PEOPLE'S DEMOCRATIC REPUBLIC OF ALGERIA
MINISTRY OF HIGHER EDUCATION AND SCIENTIFIC RESEARCH
ABOU-BEKR BELKAID UNIVERSITY- TLEMCEN

THESIS

Presented to:

FACULTY OF SNV/STU – DEPARTMENT OF BIOLOGY

For the fulfillment of the requirements for the degree of:

DOCTORATE (PhD) – L.M.D. System

Specialty: Transformation and Valorization in Agro-Food Sciences

By :

Miss LAMRAOUI Ghada

On the topic

Valorization of Agro-Industrial Residues (Date Kernels and Palm Leaves) as Alternative Substrates for sustainable Mushroom (Pleurotus ostreatus) Cultivation:

Agronomic Performance, Mycochemical Profiling, and Biological Activity Evaluation

Publicly defended on [17 / 02 / 2026] at Tlemcen before the jury composed of:

Mr. BARKA Mohamed Salih	Professor	Tlemcen University	President
Mr. TEFIANI Choukri	Professor	Tlemcen University	PhD Supervisor
Mme MEROUFEL Bahia	Associate Professor (A)	Tlemcen University	Examinator
Mr BENABDELMOUMENE Djilali	Professor	Mostaganem University	Examinator
Mr BENBOUZIANE Bouasria	Associate Professor (A)	Mostaganem University	Examinator

Laboratory of Functional Agrosystems & Technologies of Agronomic Sectors
Tlemcen - Algérie

Statement of Originality

I, the undersigned, hereby declare that the work presented in this thesis entitled:

"Valorization of Agro-Industrial Residues (Date Kernels and Palm Leaves) as Alternative Substrates for Sustainable Mushroom (*Pleurotus ostreatus*) Cultivation: Agronomic Performance, Phytochemical Profiling, and Biological Activity Evaluation"

is the result of my own independent research carried out under the supervision of Professor Choukri Tefiani

I affirm that:

- This thesis has not been submitted, in whole or in part, for the award of any other degree or qualification at this or any other institution.
- All sources of information and data used in this work have been duly acknowledged.
- Where the work of others has been cited or reproduced, it has been clearly indicated and referenced according to academic standards.
- Experimental procedures, results, and interpretations are presented with honesty and integrity, in line with the ethical guidelines of scientific research.

I take full responsibility for the originality of the content of this thesis.

Tlemcen, Algeria
25 / 11 /2025

Ghada Lamraoui
PhD Candidate

Dedication

To every guiding hand,

To every voice of care,

To those who lit my path

When shadows gathered there.

This work is not mine alone,

it carries all your grace

Each page a quiet echo

Of your kindness and embrace.

So I gift this humble thesis

To every heart that stayed,

Through patience, strength, and wisdom

The journey's debt is paid

Acknowledgement

Once upon a time, a curious student set out on a long journey called "PhD research. The path was steep, full of sleepless nights, unanswered questions, and endless revisions. Yet at every turn, there were companions who made the road lighter.

At the very beginning, the journey started at the gates of SNV/ATU faculty of ABOUBAKR BELKAID university of Tlemcen, a wise guide appeared -my supervisor-whose patience and guidance became the compass that kept me moving in the right direction. Without this light, I would have been lost in the fog of doubt.

Behind me, like the strongest roots of an ancient tree, stood my parents. Their unwavering belief and quiet sacrifices gave me the strength to keep going, even when I thought of giving up. Their trust was the foundation upon which this work stands.

Beside me, from the very first steps until the end, walked a companion who shared this journey in all its colors. Together we carried the weight of challenges, celebrated the smallest victories, and found courage in the hardest moments. This bond was not walked alone—it was extended through her family, whose kindness and support turned heavy days into lighter ones. Their home and hearts became a shelter of generosity and friendship, reminding me that this journey was never mine alone.

I also crossed paths with dedicated researchers in various laboratories and research centers; their exchanges of ideas, encouragements, and technical help were sparks that enriched this thesis in ways I could not have imagined alone

And all along the roads never missing the faculty community starting with the dean, vice dean, teachers, laboratory engineers, administrators and so many others whose invisible hands and quite contributions made this journey possible

This thesis is not only the story of my effort but the story of a community walking with me, step by step, until the final pages was written. To all of you, I owe my deepest gratitude

"Thank you all"

Ghada Lamraoui

List of Publications

Lamraoui, G., Tefiani, C., Maouedj, A., Chaalel, A., Spiga, N., Zied, D. C., Rouar, S., Jang, K.Y., Boufahj, F., Elfalleh, W., Bendif, H. (2025). Promoting Yield and Oyster Mushroom Cycle Production by Using Date Kernel and Wheat Straw Mixture as a Cultivation Substrate. *BioResources*, *20*(3). DOI:10.15376/biores.20.3.7421-7434 https://ojs.bioresources.com/index.php/BRJ/article/view/24840/2090

Abstract

Agro-industrial residues such as date kernels and palm leaves were evaluated as alternative substrates for *Pleurotus ostreatus* cultivation. Nine formulations were prepared by substituting wheat straw (WS) with date kernels or palm leaves (25, 50, 75 & 100%) and inoculated at 5% spawn (w/w). Growth parameters, yield, phytochemical composition, and biological activities were assessed.

date kernels and palm leave only based substrate reduced spawning time (12 to 17d) and produced less yield (around 220g) compared to WS in which needed 20,6d to full colonization to produce 374g as total yield. Total phenolic content reached 24.85 mg GAE/g extract in K25 compared to 13.27 mg GAE/g in P100. Total flavonoid content ranged from 4.12 to 9.46 mg QE/g . LC-MS analysis identified major phenolic constituents including luteolin, quercetin, apigenin, and gallic acid derivatives. Antioxidant assays demonstrated pronounced radical scavenging and metal chelating activities in date kernel–based substrates. DPPH IC_{50} values ranged from 546.88 to 649.32 ± 9.54 µg/mL, ABTS from 152.35 to 190.29 µg/mL, hydroxyl radical scavenging from 873.71 to 1019.80 µg/mL, and ferrous ion chelating activity (FIC) from 84.54 to 93.15 µg/mL. In contrast, palm leaf–based substrates exhibited superior reducing capacity and copper chelation, with FRAP values ranging from 24.66 to 33.35 µg/mL, CUPRAC from 98.51 to 182.95 µg/mL, and copper chelating activity (CCA) from 511.88 to 710.18 µg/mL. Enzyme inhibition assays (1 mg/mL) revealed weak inhibitory effects against α-amylase (6.2–30.01%), acetylcholinesterase (5.35–52.86%), butyrylcholinesterase (15.8–35.75%), and lipase (2.96–14.21%). However, marked tyrosinase inhibition was observed in palm-based substrates (IC_{50}: 266.68–575.98 µg/mL), while kernel-based substrates showed stronger urease inhibition (IC_{50}: 320.77–570.32 µg/mL). First-flush extracts from treatments with lower wheat straw proportions exhibited notable anti-inflammatory activity (IC_{50}: 126.54 and 149.53 µg/mL for P25 and K25; 155.25 and 245.82 µg/mL for P100 and K100). Moderate antibacterial activity was recorded against Gram-positive bacteria.

Overall, partial substitution of wheat straw with 25% date kernels supports mycelial colonization (12 d), early primordia formation (16 d), and the highest total yield (478.07 g), superior bioactive properties supporting sustainable, value-added cultivation.

Key words: agronomical performance; Agro-waste; biological activities; Date kernels; Mushroom cultivation; Palm leaves; Pleurotus ostreatus.

Résumé

Les résidus agro-industriels tels que les noyaux de dattes et les feuilles de palmier ont été évalués comme substrats alternatifs pour la culture de Pleurotus ostreatus. Neuf formulations ont été préparées en substituant la paille de blé par des noyaux de dattes ou des feuilles de palmier (25, 50, 75 et 100 %), puis inoculées avec un taux de semence de 5 % (p/p). Les paramètres de croissance, le rendement, la composition phytochimique et les activités biologiques ont été évalués.

Les substrats K100 et P100 ont réduit le temps de colonisation (12 à 17 j) mais ont produit un rendement plus faible (environ 220 g) comparativement à la paille de blé, qui nécessitait 20,6 jours pour une colonisation complète et a généré un rendement total de 374 g. La teneur totale en composés phénoliques a atteint 24,85 mg EAG/g d'extrait dans K25 contre 13,27 mg EAG/g dans P100. La teneur totale en flavonoïdes variait de 4,12 à 9,46 mg EQ/g. L'analyse LC-MS a permis d'identifier les principaux constituants phénoliques, notamment la lutéoline, la quercétine, l'apigénine et des dérivés de l'acide gallique. Les tests antioxydants ont mis en évidence une forte activité de piégeage des radicaux libres et de chélation des métaux dans les substrats à base de noyaux de dattes. Les valeurs d'IC_{50} du DPPH variaient de 546,88 à 649,32 ± 9,54 µg/mL, celles de l'ABTS de 152,35 à 190,29 µg/mL, le piégeage du radical hydroxyle de 873,71 à 1019,80 µg/mL, et l'activité chélatrice du fer de 84,54 à 93,15 µg/mL. En revanche, les substrats à base de feuilles de palmier ont montré une capacité réductrice et une chélation du cuivre supérieures, avec des valeurs FRAP comprises entre 24,66 et 33,35 µg/mL, CUPRAC entre 98,51 et 182,95 µg/mL, et CCA entre 511,88 et 710,18 µg/mL. Les essais d'inhibition enzymatique (1 mg/mL) ont révélé une faible inhibition de l'α-amylase (6,2–30,01 %), de l'acétylcholinestérase (5,35–52,86 %), de la butyrylcholinestérase (15,8–35,75 %) et de la lipase (2,96–14,21 %). Toutefois, une inhibition marquée de la tyrosinase a été observée dans les substrats à base de feuilles de palmier (IC_{50} : 266,68–575,98 µg/mL), tandis que les substrats à base de noyaux de dattes ont montré une inhibition plus importante de l'uréase (IC_{50} : 320,77–570,32 µg/mL). Les extraits de la première volée issus des traitements contenant une faible proportion de paille de blé ont présenté une activité anti-inflammatoire notable (IC_{50} : 126,54 et 149,53 µg/mL pour P25 et K25 ; 155,25 et 245,82 µg/mL pour P100 et K100). Une activité antibactérienne modérée a été enregistrée contre les bactéries Gram positives.

La substitution partielle de la paille de blé par 25 % de noyaux de dattes a favorisé une colonisation mycélienne rapide (12 j), une formation précoce des primordia (16 j) et le

rendement total le plus élevé (478,07 g), tout en améliorant les propriétés bioactives, soutenant ainsi une stratégie de valorisation durable à forte valeur ajoutée.

Mots-clés : performance agronomique ; résidus agro-industriels ; activités biologiques ; noyaux de dattes ; culture de champignons ; feuilles de palmier ; *Pleurotus ostreatus*.

الملخص

تم رسكلة مخلفات الصناعات الزراعية مثل نوى التمور وسعف النخيل كركائز بديلة لزراعة فطر *Pleurotus ostreatus*. تم إعداد تسع خلائط من قش القمح (WS) مع نوى التمور أو سعف النخيل بنسب 25 و50 و75 و100%، ثم زرعت بنسبة 5% (وزن/وزن) ليتم خلالها تقييم مؤشرات النمو، والمردود، والتركيب الكيميائي النباتي، والأنشطة البيولوجية.

أظهرت الخلائط المعتمدة كليًا على نوى التمور أو سعف النخيل انخفاضًا في مدة التحضين (12 إلى 17 يومًا)، إلا أنها أعطت مردودًا أقل (حوالي 220 غ) مقارنة بقش القمح الذي احتاج إلى 20.6 يومًا لاستكمال استعمار الميسيليوم وحقق مردودًا إجماليًا قدره 374 غ. بلغت المحتويات الكلية من المركبات الفينولية 24.85 ملغ مكافئ حمض الغاليك/غ من المستخلص في معاملة K25 مقابل 13.27 ملغ فيP100 ، بينما تراوح محتوى الفلافونويدات الكلي بين 4.12 و9.46 ملغ مكافئ كيرسيتين/غ. وأظهر تحليل LC-MS وجود مركبات فينولية رئيسية مثل اللوتيولين، والكيرسيتين، والأبيجينين، ومشتقات حمض الغاليك.

كشفت اختبارات النشاط المضاد للأكسدة عن فعالية مرتفعة في اصطياد الجذور الحرة وخلب المعادن في الركائز المعتمدة على نوى التمور؛ حيث تراوحت قيم IC_{50} لاختبار DPPH بين 546.88 و649.32 ± 9.54 ميكروغرام/مل، ولاختبار ABTSبين 152.35 و190.29 ميكروغرام/مل، ولاصطياد الجذر الهيدروكسيلي بين 873.71 و1019.80 ميكروغرام/مل، بينما تراوحت قدرة خلب الحديد (FIC) بين 84.54 و93.15 ميكروغرام/مل. في المقابل، أظهرت خلائط سعف النخيل قدرة اختزالية وخلبًا للنحاس أعلى، حيث تراوحت قيم FRAP بين 24.66 و33.35 ميكروغرام/مل، و CUPRACبين 98.51 و182.95 ميكروغرام/مل، و CCAبين 511.88 و710.18 ميكروغرام/مل. أظهرت اختبارات تثبيط الإنزيمات (1 ملغ/مل) تثبيطًا ضعيفًا لإنزيم-α أميلاز (6.2–30.01%)، وأستيل كولين إستيراز (5.35–52.86%)، وبوتيريل كولين إستيراز (15.8–35.75%)، وليباز (2.96–14.21%). في المقابل، سُجِّل تثبيط ملحوظ لإنزيم التيروزيناز في خلائط سعف النخيل 266.68–575.98 :IC_{50} ميكروغرام/مل، وتثبيط أقوى لإنزيم اليورياز في خلائط نوى التمور 320.77–570.32 :IC_{50}ميكروغرام/مل .كما أظهرت مستخلصات الدفعة الأولى من الخلائط ذات النسبة المنخفضة من قش القمح نشاطًا مضادًا للالتهاب ملحوظًا:IC_{50} 126.54 و149.53 ميكروغرام/مل لـ P25 وK25؛ و155.25 و245.82 ميكروغرام/مل لـ P100 و K100 وتم تسجيل نشاط مضاد بكتيري متوسط ضد البكتيريا ذات الغرام الموجب.

بصفة عامة، أدى الاستبدال الجزئي لقش القمح بنسبة 25% من نوى التمور إلى تسريع الاستعمار الميسيليومي (12 يومًا)، وتحفيز تكوين البراعم الأولية مبكرًا (16 يومًا)، وتحقيق أعلى مردود إجمالي (478.07 غ)، إلى جانب تعزيز الخصائص البيولوجية الفعالة، مما يدعم استراتيجية استدامة ذات قيمة مضافة في زراعة الفطر.

الكلمات المفتاحية: الأداء الزراعي؛ المخلفات الزراعية؛ الأنشطة البيولوجية؛ نوى التمر؛ زراعة الفطر؛ أوراق النخيل؛ Pleurotus ostreatus.

Table of Content

list of Figures

List of Tables

List of Abbreviations

- **ABTS** – 2,2′-azino-bis(3-ethylbenzothiazoline-6-sulfonic acid)
- **AChE** – Acetylcholinesterase
- **BChE** – Butyrylcholinesterase
- **BE** – Biological Efficiency
- **C** – Carbon
- **C/N** – Carbon-to-Nitrogen ratio
- **$CaCO_3$** – Calcium Carbonate
- **CCA** – Copper Chelating Activity
- **CUPRAC** – Cupric Ion Reducing Antioxidant Capacity
- **DM** – Dry Matter
- **DPPH** – 2,2-diphenyl-1-picrylhydrazyl
- **DW** – Dry Weight
- **EC_{50}** – Effective Concentration at 50% response
- **EDTA** – Ethylenediaminetetraacetic acid
- **EDTAE** – Ethylenediaminetetraacetic acid equivalent
- **FIC** – Ferrous Ion Chelating activity
- **FRAP** – Ferric Reducing Antioxidant Power
- **FTIR** – Fourier Transform Infrared Spectroscopy
- **GAE** – Gallic Acid Equivalent
- **HR** – Hydroxyl Radical
- **IC_{50}** – Half Maximal Inhibitory Concentration
- **K25, K50, K75, K100** – Substrate formulations with 25%, 50%, 75%, and 100% date kernels
- **LC-MS/MS** – Liquid Chromatography–Tandem Mass Spectrometry
- **N** –Nitrogen
- **P25, P50, P75, P100** – Substrate formulations with 25%, 50%, 75%, and 100% palm leaves
- **PBS** – Phosphate-Buffered Saline
- **QE** – Quercetin Equivalent
- **TAC** – Total Antioxidant Capacity
- **TE**– Trolox Equivalent
- **TFC** – Total Flavonoid Content
- **TPC** – Total Phenolic Content
- **UHPLC** – Ultra-High Performance Liquid Chromatography
- **WS** – Wheat Straw

INTRODUCTION

1. INTRODUCTION

Edible mushrooms represent a valuable resource with multidimensional importance spanning nutrition, medicine, and socio-economic development. From a nutritional perspective, they are rich in high-quality proteins, dietary fibers, vitamins, and essential minerals, while containing very little fat and calories. This composition makes them an excellent component of balanced diets and a contributor to health promotion. In addition, mushrooms are a natural source of bioactive compounds such as polysaccharides, phenolics, and flavonoids, which exhibit antioxidant, anti-inflammatory, and immunomodulatory properties, thereby supporting overall well-being and reducing the risk of chronic diseases (**Valverde *et al*., 2015; Assemie & Abaya, 2022**).

Beyond their nutritional role, mushrooms have attracted considerable scientific attention for their therapeutic potential. Isolated compounds from different species have demonstrated promising activities against various health conditions, including cancer, diabetes, neurodegenerative disorders, and microbial infections. Their antioxidant constituents are particularly effective in mitigating oxidative stress associated with aging and several pathological processes. Moreover, certain mushroom extracts display enzyme inhibitory activities that may aid in the management of disorders such as Alzheimer's disease, obesity, and metabolic dysfunctions. These health-promoting properties highlight their growing relevance in the development of nutraceuticals and pharmaceuticals (**Venturella *et al*., 2021; Ambhore *et al*., 2024**).

Pleurotus ostreatus, commonly known as the oyster mushroom, belongs to the *Basidiomycota* phylum and the *Pleurotaceae* family. Originally native to China, and now distributed worldwide. It produces clustered fruiting bodies that resemble oyster shells, which is the origin of its common name. The fruiting bodies have a white, firm flesh of varying thickness, with white to cream-colored gills that run down an off-center stalk (stipe). The spores are white to lilac-gray, complementing the mushroom's distinctive morphology and texture (**Seethapathy *et al*., 2023; National Center for Biotechnology Information, 2025**).

It serves as an excellent model species due to its highly valued both nutritionally and medicinally, It provides high-quality proteins, dietary fibers, essential amino acids, and a wide range of vitamins—particularly B-complex vitamins—alongside key minerals such as potassium, phosphorus, and iron, while maintaining a low content of fat and calories, making it a beneficial addition to a healthy diet. Its carbohydrate fraction is dominated by

polysaccharides, especially β-glucans, which not only contribute to dietary fiber but also play an important role in conferring functional health benefits. The chemical composition of P. ostreatus is dynamic, varying with substrate composition and fungal metabolism, while the levels of bioactive compounds such as phenolics and flavonoids fluctuate during the cultivation cycle, with flavonoids typically peaking in early flushes and phenolics increasing in later ones. Beyond its nutritional value, the species has been extensively studied for its medicinal potential, being a rich source of bioactive metabolites including polysaccharides, phenolics, flavonoids, and terpenoids (**Elkanah *et al*., 2022; Irshad *et al*., 2023; Effiong *et al*., 2024a**). These compounds endow the mushroom with strong antioxidant properties, enabling effective scavenging of free radicals and reduction of oxidative stress, mechanisms that are central to the prevention of chronic diseases such as cardiovascular disorders, cancer, and neurodegenerative conditions (**Effiong *et al*., 2024b**). In addition, P. ostreatus exhibits notable anti-inflammatory activity by inhibiting protein denaturation and modulating inflammatory mediators, suggesting its usefulness in managing arthritis and related disorders (**Jayasuriya *et al*., 2020**). Antimicrobial effects have also been reported, with extracts showing inhibitory action against a range of bacterial and fungal pathogens (**Yakobi *et al*., 2023**). Furthermore, enzyme-inhibitory activities have been documented, including inhibition of acetylcholinesterase and butyrylcholinesterase, indicating therapeutic potential for Alzheimer's disease, as well as α-amylase and tyrosinase inhibition, relevant in combating infections and skin disorders (**Alam *et al*., 2010; Talkad *et al*., 2015; Bello *et al*., 2017**). Moreover, P. ostreatus is highly adaptable and able to use lignocellulolytical enzymes to decompose materials and use it as nutrients for their growth, enhancing its potential for sustainable cultivation and bioconversion of organic residues. This adaptability, combined with its fast growth rate, supports cost-effective mushroom production and environmental applications such as waste recycling, its cultivation is often associated with the recycling of vast amounts of agro-industrial waste (**Luz *et al*., 2012; Ganash *et al*., 2021**).

Agro-industrial wastes such as date kernels and palm leave present significant challenges in waste management due to their volume, composition, and environmental impact. Date kernels, a byproduct of date fruit processing, and palm leaves, abundantly generated from palm cultivation – generating approximately 1 million tons of date seeds and more than 55000 tons of palm leaves are produced annually, are rich in lignocellulosic materials that are resistant to rapid decomposition (**Hegazy *et al*., 2015; Bouallegue *et al*., 2019; Alsulami *et al*., 2023; Arab News, 2023**). Improper disposal methods, including open burning and landfilling,

contribute to air pollution through the release of greenhouse gases and particulate matter, as well as soil and water contamination. Additionally, the accumulation of these agro-wastes can create breeding grounds for pests and pathogens, posing risks to public health and agricultural productivity. The inherent resistance of their fibrous and lignified structure complicates conventional waste management approaches, leading to underutilization and environmental burdens (**Ahmed, 2024; Herzallah *et al*., 2025; Suliman & Tahir, 2025**).

The pressing need to transform these agro-industrial residues into valuable resources stems from environmental, economic, and sustainability considerations. Valorization involves converting date kernels and palm leaves into useful products, thereby minimizing waste and supporting circular economy principles. These residues possess considerable potential as substrates for mushroom cultivation, bioenergy production, bioactive compound extraction, and biomaterial development, leveraging their rich carbon and nutrient content (**Shokrollahi *et al*., 2023; Manai *et al*., 2024**). Utilizing these wastes in biotechnological applications not only reduces environmental pollution but also generates economic value by producing food, feed, pharmaceuticals, and industrial enzymes. Moreover, valorization aligns with global efforts to promote sustainable agriculture and waste reduction, fostering resilience in agro-industrial systems and contributing to resource efficiency and climate change mitigation.

Using agro-industrial wastes such as date kernels and palm leaves as substrates for mushroom cultivation promotes environmental sustainability and considered as climate-friendly practice by reducing agricultural waste accumulation and mitigating associated pollution. Instead of disposing of these lignocellulosic wastes through burning or landfilling—which generate greenhouse gases, soil degradation, and water contamination—their reuse valorizes the biomass, closing nutrient cycles. This recycling approach lowers environmental footprints, conserves natural resources by decreasing reliance on virgin materials, and contributes to sustainable waste management practices in agricultural regions (**El-mously, 2023**)

In recent years, the valorization of agro-industrial by-products as substrates has gained significant attention, offering dual benefits of waste management and food production. Many literature proved that *Pleurotus ostreatus* can be cultivated on agricultural residues whether it it generated during the crop harvesting process like: wheat straw, chickpea straw, coffee leaves, rice straw, banana straw, and palm leaf, (**Bonatti et al., 2004; Iqbal *et al*., 2005; Murthy and Manonmani, 2008; Al-Qarawi *et al*., 2013; Abdulhadi and Hassan, 2013; Alananbeh *et al*., 2014**), or on process residues generated during the further processing of the crops like husks,

coffee pulp, coffee husk, coffee parchment, corn cobs, sunflower heads, saw dust, acacia wood, fig tree, rain tree, Mahogany tree, Eucalyptus tree, banana leaves, cotton waste, cherry husk, and coconut residue **(Iqbal *et al*., 2005; Salmones *et al*., 2005; Vetayasuporn, 2007; Murthy and Manonmani, 2008; Bhattacharjya *et al*., 2015; Hoa *et al*., 2015; Varghese and Amritkumar, 2020; Dissasa, 2022)**, and also on industrial residues produced by the food, fruit and vegetable processing industries; sugarcane bagasse, (**Iqbal *et al*., 2005; Hoa *et al*., 2015)**, palm empty fruit bunch, and palm pressed fibre (**Tabi *et al*., 2008**).

Their suitability depends on their lignin content, nutrient composition, and physical properties affecting aeration and moisture retention. For instance, sugarcane bagasse and banana leaves have been reported to support mycelial growth and fruiting with varied runtimes comparable or longer than wheat straw. Maize cobs and cottonseed hulls are also favorable substrates due to their physical texture and nutrient availability. These agro-wastes may require supplementation or mixing strategies to optimize yields (**Emiru *et* al., 2016; Dubey *et al*., 2019; Desisa *et al*., 2024)**. Wheat straw, in particular, supports robust fruiting body development with good yields. However, its high lignin content can delay colonization and pinhead appearance, and substrate preparation may require particle size adjustment to optimize aeration. Supplementation or mixing with nitrogen-rich residues, has been shown to enhance nutrient balance, accelerate growth phases, and increase biological efficiency (**Yang *et al*., 2013**).

In *Pleurotus ostreatus* cultivation studies, the growth cycle is a fundamental agronomic parameter that encompasses several stages from inoculation to the final harvest. Key measured intervals typically include the spawn run time (mycelial colonization), pinhead formation, fruiting body maturation, and the timing between successive flushes. Literature commonly reports spawn run times ranging from 12 to 26 days depending on substrate and species, with *Pleurotus ostreatus* showing variability influenced by substrate composition and environmental conditions. Pinhead or primordia formation usually occurs within 3 to 31 days following full colonization, with total fruiting body development spanning approximately 33 to 38 days. The interval between flushes often lengthens with each successive harvest, generally lasting from one to several weeks. These phases combined define the crop cycle duration, which in commercial cultivation can vary from around 50 to over 96 days, subject to substrate quality, spawn type, and cultivation management practices (**Paudel and Dhakal, 2020; Raman *et al*., 2021; Tupa *et al*., 2022; Östbring *et al*., 2023**).

In mushroom cultivation studies, yield is typically expressed as the fresh weight per cultivation bag and evaluated flush by flush to track productivity throughout the crop cycle. The first flush usually contributes the highest proportion of total yield, often accounting for 40–60% of the cumulative production, while subsequent flushes tend to produce progressively lower outputs. Studies emphasize the importance of substrate nutrient availability, particularly nitrogen content, on maximizing yields. Supplementation or mixing agricultural residues, such as wheat straw with nitrogen-rich additions, has been shown to enhance yield performance. Yield declines in later flushes are generally attributed to nutrient depletion and accumulation of metabolic inhibitors in the substrate (**Zakil *et al*., 2019; Argaw *et al*., 2023; Gebru, Belete, & Faye, 2024**).

Biological efficiency, defined as the ratio of fresh mushroom weight harvested to the dry weight of the substrate expressed as a percentage, is a critical standardized index used to compare substrate productivity. BE values reported for *Pleurotus ostreatus* range from 30% to over 100%, depending on substrate formulation and cultivation conditions. Commercial substrates such as wheat straw or supplemented agro-residues often yield BE values between 50% and 90%. Studies indicate that substrates with balanced carbon-to-nitrogen ratios and optimal physical structure support higher BE by facilitating efficient mycelial growth and nutrient conversion. BE tends to correlate positively with overall yield but can be influenced by factors such as flush number, substrate particle size, moisture retention, and contamination levels. (**Tekeste *et al*., 2020; Wiafe-Kwagyan *et al*., 2022; Gebru, Belete, & Faye, 2024**)

The substrate used for cultivating *Pleurotus ostreatus* not only affects its growth performance but also significantly influences nutritional quality, impacting protein content, mineral composition, vitamins, and amino acid profiles. Various lignocellulosic substrates provide different nutrient availabilities that affect mushroom growth and nutritional yield. For instance, sugarcane bagasse has been identified as a particularly suitable substrate for producing mushrooms with enhanced nutritional profiles, including higher protein content and enriched minerals such as potassium, iron, and magnesium. Additionally, substrates supplemented with nutrient-rich materials like rice bran and wheat bran further improve the dietary quality by increasing essential vitamins (C, E, B-complex) and beneficial bioactive compounds. Mushrooms grown on these substrates demonstrate moderate protein and fiber content alongside low fat and ash levels, making them a valuable functional food. The amino acid analysis reveals the presence of essential amino acids such as lysine in high amounts, contributing to the mushroom's role in combating nutrition-related disorders. The variation in

moisture content also affects shelf life and metabolic functions, while low sodium content qualifies P. ostreatus as a suitable food for hypertensive individuals (**Hoa *et al*., 2015; Elkanah *et al.*, 2022; Effiong *et al*., 2024a**).

Moreover, Different substrates impact the production of phenolic compounds and bioactive metabolites that exhibit antitumor, antioxidant, antimicrobial, antihypertensive, and antihyperglycemic activities. Studies show that different lignocellulosic and agricultural residues, result in variations in total phenolic content and antioxidant capacity of the mushrooms. For example, P. ostreatus cultivated on alder (Alnus glutinosa) sawdust exhibited the highest antioxidant activity and phenolic content compared to other substrates, highlighting the significant impact of substrate type on bioactive compound accumulation (**Kılıç *et al.*, 2024**). Research on peach palm by-products as substrates revealed enhanced phenolic acid content, including specific compounds like gallic, vanillic, trans-cinnamic, ferulic, and coumaric acids, all known for their potent antioxidant properties. These phenolic acids contribute to scavenging free radicals, reducing oxidative stress, and improving the overall antioxidant capacity measured by assays such as FRAP and ABTS (**Valério *et al*., 2024**). Additionally, supplementing substrates with components like wheat bran has been shown to increase levels of bioactive compounds such as vitamin E, phenol, fatty acids, and terpenoids, which collectively enhance the antioxidant and antimicrobial activities of the mushrooms (**Mkhize *et al*., 2022**). Outside its well-known antioxidant activity, *Pleurotus ostreatus* exhibits a range of important medicinal properties influenced by substrate and cultivation conditions. It demonstrates significant antitumor effects through multiple mechanisms, including the suppression of cancer cell proliferation, induction of apoptosis, and regulation of cell cycle arrest. Bioactive compounds such as polysaccharides (notably β-glucans), proteoglycans, and phenolic molecules enhance the immune system by stimulating natural killer cells and macrophages, which attack cancerous cells (**Effiong *et al*., 2024a**)

Beyond anticancer activity, anti-inflammatory and anti-Alzheimer is also affected, through multiple mechanisms. For example, extracts from P. ostreatus significantly reduced inflammation in carrageenan-induced paw edema models, showing comparable efficacy to anti-inflammatory drugs like indomethacin. The degree of inhibition may also relate to the substrate's influence on the synthesis of terpenoids, tannins, and polysaccharides, which contribute to antihistamine activity and membrane stabilization. Furthermore, certain substrates rich in specific nutrients can boost the mushroom’s ability to downregulate pro-inflammatory cytokines such as TNF-α and inhibit pathways involving nuclear factor kappa B (NF-κB), thus

attenuating inflammatory responses. Studies reveal that mushrooms grown on substrates such as barley straw and other agricultural wastes exhibit enhanced anti-inflammatory effects (**Rivero-Pérez *et al*., 2016; Jayasuriya *et al*., 2020; Bassi *et al*., 2024**). Importantly, such anti-inflammatory activity may also translate into neuroprotective effects relevant to Alzheimer's disease, as inflammation is a key factor in its pathology. Emerging research suggests that regular consumption of *Pleurotus ostreatus* can modulate inflammatory pathways and oxidative stress, thereby potentially reducing neuroinflammation and cognitive decline. This aligns with findings that Pleurotus extracts inhibit nuclear factor kappa B (NF-κB) activation and pro-inflammatory cytokine secretion, mechanisms implicated in Alzheimer's disease progression (**Agunloye *et al*., 2021; Silva *et al*., 2023**).

Other studies have shown the varying degrees of inhibitory effects on carbohydrate-hydrolyzing enzymes like α-amylase and α-glucosidase, which are key targets in managing postprandial blood glucose levels in diabetes. For example, mushrooms cultivated on rice bran/sawdust substrate showed stronger α-amylase inhibition, while those grown on rice bran showed better α-glucosidase inhibition (**Ekundayo *et al*., 2017; Chukwurah *et al*., 2023**), indicating that substrate composition modulates the profile and concentration of bioactive compounds responsible for these effects. Additionally, supplementation of substrates with nutrient-rich components like wheat bran can enhance the yield and concentration of bioactive compounds such as phenolics, terpenoids, and fatty acids, further boosting the antidiabetic potential (**Mkhize *et al*., 2016**). Besides antidiabetic effects, substrate composition also influences the antityrosinase activity of P. ostreatus, relevant to skin hyperpigmentation disorders. Antityrosinase activity is linked to compounds like phenolics and flavonoids, whose levels are affected by substrate type and supplements during cultivation (**Alam *et al*., 2010; Fakoya *et al*., 2020**).

Date kernel, derived from the fruiting seeds of *Phoenix dactylifera L.*, has been explored as a lignocellulosic substrate for *Pleurotus ostreatus* cultivation in recent years. Prior studies highlight the suitability of date kernel due to its considerable carbon and nitrogen content, which supports vigorous mycelial colonization and mushroom fruiting (**Abdulhadi and Hassan, 2013; Al-Qarawi *et al*., 2013**). The substrate typically contains around 4% protein and a high proportion of cellulose, hemicellulose, and lignin, providing both nutrients and structural components essential for fungal growth (**Kocheki 2015; Nabili *et al*., 2017; Abu-Thabit *et al*., 2020**).

Research has demonstrated that date kernel substrates can significantly enhance colonization speed, reducing spawn run times compared to more fibrous materials like wheat straw. This fast colonization is attributed to the nutrient richness and availability of phenolic precursors which stimulate fungal enzyme activity. Several studies corroborate the efficacy of date kernel in increasing mushroom yield and biological efficiency, often matching or exceeding yields obtained from conventional substrates such as wheat straw or sawdust (**Alananbeh *et al*., 2014; Tekeste *et al*., 2020**). Moreover, the partial degradation of date kernel components by fungal cellulases, hemicellulases, and ligninases releases soluble carbohydrates and phenolic compounds that the fungus utilizes to synthesize secondary metabolites (**He *et al*., 2024**). These bioactive molecules not only improve mushroom nutritional and medicinal properties but also enhance extraction yields in post-harvest analysis. However, a high C/N ratio may influence substrate performance by modulating enzyme production and mycelial expansion (**Mahdi *et al*., 2015; Nwaokobia *et al*., 2018**).

Palm leaves consist mainly of cellulose, hemicellulose, and lignin, providing a carbon-rich but nitrogen-deficient composition. Their fibrous and lignified nature makes them mechanically strong yet biologically resistant to degradation compared with softer agro-residues, often leading to slower mycelial colonization and growth. Oyster mushroom cultivation on dried palm leaves has shown reduced colonization rates compared with paddy straw and related substrates, largely due to their lower nitrogen content and structural rigidity. Nonetheless, palm leaves can still sustain fungal growth and fruiting, although yields are generally lower than those obtained with nutrient-rich materials. When incorporated into mixed substrates, palm residues modify the overall carbon-to-nitrogen (C/N) ratio and nutrient profile, thereby influencing fungal metabolism and primordia initiation. Similar trends have been reported with palm press fiber and oil palm fronds, where both chemical composition and physical properties affected mushroom productivity and growth patterns suggesting that palm leaves are a useful substrate component, especially when supplemented with additional nutrients to improve substrate quality (**Lopez-Llorca *et al*., 1999; David & Mshandete, 2023**).

The limited nitrogen content of palm leaves often slows fungal colonization when compared to alternative substrates such as soybean straw or cottonseed hulls (**Du *et al*., 2019; Díaz-Ariza *et al*., 2021)**. However, supplementation with nitrogen-rich agro-wastes like wheat bran, rice straw, or sawdust has been shown to improve nutritional balance, accelerate colonization, and enhance biological efficiency and fruiting body yield. Nutritional evaluations of P. ostreatus grown on palm-based substrates indicate that the mushrooms retain a favorable

proximate composition, particularly in terms of carbohydrates, dietary fiber, and essential minerals, frequently comparable to or even exceeding those cultivated on conventional substrates. In addition, palm residues influence morphological traits such as cap diameter, stipe length, and overall biomass, underscoring the role of substrate composition in determining both yield and marketable quality (**Alananbeh *et al*., 2014; Owaid *et al*., 2016; Bellettini *et al*., 2019**). In some investigations, they further highlight the functional potential of mushrooms cultivated on palm substrates. Extracts derived from these mushrooms consistently display high levels of phenolics and flavonoids, correlating with strong antioxidant and notable anti-inflammatory activity (**Elkanah *et al*., 2022; Valério *et al*., 2024**). All this is considered as evidence of of the usefull of date palm leaves and related and similar by-products as sustainable lignocellulosic resources for P. ostreatus cultivation.

Although agro-industrial residues such as date kernels and palm leaves are abundantly available in many regions, their potential as substrates for *Pleurotus ostreatus* cultivation remains comparatively underexplored relative to conventional materials like wheat straw. Most existing research has concentrated on traditional lignocellulosic substrates, leaving limited experimental evidence regarding the suitability of date kernels and date palm leaves in terms of growth performance, yield, and mushroom quality. This lack of data constrains understanding of how their distinctive chemical compositions—characterized by specific carbon-to-nitrogen ratios and polyphenolic contents—affect mycelial colonization, fruiting dynamics, and the biosynthesis of secondary metabolites. Moreover, optimal substrate proportions, pretreatment methods, and supplementation strategies for maximizing both agronomic performance and bioactive compound production remain insufficiently studied, hindering their broader adoption and valorization within sustainable mushroom production systems.

Current investigations often address either agronomic performance parameters (e.g., spawn running time, biological efficiency, and yield) or the biological activities of mushroom extracts in isolation. Few studies, however, integrate these aspects to examine how substrate composition and cultivation conditions simultaneously influence productivity and the functional properties of harvested mushrooms. This compartmentalized approach limits insights into potential correlations between cultivation variables and the accumulation of health-promoting compounds. In particular, the temporal dynamics of bioactive metabolite production across successive flushes remain largely unexplored, despite their importance for optimizing both yield and nutraceutical potential. Comprehensive and integrative studies are

therefore essential for designing cultivation strategies that enhance both mushroom productivity and functional value, enabling more targeted production of mushrooms for functional food and therapeutic applications.

Additional research gaps include the scarcity of comparative analyses conducted under different geographic and climatic conditions, which strongly influence substrate chemistry and fungal metabolism. Mechanistic studies are also limited, particularly those investigating how specific nutrients, structural polysaccharides, or phenolic precursors in substrates such as date kernels and palm leaves modulate enzymatic activity and the biosynthetic pathways of secondary metabolites. Furthermore, the absence of standardized methodologies for evaluating bioactive properties and linking them directly to cultivation strategies complicates inter-study comparisons and restricts the scalability of findings to industrial applications. Addressing these gaps through multidisciplinary research approaches would significantly advance the sustainable valorization of palm-based residues, supporting both efficient mushroom cultivation and the development of high-value functional foods or therapeutic products.

Addressing the research gap surrounding unconventional substrates such as date kernels and palm leaves requires systematic investigations into their performance both individually and in mixtures, their impact on mushroom growth physiology, and the interactions between substrate constituents and fungal metabolism.

While agronomic performance and yield remain fundamental for evaluating substrate suitability, the growing demand for functional foods and nutraceuticals has shifted the focus toward comprehensive profiling of bioactive compounds and associated health benefits. *Pleurotus ostreatus* is increasingly valued not only for its nutritional content but also for its repertoire of bioactive metabolites—phenolics, flavonoids, polysaccharides, and antioxidants—with demonstrated anti-inflammatory, antimicrobial, and enzyme-inhibitory properties. This dual importance highlights the need to assess both productivity and biofunctional attributes when exploring alternative substrates. Despite this, the majority of existing studies emphasize yield optimization, with relatively little attention given to the functional properties of mushrooms cultivated on novel agro-wastes. Data remain sparse regarding how substrate composition, mushroom developmental stage, and post-harvest processing influence the variability of bioactive compounds, particularly when using residues like date kernels and palm leaves. Moreover, many investigations rely on single antioxidant assays or narrowly focused bioactivity evaluations, limiting holistic insights into the broader functional potential of mushrooms.

To bridge these gaps, the present study makes a unique contribution to the intersection of agro-waste valorization, mushroom agronomy, and bioactive property assessment by rigorously evaluating the use of date kernels and palm leaves—alone and in blends with wheat straw—as substrates for *Pleurotus ostreatus* cultivation. Through standardized cultivation protocols adapted to local conditions, it comprehensively monitors critical agronomic parameters such as mycelium colonization duration, primordia emergence, flush number and spacing, total cropping cycle, yield, and biological efficiency. This enables a robust comparison of substrate performance, highlighting the potential advantages and limitations of these non-conventional agro-wastes.

In parallel, the study applies advanced chemical and biochemical analyses including 80% methanolic extraction, total phenolic and flavonoid quantification, Fourier-transform infrared spectroscopy (FTIR), and liquid chromatography–mass spectrometry (LC-MS/MS) for detailed metabolite profiling of mushroom fruiting bodies harvested from different substrates and flushes, with multifaceted bioactivity assessments including antioxidant activity through scavenging assays (DPPH, ABTS, hydroxyl radicals), reducing power (FRAP, CUPRAC, TAC), metal chelating evaluation, along with enzyme inhibition analyses (tyrosinase, urease, α-amylase, acetyl/butyrylcholinesterase, lipase), anti-inflammatory and anti-bacterial tests, provide a functional bioactivity database, linking chemical composition to biological potential.

The primary objective of this study is to valorize local agro-industrial residues, specifically date kernels and palm leaves and evaluate the potential of their use as alternative substrates for the cultivation of *Pleurotus ostreatus*. This includes assessing their effectiveness in supporting mushroom growth, yield, and productivity, while simultaneously investigating the impact of these substrates on the chemical composition and bioactive properties of the resulting mushroom fruiting bodies which break the main aim into smaller, actionable steps leading into the following secondary objectives:

1. To formulate and standardize substrate mixtures incorporating date kernels and palm leaves with wheat straw in various proportions for *Pleurotus ostreatus* cultivation. This objective addresses the knowledge gap regarding the suitability and optimization of these underutilized agro-wastes as substrates. Formulating mixtures will help identify optimal combinations that balance nutrient availability and physical characteristics conducive to fungal growth.

2. To characterize the chemical properties of the formulated substrates, including total carbon, nitrogen content, and C/N ratios, and to study their influence on mycelial colonization, pinhead formation, and total cropping cycle. This knowledge will inform substrate management strategies to optimize productivity.
3. To evaluate the agronomic performance of *Pleurotus ostreatus* cultivated on the different substrate mixtures by measuring spawn run duration, time for first pinning appearance, number of flushes, flush intervals, yield per flush, and biological efficiency. By assessing these parameters, the study fills gaps identified in substrate efficacy for mushroom farming, providing comparative data against established substrates and contributing to the optimization of sustainable production systems.
4. To perform detailed chemical characterization of mushroom fruiting bodies grown on these substrates, focusing on extraction yield, total phenolic content (TPC), total flavonoid content (TFC), and profiling of bioactive compounds using FTIR and LC-MS/MS techniques. Identifying phenolics, flavonoids, and other bioactive substances through advanced spectroscopic (FTIR) and chromatographic (LC-MS/MS) analyses substantiate the quality and health-promoting aspects of the mushrooms produced.
5. To assess the antioxidant, anti-browning, and other medicinal activities of *Pleurotus ostreatus* extracts from different flushes and substrate formulations, to provide a complete understanding of the biofunctional properties, addressing an important research gap in linking substrate type to bioactivity potential
6. To analyze the relationship between substrate composition, mushroom developmental stage (flush number), and the accumulation of bioactive compounds and biological activities. This targets elucidation of dynamic metabolite profiles and functional bioactivities across sequential flushes, which can inform harvesting strategies to maximize the nutraceutical value of cultivated *Pleurotus ostreatus*.
7. To evaluate the antibacterial efficacy of mushroom extracts against selected Gram-positive and Gram-negative bacteria.which will fill the gap of the lack of comparative studies concerning antimicrobial properties of *pleurotus ostreatus* mushroom cultivated on diverse agro-waste substrates

These objectives give rise to research questions focused on how palm residues influence mushroom growth parameters, metabolite accumulation, and functional properties, specifically:

1. Can date kernels and palm leaves, individually or combined with wheat straw, support effective mycelial growth, primordia formation, and fruiting of *Pleurotus ostreatus* compared to traditional substrates?
2. How do the carbon, nitrogen content, and C/N ratio of these substrates influence mycelial colonization rates, flush numbers, and yield outcomes in *Pleurotus ostreatus* cultivation?
3. What are the variations in total phenolic and flavonoid contents in mushrooms grown on these substrates, and how do these levels change across successive flushes?
4. How do antioxidant activities measured by multiple assays correlate with substrate composition and flush number in *Pleurotus ostreatus* extracts?
5. What medicinal properties, through enzyme inhibition (tyrosinase, urease, α-amylase, lipase, acetyl- and butyrylcholinesterase inhibition) and anti-inflammatory potential, can be exhibited by mushroom extracts from different substrates, and how does their potency vary temporally across flush development?
6. What is the antibacterial efficacy spectrum of *Pleurotus ostreatus* extracts grown on date kernel and palm leaf substrates against selected Gram-positive and Gram-negative bacteria?

In turn, these questions inform the development of the hypotheses, which propose the expected relationships between the utilization of palm residues and enhancements in both cultivation outcomes and the mushrooms' bioactive potential, specifically:

1. Date kernels and palm leaves, alone or in combination with wheat straw, can serve as efficient and sustainable substrates for the cultivation of *Pleurotus ostreatus*.
2. Mushrooms cultivated on date kernel and palm leaf-based substrates will contain rich profiles of bioactive compounds, including phenolics and flavonoids, which will vary across substrate composition and flush number.
3. Extracts from *Pleurotus ostreatus* grown on these substrates will exhibit strong antioxidant activities measured by diverse assays (DPPH, ABTS, FRAP, TAC, CUPRAC), influenced by substrate type and developmental stage of the mushroom.
4. Mushroom extracts will demonstrate significant enzyme inhibition activities, including anti-inflammatory (protein denaturation inhibition), anti-tyrosinase, anti-urease, and

other clinically relevant enzyme inhibition, with activity levels modulated by substrate composition and flush stage.

5. The antibacterial activity of *Pleurotus ostreatus* extracts will primarily affect Gram-positive bacteria more than Gram-negative species, with efficacy influenced by substrate treatment and mushroom maturity.

By formulating these hypotheses, this study aims to advance scientific understanding and practical applications of agro-waste valorization in *Pleurotus ostreatus* cultivation. By exploring underutilized residues such as date kernels and palm leaves as substrates, the research is expected to generate valuable insights into how substrate composition may influence mushroom growth, metabolite production, and functional bioactivities. These unconventional substrates have the potential to yield mushrooms with promising antioxidant, phenolic, enzyme inhibitory, and anti-inflammatory properties, thereby highlighting their relevance for functional foods, nutraceuticals, and natural therapeutics.

Testing these predictions is anticipated to address existing research gaps while contributing to agricultural waste management, cost-effective mushroom production, and local resource utilization. The study also seeks to support circular economy principles by transforming agro-industrial residues into valuable biomass, reducing environmental pollution, and enhancing food security through the production of nutritious, health-promoting mushrooms.

Beyond scientific contributions, the findings are expected to carry broader socio-economic implications: improving rural livelihoods, fostering sustainable agribusiness, and supporting public health through natural bioactive compounds. Overall, this research is positioned to integrate environmental sustainability, economic development, and human well-being, offering a model for innovative, eco-friendly, and socially impactful mushroom cultivation practices.

In line with its significance for sustainable agro-waste valorization, enhanced mushroom productivity, and the development of functional foods with potential health benefits, this study is scoped to investigate the use of underutilized residues—specifically date kernels and palm leaves—as alternative substrates for *Pleurotus ostreatus* cultivation. The research focuses on evaluating key agronomic parameters, including spawn run duration, pinhead formation, fruiting body development, yield, and flush productivity, alongside assessments of chemical composition and the accumulation of bioactive metabolites such as phenolics, flavonoids, and antioxidants. Furthermore, functional properties, including antioxidant capacity and enzyme inhibitory activities, are examined to provide an integrated understanding of the nutritional and

therapeutic potential of mushrooms cultivated on these substrates. By defining these boundaries, the study maintains a targeted investigation that emphasizes its environmental, economic, and health-related relevance, while offering practical insights for low-cost and sustainable mushroom cultivation. This focused scope also aims to generate data that may inform substrate optimization, waste management strategies, and the design of functional foods and nutraceuticals, thereby contributing to the broader objectives of circular economy, food security, and human well-being.

And while the scope of this study is carefully defined to evaluate the effects of date kernels, palm leaves, and wheat straw on *Pleurotus ostreatus* growth, bioactive compound accumulation, and functional activities, several inherent limitations naturally arise from these boundaries. The research was conducted under controlled laboratory conditions, ensuring reproducibility but not fully replicating the environmental variability of commercial or field cultivation, which may influence mushroom development and metabolite synthesis. Furthermore, the focus on specific substrates sourced from defined locations and prepared in particular ways limits the generalizability of the findings to other lignocellulosic materials or substrates with different composition, origin, or particle size. Methodological choices, including the use of 80% methanol for extraction and a selected panel of bioactivity assays, also constrain the chemical profile and functional properties captured in this study. Finally, the assessment was limited to sequential flushes without exploring long-term cultivation, substrate reusability beyond three flushes, large-scale feasibility, or economic implications. These limitations delineate the study's scope while highlighting areas for future research to expand applicability to commercial production and broader functional applications.

Considering the defined scope and inherent limitations, the thesis is organized into IMRAD (Introduction, Materials and Methods, Results, and Discussion) structure, providing a systematic and coherent presentation of the study conducted on *Pleurotus ostreatus* cultivation and bioactivity assessment.

The Introduction chapter establishes the research background by identifying gaps and outlining the objectives, research questions and hypotheses. It discusses the significance of the study, along with its scope and limitations. The chapter sets the context by emphasizing the importance of mushroom cultivation, particularly the use of agro-waste as substrates. It further addresses the investigation of the biochemical and biological properties of *Pleurotus ostreatus*, highlighting its potential applications in food and medicine.

The Materials and Methods chapter details the experimental procedures employed throughout the research. It comprehensively describes the preparation and formulation of substrates derived from date kernels, palm leaves, and wheat straw; the inoculation and cultivation protocols under controlled environmental conditions; and the harvesting techniques. It further explains the methodologies used for post-harvest processing, extract preparation, and the variety of analytical techniques implemented to evaluate phenolic and flavonoid contents, chemical profiling via FTIR and LC-MS, and the extensive suite of biological activity assays including antioxidant, anti-inflammatory, enzyme inhibition and antibacterial tests.

The Results and Discussion chapter presents and interprets the findings from the cultivation performance parameters, yield data, chemical characterization, and biological activity assessments. This integrative section compares the effects of different substrate treatments and flushes on mushroom growth, biochemical profiles, and bioactivities, relating results to existing literature and discussing the implications and potential applications of the findings. It explores correlations, substrate influences, and metabolic insights that support conclusions drawn from the data.

The final chapter, Conclusion and Recommendations, synthesizes the key outcomes of the study, emphasizing major contributions to mushroom cultivation knowledge and bioactive compound research. It highlights the practical implications for sustainable substrate use and biomedical potential of *Pleurotus ostreatus*. This chapter also provides recommendations for future research directions, including scaling, additional bioactivity explorations, and methodological enhancements to expand understanding and applications. Following the main chapters, the thesis includes a References section, listing all cited sources, and Appendices, which provide supplementary materials such as raw data, extended tables, and methodological details. Together, this structure provides a clear, logical progression from research context through experimental execution to data interpretation and conclusion, guiding the reader effectively through the comprehensive study.

MATERIALS AND METHODS

2. MATERIAL AND METHODS

The present study was conducted through two complementary components. The first consisted of an agronomical investigation focusing on the cultivation of *Pleurotus ostreatus* using different substrate formulations and growth conditions. The second involved laboratory-based analyses aimed at characterizing the biochemical properties and evaluating the bioactivities of the mushroom extracts. The methods were conducted following established scientific protocols.

2.1.Mushroom Cultivation

The cultivation of *Pleurotus ostreatus* was conducted in accordance with protocols described in the literature, with minor adjustments made to adapt the process to local conditions (**Oei & Nieuwenhuijzen, 2005; Kadhila-Muandingi *et al.*, 2008; Biswas *et al.*, 2011)**. The procedure resumed in Figure 1, comprised substrate preparation, inoculation with fungal spawn, and the maintenance of controlled environmental parameters, including temperature, humidity, and light, to support mycelial colonization and fruiting. The growth process was regularly monitored, and conditions were adjusted when necessary to ensure optimal development of the mushroom in line with established cultivation practices.

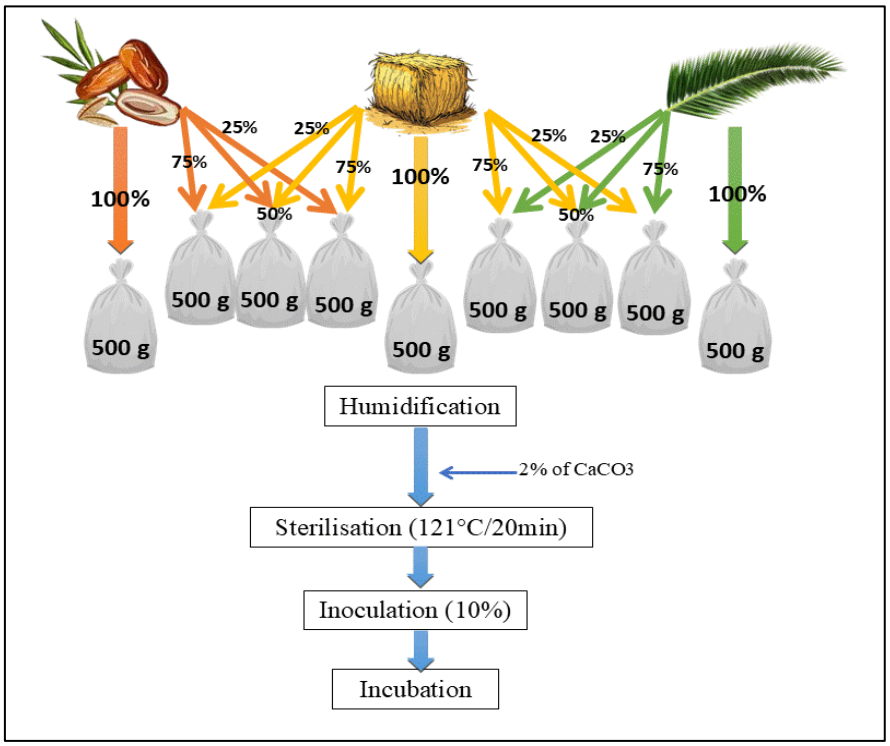

Figure 1: Substrate Preparation and Cultivation Process of *Pleurotus ostreatus*

2.1.1. Substrate Preparation

A total of nine substrate formulations were evaluated for *Pleurotus ostreatus* cultivation, prepared from three agro-industrial residues: date kernels (K), palm leaves (P), and wheat straw (WS). Date kernels were obtained from local processors of date flour specifically derived from the cultivar *Phoenix dactylifera* L. (Mech Degla) in the Biskra region. Palm leaves were collected from the Technical Institute for the Development of Saharan Agronomy (ITDAS, Biskra, Algeria), while wheat straw was sourced from an agricultural farm in the Batna region.

Prior to substrate formulation, the agro-residues were processed as follows: date kernels were ground to particles of 0.2–0.5 cm using a stainless-steel grinder, whereas palm leaves and wheat straw were cut into fragments of 2–4 cm (Figure 2). The nine substrate mixtures were prepared according to the proportions presented in Table 1. For each treatment, five replicate bags containing 500 g of substrate were prepared. Substrates were hydrated by overnight soaking in water, followed by drainage to remove excess moisture. The substrates were then transferred into polypropylene bags, supplemented with 2% $CaCO_3$, sealed, and sterilized in an autoclave at 121 °C for 20 min. After sterilization, the bags were cooled under aseptic conditions prior to inoculation.

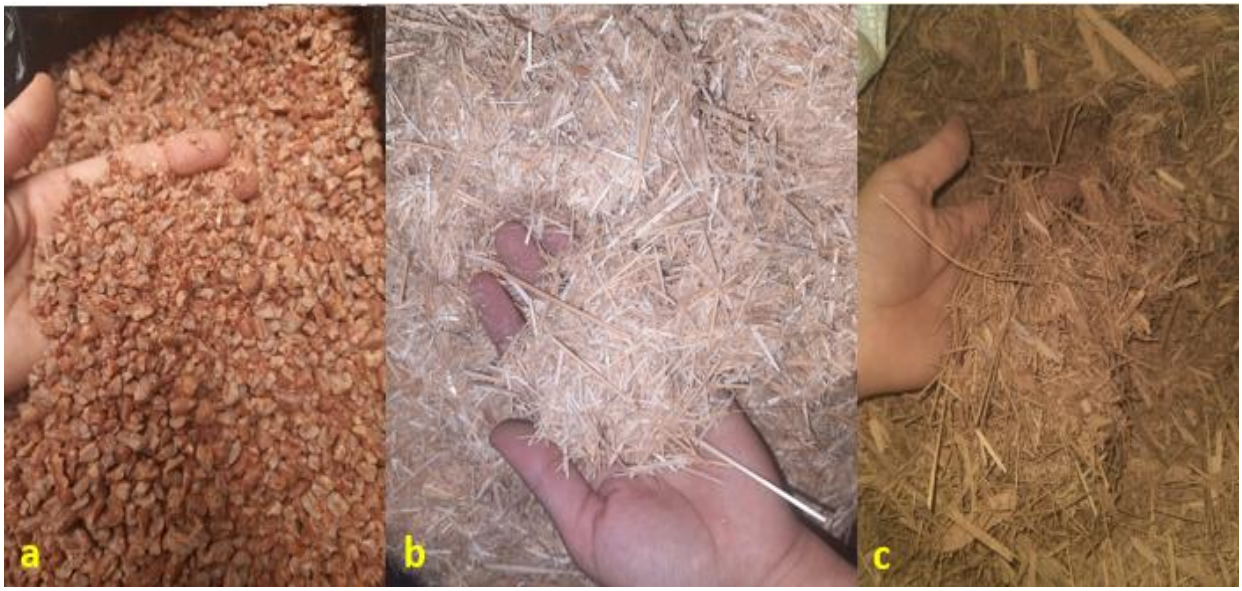

Figure 2: Processed Agricultural Residues Used as Substrates

(a: ground date kernel; b: chopped wheat straw; c: cut palm leaves)

Table 1: Proportional Composition of Waste Materials in Substrate Formulations

Substrate	Agro-waste proportion (%)		
	Wheat straw	**Date kernel**	**Palm leaves**
WS	100	0	0
K25	75	25	0
K50	50	50	0
K75	25	75	0
K100	0	100	0
P25	75	0	25
P50	50	0	50
P75	25	0	75
P100	0	0	100

2.1.2. Substrate Analysis

Each formulated substrate used for mushroom cultivation was ground into powder, weighed, and analyzed with a CHN-628 elemental analyzer (LECO Corporation, Michigan, USA) to determine total carbon and nitrogen contents. The measurements were carried out at the National Institute of Horticultural and Herbal Science, Eumseong, South Korea.

2.1.3. Inoculation and Cultivation Conditions

Following sterilization and cooling, the substrates were aseptically inoculated with 10% (w/w) spawn, placed centrally within each bag, and subsequently resealed. The inoculated bags were incubated in a dark environment at a controlled temperature of 23–27 °C until complete mycelial colonization was achieved. Upon full colonization, the bags were transferred to a fruiting chamber, where openings in the form of an “X” were cut into the polypropylene surface to facilitate primordia emergence. Fruiting conditions were maintained at 15–17 °C with a relative humidity of 85–95%, regulated using automated sensor-based systems (Figure 3).

Figure 3: mushroom cultivation process

(a: substrate bags; b: inoculation; c: incubation for spawning; d: mycelium full colonization; e: incubation for fructification; f: primordia appearance)

2.1.4. Fruiting Bodies Harvesting

The harvesting of *Pleurotus ostreatus* fruiting bodies was conducted with particular care to preserve product quality and to sustain subsequent flushes. Fruiting bodies were collected at the commercial maturity stage, defined by caps that remained slightly in-rolled at the margins and prior to the onset of upward curling. Overmature specimens, characterized by flattened or upturned caps and visible spore release, were excluded due to their rapid post-harvest deterioration and negative impact on subsequent yields. Harvesting was performed manually by gently twisting or pulling entire clusters at the stipe base to ensure complete detachment, while minimizing substrate disturbance. This practice was applied to prevent residual stipe tissue and substrate damage, which could otherwise facilitate contamination and compromise future flush production.

2.1.5. Agronomic Performance Parameters

Agronomic performance of *Pleurotus ostreatus* was evaluated based on a set of standardized cultivation parameters. The spawning run time was recorded as the number of days required for complete mycelial colonization of the substrate. Pinhead formation was noted as the interval (days) from inoculation to the visible emergence of

primordia on the substrate surface. The number of flushes produced per cultivation bag was counted, and the time separating successive flushes was measured to assess the temporal distribution of yields. The total crop cycle duration was defined as the period from inoculation until the completion of the final harvest. Yield was quantified for each flush and expressed both as fresh weight per bag and as cumulative yield across the entire crop cycle. Biological efficiency (BE) was calculated as the ratio of fresh mushroom weight obtained to the dry weight of the substrate, expressed as a percentage, thereby providing a standardized measure of productivity across treatments.

2.1.6. Post-Harvest Handling

After harvesting, the fruiting bodies were weighed, cut into small pieces, and air-dried at room temperature until a constant weight was achieved (Figure 4). The dried material was then ground into a fine powder and stored in sealed bags under refrigerated conditions for subsequent analyses.

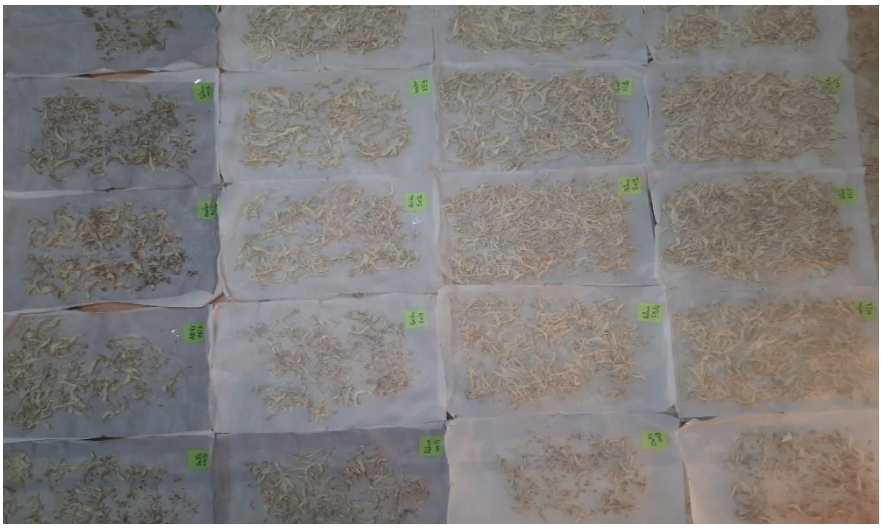

Figure 4: drying technique of harvested mushroom

2.2.Biological Activities

The biological activities of the mushroom extracts were evaluated using a comprehensive set of in vitro assays in order to characterize their bioactive compounds, antioxidant and anti-inflammatory, enzymes inhibition and antibacterial potential, following previously described standard procedures with minor modifications. All determinations were conducted in different laboratories under controlled experimental conditions and according to established methodological guidelines.

2.2.1. Extracts Preparation

The mushroom extract was prepared using maceration, a simple and gentle technique that preserves thermolabile bioactive compounds, including phenolics, flavonoids, and polysaccharides (**Osorio-Tobón, 2020**). 80% methanol (methanol:water, 80:20 v/v) was employed as the extraction solvent for 5 g of powdered mushroom, as this mixture provides an optimal polarity to solubilize both moderately and highly polar compounds, yielding higher amounts of phenolics and flavonoids compared to pure methanol (**Gonfa *et al.*, 2020**). To enhance extraction efficiency, two successive extractions were carried out—first for 48 hours with 200 mL of solvent, followed by a second extraction for 24 hours with 100 mL—ensuring that both readily soluble and residual compounds embedded in the solid matrix were recovered (Figure 5). The prolonged contact between solvent and mushroom powder allows maximal diffusion of bioactive molecules (**Đurović *et al.*, 2022**). Both extractions filtrates were combined, and the solvent was removed using a rotary evaporator to obtain the dry extract. The extraction yield was determined by weighing the flask empty and after solvent removal. The samples were labeled based on the substrate formulation and the flush number, as shown in Table 2.

Table 2: Sample Labeling According to Substrate Formulation and Flush Number

Substrate	Codes		
	1st flush	**2nd flush**	**3rd flush**
WS	WS1	WS2	WS3
K25	K25/1	K25/2	K25/3
K50	K50/1	K50/2	K50/3
K75	K75/1	K75/2	K75/3
K100	K100/1	K100/2	K100/3
P25	P25/1	P25/2	P25/3
P50	P50/1	P50/2	P50/3
P75	P75/1	P75/2	P75/3
P100	P100/1	P100/2	P100/3

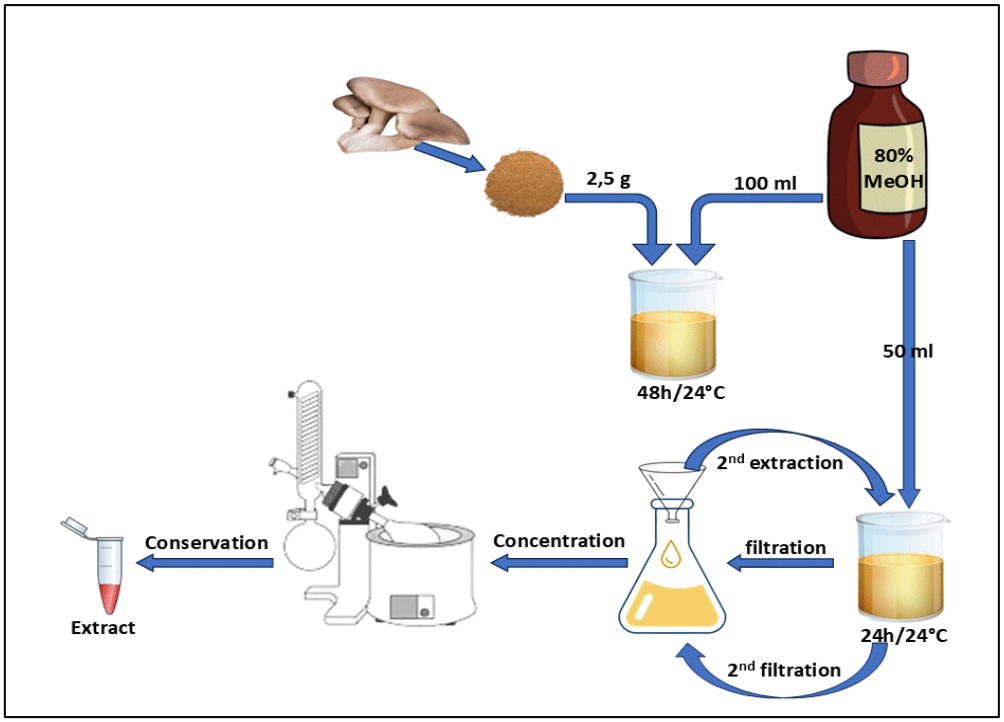

Figure 5: Extraction Procedure for *Pleurotus ostreatus* Bioactive Compounds.

2.2.2. Biochemical and Mycochemical Characterization

2.2.2.1. *Total Phenolic Content (TPC) Determination*

The TPC assay is based on the ability of phenolic compounds in a sample to reduce the Folin–Ciocalteu reagent, a mixture of phosphomolybdate and phosphotungstate, under alkaline conditions. Initially, the Folin–Ciocalteu reagent is light yellow. Upon reaction with phenolic hydroxyl groups, the reagent is reduced, producing a blue-colored complex whose intensity is proportional to the total phenolic content. The absorbance of this blue complex is measured spectrophotometrically, typically at 760–765 nm, and the results are expressed relative to a standard, such as gallic acid (**Pérez *et al.*, 2023**)

The technique used for TPC determination was developed from the protocol of **Vl (1999)** to 96-well microplate use (Figure 6). 100 µL of Folin–Ciocalteu reagent (diluted 10-fold with distilled water; 1 mL Folin–Ciocalteu and 9 mL distilled water) was added to 20 µL of mushroom extract (1 mg dissolved in 1 mL distilled water), followed by 75 µL of 7.5% sodium carbonate solution (7.5 g Na_2CO_3 dissolved in 100 mL distilled water). The mixture was kept in the dark for 2 hours, after which the absorbance was measured at 765 nm. A blank was prepared under the same conditions

by replacing the extract with distilled water. The standard curve was established using gallic acid, prepared by serial dilution (14-fold) of a 1 mg/mL stock solution in methanol and the results are expressed in mg GAE/g extract or mg GAE/g DM.

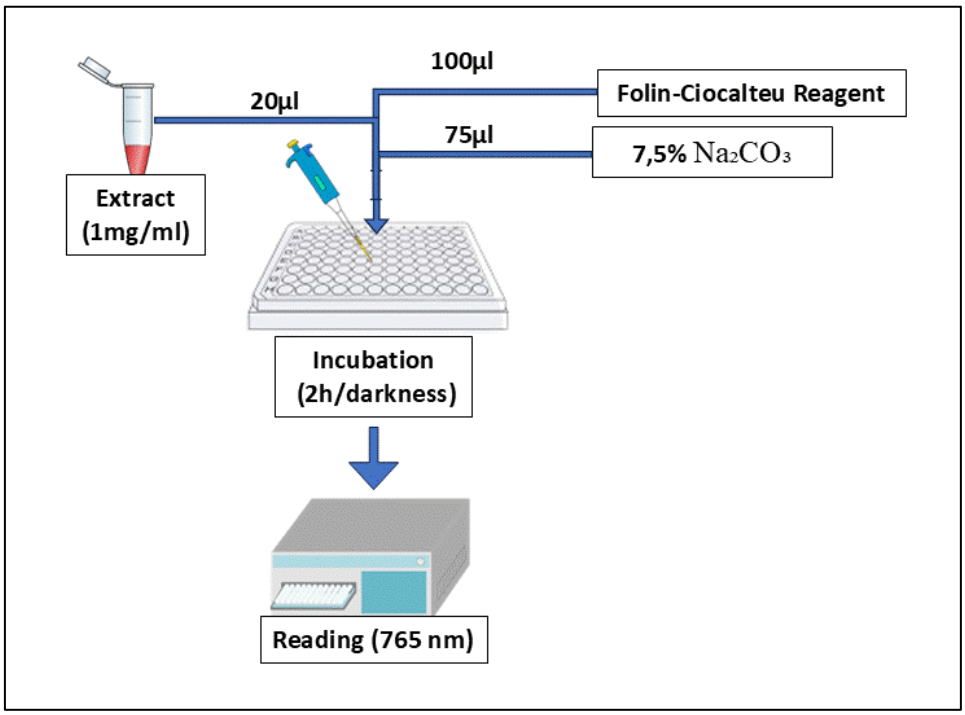

Figure 6: Experimental Protocol for the Quantification of Total phenolic Content (TPC)

2.2.2.2. *Total Flavonoid Content (TFC) Determination*

The TFC assay is based on the ability of flavonoid compounds in a sample to form complexes with aluminum chloride ($AlCl_3$) under alkaline conditions. In this assay, the sample extract is first mixed with sodium nitrite ($NaNO_2$), followed by $AlCl_3$, allowing flavonoids to form flavonoid-aluminum complexes. Subsequent addition of sodium hydroxide (NaOH) develops a pink-colored complex, the intensity of which is proportional to the flavonoid content. The absorbance of this pink coloration is measured spectrophotometrically at 510 nm, and the total flavonoid content is quantified using a quercetin standard curve, expressed as mg quercetin equivalents (QE) per gram of extract or dry matter (**Cong-Hau *et al.*, 2021**).

Using the technique developed by **Chang *et al* (2002)** The protocol was adapted to a microplate microplate use (Figure 7), 50 µL of mushroom extract (1 mg dissolved in 1 mL distilled water) was mixed in each well with 20 µL of distilled water and 15 µL

of 5% $NaNO_2$ solution (5 g $NaNO_2$ dissolved in distilled water up to 100 mL). The mixture was incubated in the dark at room temperature for 6 minutes, followed by the addition of 15 µL of 10% $AlCl_3$ solution (10 g $AlCl_3$ dissolved in distilled water up to 100 mL) and a second incubation under the same conditions for 6 minutes. Subsequently, 100 µL of 4% NaOH solution (4 g NaOH dissolved in distilled water up to 100 mL) was added, and the plate was incubated for 30 minutes in the dark. Absorbance was then measured at 510 nm. A blank was prepared under identical conditions by replacing the extract with distilled water. The standard curve was prepared using quercetin, obtained by serial 14-fold dilution of a 1 mg/mL stock solution in methanol. Results were expressed as mg QE/g extract or mg QE/g dry matter (DM).

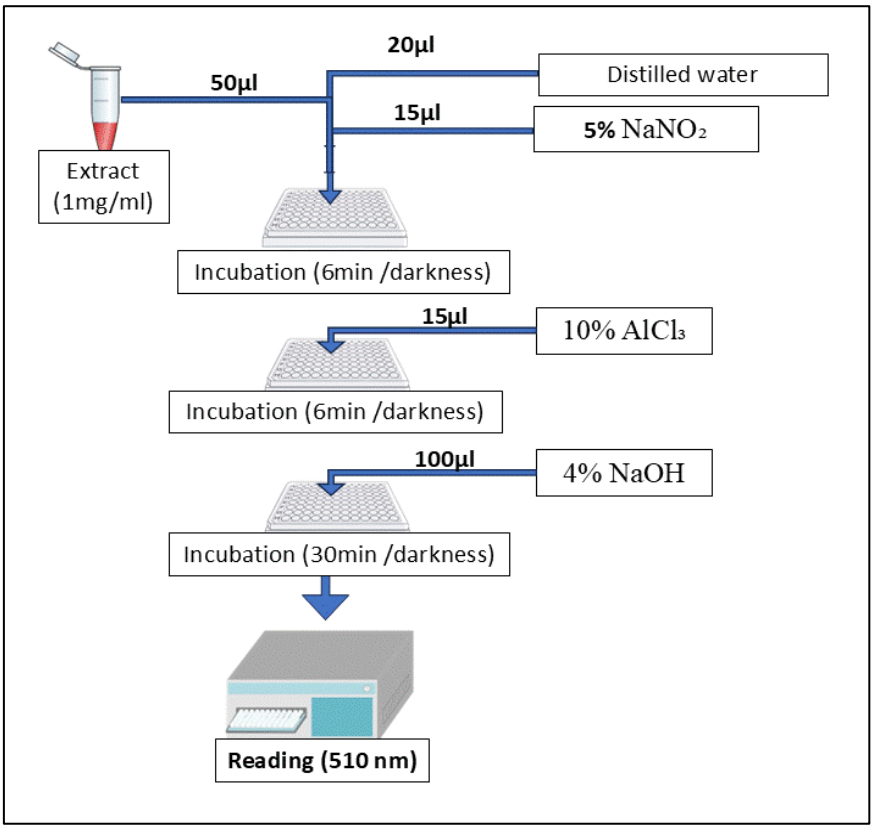

Figure 7: Experimental Protocol for the Quantification of Total Flavonoid Content (TFC)

2.2.2.3. Fourier Transform Infrared (FTIR) Analysis

Fourier Transform Infrared (FTIR) spectroscopy was employed to characterize the functional groups present in the mushroom extracts. The technique is based on the principle that molecules absorb infrared radiation at specific frequencies corresponding to the vibrational transitions of chemical bonds. When the sample is irradiated with a broad spectrum of IR light, certain wavelengths are absorbed depending on the functional groups present, generating a unique absorption pattern known as a molecular fingerprint. The instrument uses a Michelson interferometer to collect an interferogram, which is then converted into a spectrum by Fourier transformation (**Smith, 2011**). The resulting FTIR spectrum, typically expressed as absorbance versus wavenumber (cm^{-1}), was used to identify characteristic peaks associated with major bioactive compounds in the extracts.

In this study, spectral acquisition was carried out on an Agilent FTIR spectrometer equipped with an Attenuated Total Reflectance (ATR) accessory in Igdir university -Turkey-. Prior to analysis, the ATR crystal was cleaned with ethanol and dried. A small quantity of the dried mushroom powder or extract was directly placed on the ATR crystal surface, ensuring uniform contact.

Spectra were recorded in the range of 4000–650 cm^{-1} with a resolution of 8 cm^{-1}, using triangular apodization. Each spectrum was obtained by averaging 32 scans for the sample and 32 scans for the background. The instrument status was verified to be in good condition before analysis. The acquired spectra were processed using the instrument software and compared with reference spectral libraries (Agilent ATR and Pharma_D databases) to identify characteristic absorption bands and possible functional groups.

2.2.2.4. Liquid Chromatography–Mass Spectrometry (LC-MS) Analysis

Liquid Chromatography–Mass Spectrometry (LC–MS) was conducted in research institute of terrestrial ecosystem (IRET-CNR) in Naples -Italy-, and applied to characterize the bioactive compounds present in mushroom extracts. This technique integrates the separation efficiency of liquid chromatography with the high sensitivity and structural identification capacity of mass spectrometry. During the LC step, compounds were resolved according to their polarity and interactions with both the

stationary and mobile phases. The separated analytes were subsequently introduced into the mass spectrometer via an electrospray ionization (ESI) source, which produces molecular ions under soft ionization conditions, thereby reducing fragmentation. These ions were then analyzed according to their mass-to-charge ratio (m/z) in the mass analyzer (**Allwood & Goodacre, 2010**). The generated spectra provided complementary qualitative data (retention times, m/z values, and fragmentation patterns) and quantitative data (ion intensities), allowing accurate identification and profiling of phenolics, flavonoids, and other metabolites in the extracts.

Extract solutions at a concentration of 0.1 mg/mL were prepared by dissolving 1 g of dried mushroom extract in 10 mL of DMSO. The mixture was vortexed and subsequently sonicated for 60 minutes at 45 °C to ensure complete homogenization. The prepared samples were analyzed using an Ultra-High-Performance Liquid Chromatography system (UHPLC Nexera XR LC-40, Shimadzu, Kyoto, Japan) coupled with a triple quadrupole mass spectrometer (LCMS-8060, Shimadzu Italy, Milan, Italy). Data acquisition and instrument control were managed through LabSolutions software (version 5.6, Shimadzu). Electrospray ionization (ESI) was carried out in both positive and negative ionization modes, with fast polarity switching within a single run, alternating between low-energy full scans (4 V) and high-energy ramp scans (10–60 V). The main operating conditions were as follows: nebulizing gas flow, 2.9 L/min; heating gas flow, 10 L/min; desolvation line (DL) temperature, 250 °C; interface temperature, 300 °C; heat block temperature, 400 °C; and drying gas flow, 10 L/min. Chromatographic separation was achieved on a Kinetex Polar C18 column (2.6 µm, Phenomenex Inc., USA) using a mobile phase of water and acetonitrile (95:5, v/v), both supplemented with 0.01% formic acid. Analysis was conducted mainly in negative ion mode using selected ion monitoring (SIM), except for syringic acid, which was detected under positive ionization conditions (Appendix A). Compounds were identified by comparing their molecular weight, retention time, and fragmentation patterns with an in-house spectral database. A compound was considered confirmed when its chromatographic peak area exceeded that of the blank. To discriminate between isobaric compounds, Time-Of-Flight (TOF) detection was employed in the third quadrupole, providing high-resolution mass accuracy.

2.2.3. Biological Activities Evaluation

2.2.3.1. Extract Dilutions Preparation

10 mg of mushroom extract were dissolved in 1 mL of distilled water, and a series of successive 1:2 dilutions was performed to obtain the following concentrations: 10, 5, 2.5, 1.25, 0.625, 0.3125, and 0.15625 mg/ml. These dilutions were used for subsequent biological activity assays (Figure 8).

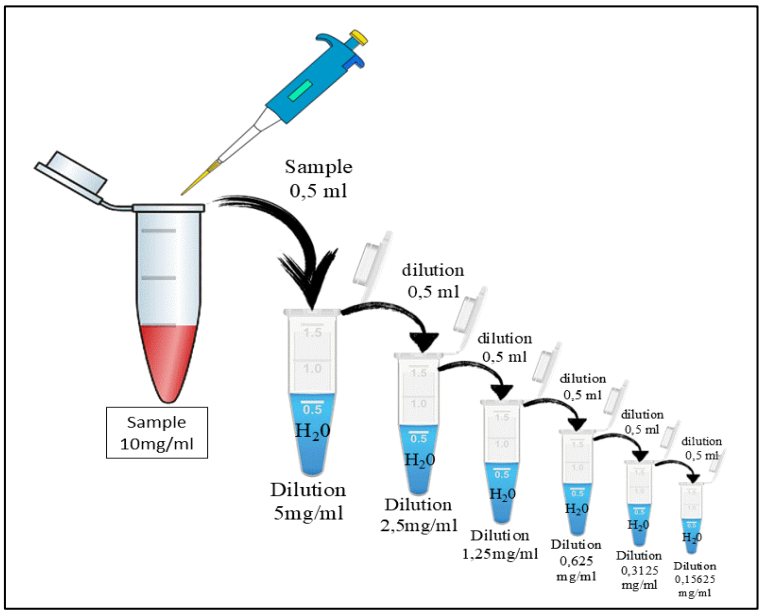

Figure 8: Dilutions preparation of *Pleurotus ostreatus* mushroom extract.

2.2.3.2. Antioxidant Activity

Antioxidant activity refers to the ability of a compound, extract, or natural product to prevent or delay oxidative damage caused by reactive oxygen and nitrogen species (ROS/RNS). Antioxidants achieve this by neutralizing free radicals, donating electrons or hydrogen atoms, or chelating metal ions that catalyze radical formation. Evaluating antioxidant activity is essential for understanding the potential health benefits of natural products and their protective effects against oxidative stress (**Flora 2009; López-Alarcón & Denicola, 2013; Pisoschi & Pop, 2015**).

Antioxidant activity in this study were performed in Research Center in Biotechnology (CRBT, Constantine, Algeria) in laboratory of biochemistry adjusting all assays to 96 well plate use. The arrangement of the assays in the microplate was carried out according to the scheme presented in Figure 9.

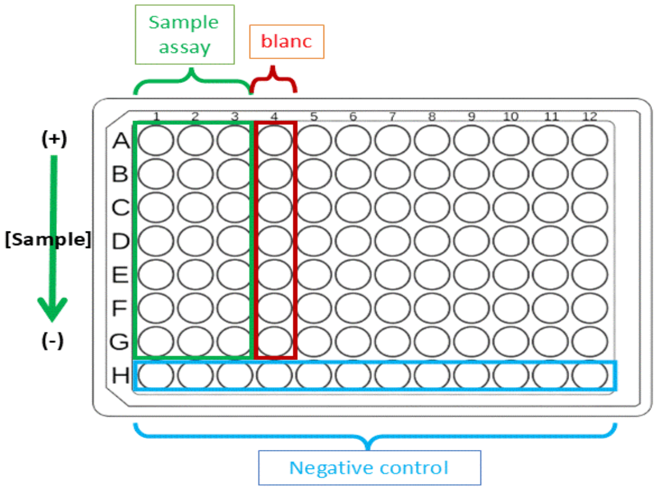

Figure 9: antioxidant assays arrangement in 96 well microplate

2.2.3.2.1. Scavenging Assays

Scavenging activity reflects the ability of a sample to neutralize free radicals or reactive oxygen/nitrogen species (ROS/RNS). It is based on the capacity of antioxidants to donate electrons or hydrogen atoms, stabilizing unstable radicals and preventing oxidative chain reactions. When exposed to a radical (e.g., DPPH, ABTS, hydroxyl, superoxide, or nitric oxide), the antioxidants reduce or quench it, leading to a measurable decrease in absorbance or fluorescence (**Sánchez-Moreno, 2002**). The scavenging activity is typically expressed either in µg/ml as the IC_{50}, representing the concentration of sample required to neutralize 50% of the radicals, or as a percentage of radical inhibition relative to a control, calculated using the equation (1); and in µM TE/g DW as an antioxidant capacity representing how many moles of Troloxgive the same antioxidant activity as 1gram of dried mushroom sample calculated using equation (2).

$$\textbf{Scavenging activity}\ (\%) = [1 - \frac{(\boldsymbol{As} - \boldsymbol{Asb})}{\boldsymbol{Anc}}] \times 100 \quad \ldots\ldots\ldots\ldots\ldots\ldots\ldots\ldots\ldots(1)$$

As: absorbance of samples (extract or standard)
Asb: absorbance of samples blank (reaction with methanol replace color changing reagent)
Anc: absorbance of negative control (reaction with methanol replacing sample)

$$\boldsymbol{TEAC} = \left[\left(\frac{\boldsymbol{IC50T}}{\boldsymbol{IC50S}}\right) \times 1000\right] \times \boldsymbol{EY} \times \left(\frac{1000}{\boldsymbol{MwT}}\right) \quad \ldots\ldots\ldots\ldots\ldots\ldots\ldots\ldots\ldots\ldots\ldots(2)$$

TEAC: Trolox equivalent antioxidant capacity
$IC_{50}T$: inhibition concentration of Trolox at 50% rate (mg/ml)
$IC_{50}S$: inhibition concentration of sample at 50% rate (mg/ml)
EY: extraction yield (g/g)
MwT: molecular weight of Trolox (250,29 g/mol)

a. DPPH Radical Scavenging Assay

The DPPH (2,2-diphenyl-1-picrylhydrazyl) assay is based on the ability of antioxidants to donate hydrogen atoms or electrons to neutralize the DPPH radical. DPPH is a stable free radical that has a deep purple color and shows a strong absorbance at 517 nm. When an antioxidant is present, it reduces the DPPH radical to its non-radical form, causing a color change from purple to yellow. The decrease in absorbance is directly proportional to the scavenging activity of the tested sample, which can be quantified as a percentage of radical inhibition relative to a control (**Kedare & Singh, 2011**).

The assay was adapted from the method of **Blois (1958**) for microplate use (Figure 10). In each well, 160 µL of DPPH solution (6 mg DPPH dissolved in 100 mL methanol) was mixed with 40 µL of extract dilution or standard (Gallic acid, Ascorbic acid, BHA, BHT, Quercetin and Trolox). The mixture was incubated in the dark for 30 minutes, and absorbance was then measured at 517 nm.

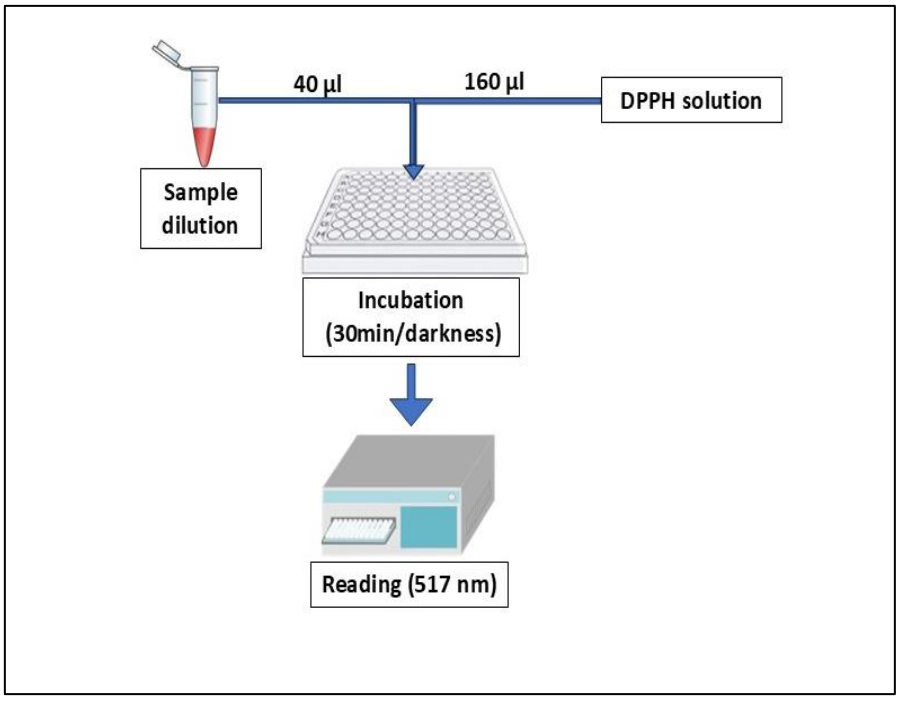

Figure 10: Protocol for Antioxidant Activity determination Using DPPH Radical Scavenging Assay

b. ABTS Radical Scavenging Assay

The ABTS (2,2'-azino-bis(3-ethylbenzothiazoline-6-sulfonic acid)) assay is based on the ability of antioxidants to quench the ABTS radical cation ($ABTS^{+}\bullet$) by donating electrons or hydrogen atoms. $ABTS^{+}\bullet$ is a blue-green colored radical that absorbs strongly at 734 nm. When an antioxidant is added, it reduces $ABTS^{+}\bullet$ to its colorless or less colored form, leading to a decrease in absorbance. The extent of this decrease is proportional to the antioxidant (scavenging) activity of the sample and can be expressed as a percentage inhibition relative to a control (**Ilyasov *et al.*, 2020**).

The ABTS radical scavenging assay was performed following the method of **Re *et al.* (1999)**, with modifications adapted for microplate use (Figure 11). A phosphate-buffered saline (PBS, pH 7.4) solution was prepared by dissolving 8 g NaCl (137 mM), 1.44 g Na_2HPO_4 (10 mM), and 0.24 g NaH_2PO_4 (1.8 mM) in distilled water, and adjusting the final volume to 1 L. The ABTS radical cation ($ABTS^{+}\bullet$) was generated by mixing equal volumes of 7 mM ABTS solution (36.02 mg ABTS dissolved in 10 mL PBS) and 2.45 mM potassium persulfate solution (6.62 mg $K_2S_2O_8$ in 10 mL PBS). The mixture was incubated in the dark for 16 h at room temperature to allow complete radical formation. For the assay, 160 µL of the $ABTS^{+}\bullet$ solution was mixed with 40 µL of the sample extract in each well, followed by incubation in darkness for 10 min. The decrease in absorbance was measured at 734 nm using a microplate reader. The standard used as positive control in this assay are: gallic acid, ascorbic acid, BHA, BHT, catechin, quecetin, and Trolox.

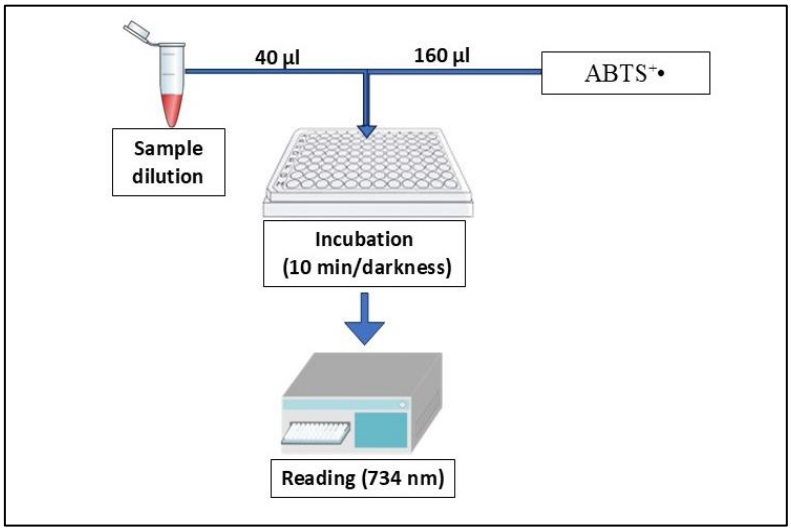

Figure 11: Protocol for Antioxidant Activity Determination Using ABTS Radical Cation Assay

c. Hydroxyl Radical Scavenging assay

The hydroxyl radical scavenging assay measures a sample's capacity to neutralize highly reactive hydroxyl radicals (•OH), which can cause damage to biomolecules such as DNA, proteins, and lipids. These radicals are commonly generated in situ through reactions like the Fenton reaction ($Fe^{2+} + H_2O_2 \rightarrow Fe^{3+} + \bullet OH + OH^-$). Antioxidants in the sample interact with the hydroxyl radicals, preventing them from reacting with a detector molecule (e.g., deoxyribose or salicylic acid). The extent of protection is determined spectrophotometrically, and the scavenging activity is expressed as the percentage of inhibition compared to a control (**Sanna & Fadda, 2022**).

Hydroxyl radical scavenging activity was determined following a modified protocol of **Smirnoff and Cumbes (1989)**. Briefly, 40 µL of sample was mixed with 24 µL of 8 mM ferrous sulfate solution (prepared by dissolving 22.24 mg $FeSO_4 \cdot 7H_2O$ in 10 mL distilled water), 20 µL of 20 mM hydrogen peroxide solution (prepared by diluting 30 µL H_2O_2 to 20 mL with distilled water), and 80 µL of 3 mM salicylic acid solution (prepared by dissolving 4 mg salicylic acid in 10 mL distilled water). The reaction mixture was incubated at 37 °C for 30 min, after which 36 µL of distilled water was added. Absorbance was then measured at 510 nm (Figure 12). Ascorbic acid, BHA and Trolox were used as standard.

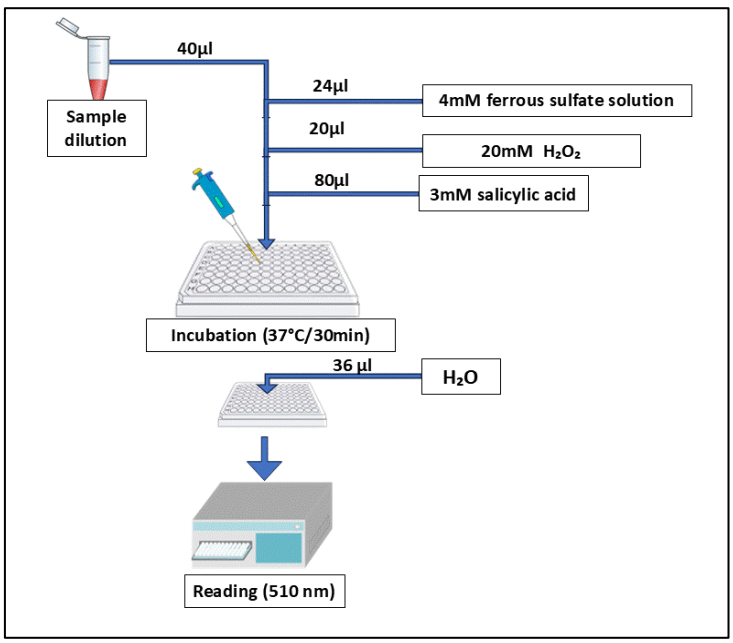

Figure 12: Protocol for Antioxidant Activity Determination Using Hydroxyl Radical Scavenging Assay

2.2.3.2.2. Reducing Power

Reducing power reflects the ability of a sample to donate electrons to reduce oxidized intermediates, which is an important mechanism of antioxidant activity. In this assay, antioxidants in the sample transfer electrons to an oxidized species (X^{+n}), leading to its conversion into a more stable, reduced form ($X^{+(n-1)}$). The reduction process is accompanied by a measurable change in color or absorbance, which is proportional to the electron-donating capacity of the sample. A higher absorbance corresponds to greater reducing (antioxidant) activity, reflecting the sample's overall potential to terminate free radical chain reactions (**Munteanu & Apetrei, 2021**). The activity is often quantified as $\mathbf{EC_{50}}$, which represents the concentration of the sample required to achieve 50% reduction, and the percentage of reducing power is calculated using the following formula:

$$\textbf{Reducing power}\ (\%) = \left[\frac{(\boldsymbol{As-Asb})}{\boldsymbol{Anc}} - \mathbf{1}\right] \times \mathbf{100} \quad \ldots\ldots\ldots\ldots\ldots\ldots\ldots\ldots(1)$$

As: absorbance of samples (extract or standard)
Asb: absorbance of samples blank (reaction with methanol replace color changing reagent)
Anc: absorbance of negative control (reaction with methanol replacing sample)

$$\boldsymbol{TEAC} = \left[\left(\frac{\boldsymbol{IC}50\boldsymbol{T}}{\boldsymbol{IC}50\boldsymbol{S}}\right) \times 1000\right] \times \boldsymbol{EY} \times \left(\frac{1000}{\boldsymbol{MwT}}\right) \quad \ldots\ldots\ldots\ldots\ldots\ldots\ldots\ldots(2)$$

TEAC: Trolox equivalent antioxidant capacity
$IC_{50}T$: inhibition concentration of Trolox at 50% rate (mg/ml)
$IC_{50}S$: inhibition concentration of sample at 50% rate (mg/ml)
EY: extraction yield (g/g)
MwT: molecular weight of Trolox (250,29 g/mol)

a. Ferric Reducing Antioxidant Power (FRAP) Assay

FRAP (ferric reducing antioxidant power) assay using the potassium ferricyanide method measures the reducing (electron-donating) ability of a sample. Initially, the reaction mixture is light yellow due to ferric ions (Fe^{3+}). Antioxidants in the sample reduce Fe^{3+} in potassium ferricyanide to ferrous ions (Fe^{2+}), which then react with ferric chloride to form a blue-colored Prussian blue complex (**Munteanu & Apetrei 2021**). The change in color intensity, measured spectrophotometrically, is directly proportional to the sample's reducing power and overall antioxidant capacity.

A modified protocol of **Oyaizu (1986)** was used to determine ferric reducing antioxidant power for samples. As indicated in Figure 13, sample extracts (10 µL) were mixed in a well plate with 40 µL of 0.2 M phosphate buffer (pH 6.6), prepared by

dissolving 22.1 g $NaH_2PO_4 \cdot H_2O$ and 5.7 g $Na_2HPO_4 \cdot 2H_2O$ in 800 mL distilled water and adjusting the pH to 6.6 with HCl, then bringing the final volume to 1 L with distilled water. To this mixture, 50 µL of 1% (w/v) potassium ferricyanide (100ml mixture of 1g $[K_3Fe(CN)_6]$ and distilled water) was added, followed by incubation at 50°C for 20 min. After incubation, 50 µL of 10% trichloroacetic acid (1g TCA in 10 ml distilled water) was added, along with 40 µL of distilled water and 10 µL of 0.1% ferric chloride (0.1 g $FeCl_3$ dissolved in distilled water up to 100 ml). The resulting solution's absorbance was measured at 700 nm to evaluate the sample's reducing capacity. The positive control replaced the sample with standards dilution of Gallic and Ascorbic acid, BHA, BHT, Catechin, Quercetin and Trolox.

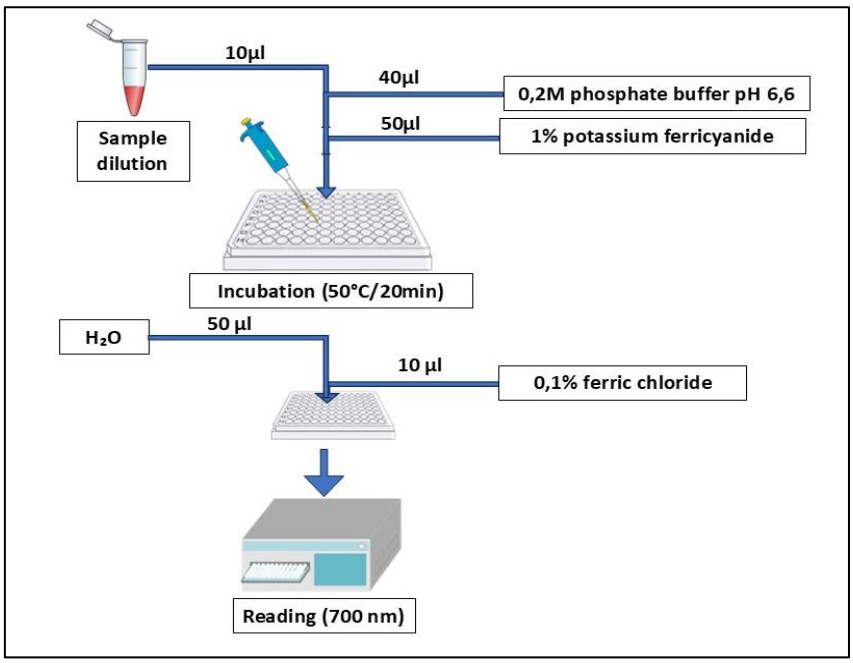

Figure 13: Protocol for Antioxidant Activity Determination Using Ferric Reducing Antioxidant Power (FRAP) Assay

b. Cupric Ion Reducing Antioxidant Capacity (CUPRAC) Assay

CUPRAC (cupric reducing antioxidant capacity) assay measures the reducing ability of a sample through its electron-donating potential. Initially, the reaction mixture is colorless, containing cupric ions (Cu^{2+}) complexed with neocuproine. Antioxidants in the sample reduce Cu^{2+} to cuprous ions (Cu^{+}), forming a yellow-orange colored Cu^{+}–neocuproine complex (**Apak *et al.*, 2008**). The intensity of this color change, measured spectrophotometrically, is directly proportional to the sample's reducing power and overall antioxidant capacity.

The Cupric reducing antioxidant capacity assay was modified from **Apak *et al.* (2004)** to microplate use. Three solutions were prepared: Solution S1 was obtained by dissolving 1.927g ammonium acetate ($ACNH_4$) in 25 mL distilled water to yield a transparent solution at pH 7.0. Solution S2 was prepared by dissolving 0.039 g neocuproine in 25 mL methanol. Solution S3, a blue solution, was prepared by dissolving 0.042625 g $CuCl_3 \cdot 2H_2O$ in 25 mL distilled water (source of Cu^2 ions). The assay was performed by mixing 40 µL of the sample with 60 µL of S1, 50 µL of S2, and 50 µL of S3. The mixture was incubated at room temperature for 1 hour, and absorbance was measured at 450 nm (Figure 14). The standards used for this assay are dilutions of BHA, BHT, Catechin, and Trolox.

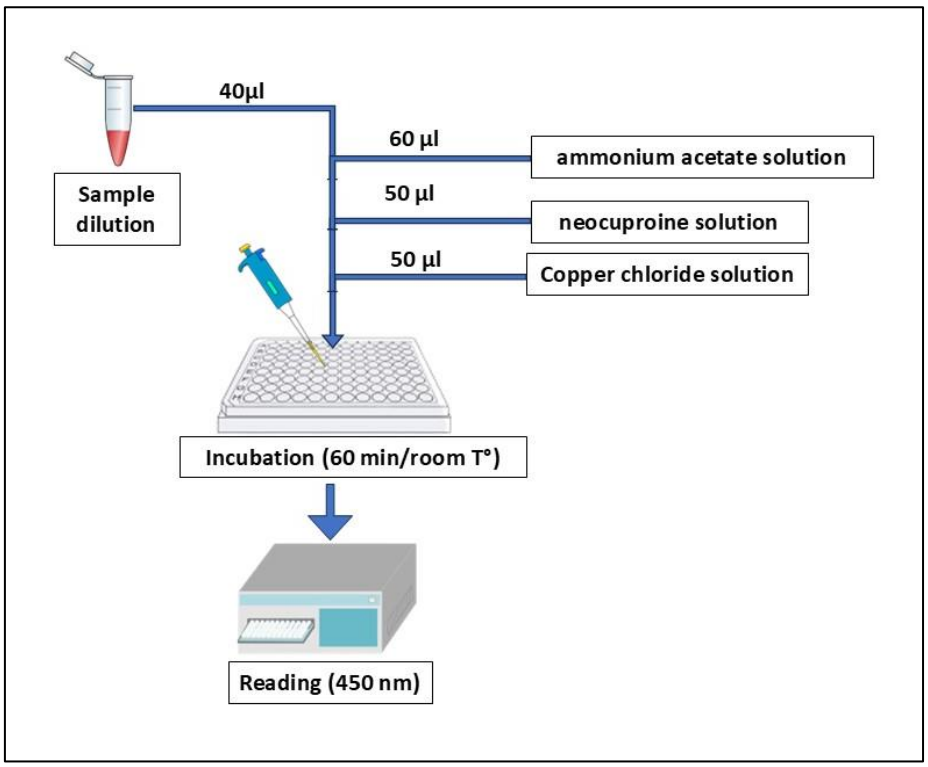

Figure 14: Protocol for Antioxidant Activity Determination Using Cupric Ion Reducing Antioxidant Capacity (CUPRAC) Assay

c. Total Antioxidant Capacity (TAC) Assay

The total antioxidant capacity (TAC) of the extracts was assessed using the phosphomolybdate method, which relies on the reduction of molybdenum (VI) [Mo(VI)] to molybdenum (V) [Mo(V)] by antioxidants under strongly acidic conditions. In this assay, ammonium molybdate serves as the source of Mo(VI), which

is reduced by the antioxidants present in the sample. The reduced Mo(V) subsequently forms a stable green phosphate–Mo(V) complex in the presence of sodium phosphate, which supplies the phosphate ions necessary for complex formation. The reaction takes place in an acidic medium maintained by sulfuric acid, which ensures proper reduction and stabilization of the chromogenic complex. The resulting green coloration, measured spectrophotometrically at 695 nm, is directly proportional to the electron-donating capacity of the antioxidants, reflecting the overall antioxidant potential of the sample (**Prieto *et al.*, 1999**).

Prieto *et al.* (1999) modified assay of total antioxidant capacity using phosphomolydate was conducted as indicated in Figure 15, by mixing in Eppendorf tube, 0.1 ml of sample with 1ml of an equal-volume reagent solution composed of 28 mM sodium phosphate (prepared by dissolving 0.7949 g Na_2HPO_4 or 0.67188 g NaH_2PO_4 in 200 mL distilled water), 4 mM ammonium molybdate (0.9311 g in 200 mL distilled water), and 0.6 M sulfuric acid (6.7 mL concentrated H_2SO_4 diluted to 200 mL with distilled water). The reaction mixtures were incubated at 95 °C in a water bath for 90 min. After incubation, 200 µL of each mixture was transferred to a 96-well microplate, and absorbance was measured at 695 nm. several standards used as positive control in this study (Gallic and Ascorbic acids, BHA, BHT, Catechin, Quercetin and Trolox).

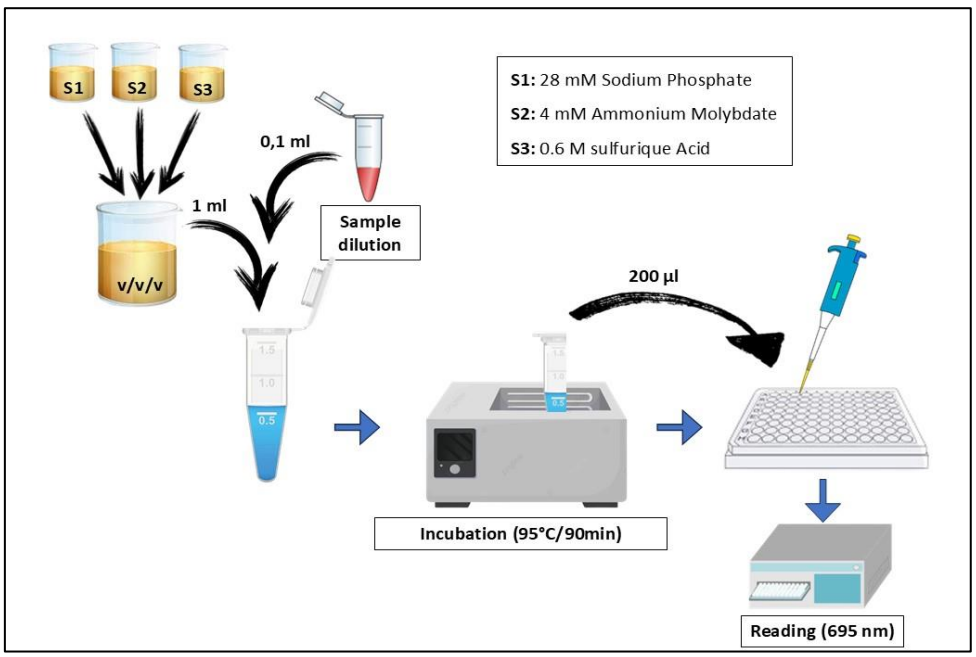

Figure 15: Protocol for Antioxidant Activity Determination Using Total Antioxidant Capacity (TAC) Assay

2.2.3.2.3. Chelating Ability

Metal chelating ability represents the potential of a sample to bind transition metal ions, thereby inhibiting their participation in redox reactions that generate reactive oxygen species. In the assays, metal ions in the reaction medium can form colored complexes with a chromogenic indicator. The presence of chelating compounds in the sample competes with the indicator for the metal ions, leading to a reduction in the intensity of the colored complex (**Gulcin & Alwasel, 2022**). The extent of this decrease, measured spectrophotometrically, provides a quantitative estimate of the sample's metal-chelating capacity and is typically expressed as a percentage of inhibition relative to a control using the following equation:

$$\boldsymbol{Chelating\ ability}(\%) = \left[1 - \frac{(\boldsymbol{As - Asb})}{\boldsymbol{Anc}}\right] \times 100 \ldots\ldots\ldots\ldots\ldots\ldots\ldots\ldots\ldots\ldots\ldots\ldots\ldots\ldots(1)$$

As: absorbance of samples (extract or standard)
Asb: absorbance of samples blank (reaction with methanol replace color changing reagent)
Anc: absorbance of negative control (reaction with methanol replacing sample)

$$\boldsymbol{EDTAEAC} = \left[\left(\frac{\boldsymbol{IC50EDTA}}{\boldsymbol{IC50S}}\right) \times 1000\right] \times \boldsymbol{EY} \times \left(\frac{1000}{\boldsymbol{MwEDTA}}\right) \quad \ldots\ldots\ldots\ldots\ldots\ldots\ldots\ldots\ldots\ldots\ldots(2)$$

TEAC: Trolox equivalent antioxidant capacity
IC_{50}EDTA: inhibition concentration of Trolox at 50% rate (mg/ml)
IC_{50}S: inhibition concentration of sample at 50% rate (mg/ml)
EY: extraction yield (g/g)
MwEDTA: molecular weight of Trolox (372,24 g/mol)

EDTA-Na_2 standard is used as positive control for chelating assay.

a. Ferrous Ion Chelating (FIC) Assay

Ferrous ion chelating (FIC) assay evaluates the ability of a sample to bind ferrous ions (Fe^{2+}) and prevent their interaction with a chromogenic reagent. In this method, ferrous ions initially form a purple/red-colored complex with ferrozine. When chelating agents are present in the sample, they compete with ferrozine for binding to Fe^{2+}, reducing the formation of the colored complex. The resulting decrease in color intensity, measured spectrophotometrically, is proportional to the sample's metal-chelating capacity and is typically expressed as a percentage inhibition relative to a control (**Butt *et al.*, 2014**).

The assay was performed following the method of **Decker & Welch (1990**), modified for 96-well microplate use (Figure 16). In each well, 40 µL of methanol was mixed with 40 µL of the sample, followed by 40 µL of 0.2 mM Fe^{2+} solution (prepared

by dissolving 4 mg $FeCl_3 \cdot 2H_2O$ in 100 mL distilled water) and 80 µL of 0.5 mM ferrozine solution (2.5 mg ferrozine dissolved in 10 mL distilled water). The mixture was incubated at room temperature for 10 min, and absorbance was measured at 562nm.

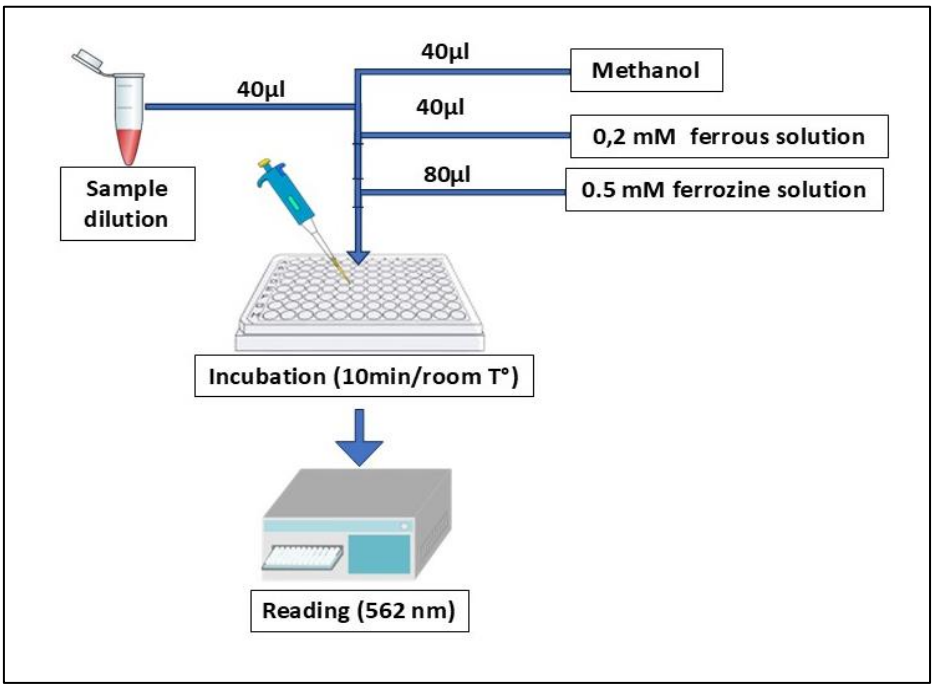

Figure 16: Protocol for Antioxidant Activity Determination Using Ferrous Ion Chelating (FIC) Assay

b. Copper Chelating Activity (CCA) Assay

The copper chelating activity (CCA) assay evaluates the ability of a sample to bind cupric ions (Cu^{2+}), thereby preventing their participation in redox reactions that generate reactive oxygen species. In this assay, Cu^{2+} ions initially form a blue-colored complex with the chromogenic indicator pyrocatechol violet (PV). When chelating compounds are present in the sample, they compete with PV for Cu^{2+} binding, reducing the formation of the PV–Cu^{2+} complex. (**Yadav & Zelder, 2021**). The resulting decrease in absorbance, measured spectrophotometrically, is proportional to the sample's copper-chelating capacity and is expressed as a percentage of inhibition relative to a control.

The CCA assay was performed following a modified protocol based on **Sánchez-Vioque *et al*. (2013)**. In each well, 40 µL of the sample was mixed with 140 µL of 50 mM sodium acetate buffer (pH 6.0) and 10 µL of 5 mM [$CuSO_4 \cdot 5H_2O$] solution (12.5 mg dissolved in 10 mL buffer). The mixture was incubated for 30 min at

room temperature, followed by the addition of 10 µL of 4 mM pyrocatechol violet (PV) solution (15.4 mg dissolved in 10 mL buffer). After a further 30 min incubation, the absorbance was measured at 632 nm (Figure 17).

The sodium acetate buffer was prepared by mixing 5.22 mL of a solution containing 1.148 mL of acetic acid complete with distilled water to 200 mL with 94.78 mL of a solution prepared by dissolving 1.64 g of sodium acetate in 200 mL of distilled water.

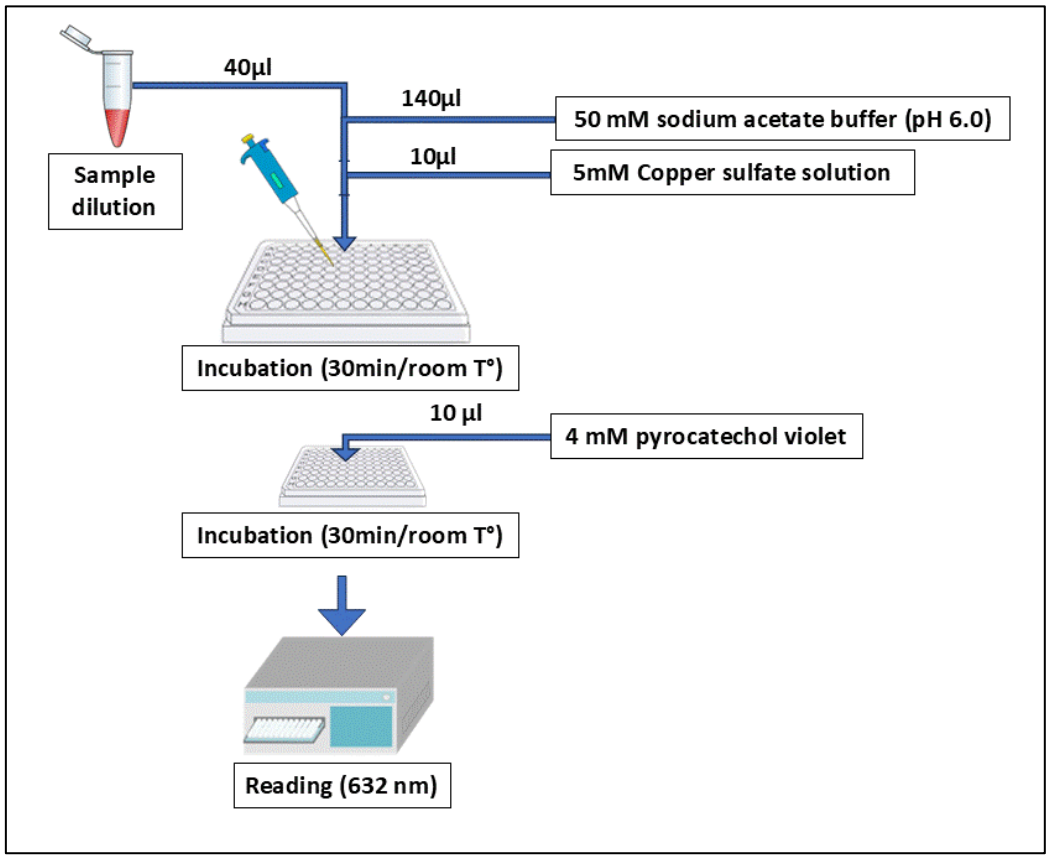

Figure 17: Protocol for Antioxidant Activity Determination Using the Copper Chelating Activity (CCA) Assay

2.2.3.3. Anti-Inflammatory Activity

Inflammation is a physiological response to injury, infection, or chemical stimuli, but chronic or excessive inflammation can lead to various diseases, including arthritis, cardiovascular disorders, and neurodegenerative conditions. Evaluating the anti-inflammatory potential of natural products or synthetic compounds is important for identifying agents that can modulate inflammatory responses, inhibit protein denaturation, and prevent tissue damage, thereby contributing to therapeutic development (**Gaikwad *et al.*, 2025**).

The BSA (bovine serum albumin) assay is based on the ability of a sample to inhibit heat-induced protein denaturation, a process that mimics inflammatory protein damage. Under stress (e.g., elevated temperature), BSA denatures, leading to structural changes that increase turbidity or alter absorbance. When a sample with anti-inflammatory properties is added, it stabilizes the protein structure and prevents denaturation, resulting in a measurable reduction in turbidity or absorbance (**Drăgan *et al.*, 2016**). The percentage inhibition of protein denaturation reflects the sample's anti-inflammatory activity and is calculated relative to a control.

The assay was carried out according to **Kandikattu *et al.* (2013**) with some modifications to adapt it for microplate use. Each well was filled with 100 µL of sample and 0.6% BSA prepared in Tris-HCl buffer (0.6072 g Tris dissolved in 100 mL of water, adjusted to pH 6.6 with HCl). The plate was incubated at 37 °C for 15 min and then placed in a 72 °C water bath for 5 min. After cooling, absorbance was measured at 660 nm using a microplate reader (Figure 18).

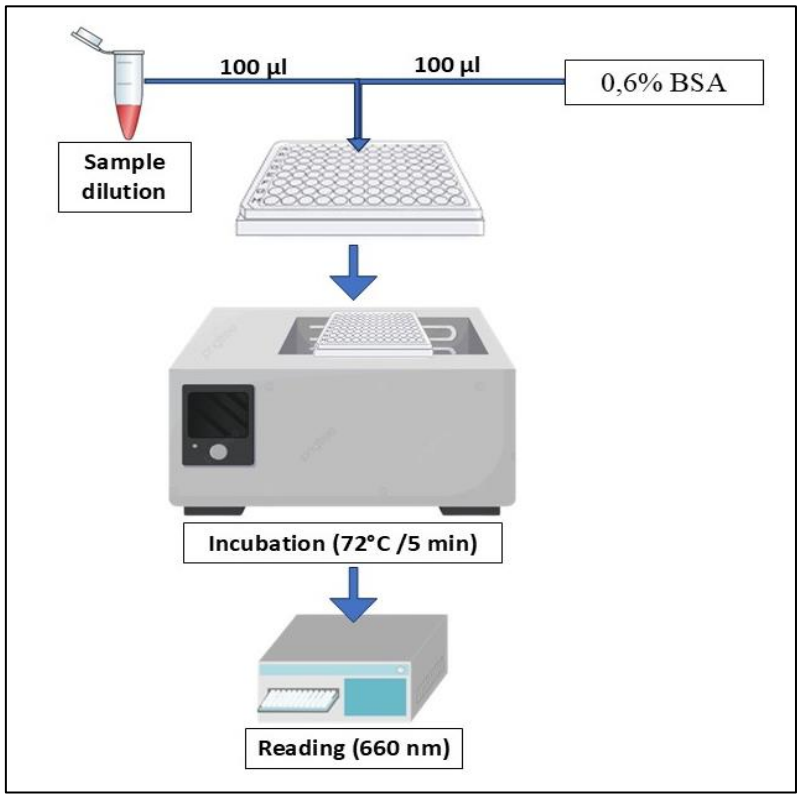

Figure 18: Protocol for Anti-Inflammatory Activity Determination Using the Protein Denaturation Inhibition Assay

The distribution of the assay in the microplate, was as the same as antoxidant activity in Figure 9, the sample blank consisted of 0.1 mL sample mixed with 0.1 mL Tris-HCl (replacing the BSA solution). The negative control consisted of 0.1 mL BSA solution mixed with 0.1 mL distilled water, ensuring complete BSA denaturation in the absence of inhibitors. Diclofenac was used as the standard, prepared in 24 successive two-fold (1:2) dilutions starting from 25 mg/ml. The inhibition of protein denaturation, reflecting anti-inflammatory potential, was calculated as follows:

$$\textbf{Enzyme inhibition}\ (\%) = [1 - \frac{(\boldsymbol{As - Asb})}{\boldsymbol{Anc}}] \times 100$$

A_s = Absorbance of the reaction with enzyme + test sample
$\mathbf{A_{sb}}$ = Absorbance of the sample blank (corrects for color/turbidity of extract).
$\mathbf{A_{nc}}$ = Absorbance of the negative control (represents 100% enzyme activity).

2.2.3.4. Enzyme Inhibition Activity

The enzyme inhibition activity assays, as the antioxidant activity determinations, were carried out in the Laboratory of Biochemistry at the Research Center in Biotechnology (CRBT), Constantine, Algeria.

2.2.3.4.1. Tyrosinase Inhibition Assay

Tyrosinase is a key enzyme in the biosynthesis of melanin, catalyzing the oxidation of tyrosine to DOPA and subsequently to dopaquinone. Overactivity of tyrosinase can lead to hyperpigmentation disorders, age spots, and uneven skin tone, while excessive melanin formation is associated with certain dermatological conditions. Evaluating tyrosinase inhibitory activity of natural or synthetic compounds is therefore important for identifying potential skin-whitening, depigmenting, or anti-hyperpigmentation agents in cosmetic and pharmaceutical applications (**Pillaiyar *et al.*, 2017**).

The tyrosinase inhibition assay evaluates the ability of a sample to inhibit the enzymatic oxidation of L-tyrosine (or L-DOPA) by tyrosinase. Initially, the reaction mixture is colorless or pale yellow. In the absence of inhibitors, tyrosinase catalyzes the conversion of L-tyrosine to DOPA and subsequently to dopaquinone, which polymerizes to form a dark-colored product. When an inhibitor is present, the formation of this colored product is reduced, resulting in less intense color development. The degree of tyrosinase inhibition is quantified by measuring the change in absorbance relative to a control. (**Chang, 2009; He *et al.*, 2022**)

Tyrosinase was extracted from fresh fruiting bodies of *Agaricus bisporus* as mentioned in **Zaidi *et al.* (2014)** mith modification (Figure 19). Briefly, 100 g of chilled, sliced mushrooms were homogenized in 120 mL of ice-cold phosphate-buffered saline (PBS, pH 7.0) using a pre-cooled blender for 30 seconds. The homogenate was stirred on ice for 30 minutes to facilitate enzyme release, followed by filtration through double-layered cheesecloth. The filtrate was centrifuged at 18 000 × g for 30 min at 4 °C, and the resulting supernatant was collected as the crude tyrosinase extract. This preparation was immediately used for enzymatic assays.

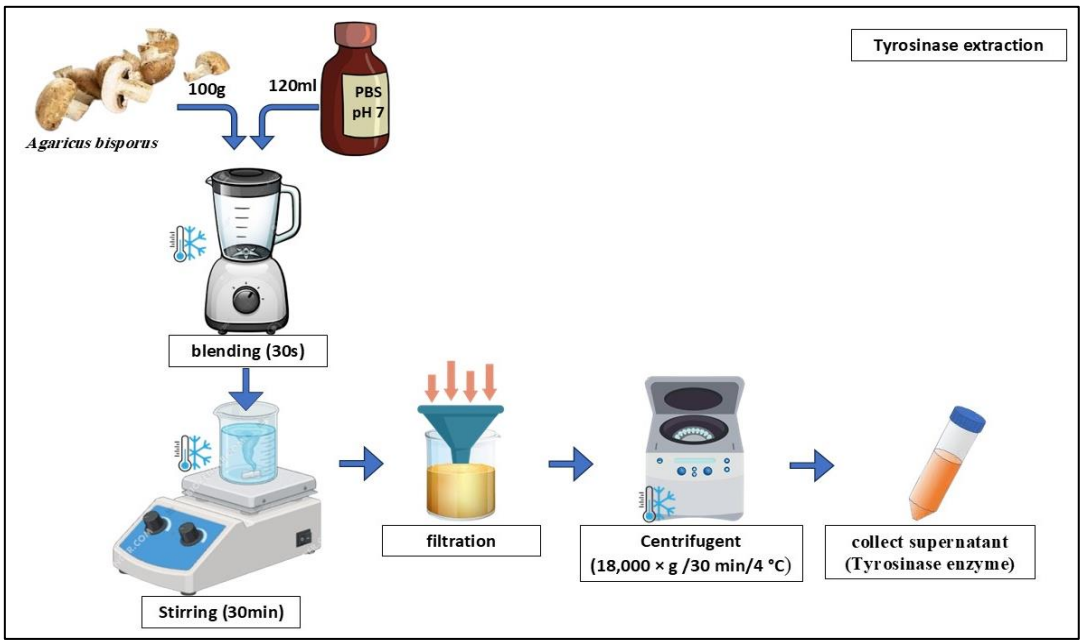

Figure 19: Protocol of tyrosinase enzyme extraction from *Agaricus bisporus* mushroom

Mesuring the enzyme inhibition was practiced according to a modified protocol of **Deveci *et al.* (2018)**, 150 µL of PBS (pH 6.8), 10 µL of the sample (or Kojic acid for positive control), and 20 µL of tyrosinase enzyme solution were added to each well of a microplate. The mixture was incubated at 37 °C for 10 min, followed by the addition of 20 µL of 5 mM L-DOPA. After a second incubation at 37 °C for 10 min, absorbance was measured at 475 nm using a microplate reader (Figure 20). The standard used fir this assay was kojic acid. The percentage of enzyme inhibition was determined using the following equation: $\textbf{tyrosinase inhibition}\ (\%) = [1 - \frac{(As - Asb)}{Anc}] \times 100$

A_s = Absorbance of the reaction with enzyme + test sample
$\mathbf{A_{sb}}$ = Absorbance of the sample blank (corrects for color/turbidity of extract).
$\mathbf{A_{nc}}$ = Absorbance of the negative control (represents 100% enzyme activity).

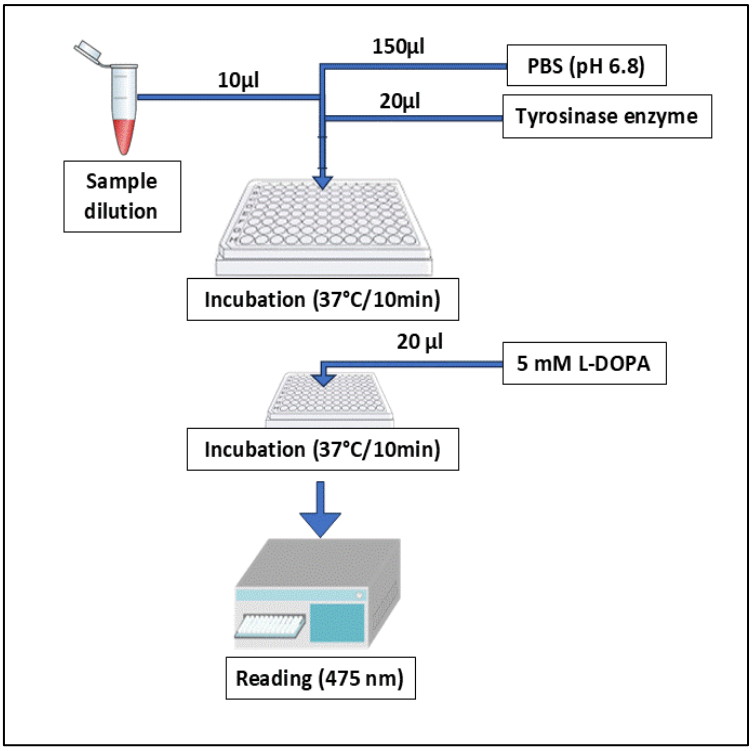

Figure 20: Protocol for anti-pigmentation activity Using Tyrosinase Inhibition Assay

2.2.3.4.2. Urease Inhibition Assay

Urease is an enzyme that catalyzes the hydrolysis of urea into ammonia and carbon dioxide. Overactivity of urease is associated with several medical and agricultural problems, including peptic ulcers, urinary tract infections, and soil nitrogen loss. Evaluating urease inhibitory activity of compounds is important for identifying potential therapeutic agents to control urease-related infections and disorders, as well as for developing strategies to reduce nitrogen loss in agriculture (**Kissel *et al.*, 1988; Follmer, 2010**).

This assay assesses the capacity of a sample to inhibit the urease-catalyzed hydrolysis of urea. The reaction mixture, initially pale yellow due to the presence of urea, phenol, and alkaline reagents, undergoes a color change in the absence of inhibitors. Urease activity generates ammonia, which reacts with the phenol and alkaline reagents, including sodium nitroprusside, producing a blue indophenol complex. Samples with urease inhibitory properties reduce ammonia formation, thereby limiting the development of the blue color. The intensity of the blue coloration, measured spectrophotometrically, correlates with enzyme activity, and the percentage inhibition is calculated relative to a control (**Mahernia *et al.*, 2015**).

Urease inhibitory activity was assessed following the method of **Weatherburn (1967)**, with modifications for microplate application as in Figure 21. In each well, 10 µL of test sample (or Thiourea as positive control) was combined with 25 µL of urease solution (1 mg/mL in buffer, pH 7) and 50 µL of urea substrate (0.2553 g urea dissolved in 25 mL buffer, pH 8.2). Subsequently, 45 µL of phenol reagent [2 g phenol in 25 mL distilled water mixed with 25 mg sodium nitroprusside ($Na_2[Fe(CN)_5NO]\cdot 2H_2O$) in 25 mL distilled water] and 70 µL of alkaline reagent (0.7125 g NaOH in 25 mL distilled water mixed with 1.175 mL NaOCl in 25 mL distilled water) were added. The reaction mixtures were incubated at 30 °C for 50 min, after which the absorbance was recorded at 630 nm using a microplate reader. The inhibtion equation is as following:

$$\textbf{Urease inhibition}\ (\%) = [1 - \frac{(\boldsymbol{As} - \boldsymbol{Asb})}{\boldsymbol{Anc}}] \times 100$$

A_s = Absorbance of the reaction with enzyme + test sample
$\mathbf{A_{sb}}$ = Absorbance of the sample blank (corrects for color/turbidity of extract).
$\mathbf{A_{nc}}$ = Absorbance of the negative control (represents 100% enzyme activity).

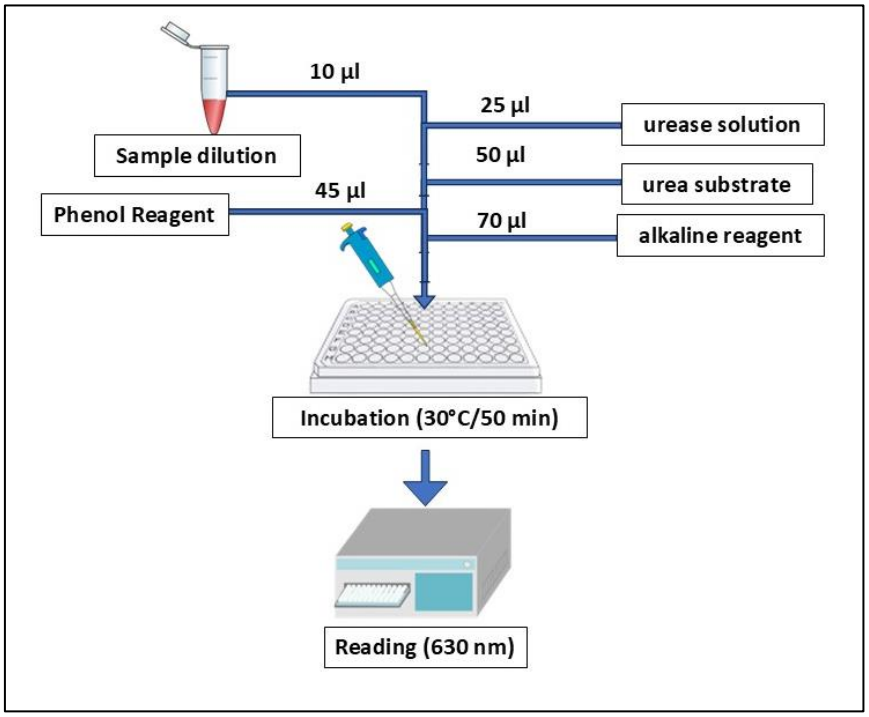

Figure 21: Protocol for anti-ulcer Activity Determination Using Urease Inhibition Assay

2.2.3.4.3. α amylase Inhibition Assay

α-Amylase is a key digestive enzyme that hydrolyzes starch into maltose and glucose. Overactivity of α-amylase can lead to rapid postprandial increases in blood glucose, contributing to hyperglycemia and type 2 diabetes (**Souza, 2010**). Evaluating the α-amylase inhibitory potential of natural or synthetic compounds is therefore important for identifying agents that can help manage blood glucose levels and control diabetes.

the reaction mixture containing starch and IKI solution exhibits an orange color, reflecting the formation of a preliminary starch-iodine complex under the assay conditions. In the absence of inhibitors, α-amylase hydrolyzes starch into smaller sugars, which disrupt the complex and lead to a paler color. When a sample contains an α-amylase inhibitor, starch degradation is reduced, and the starch-iodine complex is preserved, resulting in a brown color (**Rendleman Jr, 2003**). The intensity of this brown coloration, measured spectrophotometrically, is proportional to the degree of enzyme inhibition, and the percentage inhibition is calculated relative to a control

The α-amylase inhibition assay was performed in a microplate format based on the procedure described by **Zinjarde *et al*. (2011**) which was loaded as Figure 22, with appropriate modifications as follows: In each well, 25 µL of the sample was mixed with 50 µL of α-amylase solution (1 U). The mixture was incubated at 37 °C for 10 min, followed by the addition of 50 µL of 0.1% starch solution and a further incubation at 37 °C for 10 min. The reaction was then terminated by adding 25 µL of 1 M HCl, after which 100 µL of IKI solution (5 mM KI and 5 mM I_2) was added. The plate was incubated briefly, and absorbance was measured at 630 nm using a microplate reader (Figure 23). Inhibition (%) was determined according to the following equation:

$$\textbf{Enzyme inhibition}\ (\%) = [1 - \frac{(\boldsymbol{As - Asb})}{(\boldsymbol{Ac - Ae})}] \times 100$$

A_c=Absorbance of substrate control correspanding to maximum color intensity of the starch [no enzyme and substrate]
A_e=Absorbance of enzyme control correspanding to 0% inhibition and 100% enzyme activity [no inhibitos]
As=Absorbance of sample
A_{sb}=Absorbance sample blank

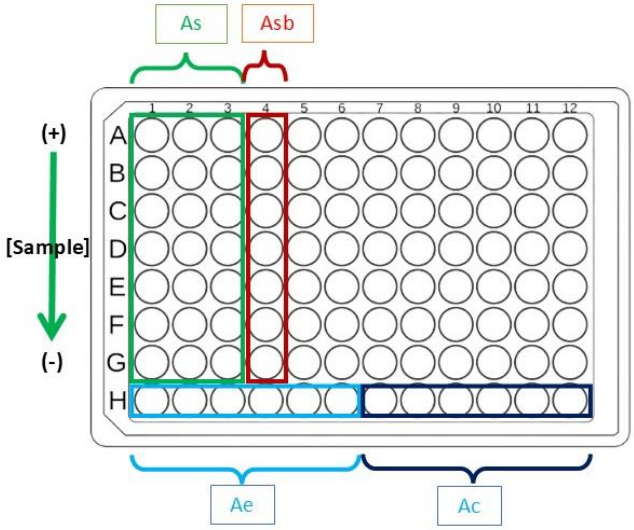

Figure 22: α-amylase assays arrangement in 96 well microplate

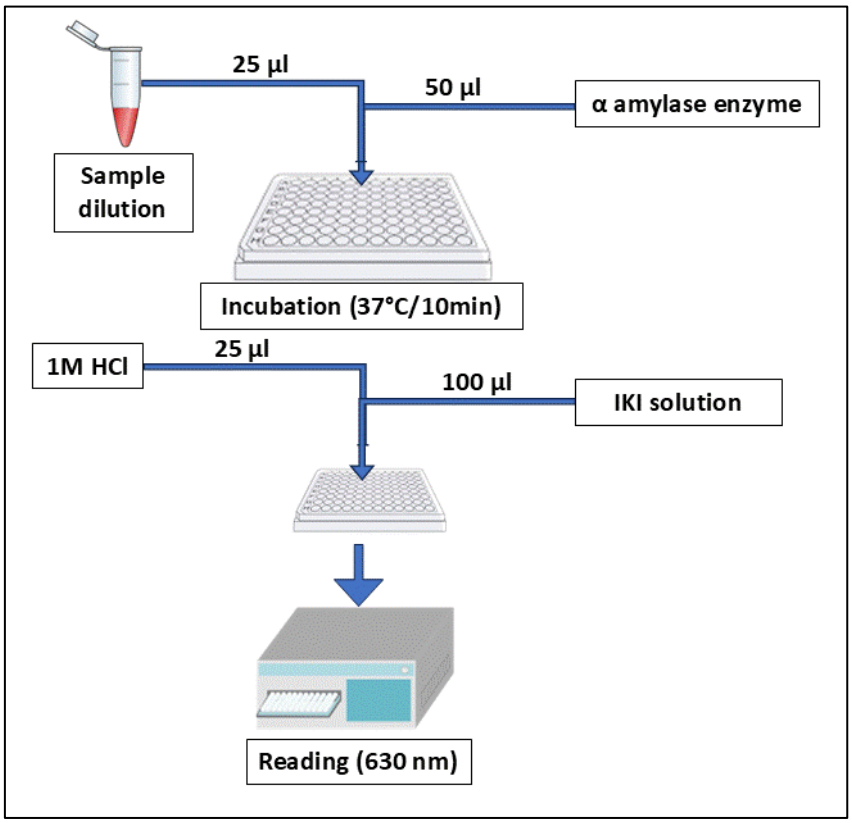

Figure 23: Protocol for anti-diabetic Activity Determination Using α-amylase Inhibition Assay

2.2.3.4.4. Acetyl/Butyrylcholinesterase Inhibition Assay

Acetylcholinesterase (AChE) and butyrylcholinesterase (BChE) are enzymes that hydrolyze the neurotransmitters acetylcholine and butyrylcholine, respectively. Overactivity of these enzymes can reduce neurotransmitter levels, contributing to cognitive decline and neurodegenerative disorders such as Alzheimer's disease. Evaluating the inhibitory potential of natural or synthetic compounds against AChE and BChE is therefore important for identifying potential therapeutic agents that can improve cholinergic signaling and cognitive function (**Greig *et al*., 2005; Caeiro *et al*., 2021**).

These assays are based on the ability of a sample to inhibit enzyme-catalyzed hydrolysis of acetylthiocholine or butyrylthiocholine. Initially, the reaction mixture containing the enzyme, substrate, and chromogenic reagent (such as DTNB, Ellman's reagent) is colorless or pale yellow. In the absence of inhibitors, the enzymes hydrolyze the substrate to release thiocholine, which reacts with DTNB to produce a yellow-colored 5-thio-2-nitrobenzoate anion. When an inhibitor is present, substrate hydrolysis is reduced, diminishing the formation of the yellow color (**Kostelnik & Pohanka, 2018**). The intensity of the yellow coloration, measured spectrophotometrically, is proportional to enzyme activity, and the degree of inhibition is calculated relative to a control.

The inhibitory activities of acetylcholinesterase and butyrylcholinesterase were determined using the method of **Ellman *et al.* (1961**) with mesurement of microplate well volume (Figure 24). A reaction mixture containing 150 µL of 100 mM sodium phosphate buffer (pH 8.0), 10 µL of the sample, and 20 µL of enzyme solution [AChE (5.32×10^{-3} U) or BChE (6.85×10^{-3} U)] was incubated at 25 °C for 15 minutes. Subsequently, 10 µL of 0.5 mM DTNB (prepared by dissolving 16 mg DTNB and 7.5 mg $NaHCO_3$ in 8 mL phosphate buffer, pH 8) and either 10 µL of 0.71 mM acetylthiocholine iodide (16 mg ACI in 8 mL phosphate buffer, pH 8) for AChE, or 10 µL of 0.2 mM butyrylthiocholine chloride (4 mg BCI in 8 mL phosphate buffer, pH 8) for BChE, were added to each reaction well. The mixture was then incubated at room temperature for 15 minutes, and the absorbance was measured at 412 nm. The activity is measured as the following equation:

$$\textbf{inhibition}\ (\%) = [1 - \frac{(\boldsymbol{As} - \boldsymbol{Asb})}{\boldsymbol{Anc}}] \times 100$$

A_s = Absorbance of the reaction with enzyme + test sample
$\mathbf{A_{sb}}$ = Absorbance of the sample blank (corrects for color/turbidity of extract).
$\mathbf{A_{nc}}$ = Absorbance of the negative control (represents 100% enzyme activity).

The phosphate buffer pH 8.0 is prepared by mixing 5.3ml of NaH_2PO_4 (1.56 g of [NaH_2PO_4, $2H_2O$] in 100 ml of H_2O) and 94.5ml of Na2HPO4 (8.890 g of[Na_2HPO_4, $2H_2O$] in 500 ml of H_2O).

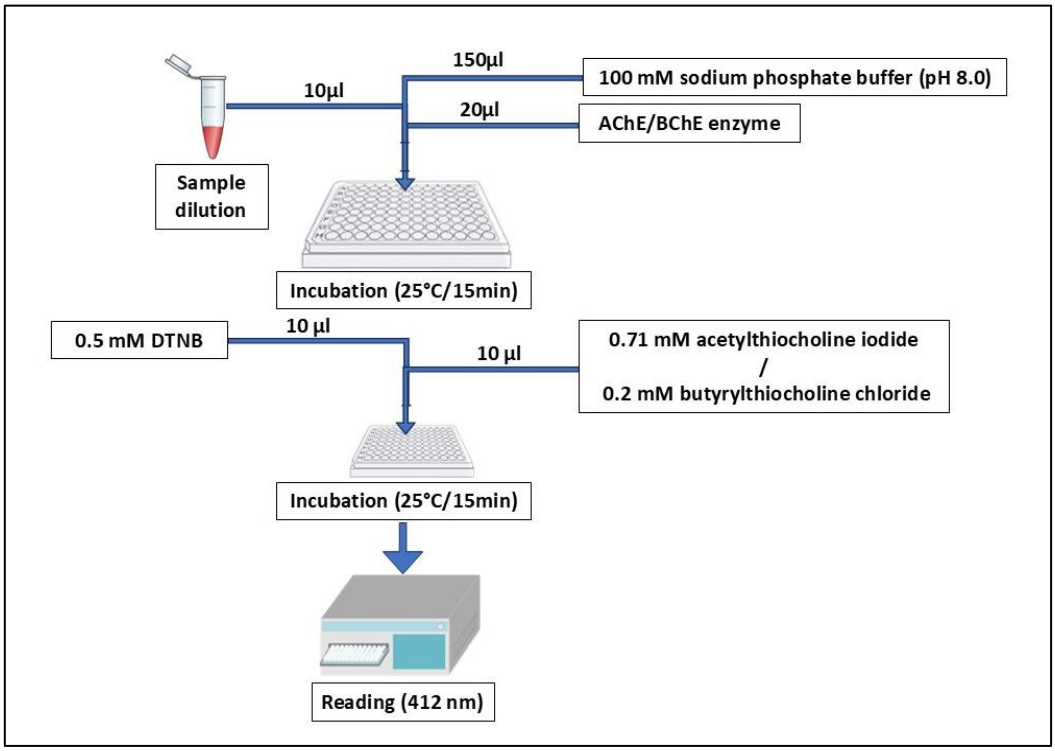

Figure 24: Protocol for anti- Anti-Alzheimer Activity Determination Using acetylcholinesterase and butyrylcholinesterase Inhibition Assay

2.2.3.4.5. *Pancreatic Lipase Inhibition Assay*

Lipases are enzymes that catalyze the hydrolysis of dietary triglycerides into glycerol and free fatty acids, facilitating fat absorption in the digestive system. Overactivity of pancreatic lipase can contribute to excessive fat digestion and absorption, which is associated with obesity and related metabolic disorders (**Singh, 2022**). Evaluating the lipase inhibitory potential of natural or synthetic compounds is therefore important for identifying agents that may help control obesity, manage lipid metabolism, and support weight management therapies.

The assay is based on the reaction of lipase with p-nitrophenyl palmitate (p-NPP) in buffer, which is initially colorless. In the absence of inhibitors, lipase hydrolyzes p-NPP to release p-nitrophenol, producing a yellow color. In the presence of a lipase inhibitor, hydrolysis is reduced, resulting in a less intense yellow coloration (**Syedd-León *et al.*, 2020**).

lipase inhibitory activity was determined using *p*-nitrophenyl palmitate as substrate, following a spectrophotometric method of **Souza *et al* (2011)** with modifications (Figure 25). 50 µL of sample extract was mixed with 100 µL of pancreatic lipase solution (1 mg/mL in 50 mM Tris–HCl buffer, pH 8.0) and pre-incubated at 37 °C for 20 min. The reaction was initiated by adding 50 µL of *p*-NPP solution (prepared by dissolving 3.8 mg *p*-NPP in 2 mL DMSO), and the mixture was further incubated at 37 °C for 2 h. The release of *p*-nitrophenol was measured at 405 nm using a microplate reader. Tris–HCl buffer was prepared by dissolving 1.21 g Tris in 200 mL distilled water and adjusting the pH to 8.0 with HCl. Appropriate blanks and controls were included to correct for background absorbance of enzyme, substrate and extracts. The inhibition rate is measured using the following equation:

$$\textbf{Lipase inhibition } (\%) = [1 - \frac{(As - Asb)}{Anc}] \times 100$$

$\mathbf{A_s}$ = Absorbance of the reaction with enzyme + test sample
$\mathbf{A_{sb}}$ = Absorbance of the sample blank (corrects for color/turbidity of extract).
$\mathbf{A_{nc}}$ = Absorbance of the negative control (represents 100% enzyme activity).

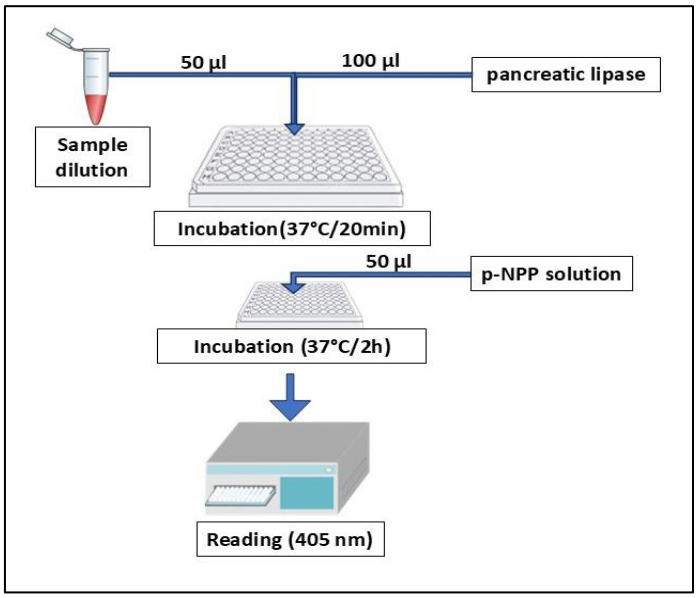

Figure 25: Protocol for anti- obesity Activity Determination Using Lipase Inhibition Assay

2.2.3.5. Antibacterial Activity

The antibacterial activity of the extracts was evaluated in the Pharmaceutical Sciences Research Center (C.R.S.P. Constatine, Algeria) and in Pasteur Institute (Algiers, Algeria) to determine their ability to inhibit the growth of Gram-positive and Gram-negative bacteria. Standardized methods resumed in Figure 26, were applied to assess the effectiveness of the samples against reference strains, providing reliable data on their potential antimicrobial properties.

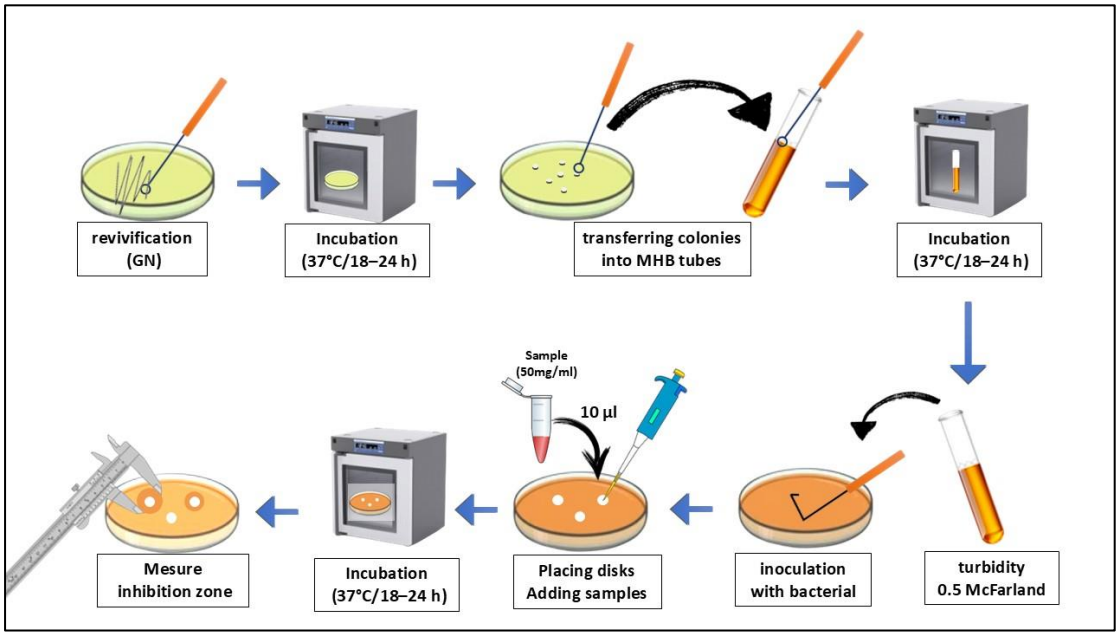

Figure 26: protocol for anti- bacterial Activity Determination Using disk diffusion Assay

2.2.3.5.1. <u>Bacterial Strains</u>

The antibacterial activity of the extracts was assessed against a selection of Gram-positive and Gram-negative bacteria. Gram-positive strains included *Staphylococcus aureus* (ATCC 25923), *Bacillus subtilis* (ATCC 6633), *Bacillus cereus* (ATCC 11778), and *Enterococcus faecalis* (ATCC 29212), while Gram-negative strains comprised *Escherichia coli* (ATCC 25922), *Klebsiella pneumoniae* (ATCC 700603), *Pseudomonas aeruginosa* (ATCC 27853), and *Salmonella* spp. All reference strains were obtained from ATCC and were used to standardize the antibacterial assays.

2.2.3.5.2. Samples Preparation

The test extracts were prepared at a concentration of 50 mg/mL in dimethyl sulfoxide (DMSO). To ensure complete dissolution and improve homogenization, the mixtures were subjected to an ultrasonic bath until a uniform solution was obtained. The prepared extracts were freshly used for the antibacterial assays to maintain stability and activity.

2.2.3.5.3. Bacteria Revival

The procedures for bacterial growth and maintenance were performed according to standard guidelines (**American Type Culture Collection [ATCC], n.d**.). Revivification of refrigerated bacterial cultures was performed by aseptically transferring a small portion of the culture using a sterile inoculating loop into fresh nutrient agar plates. The inoculated media were incubated under the species-specific optimal growth conditions (at 37°C for 18-24h), and cultures were monitored for colony formation. To enhance revival, media were pre-warmed when necessary, and all procedures were carried out under strict aseptic conditions to prevent contamination.

2.2.3.5.4. Inoculum Preparation

A bacterial suspension was prepared from a fresh, actively growing culture (18–24 h old) by transferring several well-isolated colonies from agar plates into 5 mL of sterile Mueller-Hinton broth (MHB) in a sterile test tube. The cells were thoroughly mixed to obtain a homogeneous suspension, using a vortex when necessary to disperse clumps. The suspension was then incubated at 37°C for 18–24 h, and its turbidity was adjusted to match the 0.5 McFarland standard (Figure 27), corresponding to approximately 1×10^8 CFU/mL (**Balouiri *et al.*, 2016**). The resulting suspension was used immediately for subsequent assays to ensure viability.

Figure 27: measuring turbidity of inoculum using McFarland Densitometer

2.2.3.5.5. *Disk Diffusion Assay Procedure*

The antibacterial activity of the extracts was evaluated using the disk diffusion method (**Hudzicki, 2009**). Sterile 6 mm paper disks were impregnated with 10 µL of each extract and placed onto the surface of Mueller-Hinton agar plates previously inoculated with the test bacterial strains. Amoxicillin and ampicillin were used as standard reference antibiotics, while disks with solvent alone served as negative controls. The plates were incubated at 37°C for 18–24 hours, after which the zones of inhibition around the disks were measured in millimeters to assess the antibacterial activity of the extracts. All procedures were performed under aseptic conditions to prevent contamination.

2.3.Statistical Analysis

Statistical analyses were performed to evaluate differences in cultivation performance, productivity, and bioactive properties among treatments. For cultivation performance and productivity, data were obtained from nine treatments with five replications each. For biochemical assays, including TFC, TPC, antioxidant activities, anti-inflammatory activity, and enzyme inhibition activities, a total of 27 samples were analyzed (corresponding to the three flushes of mushrooms obtained from each of the nine substrate formulations), with three replications per sample. Since the data did not meet the assumptions of normality and homogeneity of variance, non-parametric tests were applied. The Kruskal–Wallis test was used to detect overall differences among groups, followed by Dunn's post hoc test for pairwise comparisons, as it is specifically designed for non-parametric multiple group comparisons and accounts for rank-based differences more reliably than multiple Mann–Whitney tests. To control for false discovery rate across the large number of pairwise comparisons, p-values were adjusted using the Benjamini–Hochberg correction, which provides a balanced approach by maintaining statistical power while minimizing the likelihood of false positives compared with more conservative corrections such as Bonferroni **(McDonald, 2014)**. Statistical significance was considered at $p < 0.05$. IBM SPSS Statistics (IBM Corporation, version 27, Armonk, NY, USA) was used for calculating means and standard errors, Microsoft Excel (Microsoft Corporation, Excel 2016, Redmond, WA, USA) was employed to calculate activities using the respective equations and to generate graphs, and R software (RStudio, version 2025.05.1+513) was used for non-parametric testing and multiple comparison corrections.

RESULTS AND DISCUSSION

3. RESULTS AND DISCUSSION

3.1.Agronomic Performance

3.1.1. Carbon and Nitrogen Content

The analysis of carbon and nitrogen levels in tested substrates (Table 3) revealed that date kernels contained relatively higher concentrations of both carbon and nitrogen, registering values of 44.53±0.05% and 0.54±0.01% respectively in K100. In contrast, palm-based substrates exhibited lower content, with 39.19±0.74% carbon and 0.28±0.06% nitrogen in P100. A gradual increase in carbon and nitrogen was observed with greater incorporation of date kernels and a corresponding reduction of palm material. However, the carbon-to-nitrogen (C/N) ratio followed an opposite pattern: it declined with the rising proportion of date kernels and increased with more palm material, ranging from 81.87±2.02 in K100 to 164.63±4.84 in P75.

Table 3: Carbon and Nitrogen content of different substrates

SUBSTRAT	Carbon content (%)	Nitrogen content (%)	C/N
WS	42,4240 ± 0,0764^{bcd}	0,4241 ± 0,0194^{abc}	100,4461 ± 4,6175^{abc}
K25	43,7230 ± 0,1367^{abc}	0,4609 ± 0,0152^{abc}	95,0610 ± 2,8632^{abc}
K50	43,7750 ± 0,0297^{abc}	0,4753 ± 0,0148^{ab}	92,2868 ± 3,0256^{bc}
K75	44,0493 ± 0,0438^{ab}	0,5236 ± 0,0091^{a}	84,1763 ± 1,4022^{c}
K100	44,5290 ± 0,0505^{a}	0,5445 ± 0,0131^{a}	81,8743 ± 2,0222^{c}
P25	42,5967 ± 0,0577^{abcd}	0,4052 ± 0,0068^{abc}	105,1775 ± 1,7803^{abc}
P50	41,5143 ± 0,1194^{cd}	0,3313 ± 0,0135^{bc}	125,6717 ± 4,6113^{ab}
P75	40,6910 ± 0,0428^{cd}	0,2474 ± 0,0069^{c}	164,7269 ± 4,8354^{a}
P100	39,1853 ± 0,7381^{d}	0,2756 ± 0,0578^{bc}	156,5239 ± 35,5358^{ab}

The numbers in the table representing the means ± standard error, same letters over the same raw indicates groups with no significant difference ($P < 0.05$)

The concentrations of total carbon, total nitrogen, and the C/N ratio within a substrate are essential for successful mushroom cultivation, since they directly affect both mycelial colonization and the subsequent development of fruiting bodies (**Nieuwenhuijzen & Oei, 2005; Figueiró & Graciolli, 2011**).

Substrates derived from date kernels, the carbon content identified in the present study was consistent with values reported by **Hoa *et al*. (2015)**. Nevertheless, the nitrogen percentage was significantly lower, which resulted in a comparatively elevated C/N ratio. These findings

are in harmony with the conclusions of **Atila and Cetin (2024)** and **Costa *et al*. (2023)**. The fluctuations in nitrogen and carbon observed can be explained by the chemical constitution of date kernels, which are known to contain around 4% protein and more than 20% cellulose, hemicellulose, and lignin (**Kocheki, 2015; Nabili *et al*., 2017; Abu-Thabit *et al*., 2020)**.

For palm-based substrates, the proportions of carbon and nitrogen were similar to those reported by **Burezq and Davidson (2023)**. Palm leaves consist predominantly of lignocellulosic compounds—chiefly cellulose, hemicellulose, and lignin—that are abundant in carbon. The high carbon percentage highlights the structural importance of these materials, which form the cell walls of the leaves and provide rigidity and durability. This characteristic is typical of most agricultural residues and woody plant-based raw materials **(Al-Awa *et al*., 2023; Dhahi *et al*., 2024)**. Nitrogen levels in palm leaves, on the other hand, are relatively low because such tissues possess fewer proteins and nitrogen-rich molecules compared with fresh, green, non-lignified tissues. Most nitrogen in palm foliage is bound in proteins and molecules associated with photosynthesis and metabolic activity; however, as leaves age and undergo lignification, their nitrogen proportion diminishes **(Trabzuni *et al*., 2014)**.

3.1.2. Spawn Running Time

The colonization times across different treatments are summarized in Table 4. Substrate K100 demonstrated the fastest colonization, taking only 12 days**,** followed by P100 with 17 days, both of which were quicker than wheat straw (WS), which required 20.6 days**.** Substrates prepared from mixtures generally took slightly longer to reach full colonization, although these differences were not statistically significant compared with WS. Specifically, K25, P25, and K50 showed colonization times of 22.8; 22.6 and 22.2 days, respectively. Similarly, K75, P50, and P75 exhibited colonization periods of 19.8; 19.2 and 19.4 days, which did not differ significantly from each other or from WS.

Overall, the colonization times reported in this study were shorter than those documented by **Mkhize *et al*. (2016)**, who worked with maize stalks enriched with maize flour and wheat bran, and also shorter than results obtained using substrates such as sugarcane bagasse or banana leaves **(Selvaananthi & Alphonse, 2022)**. For substrates like K25, P25, and K50, colonization times were comparable to values obtained with paddy straw **(Selvaananthi & Alphonse, 2022)** and with the observations of **Atila and Cetin (2024)**, who reported about 20 days for full colonization on substrates such as poplar sawdust, lavender straw, and lavender flower waste.

Table 4: The Overall Times Measurements of *Pleurotus ostreatus* Mushroom Cultivated on Different Substrate Mixture

Substrate	Necessary time from previous stage (day)								
	spawning	1st pinhead appearance	1st flush	2nd flush	3rd flush	4th flush	5th flush	6th flush	7th flush
WS	20,6 ± 0,98^{ab}	15,8 ± 1,02^{ab}	8,2 ± 0,59^{a}	21,8 ± 1,59^{a}	39,6 ± 4,48^{ab}	24 ± 10,02^{abc}	10 ± 6,12^{a}	-^{b}	-^{a}
K25	22,8 ± 1,8^{a}	13 ± 1,55^{abc}	9,4 ± 0,93^{a}	27, ± 5,84^{a}	38,6 ± 7,98^{ab}	48,8 ± 3,17^{a}	34,2 ± 3,02^{a}	29,2 ± 12,23^{ab}	-^{a}
K50	22,2 ± 1,2^{a}	11 ± 1,27^{bc}	9 ± 0,32^{a}	18,6 ± 1,75^{a}	24,2 ± 1,77^{b}	39 ± 1,76^{abc}	35,2 ± 1,56^{a}	42,4 ± 8,84^{a}	6 ± 6^{a}
K75	19,8 ± 1,8^{abc}	9 ± 0,84^{c}	7,8 ± 0,49^{a}	21,2 ± 1,28^{a}	25,4 ± 2,14^{b}	50,6 ± 10,51^{ab}	33,4 ± 7,23^{a}	28 ± 9,7^{a}	3,2 ± 3,2^{a}
K100	12 ± 0^{c}	11,4 ± 1,29^{bc}	8 ± 0,32^{a}	16,4 ± 1,86^{a}	23,2 ± 1,39^{b}	-^{c}	-^{a}	-^{b}	-^{a}
P25	22,6 ± 1,17^{a}	14 ± 1,55^{abc}	8,6 ± 0,75^{a}	35,2 ± 12,32^{a}	35,6 ± 14,57^{ab}	21 ± 8,61^{abc}	10,4 ± 10,4^{a}	-^{b}	-^{a}
P50	19,2 ± 0,74^{abc}	12 ± 0,71^{abc}	6,4 ± 1,50^{a}	30 ± 2,55^{a}	67,4 ± 1,54^{a}	19 ± 6,24^{bc}	16,6 ± 10,37^{a}	-^{b}	-^{a}
P75	19,4 ± 1,12^{abc}	17 ± 0,45^{a}	7,6 ± 0,81^{a}	23,2 ± 4,26^{a}	22,4 ± 9,84^{b}	26,4 ± 11,6^{abc}	9,2 ± 9,2^{a}	-^{b}	-^{a}
P100	17± 0^{bc}	16,8 ± 1,2^{a}	8,6 ± 2,06^{a}	29,6 ± 2,54^{a}	46,6 ± 12,35^{ab}	34,6 ± 9,64^{abc}	5,6± 5,6^{a}	-^{b}	-^{a}

substrate	Necessary time of different stages (day)					
	From inoculation to pinning	From inoculation to 1st flush	From inoculation to 3rd flush	From 1st to 3rd flush	From 1st to last flush	From inoculation to last flush
WS	36,4 ± 1,99^{a}	44,6 ± 1,54^{a}	106 ± 3,98^{ab}	69,6 ± 5,23^{abc}	103,6 ± 8,99^{bc}	140± 10,46^{bcd}
K25	35,8 ± 1,96^{ab}	45,2 ± 2,75^{a}	110,8 ± 11,03^{ab}	75 ± 11,19^{abc}	187,2 ± 9,2^{a}	223 ± 8,31^{a}
K50	33,2 ± 1,56^{abc}	42,2 ± 1,59^{ab}	85 ± 2,59^{bc}	51,8 ± 3,34^{bc}	174,4 ± 10,22^{ab}	207,6 ± 9,32^{ab}
K75	28,8 ± 1,11^{bc}	36,6 ± 1,47^{ab}	83,2 ± 1,66^{bc}	54,4 ± 1,17^{bc}	169,6 ± 11,87^{ab}	198,4 ± 11,13^{abc}
K100	23,4 ± 1,29^{c}	31,4 ± 1,5^{b}	71 ± 2,7^{c}	47,6 ± 1,5^{c}	47,6 ± 1,5^{c}	71 ± 2,7^{d}
P25	36,6 ± 0,4^{a}	45,2 ± 0,8^{a}	116 ± 9,04^{ab}	79,4 ± 9,2^{abc}	110,8 ± 22,22a^{bc}	147,4 ± 21,91^{abcd}
P50	31,2 ± 1,28^{abc}	37,6 ± 2,27^{ab}	135 ± 3,89^{a}	103,8 ± 3,41^{a}	139,40 ± 11^{abc}	170,6 ± 10,72^{abcd}
P75	36,4 ± 1,25^{ab}	44 ± 2^{a}	89,6 ± 6,31^{bc}	53,2 ± 6,26^{bc}	88,8 ± 20,93^{c}	125,2 ± 20,6^{cd}
P100	33,8 ± 1,2^{abc}	42,4 ± 2,2^{ab}	118,6 ± 8,64^{ab}	84,8 ± 9,04^{ab}	125 ± 20,35^{abc}	158,8 ± 19,81^{abcd}

The numbers in the table representing the means ± standard error, same letters over the same raw indicates groups with no significant difference (P < 0.05)

The colonization speed on K100 was similar to that observed on substrates including corn straw (with or without sugarcane bagasse), waste paper, cardboard from industry, maize cobs, and cottonseed hulls. By contrast, colonization on P100 closely resembled results obtained with substrates such as plantain midrib (either alone or in combination with corn straw and sugarcane bagasse) and rice straw **(Afify *et al*., 2012; Emiru *et al*., 2016; Iwuagwu *et al*., 2020; Subedi *et al*., 2023)**.

Mycelial growth and colonization form the first stage of mushroom cultivation, laying the groundwork for basidiocarp production. Extended spawn run periods on lignocellulosic substrates are usually linked to the slower pace of fungal hyphae on such substrates, which depends on extracellular enzymes for degradation **(Mandeel *et al*., 2005)**. **Samuel and Eugene (2012)** stressed the importance of nitrogen in stimulating mycelial development, noting that nitrogen scarcity hinders growth, whereas moderate nitrogen levels activate ligninolytic enzymes. Conversely, when nitrogen surpasses 1.5%, enzyme synthesis is repressed **(Hoa & Wang, 2015; Neelam *et al*., 2011)**. This mechanism may clarify the growth patterns on palm-based substrates.

Carbon serves as both a key source of energy and a structural building block of mycelial cells **(Walker & White, 2017)**. Because date kernels contain relatively greater amounts of both carbon and nitrogen than wheat straw (WS), they seem to foster more rapid colonization, producing quicker spawn runs when used in higher proportions. Moreover, **Stamets (2000)** indicated that prolonged colonization phases can also stem from compact substrates with fine particle sizes, as these restrict aeration and impede hyphal expansion.

3.1.3. Pinhead Formation

Once bags were completely colonized with mycelium, they were transferred into another room to monitor subsequent growth stages, beginning with the time required for the first pinhead appearance. Substrates P75 and P100 exhibited the longest intervals, requiring 16.8 and 17 days respectively for the emergence of initial primordia, followed by WS at 15.8 days**.** In contrast, K75 displayed a shorter period of 9 days, followed by K50 and K100 with 11 and 11.4 days, respectively. The remaining treatments—K25, P25, and P50—showed no significant differences across the groups (Table 4).

When combining both spawn run and pinhead emergence, the shortest total durations were noted for K100 **(**23.4 days**)** and K75 (28.8 days**),** whereas the longest were observed on WS, P25, and P75 **(**36.4, 36.6, and 36.4 days, respectively).

The recorded interval of 9 to 17 days between full colonization and pinhead formation is in line with findings from previous studies **(Girmay *et al*., 2016; Tupa *et al*., 2020; Otieno *et al*., 2022)**. Substrates richer in lignin and cellulose usually delay primordia initiation, while those containing more readily digestible nutrients and less lignin accelerate the process **(Oei, 2003; Al-Jbouri *et al*., 2025)**. Nitrogen also plays a central role as it stimulates pinhead formation **(Tupa *et al*., 2022)**. Furthermore, it has been observed that longer spawn runs may shorten the time interval to pinhead initiation **(Dissasa, 2022)**.

3.1.4. Flushes and Total Crop Duration

After fruiting bodies matured, the clusters were harvested in flushes (Figure 28). Results in Table 4 indicated that the time required to harvest subsequent flushes increased progressively. The first harvest, occurring after primordia development, took between 6.4 and 9.4 days across all treatments, with no significant variations. Similarly, no significant differences were observed in the timing of the second flush.

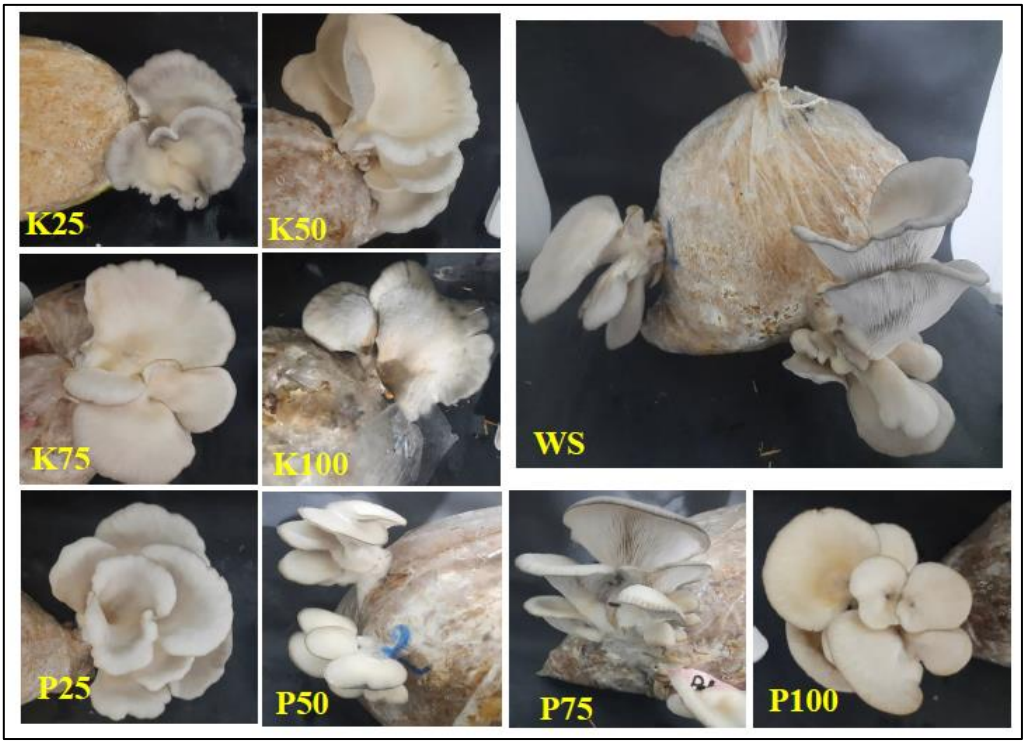

Figure 28: clusters from different substrate formulas

In contrast, significant variation was seen in the third flush. The shortest harvest times were found in K50, K75, K100, and P75 (24.2, 25.4, 23.2, and 22.4 days respectively), while P75 also recorded the longest at 67.4 days. Regarding the complete crop cycle, K100 displayed the shortest overall duration, producing three flushes within 71 days. P75 followed, requiring 125.2 days from inoculation to finish 4.2 flushes, and 89.6 days to achieve its third flush. By comparison, K25 demonstrated the longest cropping period, yielding 5.6 flushes over 223 days, with 110 days to the third flush. K50 produced the greatest number of flushes (6.2), although this did not significantly differ from K25 or K75, which required 98.4 and 83.2 days to reach approximately 5.8 and 3 flushes, respectively. Palm-containing substrates yielded between 3.4 and 4.4 flushes, with no notable differences among them.

In the literature, the time required for full fruiting body formation typically ranges between 22 and 35 days **(Emiru *et al*., 2016)**, although extended durations up to 56 days have been recorded **(Afify *et al*., 2012; Atila & Cetin, 2024)**. Since primordia maturation showed no significant differences across treatments, the primary variations must be attributed to the spawning phase, where delays in colonization and primordia initiation extended the harvesting period **(Hoa *et al*., 2015)**.

The intervals between flushes—particularly the first three—were shorter than those reported by **Paudel and Dhakal (2020)**, who noted gaps of 5–6 weeks between the first and second flush and 7–10 weeks between the second and third. This discrepancy is most likely associated with the progressive depletion of carbon and nitrogen reserves in the substrate, which slows primordia development in later flushes **(Naraian *et al*., 2008)**.

A reduced production cycle represents an important criterion for substrate selection. The total cropping time in this study, extending from inoculation to the last flush, contrasts with the 69–96 days reported by **Paudel and Dhakal (2020)** for only three flushes. Nonetheless, the results here agree with **Khanna and Garcha (1982)**, who suggested that mushroom harvesting may last up to 104 days.

The quantity and length of flushes are largely determined by nutrient reserves within the substrate. As nutrients become exhausted, both the number of flushes and total yields decrease. Substrates with higher or better-balanced nutrient availability tend to sustain more flushes, whereas those high in lignin and cellulose or generally poor in nutrients support fewer flushes because of slower degradation and limited nutrient supply for fruiting **(Sonnenberg, 2022)**. Accordingly, the differences observed across treatments in this study can be explained by

variation in spawn run length, primordia initiation, fruiting maturation, flush intervals, and the total number of flushes achieved.

3.1.5. Yield and Biological Efficiency

Following the harvesting and weighing of each flush separately, it was evident that the first flush produced the highest yield, after which output gradually declined across subsequent flushes. A substantial portion of total production was concentrated within the first three flushes. The maximum first flush yield was observed in K25 (211.6 g), while the lowest were in K100 **(**93 g**)** and P100 (98.6 g**).** The other treatments yielded between 126 and 167 g**,** without significant differences (Table 5).

K100 yielded only three flushes in total, with an overall yield of 220.2 g per bag (44.04% BE**)**—a value nearly equivalent to the first flush alone of K25 (211.6 g)—and comparable to P100, which produced 218.69 g across 3.8 flushes and 199.4 g within the first three flushes (43.7% and 39.9% BE**,** respectively).

When the first three flushes were compared across all treatments, the greatest combined yield was obtained from K25 (478.07 g), corresponding to a biological efficiency (BE**)** of 95.6%, a value not statistically different from K50 (86.3% BE**)** or K75 (83% BE) (Figure 29, Table 5).

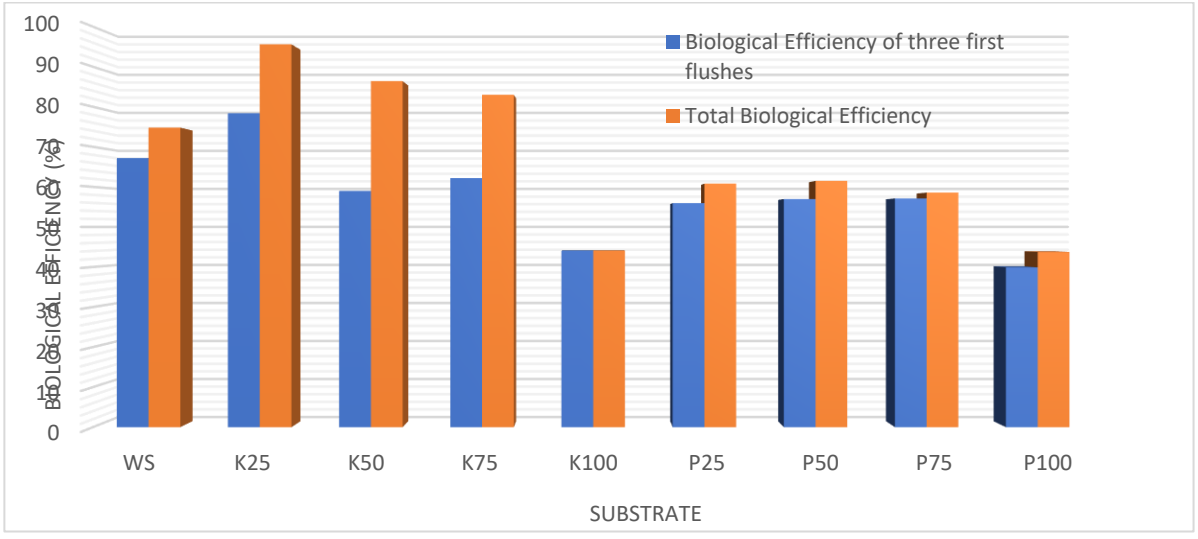

Figure 29: Mean BE of three first flushes and total BE of *Pleurotus ostreatus* mushroom cultivated on different substrate mixture

Table 5: number of flushes and Yield of *Pleurotus ostreatus* mushroom cultivated of different substrates mixture between wheat straw and date kernel.

Substrate	Total flushes	Yield (g bag^{-1})								
		1st flush	2nd flush	3rd flush	4th flush	5th flush	6th flush	7th flush	1st +2nd +3rd flush	Total yield
WS	4.2±0.58^{abcd}	167±26.86^{ab}	115.2±7.96^{a}	54.28±9.93^{a}	21.576±11.95^{abcd}	13.79±8.82^{abc}	0^{c}	0^{a}	336.48±29.98^{ab}	374.3±41.21^{ab}
K25	5.6±0.24^{abc}	211.6±5.59^{a}	109.2±10.47^{a}	71.8±15.73^{a}	43.068±10.48^{abc}	36.122±1.16^{a}	6.278±3.24^{abc}	0^{a}	392.6±21.02^{a}	478.068±28.87^{a}
K50	6.2±0.20^{a}	127.8±9.02^{ab}	74.4±16.40^{a}	93±14.99^{a}	80.2±7.02^{a}	24.892±5.08^{ab}	22.734±4.63^{a}	8.694±8.69^{a}	295.2±14.65^{abc}	431.72±12.70^{a}
K75	5.8±0.37^{ab}	126±9.51^{ab}	93.2±15.19^{a}	91.4±13.27^{a}	58.26±16.46^{ab}	18.37±2.67^{abc}	19.728±6.39^{ab}	7.8±7.80^{a}	310.6±23.19^{abc}	414.758±20.48^{a}
K100	3±0.00^{d}	93±20.91^{b}	78±8.81^{a}	49.2±6.78^{a}	0^{d}	0^{c}	0^{c}	0^{a}	220.2±15.97^{bc}	220.2±15.97^{b}
P25	3,4±0,6^{cd}	8,6 ± 0,75^{ab}	35,2±12,32^{a}	35,6±14,57^{a}	21±8,61^{abcd}	10,4±10,4^{bc}	0^{c}	0^{a}	279,65±34,42^{abc}	304,06±43,29^{ab}
P50	4,4±0,51^{abcd}	6,4 ± 1,50^{ab}	30±2,55^{a}	67,4±1,54^{a}	19±6,24^{bcd}	16,6±10,37^{abc}	0^{c}	0^{a}	284,77±17,56^{abc}	307,49±22,38^{ab}
P75	3,4 ± 0,6^{cd}	7,6 ± 0,81^{ab}	23,2±4,26^{a}	22,4±9,84^{a}	26,4±11,6^{cd}	9,2±9,2^{bc}	0^{c}	0^{a}	285,6±36,80^{abc}	292,91±35,2^{ab}
P100	3,8±0,49^{bcd}	8,6 ± 2,06^{b}	29,6±2,54^{a}	46,6±12,35^{a}	34,6±9,64^{abcd}	5,6±5,6^{bc}	0^{c}	0^{a}	199,4±15,84^{c}	218,69±18,27^{b}

he numbers in the table representing the means ± standard error, same letters over the same raw indicates groups with no significant difference ($P < 0.05$)

Yield represents a decisive parameter in selecting a substrate. The progressive decline in yield across flushes, as noted in this experiment, aligns with previous reports **(Hoa *et al*., 2015; Dedousi *et al*., 2023)**. Such distribution is a common pattern in Pleurotus spp**. (Rizki & Tamai, 2011; Koutrotsios *et al*., 2018; Melanouri *et al*., 2022)**. The major explanation for yield reduction in later flushes is the depletion of readily available nutrients within the substrate, which provide both energy and building blocks for fruiting. The initial flush usually utilizes the most accessible nutrient fraction, while subsequent flushes depend on harder-to-access reserves, causing a decline in productivity. Additionally, the build-up of metabolic byproducts and inhibitory substances may further suppress fungal growth and reduce yields in later flushes **(Naim *et al*., 2020)**.

When considering solely the first flush, the yield obtained with K25 was on par with the findings of **Subedi *et al*. (2023)** using mixtures of rice straw and water hyacinth, and it even exceeded the yields recorded by **Bhatti *et al*. (2007)** for wheat straw substrates. Remarkably, the maximum cumulative yield achieved with K25 in this research corresponded to the minimum yield reported by **Subedi *et al*. (2023)**, whereas even the lowest yield registered for K100 was higher than most of the values documented by **Emiru *et al*. (2016).**

When assessing all flushes collectively, the combination of date kernel and wheat straw produced yields and biological efficiencies comparable to those observed by **Sales-Campos *et al*. (2011)** in coconut–sawdust mixtures. However, the yield of K75 was notably greater than that of K25. A separate investigation involving date kernel **(Abdulhadi & Hassan, 2013)** also reported a biological efficiency for K100 that aligns with the present findings. These patterns most likely reflect the nutritional shortcomings of lignocellulosic materials, which characteristically contain little protein and therefore are less favorable for mushroom growth **(Obodai *et al*., 2002)**. Supplementation with nitrogen-rich substrates has been shown to enhance both yield and product quality in Pleurotus species **(Mahari *et al*., 2020)**. Nevertheless, date palm leaves are marked by a high carbon-to-nitrogen ratio because of their low nitrogen content, which slows down mycelial colonization, postpones the development of pinheads and fruiting bodies, and in the end reduces yield and biological efficiency **(Ali *et al*., 2018)**.

3.2.Biochemical and Mycochemical Characterization

3.2.1. Extraction Yield

Extraction yield varied substantially according to the substrate employed (Figure 30 and appendix B). Palm-based treatments yielded the highest outputs (combining four treatments across three flushes) when compared with date kernel treatments, and among them, P100 displayed the greatest yield. The highest yield recorded in the study was in the second flush of P100 (39.12%), followed by P25 (38%), K25 (37.56%), and the third flush of WS (40.32%), the latter being the sole treatment that showed an increase in extraction yield as harvesting progressed. K75 and K100 demonstrated nearly identical yields across treatments and flushes, similar also to P75, ranging between 27.68% and 32.80%. K50 exhibited the lowest yield among all treatments, with almost no flush-to-flush variation, ranging from 22.32% to 34.84%; specifically, the second flush of P50 (23.6%) and the third flush of P25 (24.04%) represented the lowest values.

The maximum yield reported here matches the findings of **Irshad *et al*. (2023)** using water extraction. Conversely, the lowest yield is consistent with the observations of **Gąsecka *et al*. (2016)** when employing the same extraction solvent (80% methanol in water), though it was still higher than the results documented by **and Oyetayo (2011).**

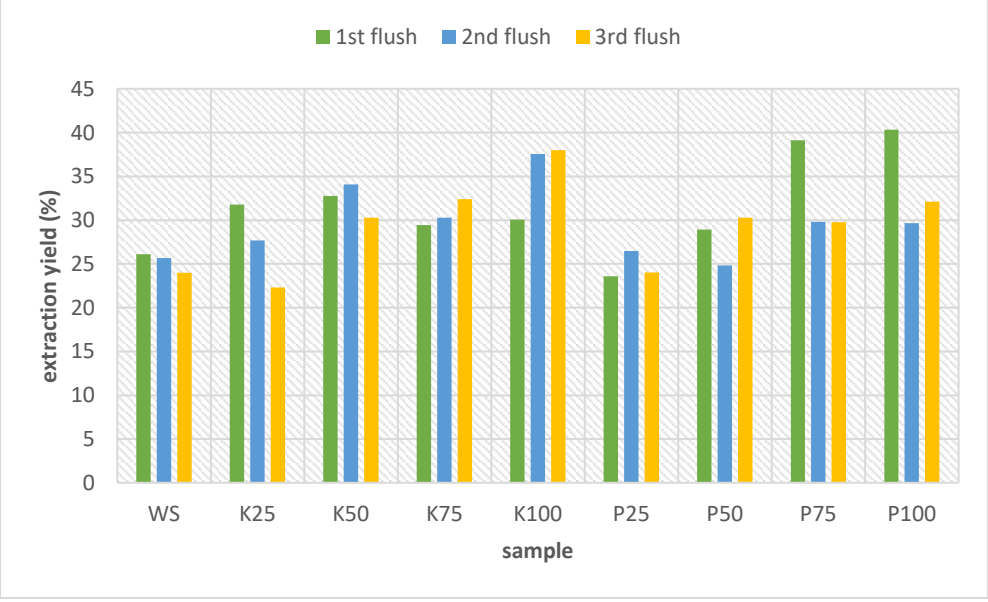

Figure 30: Extraction yield from three first flushes of *Pleurotus ostreatus* mushrooms grown on different substrate formulas.

3.2.2. Total Phenolic and Flavonoid Content (TPC, TFC)

TPC and TFC were measured in both mg per g of extract (Figure 31 and 32) and mg per g of dry mushroom (Figure 33 and 34), allowing assessment of extract concentration as well as the nutritional composition of the mushroom biomass and all data are available in Appendix C with the significant difference in Table C1and the standard curves in Figure C1 and C2. The two parameters were differently influenced by the type of substrate, the proportion of combinations, and the flush sequence.

Flush order had a marked impact: TFC was typically maximized in the first flushes; TPC peaked in the second flushes, while the third flushes generally showed decreased levels of bioactive compounds despite occasionally maintaining high yields. Expressed per g of dry mushroom, the highest TPC was observed in the third flush of date kernel treatments and the first flush of palm-based treatments, whereas TFC was greatest in the first flush across most of the substrates.

The relationship between extraction yield and phenolic/flavonoid content revealed a negative correlation for both TPC and TFC when expressed per g of extract (–0.26 and –0.46, respectively), indicating that higher extraction yield tended to correspond to slightly lower phenolic and flavonoid concentrations in the extract. However, positive correlations (+0.23 for TPC and +0.20 for TFC) were noted when expressed per g of dry mushroom, suggesting that higher extraction yields resulted in greater total phenolic and flavonoid content per mushroom unit (Figure 35).

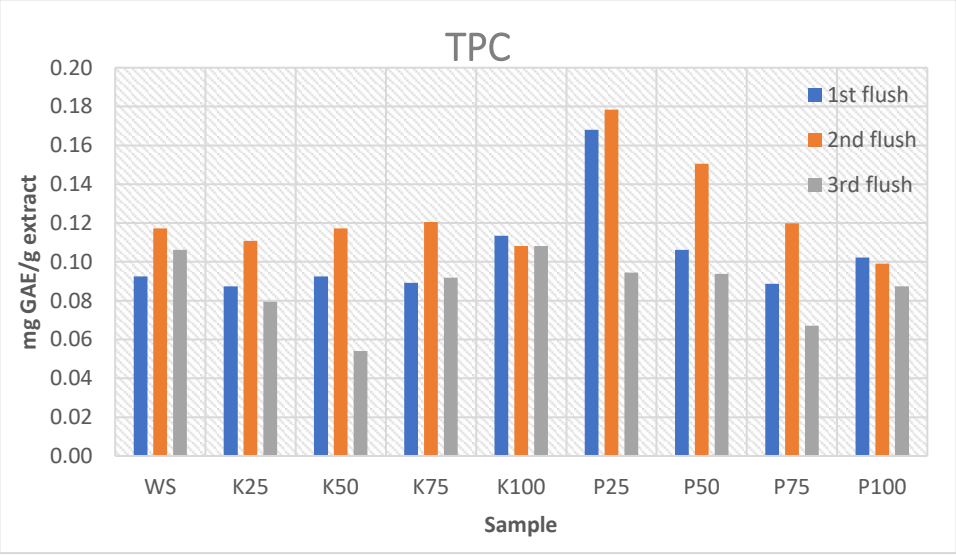

Figure 31: total phenolic content (TPC) of *Pleurotus ostreatus* mushroom extract (mg GAE/g)

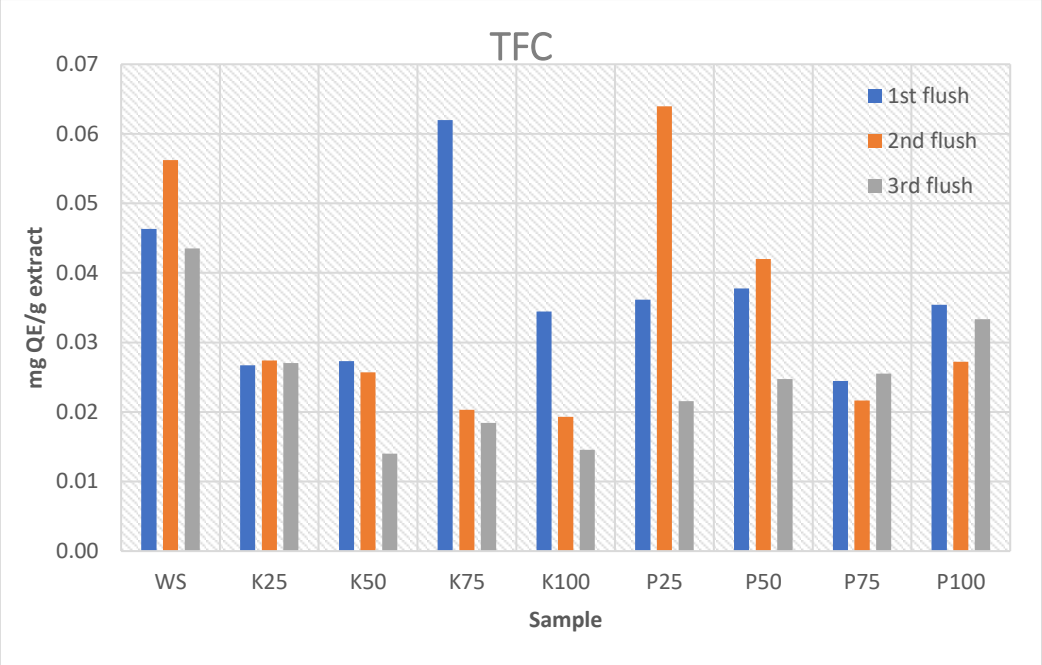

Figure 32: total flavonoids content (TFC) of *Pleurotus ostreatus* mushroom extract (mg QE/g)

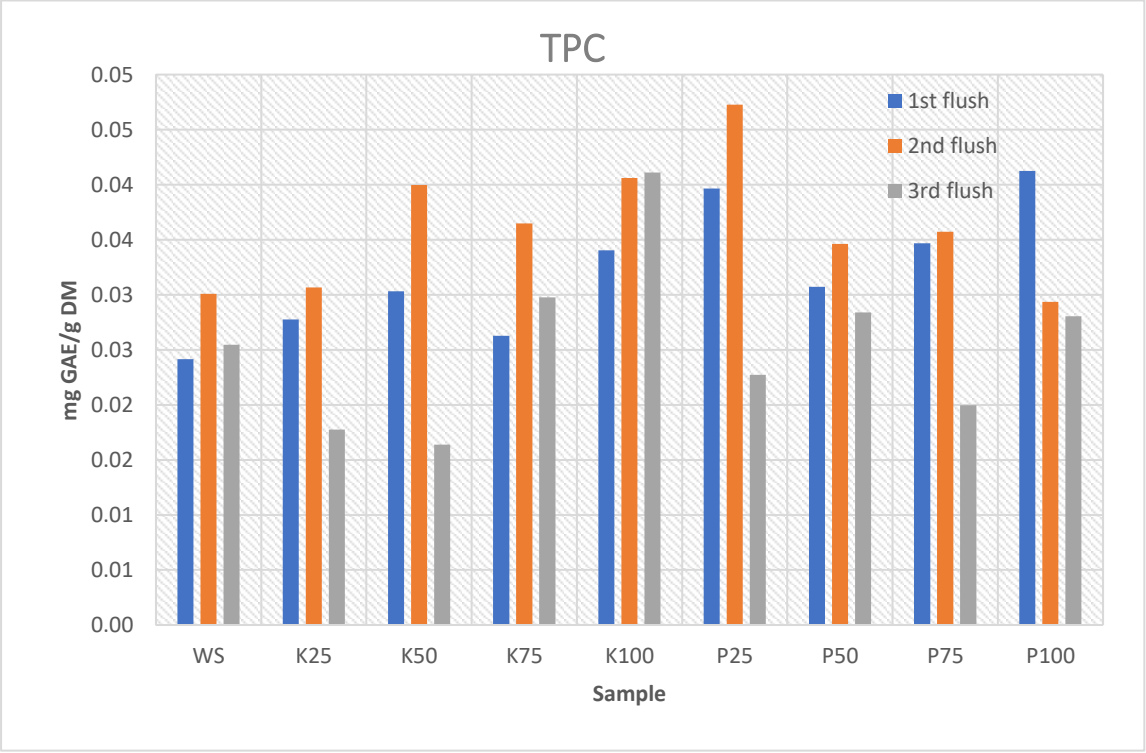

Figure 33: total phenolic content (TPC) of *Pleurotus ostreatus* mushroom powder (mg GAE/g)

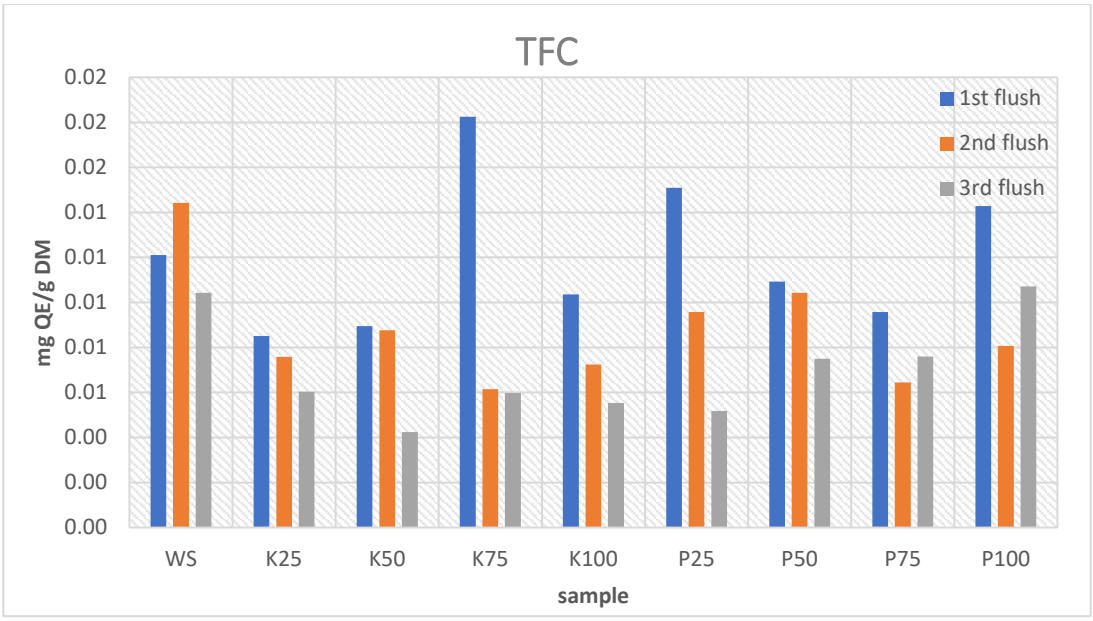

Figure 34: total flavonoids content (TFC) of *Pleurotus ostreatus* mushroom powder (mg QE/g)

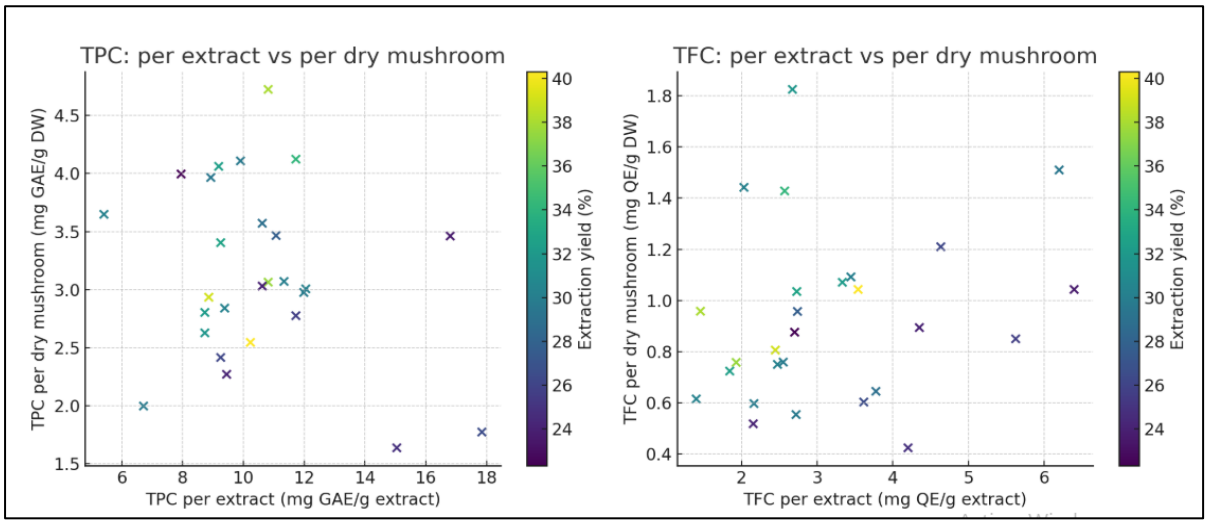

Figure 35: correlation between TPC, TFC and extraction yield

The highest extraction yields—such as the first flush of P100 (40.32%) and P75 (39.12%), and the second and third flushes of K100 (37.56% and 38%, respectively)—recorded TPC values of 10.229 mg GAE/g extract and 8.86 mg GAE/g extract, respectively. On the other hand, the lowest yields observed in the third flush of WS, K25, and P25 (23.98%, 22.32%, and 24.04%, respectively), as well as the second flush of P50 (24.84%) and the first flush of P25 (23.6%), displayed TPC

values ranging between 7.949 and 16.804 mg GAE/g extract and TFC values between 2.115 and 6.397 mg QE/g extract.

Outliers such as P75/1 (high yield but low TPC) and P25/2 (low yield but very high TPC) confirmed that extraction yield and phenolic/flavonoid concentrations are not directly proportional, underscoring a trade-off between extract quantity and bioactive richness.

When expressed per g of dry mushroom (DM), these patterns persisted but with some differences. Palm-based substrates still led in phenolic abundance, though the advantage was less pronounced since high-yield treatments also delivered more total bioactive compounds per mushroom despite their extracts being more diluted. P25/1 (3.462 GAE/g DM) and P25/2 (1.774 GAE/g DM) remained among the top TPC values per DM, but high-yield treatments such as K100/3 (4.725 GAE/g DM) and K50/2 (4.124 GAE/g DM) also displayed competitive TPC due to their greater extractable mass. For TFC, wheat straw showed relatively stable values across flushes, while kernel-based substrates demonstrated a sharper decline in later flushes. Samples with both reasonable yields and high concentrations—such as P25/1 (23.6% yield; 16.804 mg GAE/g and 6.397 mg QE/g per extract)—or with high yield but moderate concentrations like K50/2 (34.08% yield; 11.726 mg GAE/g and 2.57 mg QE/g per extract)—proved capable of maximizing total phenolic and flavonoid recovery per unit mushroom (3.462 mg GAE/g and 1.043 mg QE/g for P25/1; 4.124 mg GAE/g and 1.428 mg QE/g for K50/2).

Gąsecka *et al.* (2016) found that *P. ostreatus* cultivated on wheat straw supplemented with Se and Zn achieved TPC values of 13.38 mg GAE/g extract and TFC values of 2.72 mg QE/g extract, lower than the maximum values reported in the present study. However, these remain below several studies of wild mushrooms or cultivation on coconut **(Fakoya *et al.*, 2020; Mihai *et al.*, 2022)** and above cultivation with oil palm supplemented with rice bran, gypsum, and lime in tea or espresso waste **(Sulistiany *et al.*, 2016; Yılmaz *et al.*, 2017)**.

The TFC values reported here (mostly between 0.4 and 1.8 mg QE/g DW) align with prior studies on *Pleurotus* species that recorded TFC between 0.5 and 2.0 mg QE/g DW, depending on extraction technique and substrate **(Gąsecka *et al.*, 2016; Pandey *et al.*, 2023)**. The higher values for palm-based substrates support earlier findings that

substrates rich in polyphenolic precursors enhance biosynthesis of antioxidant compounds **(Mkhize *et al*., 2022; Gebru, Faye, & Belete, 2024)**.

Several other studies reported extremely low flavonoid levels in Pleurotus extracts—down to about 0.12–0.15 mg QE/g DW or even less when cultivated on oil palm residues supplemented with rice bran, gypsum, and lime, or on tea and espresso waste **(Sulistiany *et al*., 2016; Yılmaz *et al*., 2017)**. These findings confirm that flavonoid content can fall below the lowest TFC recorded in the present study (0.4 mg QE/g DW).

Extraction yield differences can be influenced by substrate richness in secondary metabolites such as phenols, alkaloids, polysaccharides, and amino acid derivatives **(Rahimah *et al*., 2019; Effiong *et al*., 2024)**. When the solvent is suitable, a metabolite-rich substrate gives higher yields, whereas nutrient-poor substrates yield less **(Bellettini *et al*., 2019; Elkhateeb *et al*., 2020)**. Rich polyphenolic or lignin substrates may stimulate enzyme and metabolite production, while poor substrates reduce biosynthesis, leading to less extractable matter **(Wu *et al*., 2023)**. Wheat straw's heavily lignified and fibrous structure limits solvent penetration, allowing only small amounts of polar compounds soluble in methanol, resulting in lower yields **(Zhang *et al*., 2022; Geremew *et al*., 2023)**. Palm-based samples, by contrast, contain more accessible fibers and less lignified tissue, which improve extraction yields and increase TPC and TFC **(Koba & Ishizaki, 1990; Tahri *et al*., 2016)**.

The relatively high extraction yields obtained from *Pleurotus ostreatus* grown on date kernel substrates can be attributed to the abundance of polyphenolic precursors in date kernels **(Habib *et al*., 2014)**, which are partly degraded by fungal enzymes such as cellulases, hemicellulases, and ligninases. This releases soluble carbohydrates, proteins, and small phenolic molecules that the fungus can assimilate and convert into secondary metabolites, which accumulate in the fruiting bodies **(Luz *et* al., 2012; Li *et al*., 2022)**, thereby increasing extractable mass. The low phenolic content in high-yield extracts may result from a dilution effect, where extract mass is dominated by non-phenolic solubles (polysaccharides, proteins, organic acids). Although nutrient-rich substrates and fungal metabolism enhance overall solubility, they do not necessarily stimulate phenolic biosynthesis, producing high yields but lower phenolic concentrations per g extract **(Torres-Martínez *et al*., 2023; Parí *et al*., 2025)**.

Similarly, dense, highly lignified structures restrict phenolic release, again producing higher yields but weaker phenolic/flavonoid concentrations **(Siddique *et al*., 2021)**.

The high TFC levels observed in first flushes can be explained by the initial abundance of precursors and metabolic energy in the fresh substrate, along with the fungus's tendency to synthesize flavonoids during early fruiting stages for protection **(Elkanah *et al*., 2022)**.

By the second flush, nutrient scarcity and stress alter metabolic priorities toward other phenolic compounds such as phenolic acids and tannins, explaining the peak in TPC at this stage **(Cardoso *et al*., 2021; Sonnenberg *et al*., 2022)**. By the third flush, substrate exhaustion, declining enzymatic activity, and increased physiological stress reduce secondary metabolite production **(Chang & Miles, 1997; Vieira Júnior, 2025)**.

Negative correlations observed for per-extract values confirm that high-yield extracts tend to be diluted with sugars, proteins, and other non-phenolic compounds **(Effiong *et al*., 2024b)**. Yet, the slightly positive correlations expressed per g DM show that larger yields still increase the total mass of phenolics and flavonoids recovered per mushroom **(Barros *et al*., 2008)**. For TPC, the weak positive correlation between extraction yield and DM values indicates that even diluted extracts can support higher phenolic recovery if yields are sufficiently large, especially when moderate-to-high yields are paired with moderate phenolic concentrations. In contrast, TFC displayed a stronger negative correlation (–0.46) with per-extract values, meaning increases in yield contribute less effectively to higher total flavonoid recovery per mushroom. Consequently, achieving high TFC per DM depends more on maintaining strong flavonoid concentration in the extract, whereas high TPC per DM can result from balancing yield with concentration.

3.2.3. Infrared Spectroscopic Profile of the Samples (FTIR)

The FTIR spectra of nearly all extracts and powdered preparations of *Pleurotus ostreatus* across the different flushes revealed the same collection of defining functional groups, reflecting a conserved chemical fingerprint among flushes, with the variations being mostly quantitative rather than qualitative.

According to **Lin-Vien *et al*. (1991)**, a broad and intense absorption region between 3200–3400 cm^{-1} corresponds to hydrogen-bonded O–H groups, whereas bands

between 2940–2850 cm^{-1} originate from C–H stretching. Amide absorptions appear near 1650 cm^{-1} and around 1540 cm^{-1}, while the strong signals spanning 1150–1020 cm^{-1} are attributed to C–O–C or C–O stretching. The region between 1465–1370 cm^{-1} represents CH_2/CH_3 bending, and a distinct band at 900–870 cm^{-1} is also detected. The significant absorbance peaks and their corresponding assignments are summarized in Table 6.

Table 6: Peak assignments of *Pleurotus ostreatus* samples

Wavenumber (cm^{-1})	**Assignment**
3400–3200 (broad)	O–H stretch (± N–H stretch)
2940–2850	C–H stretch ($–CH_2/–CH_3$)
~1700–1650	C=O stretch (amide I / conjugated carbonyls)
~1550–1530	Amide II (N–H bend + C–N stretch)
1465–1450	CH_2/CH_3 bending (scissoring)
1420–1370	O–H bend / CH_3 symmetric bend
1260–1200	C–O stretch / C–N stretch
1150–1020 (strong)	C–O–C and C–O stretch (glycosidic)
~1075–1030	C–O stretch (secondary alcohols)
900–870	β-anomeric C–H deformation / ring modes
850–700	Out-of-plane C–H bends (aromatic) & skeletal modes

In powdered samples prepared with wheat straw, the second flush was the most dominant (Figure 36), a trend also observed in the extracts (Figure 37). Conversely, in powdered samples derived from date kernel substrates, the first flush prevailed over the other flushes, with substantial overlap in the K100 treatment, suggesting that the extracts contained equivalent functional groups in comparable ratios (Figure 38). Palm-based substrates showed overlap at P75, whereas in P25 and P50 the third flush was more dominant in the O–H bending region, and the same was observed for P100 (Figure 39). Extract samples, however, generally showed predominance of the second flush,

except in K100 where it exhibited the lowest bond intensity (Figure 40). Palm-based extracts mostly overlapped, apart from P25, where the third flush presented a minor O–H peak (Figure 41).

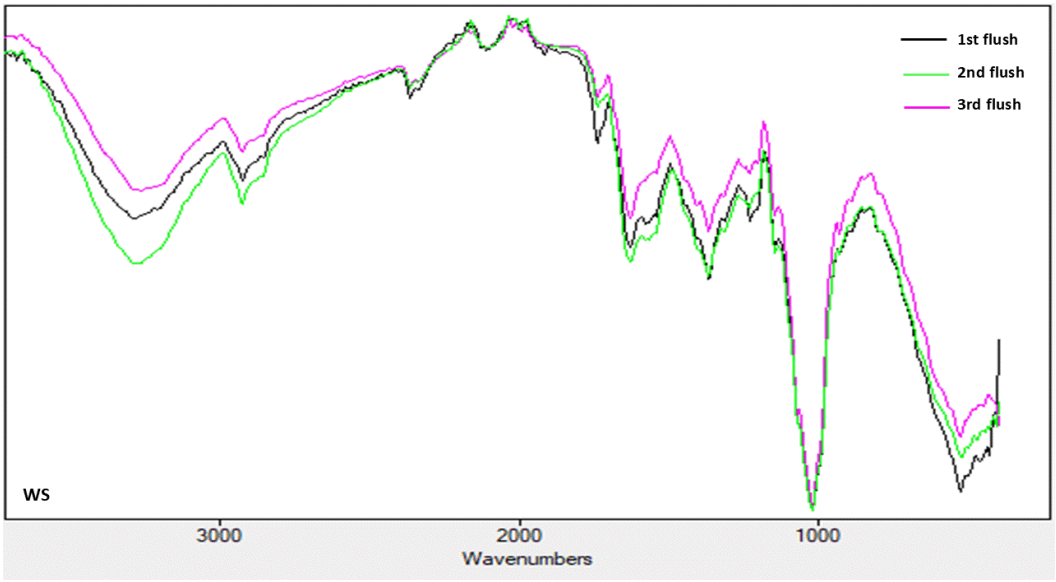

Figure 36: FTIR of WS treatment (powder)

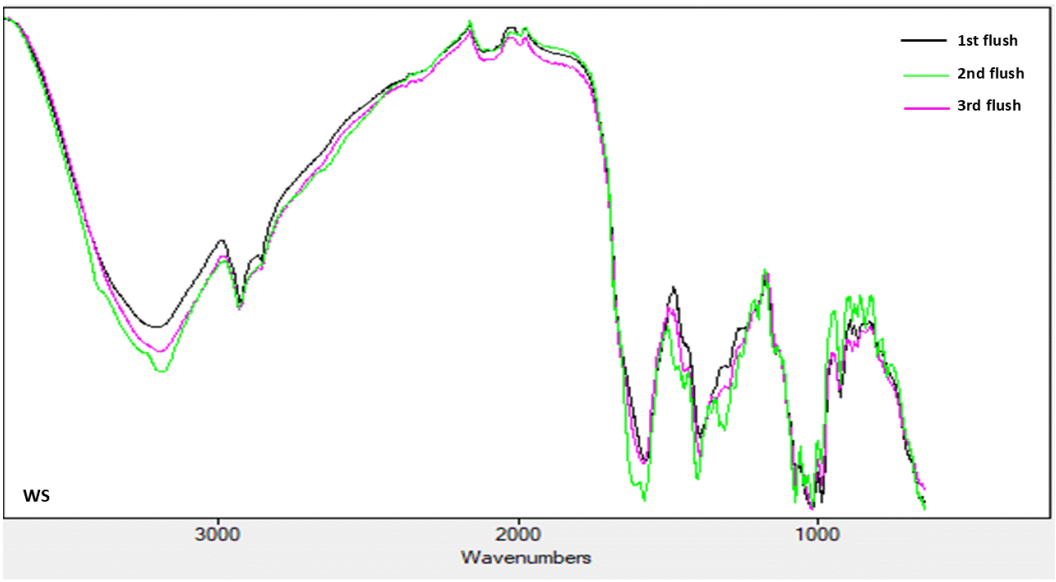

Figure 37: FTIR of WS treatment (extract)

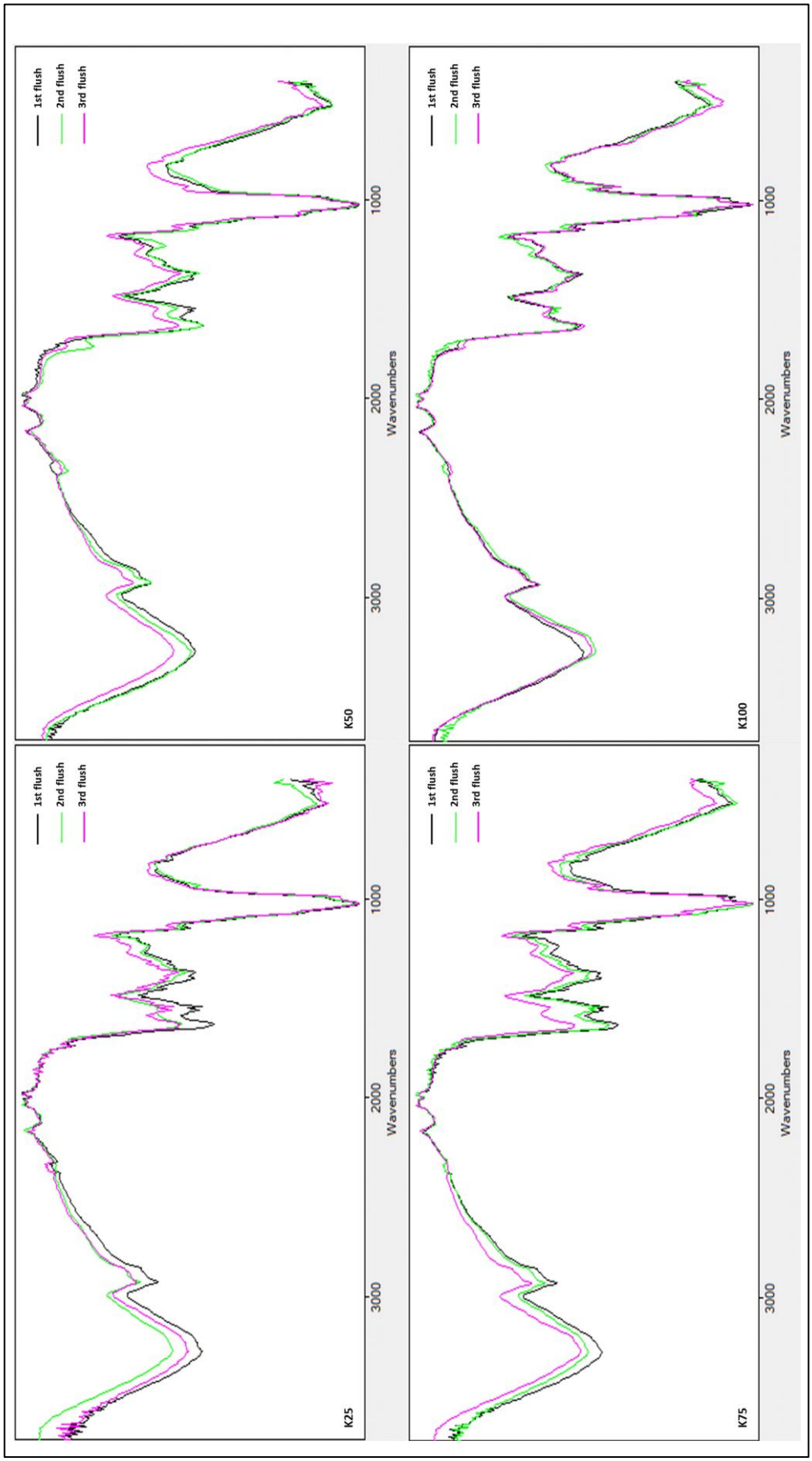

Figure 38: FTIR of K treatment (powder)

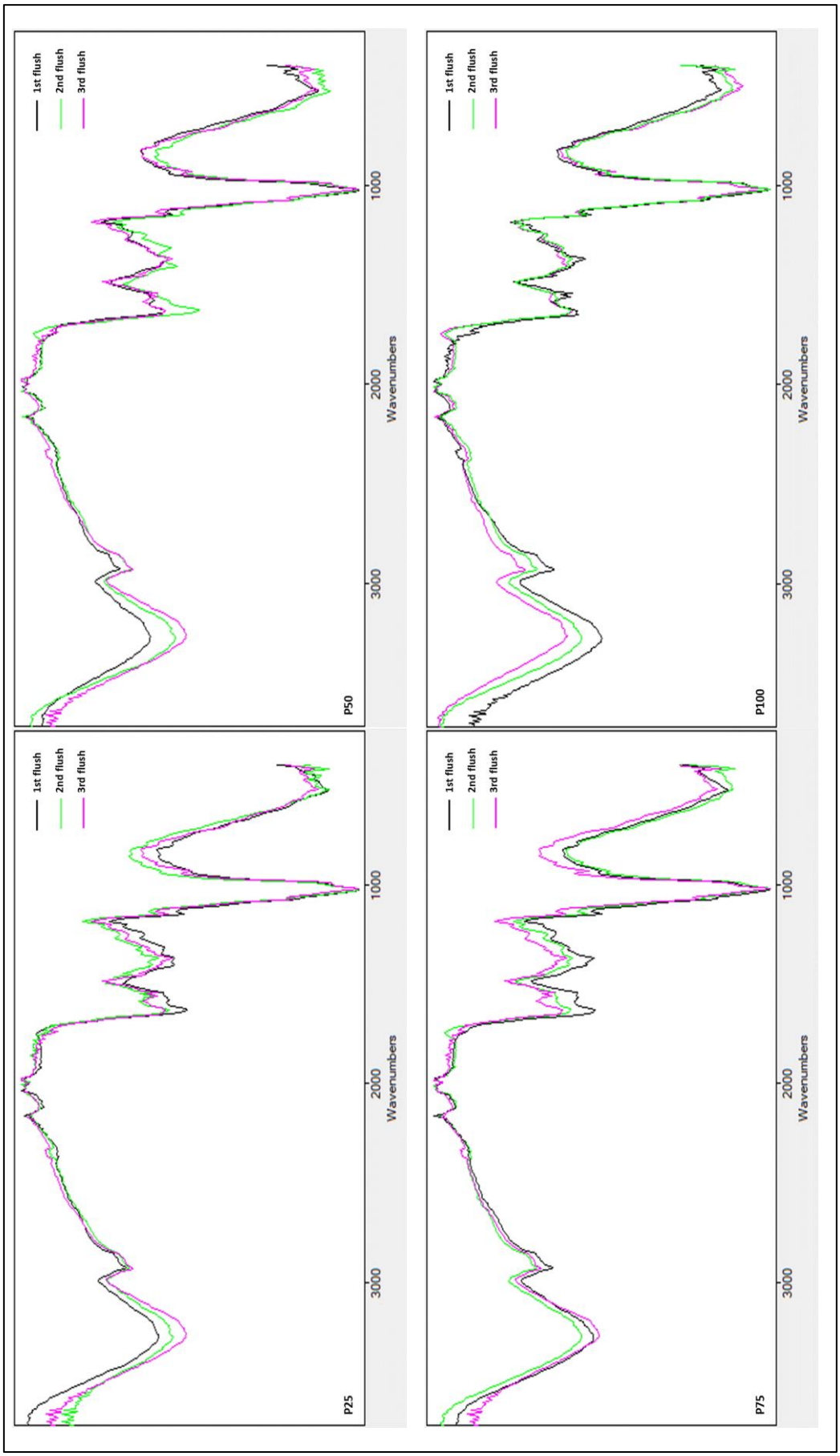

Figure 39: FTIR of P treatment (powder)

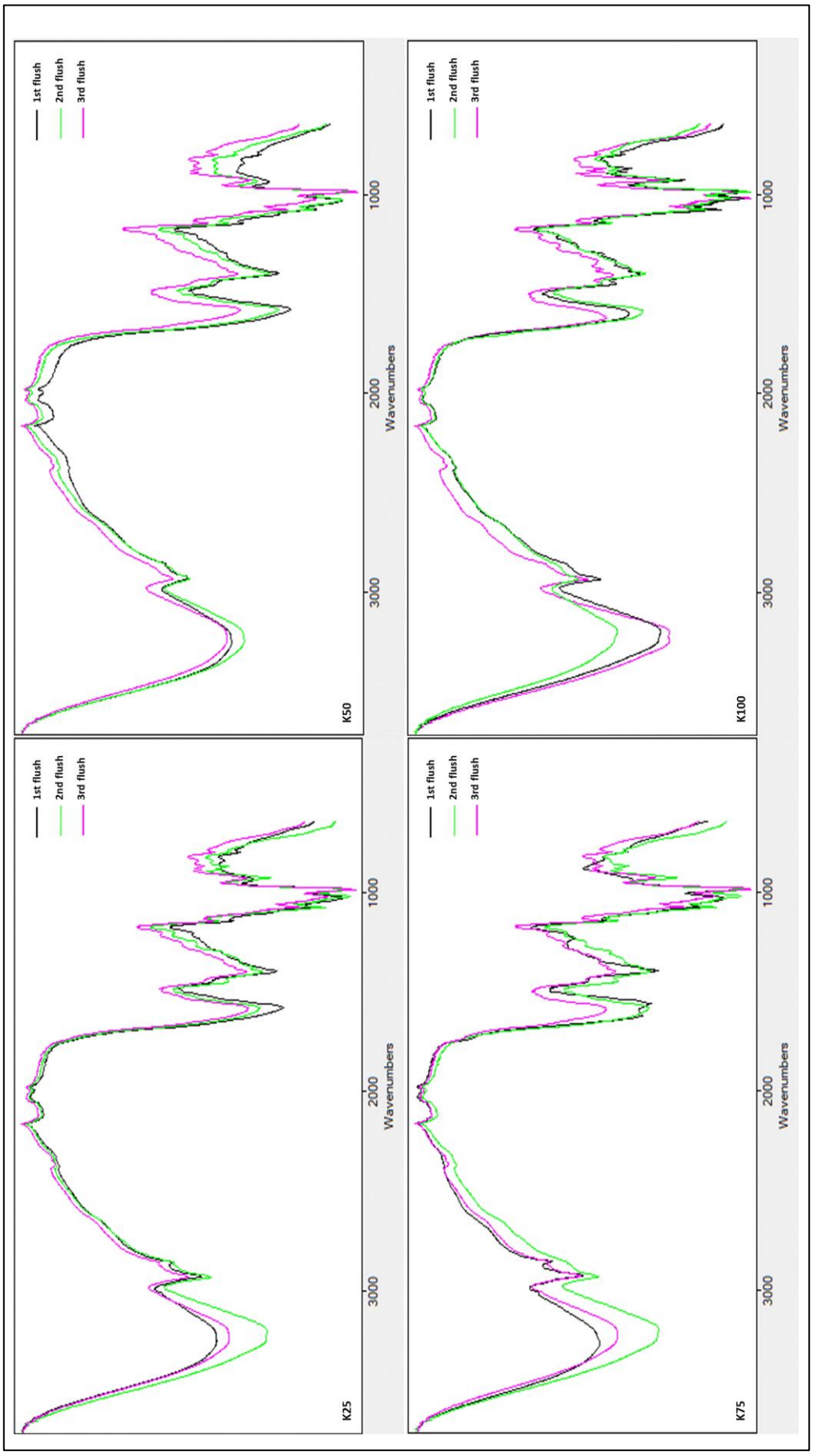

Figure 40: FTIR of K treatment (extract)

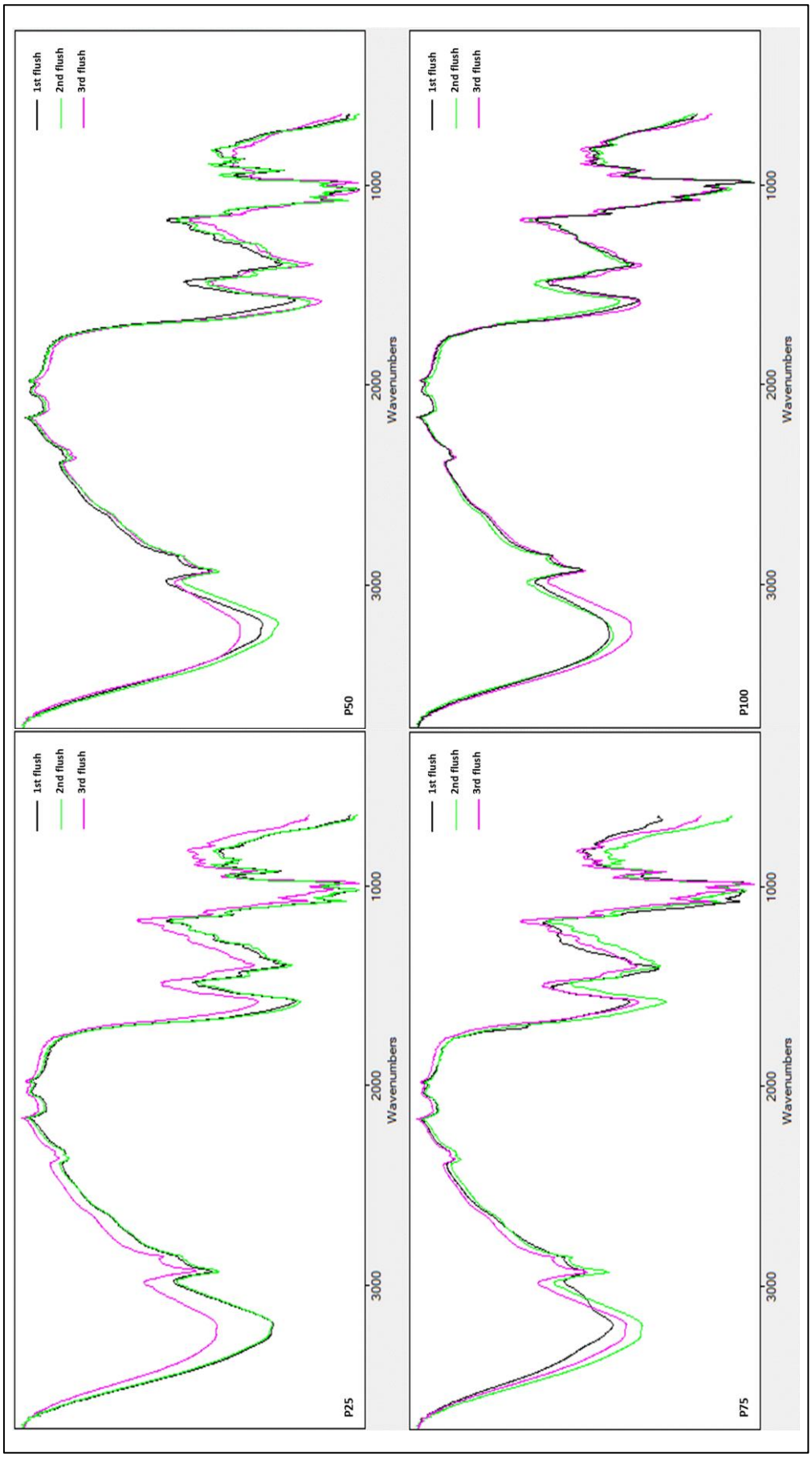

Figure 41: FTIR of P treatment (extract)

Comparisons between powdered samples and hydro-methanolic extracts revealed clear differences: the extracts displayed larger peaks in most bond regions. In date kernel substrates, the first flush yielded the highest compound content in powdered form (Appedix D, Figure D1), while in extracts, palm-based samples showed larger O–H bending peaks, with the exception of the 100% treatments (P100 and K100). In Appendix D, Figure D2 demonstrated considerable overlap among equivalent mixtures of substrates for both extract and powdered preparations. The third flush displayed overlapping peaks in date kernel and palm substrates with higher intensity than wheat straw in powdered samples, but the opposite was true in extracts (Appendix D, Figure D3). Figure D4 and D5 in Appendix D, compared the four substrate mixtures across the three flushes for both powdered and extract forms. Powdered samples overlapped within the C=O region, with slightly higher intensities at 3400–3200 cm^{-1} in mixed treatments, whereas extracts showed wheat straw dominance in the 1550–1700 cm^{-1} region.

According to **Movasaghi *et al*. (2008)**, the 3200–3400 cm^{-1} envelope corresponds to O–H stretching from polysaccharides, overlapped by N–H stretches from proteins. The 2940–2850 cm^{-1} bands represent aliphatic C–H stretches. Protein signatures appear as amide I near 1650 cm^{-1} and amide II around 1540 cm^{-1}. The fingerprint absorptions between ~1150 and 1020 cm^{-1} are linked to glycosidic bonds, consistent with β-glucan-rich polysaccharides such as pleuran **(Deng *et al*., 2025)**. Additional bending from CH_2/CH_3 groups between 1465–1370 cm^{-1} and a 900–870 cm^{-1} β-anomeric vibration confirm a carbohydrate backbone with β-linkages **(Bikmurzin *et al*., 2022)**.

Intensity comparisons revealed minor flush-to-flush variation, mostly within the O–H/amide envelopes and polysaccharide regions, reflecting differences in protein and glucan concentrations rather than the appearance of new functional groups. Overall, the spectra confirmed the consistent presence of polysaccharides (especially β-glucans), peptides/proteins and phenolic/carboxyl groups, with flush-related variation linked to concentration shifts. **Bekiaris *et al*. (2020)** observed that *P. ostreatus* cultivated on olive mill waste and olive leaves displayed more intense absorptions in amide I (~1650 cm^{-1}), amide II (~1525 cm^{-1}), and polysaccharide (~1020 cm^{-1}) bands, indicative of greater protein and glucan levels. These findings align with the current study and with earlier literature **(Baeva *et al*., 2019)**;

3.2.4. LC-MS Analysis of Bioactive Compounds

Semi-quantitative LC-MS profiling revealed a variety of phenolic and flavonoid bioactive compounds, with marked differences in concentration across the tested extracts. Table 7 lists the concentrations of selected metabolites (µg/g extract) detected in the extracts. The substrate yielding the highest level of bioactive compounds was K75 with 6014.29 µg/g, followed by K25 with 5471.25 µg/g. The lowest concentrations were observed in P75 and P100, which contained 4722.11 µg/g.

Among individual compounds, luteolin was the most abundant, followed by quercetin and apigenin. Luteolin reached its highest levels in K25 (second flush) and WS (first flush), and its lowest levels in K75 (second flush) and P50 (third flush). Notably, luteolin was absent in P75/1 (first flush). Quercetin was maximally recorded in P25 (third flush) and minimally in P75 (first flush) and P100 (third flush). Apigenin showed the lowest levels in P75 (first flush), followed by WS (third flush), K25 (third flush), K50 (second flush), and K75 (second flush), while its highest accumulation occurred in K100 (third flush). Quercetin-3-O-glucuronic acid was also identified at low concentrations, with greater amounts in K substrates—particularly K75 (third flush)—and minimal levels in palm-based treatments, where K75 lacked detection in the first flush. Other detected metabolites, present in amounts below 10 µg/g, included arbutin, caffeic acid, sinapic acid, procyanidin, rutin, and naringin, though several were absent in specific flushes. Compounds such as hesperetin and rosmarinic acid were only present as traces (<1 µg/g), suggesting their role as minor constituents. Out of the 46 compounds screened, 18 were identified in measurable concentrations in Table 7, while 28 were absent altogether, including syringic acid; gallic acid; p coumarci acid; oleochantal; hydroxytyrosol; trans ferulic acid; oleuropein; trimethoxyflavone; Amentoflavone; quercetin-3-O-glucoside; Kaempferol-3-O-glucose; Isorhamnetin- 3-O Rutinoside; Kaempferol-3-O-glucuronic acid; Kaempferol-3-O-pentose; Kaempferol-3-O-hexose deohyhexose; Vanillic acid; p-hydroxybenzoic\salicilic acid; Ferulic acid; Trans-cinnamic acid; cathechin\epicathechin; allocathechin\epigallocathechin gallate; gallocathechin\epigallocathechin; cathechin gallate; Myricetin; Tyrosol; Protocathecoic acid; Gentisic acid; Kaempeferol.

Sample P75/1 behaved anomalously, showing markedly different metabolite levels compared with P75/2 and P75/3, possibly due to errors in preparation or analysis.

Table 7: Identification and Quantification (µg/g extract) of Phenolic Compounds by LC-MS in Extracts from the First Three Flushes of Mushrooms Cultivated on Different Substrate Formulas

sample	quercetin	Luteolin	Apigenin	quercetin-3-O-glucuronic acid	syringic acid	ursolic acid	Isorhamnetin-7-O-Pentose	luteoilin 7-O-glucoside	Quercetin-3-O.hexose deoxyhexose	Chlorogenic acid	Caffeic acid	Sinapic acid	Arbutin	Procianidin	Rutin	Narigin	Hesperetin	Rosmarinic acid
ws1	391	701	335	57,69	57,95	45,43	25,76	18,92	53,37	ND	6,48	3,88	2,61	1,12	3,94	0,10	0,32	0,45
WS2	663	495	422	190,05	68,67	24,00	26,49	19,35	46,24	ND	ND	3,65	3,45	1,87	4,06	0,88	0,58	0,81
WS3	481	614	317	119,90	85,87	30,88	24,42	27,28	29,97	ND	4,52	4,36	2,74	3,38	2,23	0,78	0,46	0,60
K25/1	396	610	330	209,62	41,80	42,92	21,47	20,96	25,65	ND	3,70	4,29	1,39	2,34	1,28	0,79	0,35	0,40
K25/2	668	649	452	274,75	66,13	30,47	18,64	18,88	17,81	ND	5,00	4,22	2,32	4,46	0,55	1,12	0,57	0,72
K25/3	376	551	296	102,88	82,96	29,71	26,93	26,25	ND	34,46	4,06	3,93	1,32	5,52	ND	0,57	0,31	0,62
K50/1	230	569	405	492,92	40,86	29,29	21,28	21,07	17,35	ND	6,82	1,87	2,91	ND	1,08	1,61	0,30	0,54
K50/2	615	494	308	236,21	47,63	32,32	20,38	19,91	12,45	23,18	4,62	4,04	1,56	1,72	1,18	1,10	0,53	0,56
K50/3	300	589	408	238,38	63,54	29,65	28,62	18,96	ND	11,36	3,17	4,19	1,54	5,60	ND	1,25	0,30	0,60
K75/1	360	530	301	203,78	51,76	25,14	18,84	19,25	ND	ND	9,34	2,59	3,00	ND	ND	2,72	0,36	0,67
K75/2	668	407	280	345,84	30,68	37,25	19,25	19,79	19,43	41,93	3,03	3,36	1,96	4,87	1,89	0,83	0,56	0,50
K75/3	431	481	496	1028,31	58,92	25,70	18,43	15,03	21,75	8,55	2,04	4,23	3,57	0,18	2,17	2,05	0,35	0,76
K100/1	383	583	396	115,72	73,04	23,39	21,00	20,20	ND	ND	ND	3,26	1,57	ND	ND	0,89	0,25	0,71
K100/2	689	441	297	94,27	53,23	37,31	20,72	20,40	7,88	52,11	4,43	4,03	1,04	6,08	ND	0,26	0,59	0,51
K100/3	361	526	556	160,39	104,20	25,05	11,23	19,83	15,63	8,79	ND	4,16	2,18	3,95	0,35	0,66	0,32	0,88
P25/1	462	617	411	87,12	62,49	21,34	20,90	21,14	ND	ND	ND	ND	2,69	ND	ND	1,54	0,33	0,75
P25/2	405	456	347	79,69	50,11	31,31	21,23	24,41	14,51	ND	7,04	4,00	2,53	6,83	1,12	0,31	0,42	0,59
P25/3	733	572	457	65,87	88,25	28,15	20,71	26,15	42,31	14,40	6,32	3,77	2,81	ND	3,53	1,32	0,59	0,84
P50/1	455	551	417	422,37	50,80	32,73	22,74	22,97	66,77	15,65	5,38	2,71	3,46	ND	5,17	6,92	0,37	0,80
P50/2	361	529	370	87,74	52,46	28,59	23,00	21,87	90,18	ND	6,07	4,13	4,39	8,80	8,24	1,51	0,36	0,52
P50/3	372	405	383	51,50	82,11	31,08	20,62	23,56	28,56	29,66	4,16	4,11	2,74	3,35	2,19	3,63	0,30	0,67
P75/1	138	ND	90	ND	ND	31,28	ND	ND	ND	ND	ND	ND	0,48	3,36	ND	0,44	0,12	0,12
P75/2	367	527	330	57,16	59,56	33,85	19,73	20,09	3,77	32,72	0,24	4,33	2,07	9,67	1,20	3,53	0,33	0,44
P75/3	314	527	384	86,52	62,06	29,98	21,09	19,51	22,53	23,07	3,58	3,68	2,56	6,68	1,89	3,96	0,33	0,70
P100/1	429	540	414	156,25	ND	23,19	22,36	22,95	ND	40,17	3,53	2,99	1,50	6,91	ND	1,03	0,35	0,80
P100/2	371	521	411	165,32	107,71	32,01	21,49	25,66	ND	ND	4,07	5,43	1,75	0,21	ND	2,73	0,35	0,47
P100/3	83	570	397	126,70	91,23	28,64	18,08	15,08	23,17	12,49	2,35	4,10	1,56	7,29	2,21	2,13	0,30	0,64

ND = Not detected

Interestingly, the presence of quercetin in this study contrasts with most prior reports, since LC-MS and HPLC analyses typically detect only trace or negligible amounts of quercetin in *P. ostreatus* **(Bhekti *et al*., 2023)**. Nevertheless, luteolin was consistently abundant **(Abou Raya *et al*., 2014)**, as was apigenin **(Elhusseiny *et al*., 2021)**. Both are widely recognized for antioxidant, anti-inflammatory, and anticancer properties **(Justyńska *et al*., 2025)**. Luteolin acts as a free radical scavenger and lipid peroxidation inhibitor, whereas quercetin regulates signaling pathways and mitigates oxidative stress **(Kumar & Pandey, 2013; Boots *et al*., 2008)**. The high levels of luteolin and quercetin observed here underscore the potential of these extracts as sources of nutraceutical or pharmaceutical agents.

Secondary metabolites like arbutin, rosmarinic acid, and ursolic acid, although detected at low levels, are also linked to antimicrobial and anti-inflammatory activity **(Lee & Kim, 2012; Noor *et al*., 2022; Liu *et al*., 2024)**. Even the modest presence of rosmarinic and syringic acids, it could enhance the extracts antioxidant effectiveness through synergistic effects **(Skroza *et al*., 2022)**.

The absence of certain metabolites, such as gentisic acid, likely reflects limited biosynthesis in *P. ostreatus* or instability during processing. Compared with other reports, the non-detection of tyrosol, protocathechuic acid, kaempferol derivatives, oleuropein, oleocanthal, hydroxytyrosol, lycopene, delphinidin derivatives, and diverse flavonoid glycosides is consistent with the metabolic profile of this mushroom. Literature indicates that *P. ostreatus* metabolomes are dominated by amino acids, dipeptides, and simple phenolic acids, while more complex flavonoids and olive-associated metabolites are rare or absent **(Selvamani *et al*., 2018; Pellegrino *et al*., 2022; Valério *et al*., 2024)**. Compounds like cinnamic, ferulic, p-coumaric, gallic, and vanillic acids are more typical but vary depending on growth medium and extraction protocols. Pigments like lycopene and anthocyanins such as delphinidin are rarely observed in fungi, explaining their absence.

Mycochemical and antioxidant analyses consistently confirm that *P. ostreatus* extracts contain quantifiable phenolic and flavonoid contents, which contribute to their antioxidant potential. Detected flavonoids tend to be structurally simple, and kaempferol derivatives are either absent or only present in minimal amounts. Substrate composition exerts a major influence on amino acid and dipeptide profiles, with less impact on complex flavonoids or phenolic glycosides **(Fakoya *et al*., 2020; Pellegrino**

***et al*., 2022; Pukalski & Latowski, 2022; Effiong *et al*., 2024b)**. Thus, the non-detection of these compounds in the current study agrees with established literature, reinforcing the view that the metabolome of *P. ostreatus* is species-specific, method-dependent, and primarily composed of peptides and simple phenolics rather than complex flavonoids or olive-derived compounds.

3.3.Biological Activities

3.3.1. Antioxidant Activity

all antioxidant activities of tested samples were measured the amount needed to Achiving 50% of the activity, it is determined and expressed by the amount of mushroom extract (mg) required per mL of reaction medium, in parallel, the results were converted into µM Trolox equivalents (TE) and expressed relative to mushroom dry weight (µM TE/g DW) expressing the antioxidant capacity of the samples, the full dataset With Significant difference, is available in Appendix E, F and G.

All extract samples reported lower activity compared to standards used (Appendix H) with dominance in reducing, chelating and scavenging antioxidant activities respectively; extracts of second flush consistently displayed the highest antioxidant activity in most assays, suggesting that the fungus synthesizes larger amounts of low-molecular-weight antioxidants during this stage. Nevertheless, in specific tests such as CCA, and hydroxyl radical scavenging, the first flush outperformed the others for some samples. Substrates based on wheat straw generally gave the greatest total antioxidant capacity (TAC) and ABTS activity across flushes. By contrast, date kernel extracts exhibited stronger radical scavenging activity, whereas palm-based substrates mushroom extracts demonstrated superior reducing potential. Regarding metal chelation, mushrooms cultivated on date kernel substrates bound iron more efficiently, while palm-based substrates favored copper chelation. The same pattern was detected in measuring the antioxidant activity in dry mushroom weight.

3.3.1.1. Scavenging Activity

For DPPH activity, differences between flushes within the same substrate were minimal, except for P25 where the second and third flushes diverged significantly (Appendix E, Table E1). Figure 42 showed that strongest DPPH activity in mushroom extracts was found in the third flush of P25 (502.93 µg/ml), followed by the second and

third flushes of WS (537.54 µg/ml and 529.85 µg/ml, respectively) and the second flush of K100 (546.88 µg/ml) with no significant difference. The weakest activity was observed in P75/1 (962.02 µg/ml), followed by P25/2, P50/2, and P75/2 (936.46 µg/ml, 916.92 µg/ml, and 926.01 µg/ml, respectively). For measuring the activity in a g of powdered mushroom, where the highest activity registered was in second flush of mushroom cultivated on date based substrate specially for K100 (10,89 µM TE/g DW) with no significant difference with 3rd flush of P25, 2nd and 3rd flush of WS and the lowest at 4,13 µM TE/g DW was with 3rd flush of K25, the samples showed lower capacity in second flush of mushroom harvested from kernel based substrate while for palm based substrate was in 1st and 2nd flush (Figure 43 and Appendix E in Table E2).

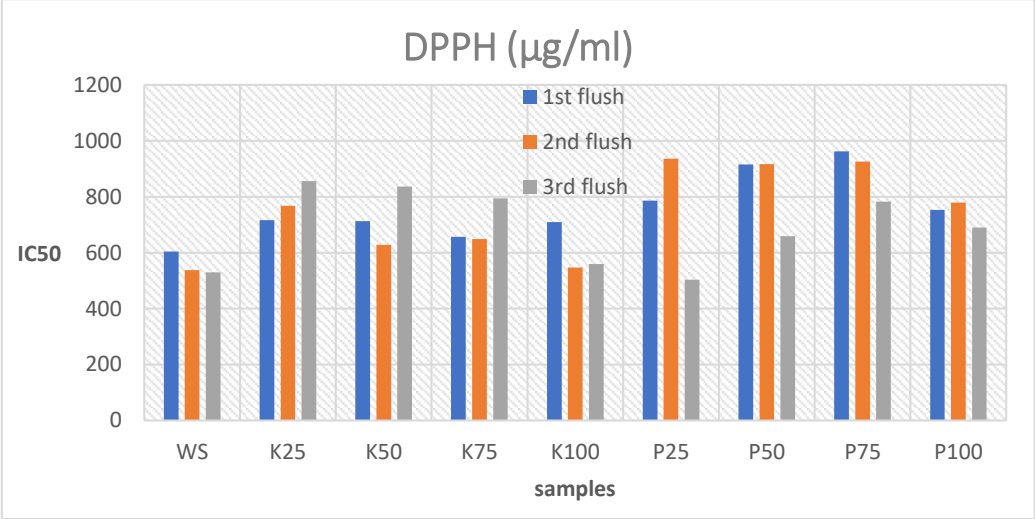

Figure 42: IC_{50} values (µg/mL) of DPPH scavenging antioxidant activity of *P.ostreatus* extracts from three first flushes cultivated on different substrate formulas.

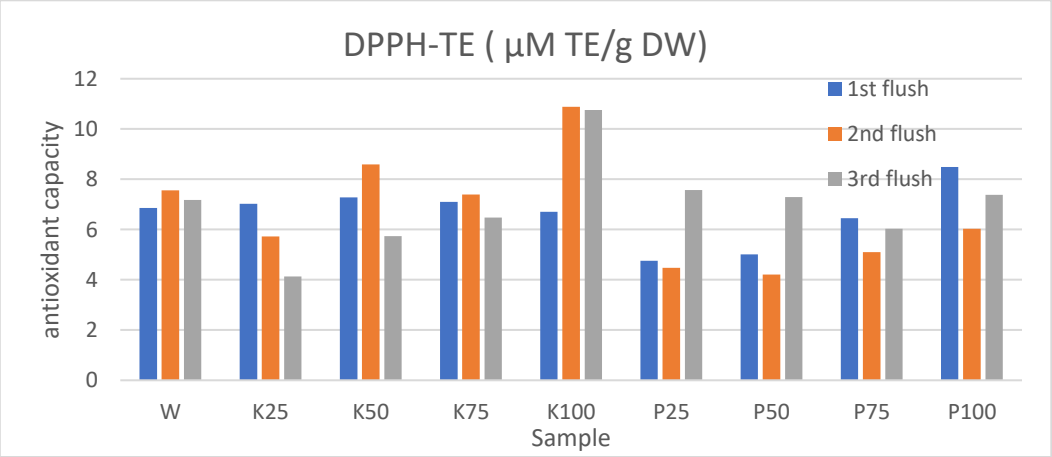

Figure 43: DPPH scavenging antioxidant capacity (µM TE/g DW) of *P.ostreatus* extracts from three first flushes cultivated on different substrate formulas.

For ABTS activity (Appendix E, Table E1), the maximum scavenging of extracts was recorded in P25/1 (122.39 µg/ml), WS/1 (142.75 µg/ml), K75/1 (152.35 µg/ml), and K75/2 (153.04 µg/ml). Palm-based substrates produced the lowest ABTS activity, ranging from 186.42 µg/ml to 1157.65 µg/ml (Figure 44). But when expressed in g of dry weight (Appendix E in Table E2), P75/1 and P100/1 showed higher activity (0,272 µM TE/g DW and 0,137 µM TE/g DW respectively) compare to WS (ranging from 0,945 to 1,263 µM TE/g DW) and K samples which registered lower activity (Figure 45).

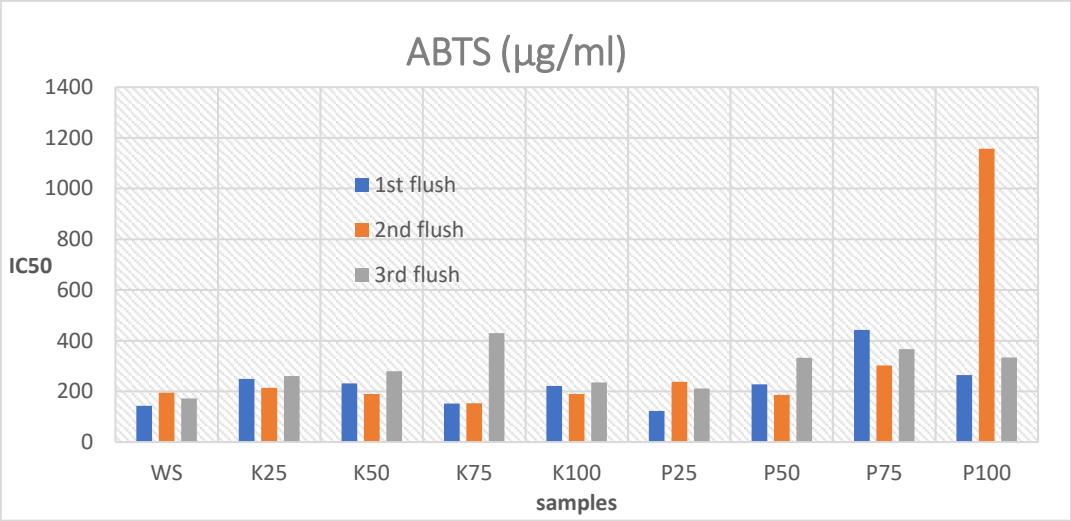

Figure 44: IC_{50} values (µg/mL) of ABTS scavenging antioxidant activity of *P.ostreatus* extracts from three first flushes cultivated on different substrate formulas.

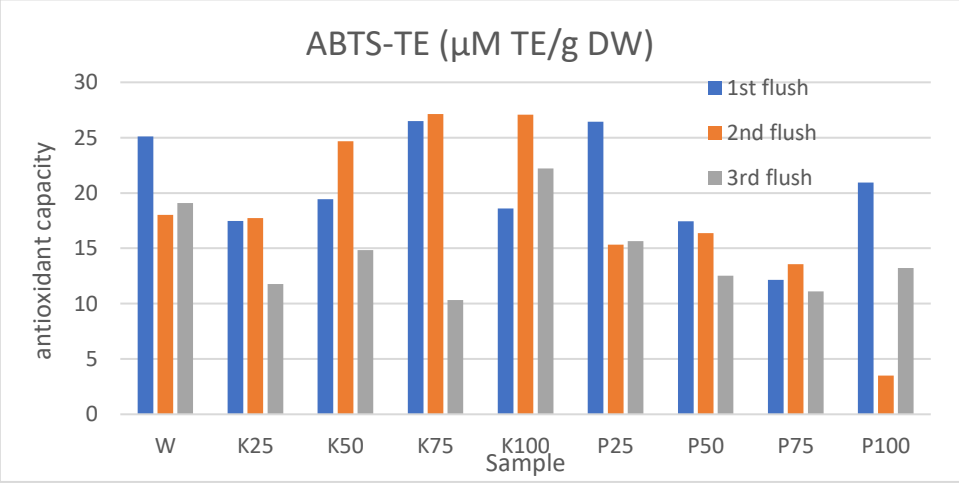

Figure 45: ABTS scavenging antioxidant capacity (µM TE/g DW) of *P.ostreatus* extracts from three first flushes cultivated on different substrate formulas.

Hydroxyl radical scavenging assays showed in Figure 46 and Appendix E in Table E1 that extracts of mushroom harvested from palm-based treatments typically gave the weakest results (1159.08–2198.84 µg/ml), except for P50/2 which, along with K100/2 (868.38 µg/ml and 837.71 µg/ml, respectively), displayed the strongest activity however, as for their activity in g of dried mushroom weight, 1st and 2nd flush of P50 and P100 registered high activity (ranging from 50,50 µM TE/g DW to 65,18 µM TE/g DW while 2nd and 3rd flush of P25 and P100 have lower activity (ranging from 21,57 µM TE/g DW to 32,74 µM TE/g DW) as shown in Figure 47 and Appendix E in Table E2, however, samples harvested from date kernel based substrate registered the highest activity in first flush with an IC50 ranging from 915,54 µg/ml to 1041,89 µg/ml and antioxidant capacity from 64,22 µM TE/g DW to 66,21 µM TE/g DW while the highest with a value 88,49 µM TE/g DW noted in 2nd flush of K100 (IC50 = 873,71 µg/ml).

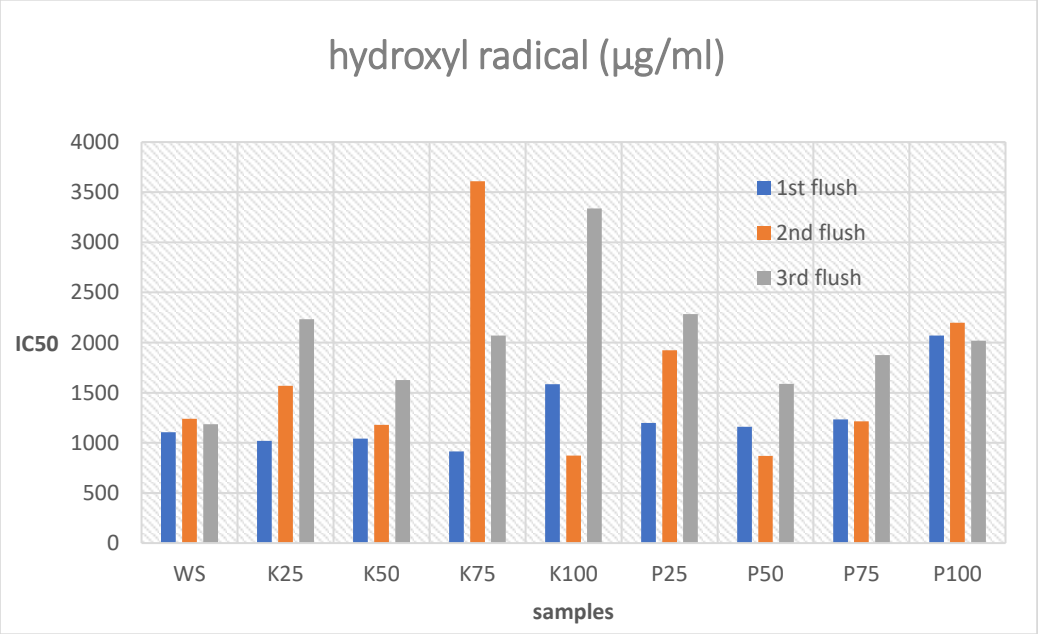

Figure 46: IC_{50} values (µg/mL) of Hydroxyl Radical scavenging antioxidant activity of *P.ostreatus* extracts from three first flushes cultivated on different substrate formulas.

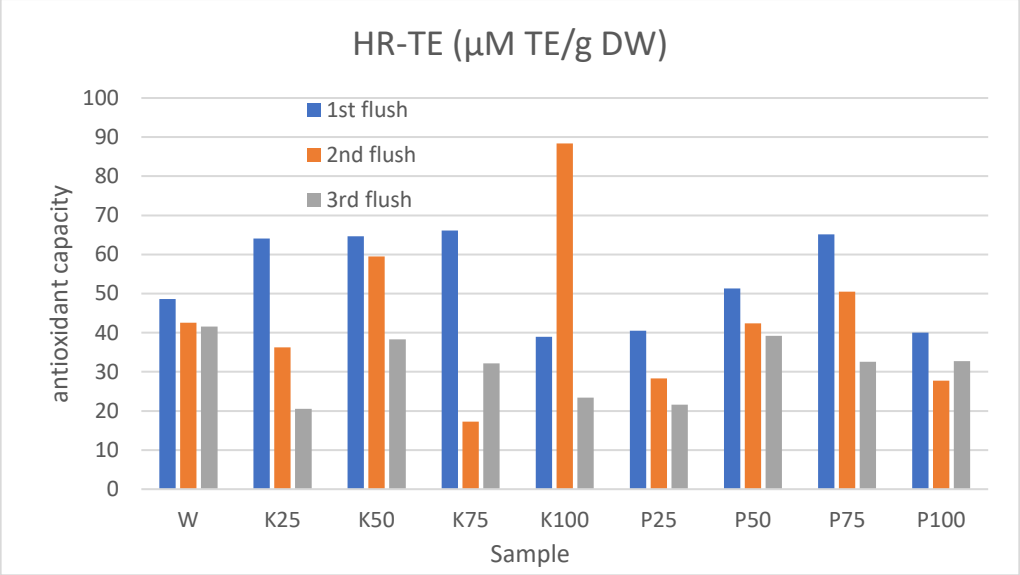

Figure 47: hydroxyl radical scavenging antioxidant capacity (µM TE/g DW) of *P.ostreatus* extracts from three first flushes cultivated on different substrate formulas.

Gebru, Faye, & Belete (2024) reported DPPH scavenging IC_{50} values of 0.46 mg/mL for *Pleurotus ostreatus* grown on field pea substrate, and as high as 13.17 mg/mL when cultivated on other agro-wastes. These results align with the present study, where IC_{50} values ranged from 0.502 to 0.936 mg/mL, indicating exceptionally strong antioxidant activity compared to findings from other studies and mushroom species **(Arbaayah & Umi Kalsom, 2013; Woldegiorgis *et al*., 2014; Leong *et al*., 2021)**. The high activity observed may be due to the solvent used, as 80% methanol generally produces more potent extracts than ethanol or hot water **(Tsai *et al*., 2009)**.

ABTS radical scavenging capacity of *P. ostreatus* varies considerably depending on the extraction method and solvent. While some studies reported weak activity IC_{50} > 500 µg/mL (**Guzmán *et al*., 2016; Fomekong *et al*., 2024)**, the values obtained here are comparatively higher, suggesting lower antioxidant activity. On the other hand, crude extracts have demonstrated very strong activity, with IC_{50} as low as 11.22 ± 1.81 µg/mL **(Elhusseiny *et al*., 2021)**. Ethanolic extracts (EE96) generally exhibit moderate activity around 108.07 µg/mL **(Rahimah et al., 2019)**, while ethyl acetate fractions incorporated in cream formulations reached values near 84.61 µg/mL.

Hydroxyl radical scavenging activity has also been documented for *P. ostreatus*. **Jayakumar *et al*. (2009)** reported an IC_{50} of 8 mg/mL for ethanolic extracts, while

other mushrooms such as *Agaricus bisporus* and methanolic extracts of black, snow, and silver ear mushrooms exhibited IC_{50} values above 5 mg/mL **(Mau *et al*., 2001; Liu *et al*., 2013)**. *Pleurotus flabellatus* (pink oyster) showed a much higher IC_{50} of 56.62 mg/mL **(Liu *et al*., 2013)**. These comparisons reinforce the effectiveness of *P. ostreatus* as a hydroxyl radical scavenger, with activity potentially enhanced when cultivated on date palm residues.

Antioxidant activity is strongly linked to phenolic compounds, particularly quercetin, one of the most effective flavonoids in both DPPH and ABTS assays due to its hydroxyl groups and conjugated double bonds **(Dolatabadi *et al*., 2013)**. In this study, kernel-based substrates yielded higher quercetin levels than palm-based ones, which likely explains the stronger activity in date kernel samples. However, hydromethanolic extraction also recovers non-phenolic antioxidants such as polysaccharides and amino acids **(Chirinang & Intarapichet, 2009; Hasan & Abdulhadi, 2023; Effiong *et al*., 2024a)**, further contributing to scavenging effects.

3.3.1.2. Reducing Power

The data in reducing power (Appendix F, Table F1) showed that in the FRAP assay, the highest activity of extracts was observed in the third flush of K50 (12.43 µg/mL), followed by the second flush of WS (20.50 µg/mL). The lowest values occurred in K25/1, K75/2, and K100/2 (75.51–78.08 µg/mL). Palm-based substrates generally showed higher FRAP activity, while date kernel substrates gave weaker results, with activity decreasing as kernel proportion increased (Figure 48). Meanwhile measuring the activity in dried mushroom showed almost the same trend when kernel based substrate demonstrate higher activity in 3rd flush with highest value in K50 (134,39 µM TE/g DW) and lowest activity in 2nd flush (from 21,72 µM TE/g DW to 28,25 µM TE/g DW) except for K25 registering the lowest activity in 3rd flush with a value of 15,75 µM TE/g DW (Figure 49 and Appendix F, Table F2). As for mushroom of palm based substrate a moderated activity is noted in 1st and 2nd flush and low in 3rd flush.

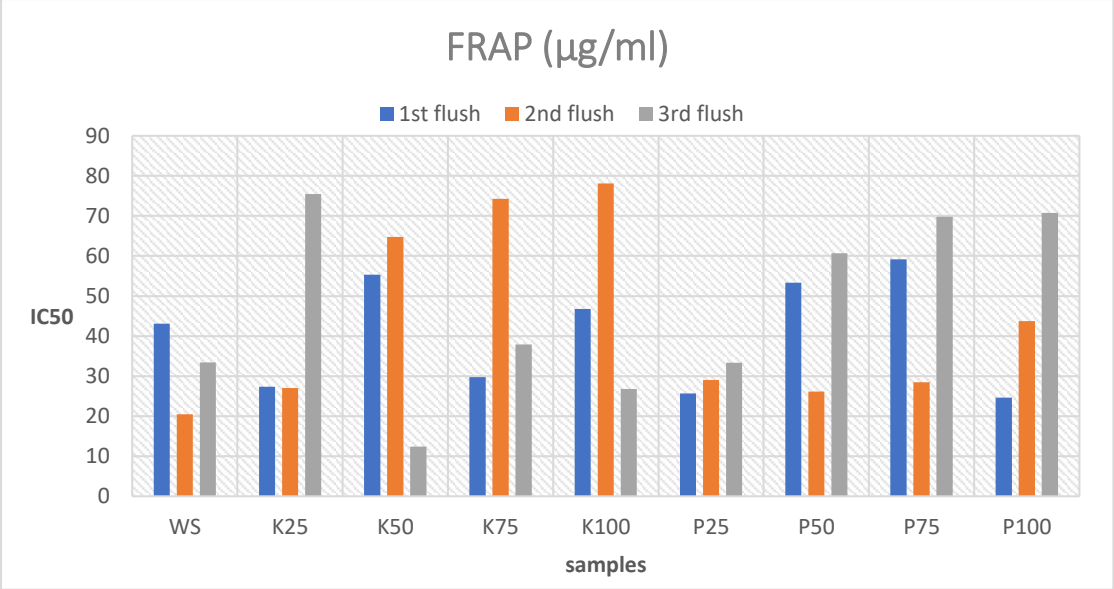

Figure 48: EC_{50} values (µg/mL) of FRAP reducing antioxidant activity of *P.ostreatus* extracts from three first flushes cultivated on different substrate formulas.

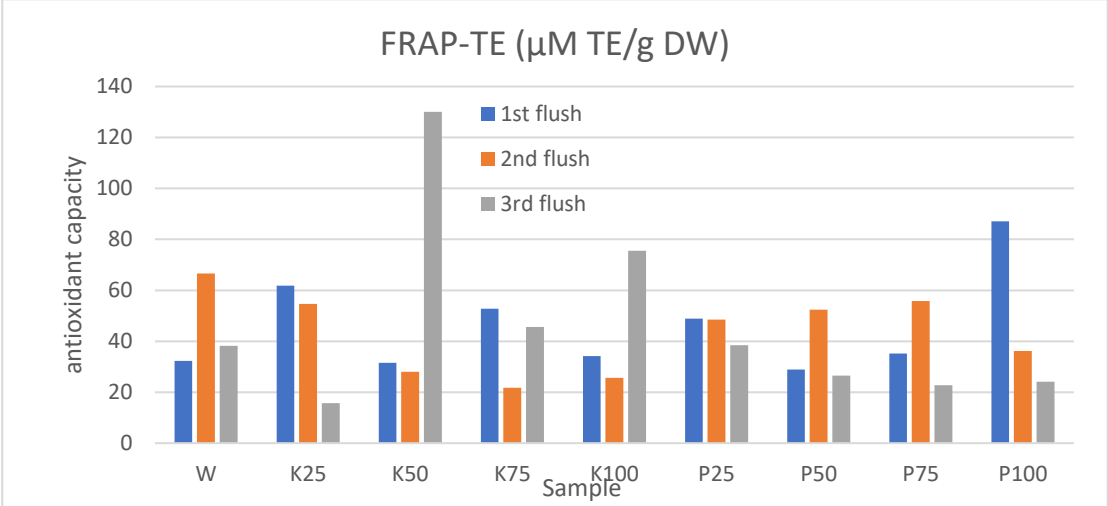

Figure 49: FRAP (µM TE/g DW) reducing antioxidant capacity of *P.ostreatus* extracts from three first flushes cultivated on different substrate formulas.

For CUPRAC, K100 in the second and third flushes and P25/2 exhibited the strongest activity (98.51–115.99 µg/mL). P25/1 (130.55 µg/mL) and P50/3 (131.37 µg/mL) also performed well, whereas wheat straw samples displayed weak activity (388.15–482.28 µg/mL). Increasing palm substrate proportions reduced CUPRAC activity, with P25 and K100 emerging as the most effective combinations (Figure 50

and Appendix F, Table F1). When expressed in µM TE/g DW (Figure 51 and Appendix F, Table F2), the same trend observed with very low activity in wheat straw based substrate (40,02 39 µM TE/g DW to 48,74 39 µM TE/g DW) and remarkable capacity in K100 (from 153,55 µM TE/g DW to 245,00 µM TE/g DW).

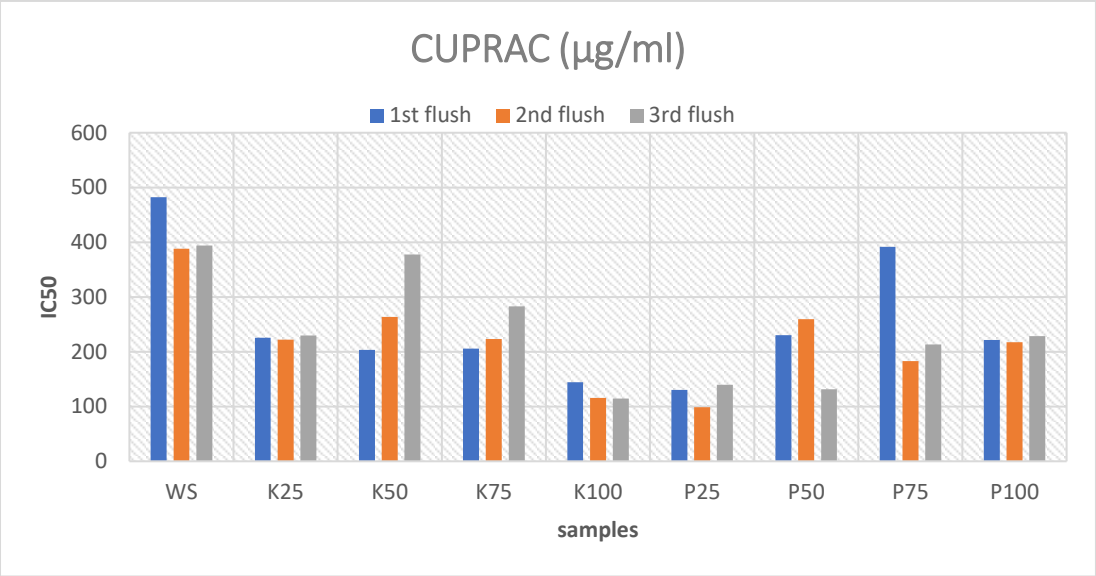

Figure 50: EC_{50} values (µg/mL) of CUPRAC antioxidant activity of *P.ostreatus* extracts from three first flushes cultivated on different substrate formulas

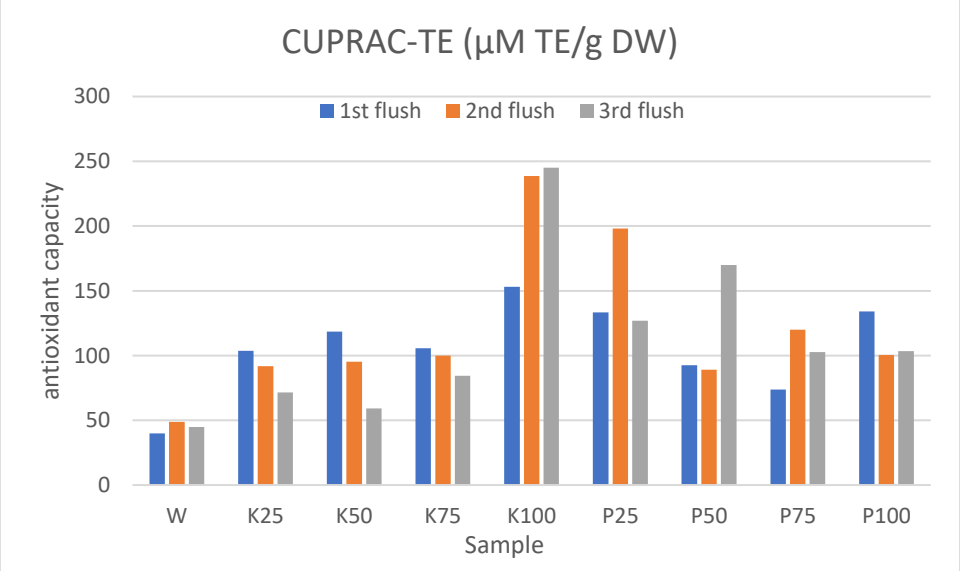

Figure 51: CUPRAC (µM TE/g DW) reducing antioxidant capacity of *P.ostreatus* extracts from three first flushes cultivated on different substrate formulas

Figure 52 and 53 (Appendix F, Table F1 and F2) showed also the same pattern in total antioxidant capacity. For mushroom extracts, wheat straw-based samples consistently demonstrated high TAC activity across flushes (76.38–96.60 µg/mL and 63,77–74,25 µM TE/g DW), with strong values recorded in K50/2 (88.85 µg/mL and 91,27 µM TE/g DW), K75/2 (98.33 µg/mL and 72,61 µM TE/g DW), P50/2 (94.40 µg/mL and 62,06 µM TE/g DW), and P25/1 (80.66 µg/mL and 68,97 µM TE/g DW). In contrast, 3rd samples of palm based substrate showed the lowest activity (145,16-225,51 µg/ml and 29,61–49,18 µM TE/g DW) with 1st flush of kernel based substrate (139,18–188,54µg/ml and 37,63–52,80 µM TE/g DW).

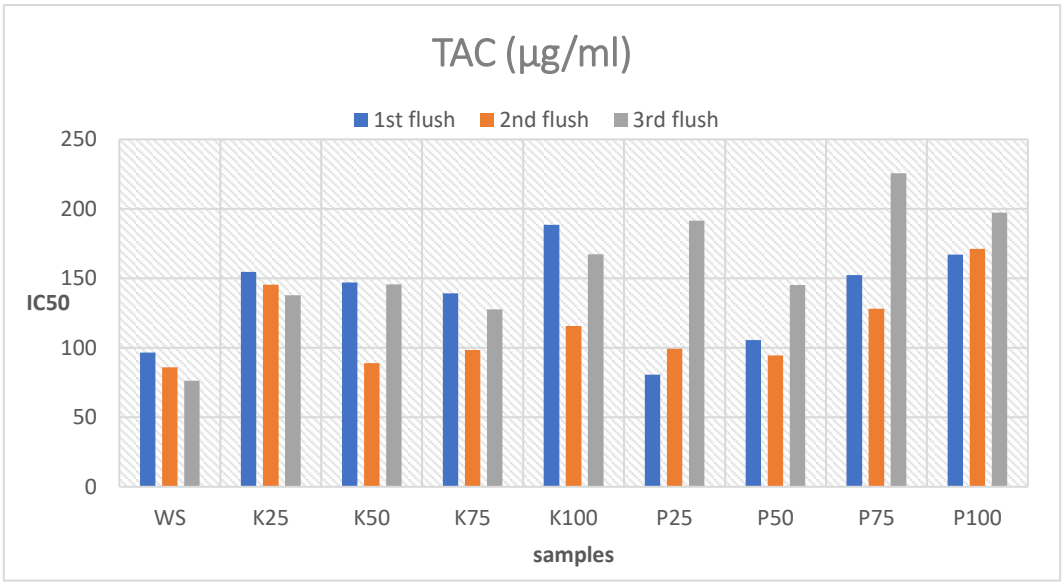

Figure 52: EC_{50} values (µg/mL) of TAC antioxidant activity of *P.ostreatus* extracts from three first flushes cultivated on different substrate formulas

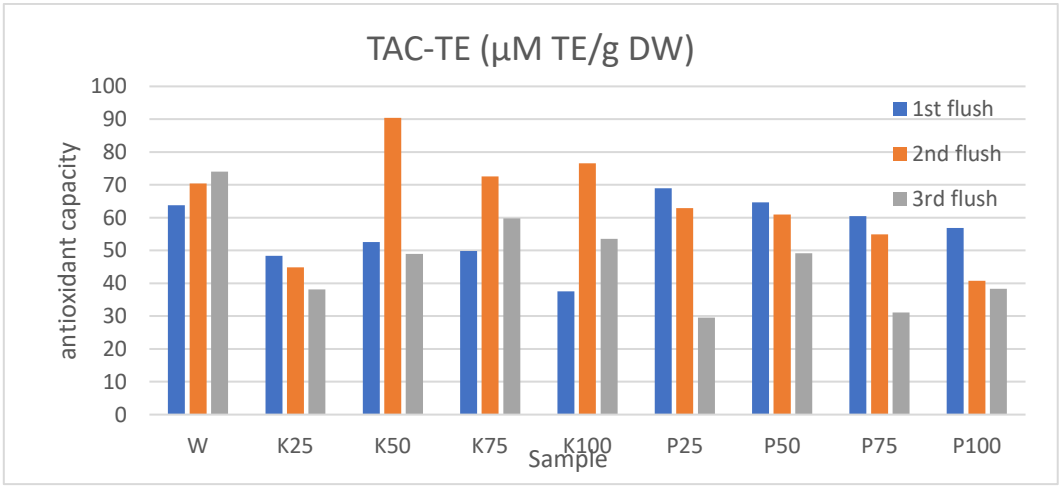

Figure 53: TAC (µM TE/g DW) reducing antioxidant capacity of *P.ostreatus* extracts from three first flushes cultivated on different substrate formulas

The FRAP assay of hydromethanolic extracts yielded EC_{50} values of 12–78 µg/mL, reflecting strong electron-donating ability. These are far lower than previously reported—for example, 3.31 mg/mL for methanolic extracts **(Reis *et al*., 2012)** and 3.85–7.7 mg/mL for lyophilized mycelium extracts **(Vamanu, 2012)**. Such differences likely stem from variations in phenolic structure and composition, as well as synergistic or antagonistic interactions among antioxidant constituents **(Munteanu & Apetrei, 2021; Bolling *et al*., 2012)**.

In CUPRAC assays, methanolic extracts of *P. ostreatus* were reported to have EC_{50} values of 433.3 µg/mL, much weaker than ethyl acetate extracts (102.3 µg/mL) or hexane extracts (236.4 µg/mL) **(Tel *et al*., 2015)**. The present study supports these findings: wheat straw-grown mushrooms showed low activity (388.01–482.28 µg/mL), while kernel- and palm-based substrates yielded stronger activity (98.51–115.99 µg/mL), comparable to ethyl acetate extracts. However, they remained less potent than certain medicinal mushrooms such as *Ganoderma lucidum* **(Tel *et al*., 2015; Duru *et al*., 2019)**. Enhanced CUPRAC activity in palm- and kernel-supplemented substrates is likely linked to their higher phenolic and lipid content, which contribute antioxidant precursors **(Atila, 2019; Mrabet *et al*., 2022; Niloy *et al*., 2025)**.

TAC assay results in this study were similar to those of *Launaea procumbens* chloroform extracts (78.3 µg/mL), though weaker than its methanolic extracts (64.27 µg/mL) **(Khan *et al*., 2012)**. Still, they were stronger than values reported for herbs like *Ziziphora taurica* 1840 µg/mL; **(Tomczyk *et al*., 2019)**, highlighting the relatively high antioxidant activity of the tested samples.

3.3.1.3. Chelating Ability

In chelating ability (Appendix G in Table G1), Date kernel substrates showed stronger ferric ion-chelating ability (Figure 54 and 55), particularly in the second flush (82.67–87.20 µg/mL and 306,31–428,78 µM EDTAE/g DW), while palm-based substrates exhibited weaker ferric chelation but stronger copper chelation, especially P50 ranging from 511.88 to 658.49 µg/mL (139,39–201,37 µM EDTAE/g DW); in contrast of K100 showing the lowest copper chelation with a value of 1921–3013 µg/mL and 35,35–70,21 µM EDTAE/g DW across flushes (Figure 56 and 57, Appendix G, Table G2).

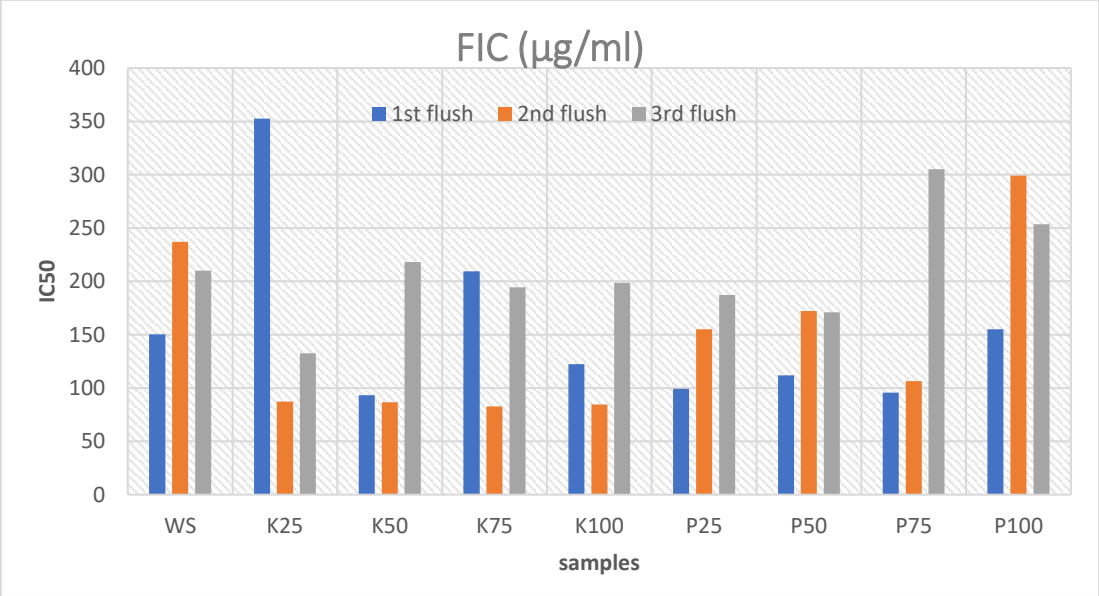

Figure 54: IC_{50} values (µg/mL) of FIC antioxidant activity of *P.ostreatus* extracts from three first flushes cultivated on different substrate formulas

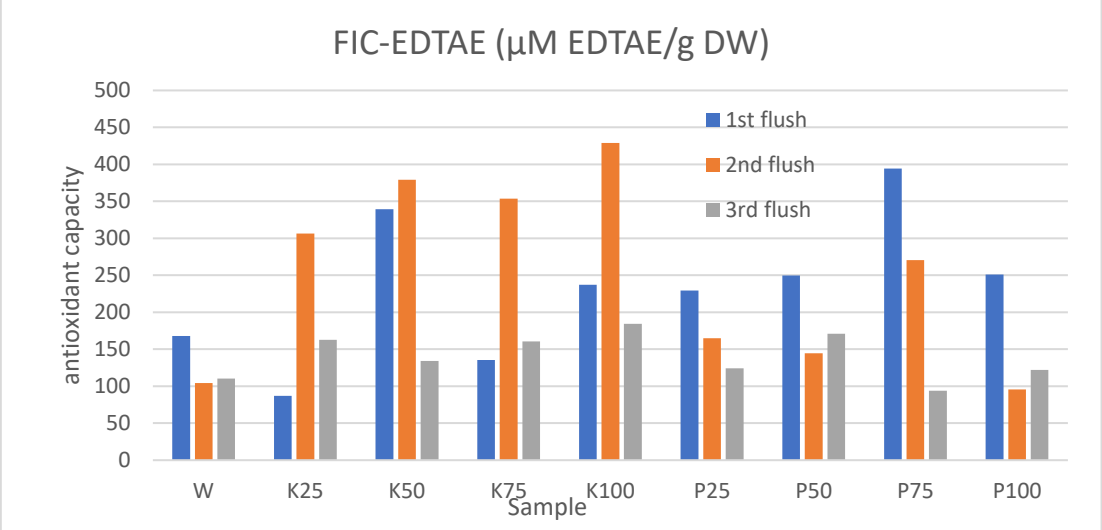

Figure 55: IC_{50} values (µM EDTAE/g DW) of FIC antioxidant activity of *P.ostreatus* extracts from three first flushes cultivated on different substrate formulas

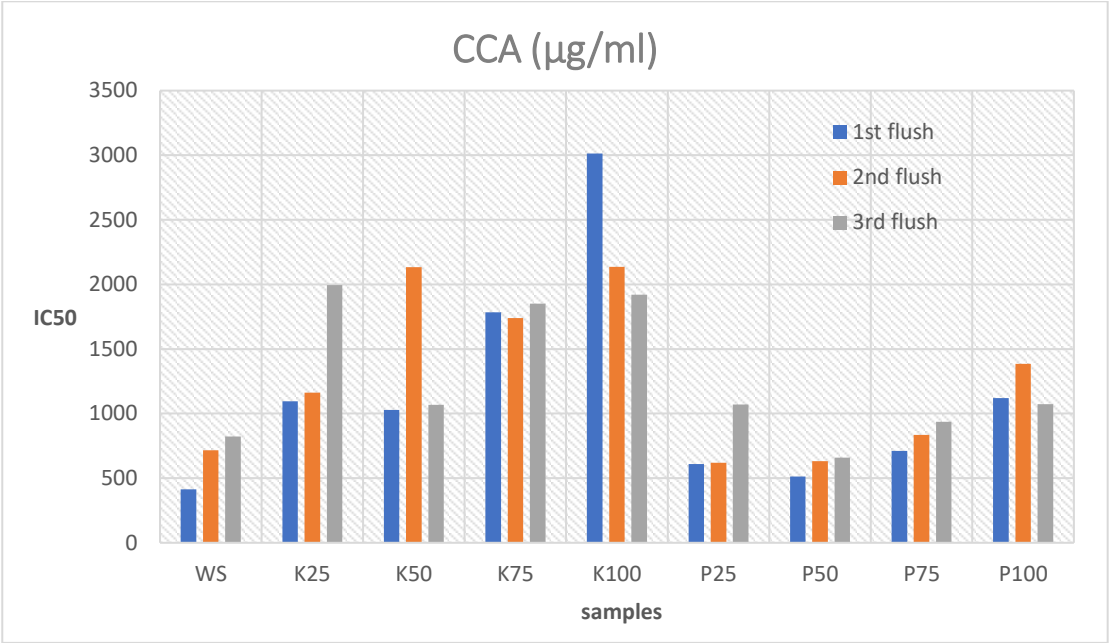

Figure 56: IC_{50} values (µg/mL) of CCA antioxidant activity of *P.ostreatus* extracts from three first flushes cultivated on different substrate formulas

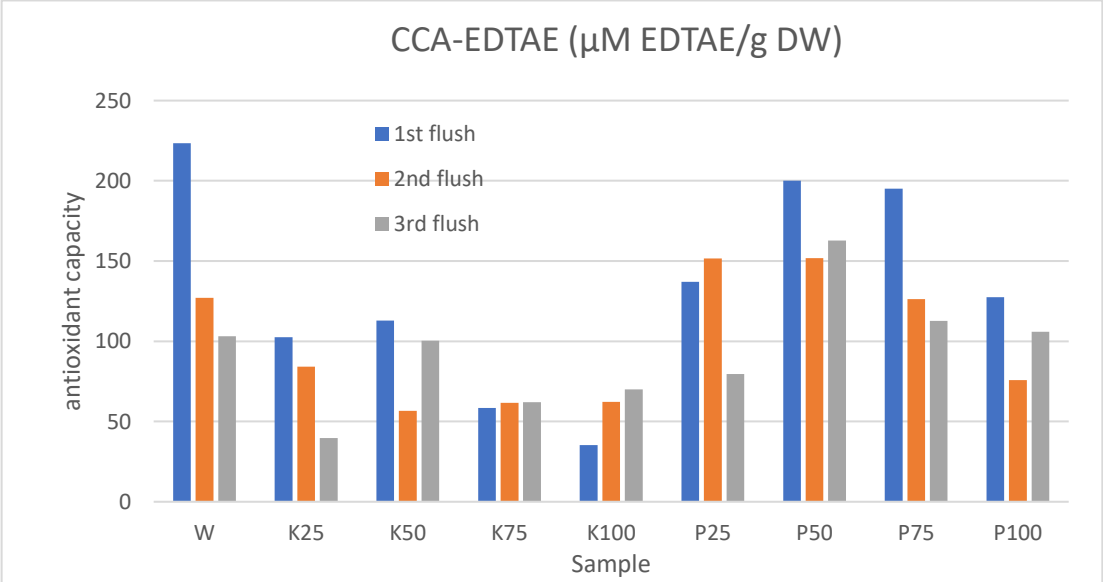

Figure 57: IC_{50} values (µM EDTAE/g DW) of CCA antioxidant activity of *P.ostreatus* extracts from three first flushes cultivated on different substrate formulas

These results align with **Muruke (2014)**, who reported effective Fe^{2+} chelation at 90–200 µg/mL. However, most literature indicates weaker activity, with IC_{50} > 1 mg/mL in *Pleurotus* species **(Huang *et al*., 2000; Jayakumar *et al*., 2009; Bamigboye *et al*., 2021)**. For copper chelation, the observed range (500–3000 µg/mL) is consistent with prior studies, though data on *P. ostreatus* remain limited. Some plant extracts, like black peppercorn and clove, and polysaccharides from *Lentinula edodes*, show much stronger activity **(Morales et al., 2020; May *et al*., 2023)**.

The stronger ferrous chelation in kernel-grown mushrooms and copper chelation in palm-grown ones likely reflect substrate's differences in phenolic and peptide metabolites. Kernel substrates, rich in polyphenols and organic acids, favor Fe^{+2} binding, while palm substrates promote nitrogen- and sulfur-containing ligands with stronger Cu^{+2} affinity **(Moran *et al*., 1997; Mohamed *et al*., 2014; Lakey-Beitia *et al*., 2021; Suleiman *et al*., 2021)**.

Antioxidant activity varied across flushes, largely depending on nutrient availability in substrates. The first flush generally yielded higher metabolite concentrations, while later flushes sometimes produced higher activity due to adaptive metabolic responses to nutrient depletion. Substrate composition and mineral content strongly influenced these patterns, explaining why certain flushes (e.g., second or third) sometimes displayed higher antioxidant capacity **(Hoa *et al*., 2015; Jin *et al*., 2018; Gebru, Faye, & Belete, 2024)**.

3.3.2. Anti-inflammatory Activity

In order to complement the evaluation of the bioactive properties of the extracts, their anti-inflammatory potential was assessed. This analysis highlights the capacity of the samples to influence inflammatory mechanisms, which are closely linked to the prevention and management of several chronic diseases. From results in Appendix I, the first flush was the most effective in reducing inflammation-related enzyme activity. Wheat straw (WS) was the most potent substrate across all flushes, with IC_{50} values between 106.73 and 124.61 µg/ml. Similarly, the first flush of P25 and P50 substrates yielded IC_{50} values of 126.54 and 132.9 µg/ml, respectively. In contrast, diminished activity was recorded in the third flush for P25, P75, and P100, where IC_{50} values reached 263.27, 368.24, and 269.82 µg/ml (Figure 58).

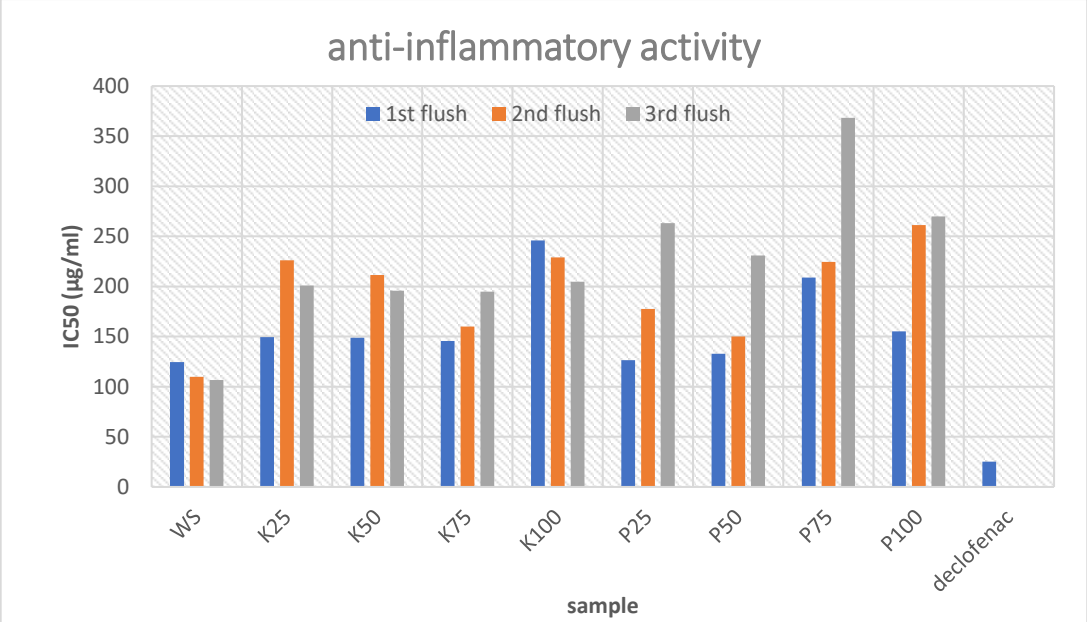

Figure 58: IC_{50} values (µg/mL) of anti-inflammatory activity of *P.ostreatus* extracts from three successive flushes cultivated on different substrate formulas.

Protein denaturation, which renders proteins biologically inactive, is associated with several inflammatory diseases, including rheumatoid arthritis, diabetes, and cancer. Thus, compounds that prevent denaturation can potentially mitigate these disorders **(Dutta 2013)**. Prior research has demonstrated that bioactive substances such as pleuran—β-glucan polysaccharide derived from oyster mushrooms—possess strong anti-inflammatory properties **(Das & Chatterjee, 1995; Nosalova *et al.*, 2001)**. However, the concentration of pleuran depends on the cultivation substrate **(Bekiaris *et al.*, 2020)**, which may explain the variations observed among the mushroom samples studied here. Comparative data indicate that *Pleurotus florida* reached an IC_{50} of 233.91 ± 9.69 µg/ml, whereas *Flammulina velutipes* exhibited much weaker activity at 625 µg/ml **(Jantrapanukorn *et al.*, 2018; Prabu & Kumuthakalavalli, 2014)**. Even some microfungi, like *Aspergillus quadrilineatus*, showed 51% protein denaturation inhibition when tested with 1 mg of methanolic mycelial extract **(Skanda & Vijayakumar, 2021)**. These comparisons confirm that certain *Pleurotus ostreatus* samples in this work rank among the strongest anti-inflammatory agents yet reported.

3.3.3. Anti-melanogenic activity

IC_{50} values for tyrosinase inhibition (Appendix J, Table J1) ranged widely, from 266.68 µg/ml in P100/2 to 1143.73 µg/ml in P25/3, while the weakest inhibition was observed in P50/1 (1143.69 µg/ml). Across all flushes, the 100% palm substrate displayed the strongest inhibitory effect, whereas the 50% palm–wheat straw mixture was the least effective (Figure 59).

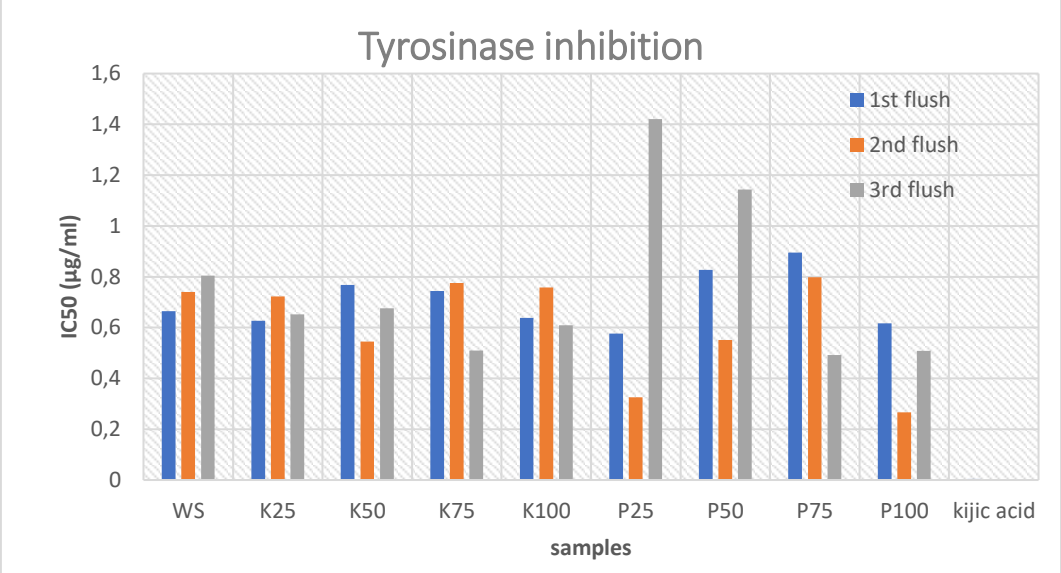

Figure 59: IC_{50} values (µg/mL) of anti-tyrosinese activity of *P. ostreatus* extracts from three successive flushes cultivated on different substrate formulas.

The inhibitory action is often attributed to phenolic hydroxyl groups in mushroom extracts, which interact with the enzyme's active site through hydrogen bonding, reducing activity. In some cases, these compounds induce steric hindrance or conformational modifications in tyrosinase **(Baek *et al.*, 2008; Kim *et al.*, 2008)**. For instance, **Alam *et al.* (2010)** reported that more than 0.5 mg/mL of *P. ostreatus* methanolic extract was required to achieve 50% inhibition, while another study indicated 0.86 mg/mL. In contrast, *Agaricus bisporus* was more potent, with an IC_{50} of 0.16 mg/mL **(Taofiq *et al.*, 2016)**. The present study produced results consistent with this literature, with the lowest IC_{50} values of *P. ostreatus* approaching those of *A. bisporus*. Nevertheless, even at their weakest, the tested samples still inhibited tyrosinase more strongly than mushrooms such as *Lactarius deliciosus*, *Cantharellus cibarius*, and *Lactarius pyrogalus* **(Çol Ayvaz *et al.*, 2019)**.

3.3.4. Anti-ulcer activity

Date kernel substrates produced stronger urease inhibition, particularly in the first flushes of K75 (380.02 µg/ml) and K100 (320.77 µg/ml). Palm substrates, by comparison, were weaker, with the poorest results in the third flush of P75 (1416.10 µg/ml) and P100 (1313.46 µg/ml) (Figure 60 and Appendix J, Table J2).
Inhibiting urease is clinically important since excessive urease activity is implicated in gastric disorders, including cancer. Prior to this study, no reports existed on *P. ostreatus* urease inhibition. Other mushrooms have been tested: *Lactarius deliciosus* (IC_{50} = 0.37 mg/mL), *Cantharellus cibarius* (0.42 mg/mL), and *Lactarius pyrogalus* (50% inhibition at comparable concentrations) **(Çol Ayvaz *et al.*, 2019)**. The inhibitory values reported here for *P. ostreatus* fall within or even surpass these ranges and were also stronger than bee-derived products such as honey, bee bread, and propolis **(Kolaylı *et al.*, 2017; Gercek *et al.*, 2024)**.

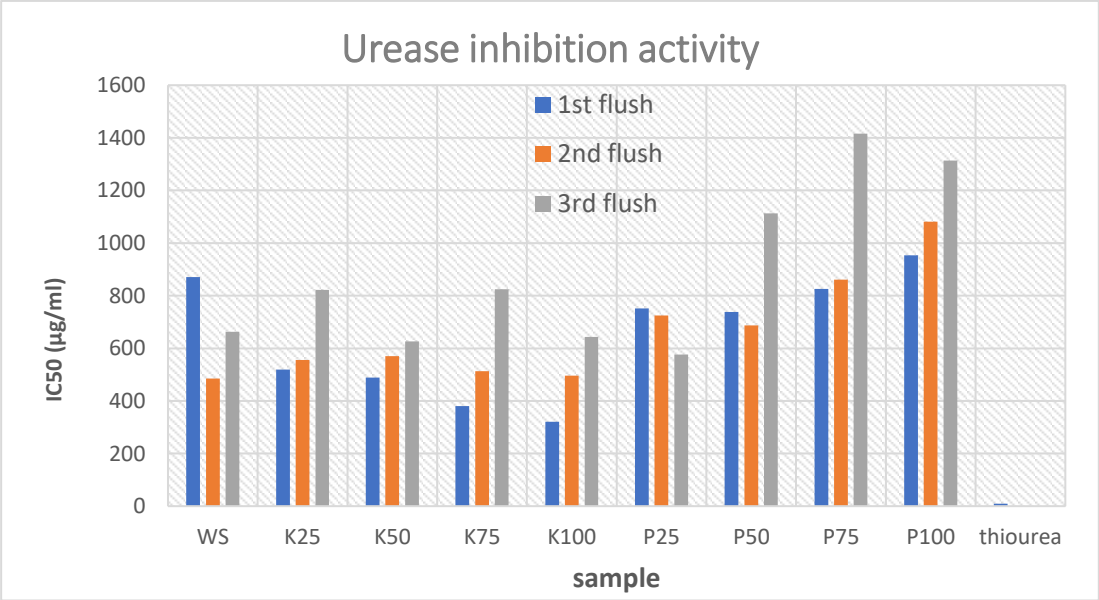

Figure 60: IC_{50} values (µg/mL) of urease inhibition activity of *P.ostreatus* extracts from three successive flushes cultivated on different substrate formulas.

3.3.5. Anti-diabetic activity

Overall, α-amylase inhibition was weak (Appendix J, Table J3). Date kernel–based extracts showed slightly better effects than palm substrates. The highest inhibition was observed in the first flush of K100, where 1 mg of extract achieved 30.02% inhibition, while the lowest was in the third flush of the same substrate (6.20%). Palm treatments were particularly weak, even in their best flush (Figure 61).

Existing literature often reports *P. ostreatus* methanolic extracts as potent α-amylase inhibitors, with less than 0.5 mg/mL sufficient to inhibit 50% of the enzyme and 1 mg/mL reaching over 90% inhibition **(Deveci *et al.*, 2021; Krishna *et al.*, 2023)**. In contrast, the present study required more than 1 mg/mL to achieve 50% inhibition, diverging from the majority of published results. However, this aligns with **Su *et al.* (2013)**, who found IC_{50} values of 2–6 mg/mL in other mushroom species. Likewise, **Shamtsyan & Pogačnik (2020)** reported <20% inhibition at 1 mg/mL hydro-alcoholic extract.

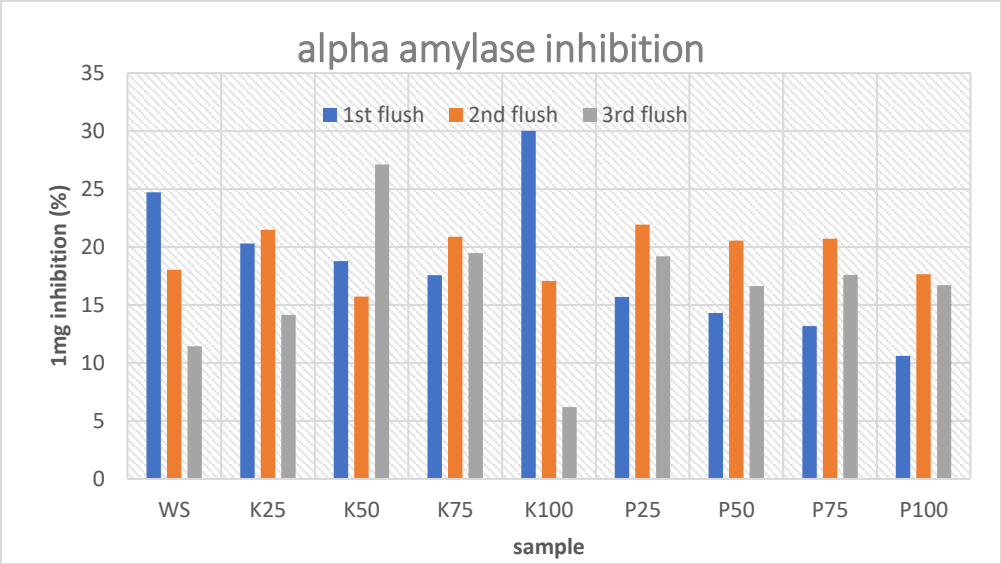

Figure 61: α-Amylase inhibition values (%) of 1mg/ml of *P.ostreatus* extracts from three successive flushes cultivated on different substrate formulas.

3.3.6. Anti-Alzheimer Activity

The highest acetylcholinesterase (AChE) inhibition occurred in palm-based samples from the third flush, with P100 showing 52.86% and P25 showing 44.82%. The lowest effect was observed in K25/3, with only 5.35%. Wheat straw extracts consistently displayed low and decreasing activity across flushes (Figure 62 and Appendix J, Table J3).

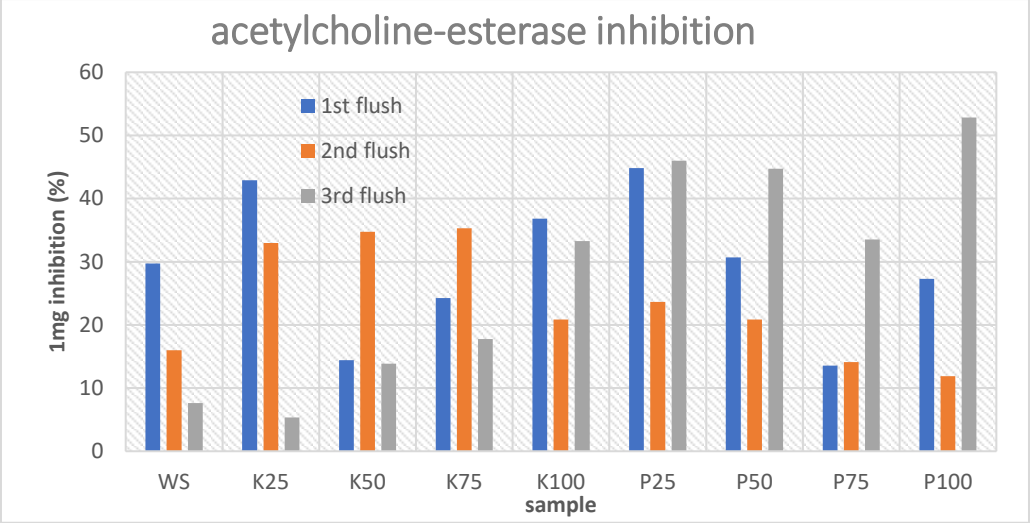

Figure 62: acetylcholine -esterase inhibition values (%) of 1mg/ml of *P.ostreatus* extracts from three successive flushes cultivated on different substrate formulas.

Butyrylcholinesterase (BChE) inhibition was stronger in date kernel substrates, especially in the second flush. Wheat straw showed the highest BChE inhibition in the first flush (35.75%), followed closely by K75/1 (35.10%). The weakest activity was found in the third flushes of K75 (15.80%) and K100 (16.17%). Palm substrates ranged from 18.69% in P75/2 to 34.30% in P100/3 (Figure 63).

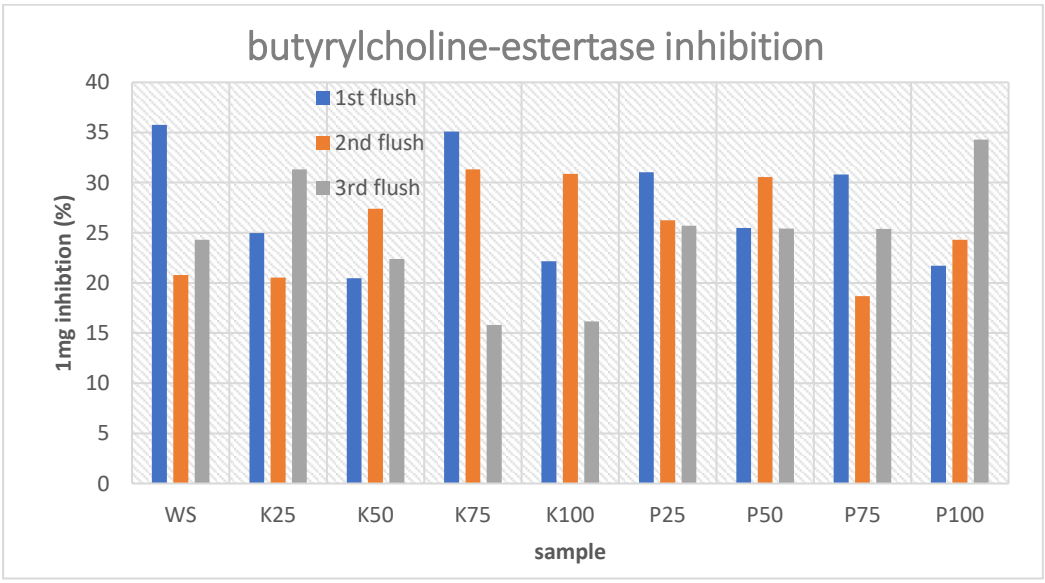

Figure 63: butyrylcholine -esterase inhibition values (%) of 1mg/ml of *P.ostreatus* extracts from three successive flushes cultivated on different substrate formulas.

These findings are comparable to **Ćilerdžić *et al.* (2019)**, who found that 1 mg of hydroethanolic *P. ostreatus* extract inhibited 37–42% of AChE. **Chamutpong *et al.* (2019)** also observed that 1.75–5.91 mg/mL extract was required to inhibit 50% of AChE. For BChE, however, the current study reported lower activity than **Dundar *et al.* (2019)**, where 200 µg/mL methanolic extract inhibited 48.21%. Despite relatively low results, *P. ostreatus* still outperforms *P. florida* in Alzheimer's prevention **(Randhawa & Shri, 2018)**.

3.3.7. Anti-obesity Activity

From data of Appendix J, Table J3, lipase inhibition was minimal, with 1 mg of extract suppressing only 2.97–14.21% of enzyme activity. Wheat straw showed the strongest effect, peaking at 14.21% in the second flush. K25 and K50 second flushes followed with 12.92% and 11.91%, respectively. The lowest inhibition was P25/3 (2.96%), closely followed by K75/3 (3.99%) (Figure 64).

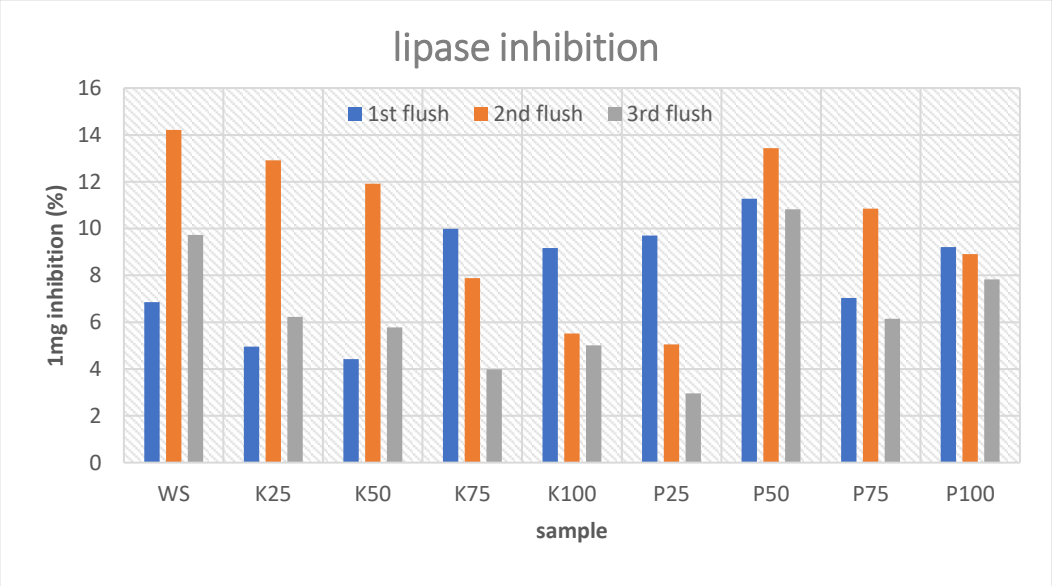

Figure 64: lipase inhibition values (%) of 1mg/ml of *P.ostreatus* extracts from three successive flushes cultivated on different substrate formulas.

Even at their best, these values were much weaker than those reported for *A. bisporus* and *P. eryngii*, which inhibited 32.2% and 20.8% of lipase using only 0.1 mg of extract **(Mizutani *et al.*, 2010; Kim *et al.*, 2023)**. The poor activity may result from the scarcity or absence of strong lipase inhibitors such as myricetin and fatty acids **(Bustos *et al.*, 2020; Effiong *et al.*, 2024a)**.

3.3.8. Anti-bacterial Activity

Antibacterial effects were tested by measuring inhibition zones (including the 6 mm disc) against Gram-positive strains (*Staphylococcus aureus*, *Bacillus cereus*, *Bacillus subtilis*, *Enterococcus faecalis*) and Gram-negative strains (*Salmonella*, *Pseudomonas aeruginosa*, *Escherichia coli*, *Klebsiella pneumoniae*). Activity varied across substrates and strains. For *E. coli*, inhibition zones were minimal, ranging from 6.00 mm (no effect) to 6.75 mm (K50/1) (Figure 65). *S. aureus* was more sensitive, with zones up to 14.67 mm (K75/2) and 12.90 mm (WS/2) (Figure 66). *K. pneumoniae* showed little to no susceptibility, mostly at 6.00 mm (Figure 67). *B. cereus* inhibition ranged from 6.20 mm (K100/2) to 9.03 mm (WS/1) (Figure 68), while *B. subtilis* ranged between 6.23 mm (P25/2) and 8.86 mm (K25/2) (Figure 69). No inhibition was detected for *P. aeruginosa*, *E. faecalis*, or *Salmonella ssp* (Figure 70, 71, 72)).

Controls confirmed much stronger effects: ampicillin produced zones between 6.28 and 41.99 mm (highest against *S. aureus*), while amoxicillin ranged from 8.69 to 49.86 mm across multiple strains. However, for *B.cereus* and *B.subtilis* some samples extract showed better activity than ampicillin.

Overall, the mushroom extracts displayed weak-to-moderate antibacterial activity, more effective against Gram-positive species than Gram-negative. This agrees with earlier findings, where *Pleurotus* extracts preferentially inhibited Gram-positive bacteria **(Gashaw *et al*., 2020)**. Previous studies typically reported zones between 10–20 mm for Gram-positive strains, with much weaker activity against Gram-negative ones. Compared to ampicillin and amoxicillin, which produced up to 42 mm and 50 mm zones, respectively, *P. ostreatus* extracts were clearly less potent **(Sutthisa & Anujakkawan, 2023)**.

The variability among samples is likely due to differences in bioactive metabolite content (polysaccharides, phenolics, flavonoids), which depend on substrate, environmental conditions, strain genetics, and fruiting stage **(Ahmed *et al*., 2022; Hasan & Abdulhadi, 2023)**. Maturity of fruiting bodies affects metabolite levels, altering antibacterial potency **(Fakoya *et al*., 2020; Polito *et al*., 2024)**. Additionally, post-harvest processing and storage conditions (temperature, humidity, light, and air exposure) can degrade bioactive compounds, further influencing activity **(Ahmed *et al*., 2022)**.

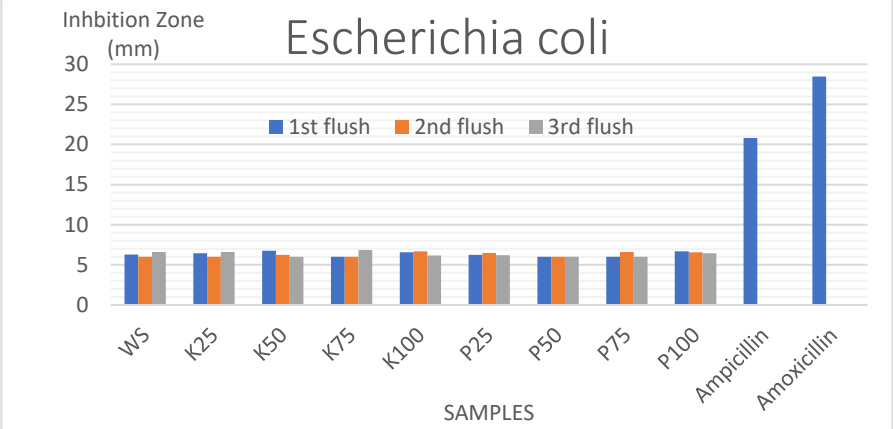

Figure 65: inhibition zone (mm) of three first flushes of *P.ostreatus* mushroom Extracts cultivated of different substrate formulas against *Escherichia coli.*

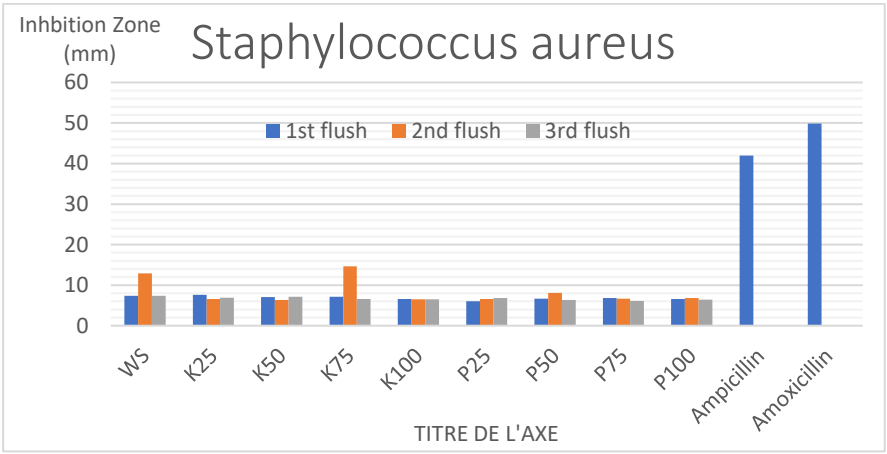

Figure 66: inhibition zone (mm) of three first flushes of *P.ostreatus* mushroom Extracts cultivated of different substrate formulas against *Staphylococcus aureus.*

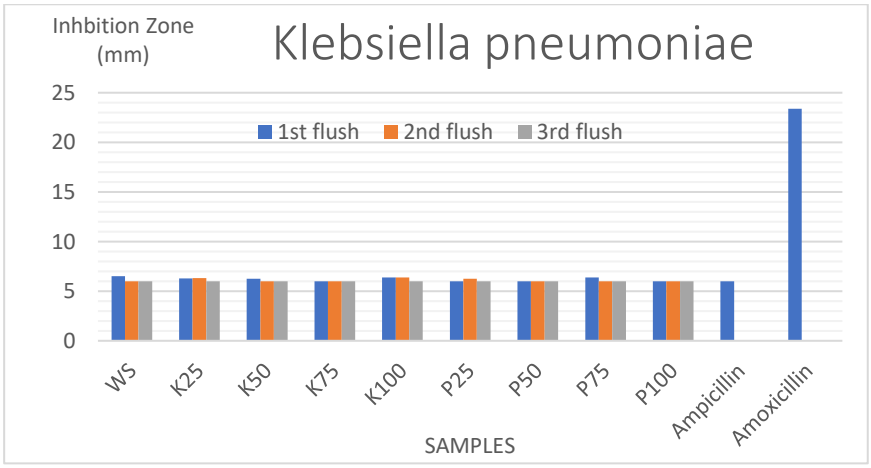

Figure 67: inhibition zone (mm) of three first flushes of *P.ostreatus* mushroom Extracts cultivated of different substrate formulas against *Klebsiella pneumoniae.*

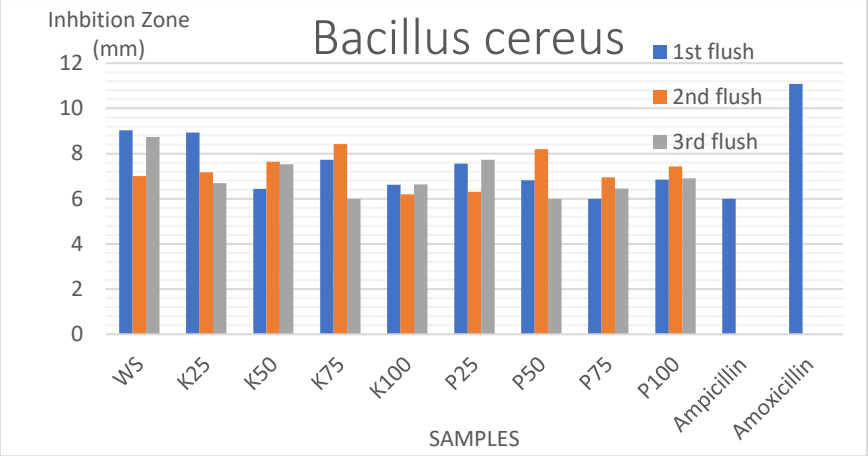

Figure 68: inhibition zone (mm) of three first flushes of *P.ostreatus* mushroom Extracts cultivated of different substrate formulas against *Bacillus cereus.*

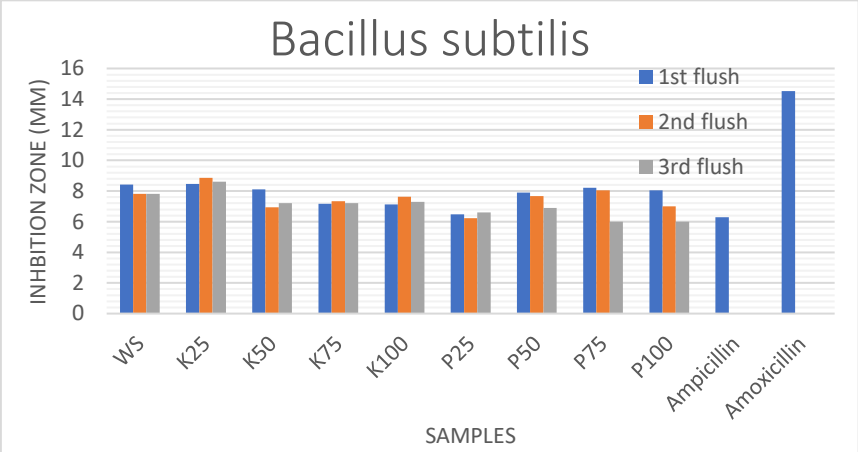

Figure 69: inhibition zone (mm) of three first flushes of *P.ostreatus* mushroom Extracts cultivated of different substrate formulas against *Bacillus subtilis.*

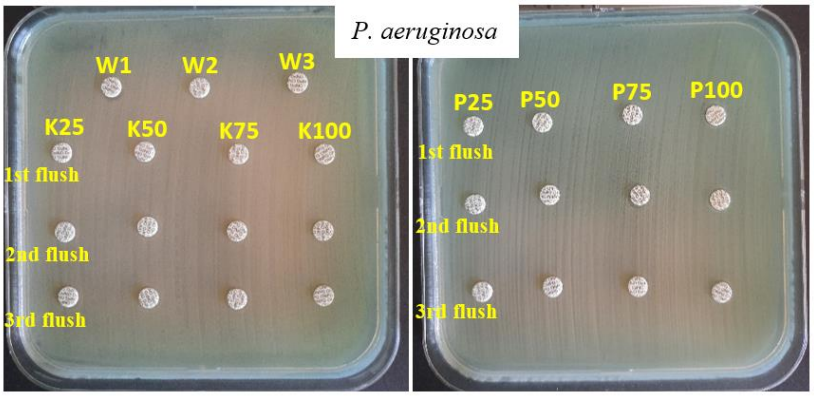

Figure 70: inhibition zone of three first flushes of *P.ostreatus* mushroom Extracts cultivated of different substrate formulas against, *P.aerogenosa*

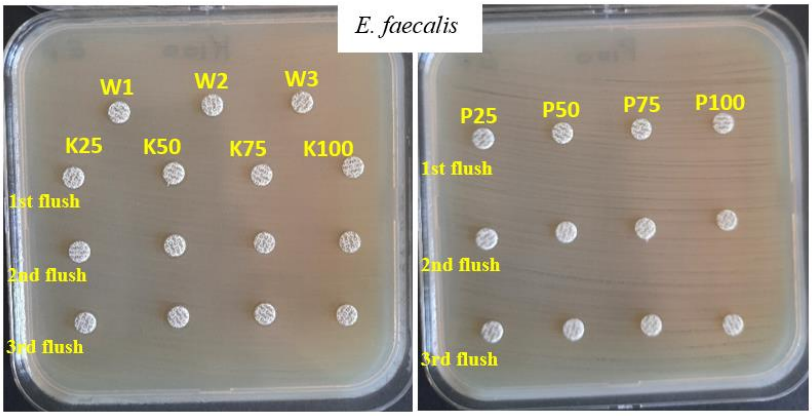

Figure 71: inhibition zone of three first flushes of *P.ostreatus* mushroom Extracts cultivated of different substrate formulas against *E. feacalis*,

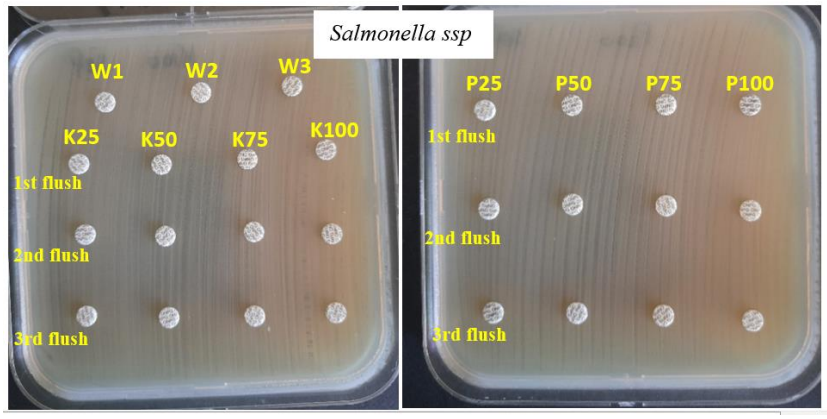

Figure 72: inhibition zone of three first flushes of *P.ostreatus* mushroom Extracts cultivated of different substrate formulas against *Selmonella ssp.*

CONCLUSION AND PERSPECTIVES

4. CONCLUSION AND PERSPECTIVES

This study demonstrated that the cultivation of *Pleurotus ostreatus* on alternative agro-waste substrates such as date kernels, palm leaves, and wheat straw is not only feasible but also highly valuable in terms of yield, biochemical composition, and functional bioactivities. Across successive flushes, variations were observed in productivity and metabolite accumulation, highlighting the influence of substrate type and cultivation stage on mushroom quality and functionality.

- Date kernel-based substrates promoted faster mycelial colonization and earlier fruiting initiation due to their higher carbon and nitrogen content, resulting in shorter crop cycles. Conversely, palm leaf substrates, characterized by higher lignin content and a higher C/N ratio, slowed colonization and pinhead formation, leading to delayed fruiting and reduced overall yields.
- Yield and biological efficiency were highest in substrates combining date kernels with wheat straw, notably K25, which showed superior cumulative yield and biological efficiency compared to pure substrates. The progressive depletion of nutrients across successive flushes caused a typical decline in yield, with the majority of productivity concentrated in first and second flush.
- Chemical analyses revealed higher extraction yields in palm-based substrates, yet these were often accompanied by lower total phenolic and flavonoid concentrations per gram of extract due to dilution effects. Date kernel-based mushrooms exhibited higher concentrations of key bioactive flavonoids such as luteolin and quercetin, which strongly correlated with antioxidant activities like DPPH and ABTS radical scavenging. FTIR spectra confirmed the presence of polysaccharides (notably β-glucans), proteins, and phenolics across all flushes, supporting the bioactive potential of the extracts.
- Antioxidant activity assays highlighted the second flush generally as richest in low-molecular-weight antioxidants, while first flushes excelled in specific scavenging and metal chelating activities. Date kernel substrates favored iron chelation, whereas palm substrates enhanced copper chelation, reflecting substrate-driven differences in metabolite profiles.

- For anti-inflammatory effects, wheat straw and date kernel substrates, either alone or combined, are recommended. However, using the first flush of lower-percentage palm-based substrates is also advisable.
- Enzyme inhibition assays indicated strong urease, and tyrosinase inhibitory effects. For anti-melanogenic (anti-browning) purpose use palm-rich substrates (especially P100 and P25 in some flushes) is recommended with 2nd flush strong for some palm mixes. For anti-ulcer (anti-urease infections) first flush of date-kernel-enriched substrates (K75, K100).
- In contrast, α-amylase, anti-Alzheimer (acetyl- and butyryl cholinesterase), inhibitions were weaker. Targeting anti-diabetic activity (α-Amylase inhibition) or slow carbohydrate breakdown, recommend first flush of higher palm-based substrate. For anti-Alzheimer / neuroprotective recommend late flushes (2^{nd} and 3^{rd}) of kernel mixed substrates and second flush of date palm-based substrate (P100)
- samples showed very low anti-obesity activity translated from almost no inhibition pancreatic lipase enzymes and therefore very low reducing of fat absorption
- Antibacterial activity was moderate and predominantly effective against Gram-positive bacteria like Staphylococcus aureus, with minimal effects against Gram-negative species. This spectrum aligns with known selective antimicrobial activities of *Pleurotus ostreatus* extracts.

Importantly, the results provided strong support for the hypotheses formulated in the introduction. The expectation that agro-waste composition would influence mushroom productivity, metabolite accumulation, and bioactivities was confirmed. Likewise, the temporal variation across flushes validated the hypothesis that developmental stage modulates both biochemical content and biological potential. The study also underscores that substrate selection governs not only agronomic parameters but also the bioactive compound profile and functional properties of *Pleurotus ostreatus*. Combining agro-industrial residues with complementary nutrient profiles, such as date kernels and palm leaves, optimizes yield and nutraceutical potential. These bioactive extracts hold promise for applications in functional foods, natural antioxidants, anti-inflammatory enzyme inhibitors, and selective antimicrobials, though their potency is generally lower than conventional pharmaceuticals.

Overall, this study advances understanding of how cultivar substrate impacts *Pleurotus ostreatus* performance and bioactivity, facilitating tailored cultivation strategies for enhanced production of health-promoting mushroom compounds.

Future studies should investigate the effect of date kernel particle size on substrate performance, with particular attention to overcoming issues of compactness and nutrient availability. Moreover, optimizing mixtures of date kernels and palm leaves in different proportions may provide suitable substrates that enhance both biological efficiency and the accumulation of bioactive compounds across successive flushes.

Advanced metabolomic and proteomic profiling of fruiting bodies harvested at different developmental stages would deepen understanding of biochemical dynamics during mushroom maturation. This knowledge could inform harvest timing strategies to optimize bioactive compound yield and functional properties.

The antioxidant, anti-inflammatory, enzyme inhibitory (anti-tyrosinaseand anti-urease), and antibacterial activities exhibited by the extracts suggest promising applications in functional food, pharmaceutical, and cosmeceutical sectors. However, the relatively modest antibacterial efficacy against Gram-negative pathogens underscores the necessity of further bioprospecting and purification efforts to isolate more potent antimicrobial agents from mushroom-derived compounds.

Since enzyme inhibition results can vary, it is important to use the same extraction methods and test bioactivities on different mushroom strains and growing conditions. This will make the results more reliable and help in creating safe, certified nutraceutical products.

Finally, integrating *Pleurotus ostreatus* cultivation with circular bioeconomy models in arid and semi-arid regions—leveraging abundant date palm residues—could significantly enhance regional agriculture sustainability, generate alternative income sources, and contribute to food security. Multidisciplinary approaches combining agronomy, biochemistry, and process engineering will be crucial to fully realize the commercial and health benefits of mushroom cultivation on agro-industrial residues.

REFERENCES

REFERENCES

Abdulhadi, A.M., Hassan, I.A. (2013). Effect of sterilization method and supplementation on the yield and storage life of oyster mushroom cultivated on date palm byproducts. *Diyala Agricultural Sciences Journal*. 5(1):170–181.

Abou Raya, M. A., Shalaby, M. T., Hafez, S. A., & Hamouda, A. M. (2014). Chemical composition and nutritional potential of some mushroom varieties cultivated in Egypt. *Journal of Food and Dairy Sciences*, *5*(6), 421-434.

Abu-Thabit, N.Y., Judeh, A.A., Hakeem, A.S., Ul-Hamid, A., Umar, Y., Ahmad, A. (2020). Isolation and characterization of microcrystalline cellulose from date seeds (Phoenix dactylifera L.). *International journal of biological macromolecules*. 155:730-739.

Afify, A.H., El-Sawah, M.M.A., Ali, M.S., El-Rahman, A. (2012). Effect of molasses on cultivation of oyster mushroom (*Pleurotus osrteatus*) on different agro-industrial wastes. *Journal of Agricultural Chemistry and Biotechnology*. 3(3):103-111.

Agunloye, O. M., & Oboh, G. (2021). Effect of diet supplemented with P. ostreatus and L. subnudus on memory index and key enzymes linked with Alzheimer's disease in streptozotocin-induced diabetes rats. *Journal of Food Biochemistry*, *45*(3), e13355.

Ahmed, H. A., Youssef, M. S., & Magraby, T. A. (2022). Antimicrobial and Antioxidant Activities of *Pleurotus Ostreatus* as Edible Oyster Mushroom in Egypt. *Journal of Environmental Studies*, *28*(1), 24-34.

Ahmed, M. F. (2024). Exploring the characteristics and effects of date palm waste on some properties of concrete: a review. *Kufa Journal of Engineering*, *15*(1).

Alam, N., Yoon, K. N., Lee, K. R., Shin, P. G., Cheong, J. C., Yoo, Y. B., Shim M. J., Lee M. W., Lee U. Y. & Lee, T. S. (2010). Antioxidant activities and tyrosinase inhibitory effects of different extracts from *Pleurotus ostreatus* fruiting bodies. *Mycobiology*, *38*(4), 295-301.

Alananbeh, K. M., Bouqellah, N. A., & Al Kaff, N. S. (2014). Cultivation of oyster mushroom *Pleurotus ostreatus* on date-palm leaves mixed with other agro-wastes in Saudi Arabia. *Saudi journal of biological sciences*, *21*(6), 616-625.

Al-Awa, Z. F. A., Sangor, F. I. M. S., Babili, S. B., Saud, A., Saleem, H., & Zaidi, S. J. (2023). Effect of leaf powdering technique on the characteristics of date palm-derived cellulose. *ACS omega*, *8*(21), 18930-18939.

Ali, N., Khairudin, H., Mohamed, M., & Hassan, O. (2018). Cultivation of *Pleurotus ostreatus* on oil palm fronds mixed with rubber tree sawdust. *Chemical Engineering Transactions*, *63*, 547-552.

Al-Jbouri, Z. S., Alsaady, M. H., & Abdulrazzaq, A. K. (2025). Evaluation of substrate efficacy and supplementation on the growth and productivity of three species of oyster mushrooms. *Journal of Ecological Engineering*, *26*(5).

Allwood, J. W., & Goodacre, R. (2010). An introduction to liquid chromatography–mass spectrometry instrumentation applied in plant metabolomic analyses. *Phytochemical Analysis: An International Journal of Plant Chemical and Biochemical Techniques*, *21*(1), 33-47.

Al-Qarawi, A. A., Abd-Allah, E. F., & Bawadiji, A. A. (2013). Production of *Pleurotus ostreatus* on date palm residues. *Journal of Pure and Applied Microbiology*, 7(2), 1093-1097.

Alsulami, R. A., El-Sayed, S. A., Eltaher, M. A., Mohammad, A., Almitani, K. H., & Mostafa, M. E. (2023). Thermal decomposition characterization and kinetic parameters estimation for date palm wastes and their blends using TGA. *Fuel*, *334*, 126600.

Ambhore, J. P., Adhao, V. S., Rafique, S. S., Telgote, A. A., Dhoran, R. S., & Shende, B. A. (2024). A concise review: Edible mushroom and their medicinal significance. *Exploration of Foods and Foodomics*, *2*(3), 183-194.

American Type Culture Collection (ATCC). *Bacteriology culture guide: Technical information on bacterial growth, propagation, preservation, and application* [Internet]. Manassas, VA: ATCC; [cited 2024 Sep 23]. Available from: https://www.atcc.org/resources/culture-guides/bacteriology-culture-guide

Apak, R., Güçlü, K., Özyürek, M., & Çelik, S. E. (2008). Mechanism of antioxidant capacity assays and the CUPRAC (cupric ion reducing antioxidant capacity) assay. *Microchimica acta*, *160*(4), 413-419.

Apak, R., Güçlü, K., Özyürek, M., & Karademir, S. E. (2004). Novel total antioxidant capacity index for dietary polyphenols and vitamins C and E, using their cupric ion reducing capability in the presence of neocuproine: CUPRAC method. *Journal of agricultural and food chemistry*, *52*(26), 7970-7981.

Arab News. (2023, February 27). *Saudi date exports soar during 2022*. Arab News. Retrieved August 30, 2025, from https://www.arabnews.com/node/2258991/saudi-arabia?utm_source=chatgpt.com

Arbaayah, H. H., & Umi Kalsom, Y. (2013). *Antioxidant Properties in the Oyster Mushrooms (Pleurotus spp.) and Split Gill Mushroom (Schizophyllum commune) Ethanolic Extracts. Mycosphere*, *4*, *661-673*.

Argaw, B., Tesfay, T., Godifey, T., & Asres, N. (2023). Growth and yield performance of oyster mushroom (P. ostreatus (Jacq.: Fr.) Kummer) using waste leaves and sawdust. *International Journal of Agronomy*, *2023*(1), 8013491.

Assemie, A., & Abaya, G. (2022). The effect of edible mushroom on health and their biochemistry. *International journal of microbiology*, *2022*(1), 8744788.

Atila, F. (2019). Compositional changes in lignocellulosic content of some agro-wastes during the production cycle of shiitake mushroom. *Scientia Horticulturae*, 245, 263-268.

Atila, F., & Cetin, M. (2024). Bioconversion of lavender oil extraction wastes through cultivation of *Pleurotus eryngii* var. ferulae: Its effects on yield, nutritional content and antioxidant capacity of the mushroom. *Biocatalysis and Agricultural Biotechnology*. 58:103138.

Baek, H. S., Rho, H. S., Yoo, J. W., Ahn, S. M., Lee, J. Y., Jeonga-Lee, J. L., Kim M. K., Kim D. H., & Chang, I. S. (2008). The inhibitory effect of new hydroxamic acid derivatives on melanogenesis. *ChemInform*, *39*(23), i.

Baeva, E., Bleha, R., Lavrova, E., Sushytskyi, L., Čopíková, J., Jablonsky, I., Klouček P. & Synytsya, A. (2019). Polysaccharides from basidiocarps of cultivating mushroom *Pleurotus ostreatus*: isolation and structural characterization. *Molecules*, *24*(15), 2740.

Balouiri, M., Sadiki, M., & Ibnsouda, S. K. (2016). Methods for in vitro evaluating antimicrobial activity: A review. *Journal of pharmaceutical analysis*, *6*(2), 71-79.

Bamigboye, C. O., Omomowo, I. O., Alao, M. B., Elegbede, J. A., & Adebayo, E. A. (2021). Free radical scavenging ability, mechanisms of action and health implications of oyster mushrooms (*Pleurotus* species).

Barros, L., Venturini, B. A., Baptista, P., Estevinho, L. M., & Ferreira, I. C. (2008). Chemical composition and biological properties of Portuguese wild mushrooms: a comprehensive study. *Journal of agricultural and food chemistry*, *56*(10), 3856-3862.

Bassi, S., Benvenuti, M., Mirata, S., Di Piazza, S., Salis, A., Damonte, G., Zotti M., & Scarfi, S. (2024). Enhanced antioxidant and anti-inflammatory activity of the extracts of *Pleurotus ostreatus* edible mushroom grown on Lavandula angustifolia residues. *Food Bioscience*, *60*, 104382.

Bekiaris, G., Tagkouli, D., Koutrotsios, G., Kalogeropoulos, N., & Zervakis, G. I. (2020). Pleurotus mushrooms content in glucans and ergosterol assessed by ATR-FTIR spectroscopy and multivariate analysis. *Foods*, *9*(4), 535.

Bellettini, M. B., Fiorda, F. A., Maieves, H. A., Teixeira, G. L., Ávila, S., Hornung, P. S., Maccari Júnior A., & Ribani, R. H. (2019). Factors affecting mushroom *Pleurotus* spp. *Saudi Journal of Biological Sciences*, *26*(4), 633-646.

Bello, M., Oluwamukomi, M. O., & Enujiugha, V. N. (2017). Anti-diabetic activity of three species of oyster mushroom. *Annals: Food Science & Technology*, *18*(2).

Bhattacharjya, D. K., Paul, R. K., Miah, M. N., & Ahmed, K. U. (2015). Comparative study on nutritional composition of oyster mushroom (*Pleurotus ostreatus* Fr.) cultivated on different sawdust substrates. *Bioresearch Communications-(BRC)*, *1*(2), 93-98.

Bhatti, M. I., Jiskani, M. M., Wagan, K. H., Pathan, M. A., & Magsi, M. R. (2007). Growth, development and yield of oyster mushroom, *Pleurotus ostreatus* (Jacq. Ex. Fr.) Kummer as affected by different spawn rates. *Pak. J. Bot*, *39*(7), 2685-2692.

Bhekti Rahimah, S., Firmansyah, A., Maharani, W., Andriane, Y., Santosa, D., & Romadhona, N. (2023). Active compound test: ethanolic extract of White Oyster Mushroom (*Pleurotus ostreatus*) Using HPLC and LC-MS. *F1000Research*, *10*, 1233.

Bikmurzin, R., Bandzevičiūtė, R., Maršalka, A., Maneikis, A., & Kalėdienė, L. (2022). FT-IR method limitations for β-glucan analysis. *Molecules*, *27*(14), 4616.

Biswas, S., Datta, M., & Ngachan, S. V. (2011). Mushrooms: A Manual for cultivation. *PHI Learning Pvt.* Ltd..

Blois, M. S. (1958). Antioxidant determinations by the use of a stable free radical. *Nature*, *181*(4617), 1199-1200.

Bolling, B. W., Chen, Y. Y., Kamil, A. G., & Oliver Chen, C. Y. (2012). Assay dilution factors confound measures of total antioxidant capacity in polyphenol-rich juices. *Journal of food science*, *77*(2), H69-H75.

Bonatti, M., Karnopp, P., Soares, H. M., & Furlan, S. A. (2004). Evaluation of *Pleurotus ostreatus* and *Pleurotus sajor-caju* nutritional characteristics when cultivated in different lignocellulosic wastes. *Food chemistry*, *88*(3), 425-428.

Boots, A. W., Haenen, G. R., & Bast, A. (2008). Health effects of quercetin: from antioxidant to nutraceutical. *European journal of pharmacology*, *585*(2-3), 325-337.

Bouallegue, K., Allaf, T., Besombes, C., Younes, R. B., & Allaf, K. (2019). Phenomenological modeling and intensification of texturing/grinding-assisted solvent oil extraction: case of date seeds (*Phoenix dactylifera* L.). *Arabian Journal of Chemistry*, *12*(8), 2398-2410.

Burezq, H. A., & Davidson, M. K. (2023). Biochar from date palm (*Phoenix dactylifera* L.) residues—a critical review. *Arabian Journal of Geosciences*, *16*(2), 101.

Bustos, A. S., Håkansson, A., Linares-Pastén, J. A., & Nilsson, L. (2020). Interaction between myricetin aggregates and lipase under simplified intestinal conditions. *Foods*, *9*(6), 777.

Butt, G. H. A. Z. A. L. A., Hussain, E. J. A. Z., & Rehman, A. B. D. U. R. (2014). Ferrous ion-chelating assay for analysis of antioxidant potential of *Sargassum* sp. and *Iyengaria* sp. *Pakistan Journal of Medical & Health Sciences.* 8(1): 202-203.

Caeiro, L., Novais, F., Saldanha, C., e Melo, T. P., Canhão, P., & Ferro, J. M. (2021). The role of acetylcholinesterase and butyrylcholinesterase activity in the development of delirium in acute stroke. *Cerebral Circulation-Cognition and Behavior*, *2*, 100017.

Cardoso, R. V., Carocho, M., Fernandes, Â., Pinela, J., Stojković, D., Soković, M., Zied D., Cobos J. D. V., González-Paramás A. M., Ferreira I. C. F. R. & Barros, L. (2021). Antioxidant and antimicrobial influence on oyster mushrooms (*Pleurotus ostreatus*) from substrate supplementation of calcium silicate. *Sustainability*, *13*(9), 5019.

Chamutpong, S., Pummarin, T., & Noysang, C. (2019). Nutritional Properties, Antioxidant and Anti-Acetylcholinesterase Activities of Pleurotus ostreatus. *Applied Mechanics and Materials*, *891*, 14-20.

Chang, C. C., Yang, M. H., Wen, H. M., & Chern, J. C. (2002). Estimation of total flavonoid content in propolis by two complementary colorimetric methods. *Journal of food and drug analysis*, *10*(3).

Chang, S. T., & Miles, P. G. (1997). Mushroom biology: concise basics and current developments. World Scientific.

Chang, T. S. (2009). An updated review of tyrosinase inhibitors. *International journal of molecular sciences*, *10*(6), 2440-2475.

Chirinang, P., & Intarapichet, K. O. (2009). Amino acids and antioxidant properties of the oyster mushrooms, *Pleurotus ostreatus* and *Pleurotus sajor-caju*. *Science Asia*, *35*(2009), 326-331.

Chukwurah, C. C., Obasi, K. O., Anaduaka, E. G., Nweze, N. E., & Eze, C. N. (2023). In vitro antidiabetic studies of aqueous extract of *Pleurotus ostreatus* grown on different substrates. *Research Journal of Phytochemistry*, *17*(1), 37–47.

Ćilerdžić, J., Galić, M., Vukojević, J., & Stajic, M. (2019). *Pleurotus ostreatus* and *Laetiporus sulphureus* (Agaricomycetes): possible agents against Alzheimer and Parkinson diseases. *International Journal of Medicinal Mushrooms*, *21*(3).

Çol Ayvaz, M., Aksu, F., & Kır, F. (2019). Phenolic profile of three wild edible mushroom extracts from Ordu, Turkey and their antioxidant properties, enzyme inhibitory activities. *British Food Journal*, *121*(6), 1248-1260.

Çol Ayvaz, M., Aksu, F., & Kır, F. (2019). Phenolic profile of three wild edible mushroom extracts from Ordu, Turkey and their antioxidant properties, enzyme inhibitory activities. *British Food Journal*, *121*(6), 1248-1260.

Cong-Hau, N., Thanh-Nho, N., Anh-Dao, L. T., & Nhon-Duc, L. (2021). Spectrophotometric determination of total flavonoid contents in tea products and their liquors under various brewing conditions. *Malaysian Journal of Analytical Sciences*, 25(5), 740-750.

Costa, A.F.P., Steffen, G.P.K., Steffen, R.B., Portela, V.O., Santana, N.A., dos Santos Richards, N.S.P., Jacques, R.J.S. (2023). The use of rice husk in the substrate composition increases Pleurotus ostreatus mushroom production and quality. *Scientia Horticulturae*. 321:112372.

Das SN and Chatterjee S. (1995). Long termtoxicity study of ART-400. *Indian Journal of Indigenous Medicine,* 16(2): 117-123,(1995)

David, A. B., & Mshandete, A. M. (2023). Valorization of palm oil wastes into oyster mushrooms (*Pleurotus* HK-37) and biogas production (Preprint). *Qeios. CC-BY 4.0*. https://doi.org/10.32388/YS6L57

Decker, E.A., & Welch, B. (1990). Role of ferritin as a lipid oxidation catalyst in muscle food. *Journal of Agricultural and Food Chemistry*, 38(3), 674–677.

Dedousi, M., Melanouri, E.M., Diamantopoulou, P. (2023). Carposome productivity of *Pleurotus ostreatus* and *Pleurotus eryngii* growing on agro-industrial residues enriched with nitrogen, calcium salts and oils. *Carbon Resources Conversion*. 6(2):150-165.

Deng, G., Liu, H., Li, J., & Wang, Y. (2025). ATR-FTIR spectroscopy combined with metabolomics to analyze the taste components of boletus bainiugan at different drying temperatures. *Food Chemistry: X*, *26*, 102324.

Desisa, B., Muleta, D., Dejene, T., Jida, M., Goshu, A., Negi, T., & Martin-Pinto, P. (2024). Utilization of local agro-industrial by-products based substrates to enhance production and dietary value of mushroom (*P. ostreatus*) in Ethiopia. *World Journal of Microbiology and Biotechnology*, *40*(9), 277.

Deveci, E., Çayan, F., Tel-Çayan, G., & Duru, M. E. (2021). Inhibitory activities of medicinal mushrooms on α-amylase and α-glucosidase-enzymes related to type 2 diabetes. *South African Journal of Botany*, *137*, 19-23.

Deveci, E., Tel-Çayan, G., & Duru, M. E. (2018). Phenolic profile, antioxidant, anticholinesterase, and anti-tyrosinase activities of the various extracts of *Ferula elaeochytris* and *Sideritis stricta*. *International journal of food properties*, *21*(1), 771-783.

Dhahi, R. M., Mohammed, M. M., & Mikhlif, H. M. (2024). Biowaste valorization of palm tree *Phoenix dactylifera* L. for nanocellulose production. *IET nanobiotechnology*, *2024*(1), 7867463.

Díaz-Ariza, L. A., Rivera, E. L., & Sánchez, N. (2021). Occurrence of arbuscular mycorrhizal fungi in leaf litter and roots of shaded coffee plantations under organic and conventional management. *Revista Brasileira de Ciência do Solo*, *45*, e0200110.

Dissasa, G. (2022). Cultivation of different oyster mushroom (*Pleurotus* species) on coffee waste and determination of their relative biological efficiency and pectinase enzyme production, Ethiopia. *International Journal of Microbiology*, *2022*(1), 5219939.

Dolatabadi, J. E. N., Mokhtarzadeh, A., Ghareghoran, S. M., & Dehghan, G. (2013). Synthesis, characterization and antioxidant property of quercetin-Tb (III) complex. *Advanced pharmaceutical bulletin*, *4*(2), 101.

Drăgan, M., Stan, C. D., Pânzariu, A., & Profire, L. (2016). Evaluation of anti-inflammatory potential of some new ferullic acid derivatives. *Farmacia*, *64*(2), 194-197.

Du, B., Kruse, J., Winkler, J. B., Alfarray, S., Schnitzler, J. P., Ache, P., Hedrich R., & Rennenberg, H. (2019). Climate and development modulate the metabolome and antioxidative system of date palm leaves. *Journal of experimental botany*, *70*(20), 5959-5969.

Dubey, D., Dhakal, B., Dhami, K., Sapkota, P., Rana, M., Poudel, N. S., & Aryal, L. (2019). Comparative study on effect of different substrates on yield performance of oyster mushroom. *Global Journal of Biology, Agriculture, Health Sciences*, *7*.

Dundar, A., Okumus, V., Ozdemir, S., Celik, K. S., Boga, M., Ozcagli, E., Ozhan G., & Yildiz, A. (2015). Antioxidant, antimicrobial, cytotoxic and anticholinesterase activities of seven mushroom species with their phenolic acid composition. *J Hortic*, *2*(4), 1-7.

Đurović, S., Domínguez, R., Pateiro, M., Teslić, N., Lorenzo, J. M., & Pavlić, B. (2022). Industrial hemp nutraceutical processing and technology. In *Industrial hemp* (pp. 191-218). Academic Press.

Duru, M. E., Tel-Çayan, G., & Deveci, E. (2019). Evaluation of phenolic profile, antioxidant and anticholinesterase effects of *Fuscoporia torulosa*. *International Journal of Secondary Metabolite*, *6*(1), 79-89.

Dutta S. (2013). Role of mushrooms as nutraceutical an overview. *International Journal of Pharma and Bio Sciences*, 4(4):59-66,

Effiong, M. E., Umeokwochi, C. P., Afolabi, I. S., & Chinedu, S. N. (2024a). Assessing the nutritional quality of *Pleurotus ostreatus* (oyster mushroom). *Frontiers in nutrition*, *10*, 1279208.

Effiong, M. E., Umeokwochi, C. P., Afolabi, I. S., & Chinedu, S. N. (2024b). Comparative antioxidant activity and phytochemical content of five extracts of *Pleurotus ostreatus* (oyster mushroom). *Scientific Reports*, *14*(1), 3794.

Ekundayo, F. O., Ekundayo, E. A., & Ayodele, B. B. (2017). Comparative studies on glucanases and β-glucosidase activities of *Pleurotus ostreatus* and *P. pulmonarius* in solid state fermentation. *Mycosphere*, *8*(8), 1051-1059.

Elhusseiny, S. M., El-Mahdy, T. S., Awad, M. F., Elleboudy, N. S., Farag, M. M., Yassein, M. A., & Aboshanab, K. M. (2021). Proteome analysis and in vitro antiviral, anticancer and antioxidant capacities of the aqueous extracts of *Lentinula edodes* and Pleurotus ostreatus edible mushrooms. *Molecules*, *26*(15), 4623.

Elkanah, F. A., Oke, M. A., & Adebayo, E. A. (2022). Substrate composition effect on the nutritional quality of Pleurotus ostreatus (MK751847) fruiting body. *Heliyon*, 8(11).

Elkhateeb, W. A., Elnahas, M. O., Thomas, P. W., & Daba, G. M. (2020). Trametes versicolor and *Dictyophora indusiata* champions of medicinal mushrooms. *Pharm Res*, *4*(1), 00019.

Ellman, G. L., Courtney, K. D., Andres Jr, V., & Featherstone, R. M. (1961). A new and rapid colorimetric determination of acetylcholinesterase activity. *Biochemical pharmacology*, *7*(2), 88-95.

El-mously, H. (2023). Date Palm Byproducts: A Sustainable Material base for the Future Bioeconomy. *London Journal of Engineering Research*, *23*(3), 19-44.

Emiru, B., & Zenebech, K. (2016). Effect of substrates on the yield, yield attribute and dietary values of oyster mushroom (*Pleurotus ostreatus*) in the pastoral regions of northern Ethiopia. *African Journal of Food, Agriculture, Nutrition and Development*, *16*(4), 11198-11218.

Fakoya, S., Adegbehingbe, K. T., & Ademakinwa, I. S. (2020). Bio-therapeutic, phytochemical screening and antioxidant efficacies of oyster mushroom (*Pleurotus ostreatus*) obtained from the wild. *Open Journal of Medical Microbiology*, *10*(2), 58-70.

Figueiró, G.G., Graciolli, L.A. (2011). Influence of the chemical composition of the substrate in the cultivation of *Pleurotus florida*. *Ciência e Agrotecnologia*. 35:924-930.

Flora, S. J. (2009). Structural, chemical and biological aspects of antioxidants for strategies against metal and metalloid exposure. *Oxidative medicine and cellular longevity*, *2*(4), 191-206.

Follmer, C. (2010). Ureases as a target for the treatment of gastric and urinary infections. *Journal of clinical pathology*, *63*(5), 424-430.

Fomekong, G. C., Nguimbou, R. M., Tsague, M. V., Djantou, E. B., & Yanou, N. N. (2024). Effect of steam cooking and particle size on the nutritional composition, phytochemicals and antioxidant activities of oyster mushroom (*Pleurotus ostreatus*) powder. *Food Science and Biotechnology*, *33*(10), 2343-2356.

Gaikwad, V. V., Gitaje, S. R., Joshi, S. D., Kharmate, S. V., Phalle, D. R., More, M. P., Mali M. A., & Shingade, P. P. (2025). Mechanisms of Inflammation Associated with Chronic Diseases: A Brief Review. *Journal of Advances in Medicine and Medical Research*, *37*(3), 48-56.

Ganash, M., Ghany, T. M. A., Al Abboud, M. A., Alawlaqi, M. M., Qanash, H., & Amin, B. H. (2021). Lignocellulolytic activity of *Pleurotus ostreatus* under solid state fermentation using silage, stover, and cobs of maize. *BioResources*, *16*(2), 3797-3807.

Gąsecka, M., Mleczek, M., Siwulski, M., & Niedzielski, P. (2016). Phenolic composition and antioxidant properties of *Pleurotus ostreatus* and *Pleurotus eryngii* enriched with selenium and zinc. *European Food Research and Technology*, *242*(5), 723-732.

Gashaw, G., Fassil, A., & Redi, F. (2020). Evaluation of the antibacterial activity of *Pleurotus* spp. cultivated on different agricultural wastes in Chiro, Ethiopia. *International Journal of Microbiology*, *2020*(1), 9312489.

Gebru, H., Belete, T., & Faye, G. (2024). Growth and Yield Performance of *Pleurotus ostreatus* Cultivated on Agricultural Residues. *Mycobiology*, *52*(6), 388-397.

Gebru, H., Faye, G., & Belete, T. (2024). Antioxidant capacity of *Pleurotus ostreatus* (Jacq.) P. Kumm influenced by growth substrates. *AMB Express*, *14*(1), 73.

Gercek, Y. C., Dagsuyu, E., Basturk, F. N., Kırkıncı, S., Yıldırım, N., Kıskanç, G., Özmener B., Unlu Y. S., Kalkan S. N., Boztaş K., Oz G. C., Yanardağ R., Bayram N. E., & Kostić, A. Ž. (2024). Enzyme inhibitory, physicochemical, and phytochemical properties and botanical sources of honey, bee pollen, bee bread, and propolis obtained from the same apiary. *Antioxidants*, *13*(12), 1483.

Geremew, A., De Winne, P., Demissie, T. A., & De Backer, H. (2023). Characterization of wheat straw fiber grown around Jimma zone, Ethiopia. *Journal of Natural Fibers*, *20*(1), 2134268.

Girmay, Z., Gorems, W., Birhanu, G., & Zewdie, S. (2016). Growth and yield performance of *Pleurotus ostreatus* (Jacq. Fr.) Kumm (oyster mushroom) on different substrates. *Amb Express*, *6*(1), 87.

Gonfa, T., Teketle, S., & Kiros, T. (2020). Effect of extraction solvent on qualitative and quantitative analysis of major phyto-constituents and in-vitro antioxidant activity evaluation of *Cadaba rotundifolia* Forssk leaf extracts. *Cogent Food & Agriculture*, *6*(1), 1853867.

González-Palma, I., Escalona-Buendía, H. B., Ponce-Alquicira, E., Téllez-Téllez, M., Gupta, V. K., Díaz-Godínez, G., & Soriano-Santos, J. (2016). Evaluation of the antioxidant activity of aqueous and methanol extracts of *Pleurotus ostreatus* in different growth stages. *Frontiers in microbiology*, *7*, 1099.

Greig, N. H., Utsuki, T., Ingram, D. K., Wang, Y., Pepeu, G., Scali, C., Yu, Q. S., Mamczarz, J., Holloway, H. W., Giordano, T., Chen, D., Furukawa, K., Sambamurti, K., Brossi A., & Lahiri, D. K. (2005). Selective butyrylcholinesterase inhibition elevates brain acetylcholine, augments learning and lowers Alzheimer β-amyloid peptide in rodent. *Proceedings of the National Academy of Sciences*, *102*(47), 17213-17218.

Gulcin, İ., & Alwasel, S. H. (2022). Metal ions, metal chelators and metal chelating assay as antioxidant method. *Processes*, *10*(1), 132.

Habib, H. M., Platat, C., Meudec, E., Cheynier, V., & Ibrahim, W. H. (2014). Polyphenolic compounds in date fruit seed (*Phoenix dactylifera*): characterisation and quantification by using UPLC-DAD-ESI-MS. *Journal of the Science of Food and Agriculture*, *94*(6), 1084-1089.

Hasan, G. Q., & Abdulhadi, S. Y. (2023). Molecular characterization of wild *Pleurotus ostreatus* (MW457626) and evaluation of $\beta $-glucans polysaccharide activities. *arXiv preprint arXiv:2303.06187*.

He, M., Peng, Q., Xu, X., Shi, B., & Qiao, Y. (2024). Antioxidant capacities and non-volatile metabolites changes after solid-state fermentation of soybean using oyster mushroom (*Pleurotus ostreatus*) mycelium. *Frontiers in Nutrition*, *11*, 1509341.

He, Y., Suyama, T. L., Kim, H., Glukhov, E., & Gerwick, W. H. (2022). Discovery of novel tyrosinase inhibitors from marine Cyanobacteria. *Frontiers in Microbiology*, *13*, 912621.

Hegazy, S., Ahmed, K., & Hiziroglu, S. (2015). Oriented Strand Board Production from Water-Treated Date Palm Fronds. *BioResources*, *10*(1).

Herzallah, L., Mansour, F., Abuarra, A., Hara, D., Abdallah, R., & Juaidi, A. (2025). Experimental and economic analysis to explore the potential of managing date palm waste to generate energy for heating applications. *Environmental Development*, *54*, 101171.

Hoa, H. T., Wang, C. L., & Wang, C. H. (2015). The effects of different substrates on the growth, yield, and nutritional composition of two oyster mushrooms (*Pleurotus ostreatus* and *Pleurotus cystidiosus*). *Mycobiology*, *43*(4), 423-434.

Hoa, H.T., Wang, C.L. (2015). The effects of temperature and nutritional conditions on mycelium growth of two oyster mushrooms (*Pleurotus ostreatus* and *Pleurotus cystidiosus*). *Mycobiology.* 43(1):14-23.

Huang, L. C., & Mau, J. L. (2000). Antioxidant properties and polysaccharide composition analysis of *Antrodia camphorata* and *Agaricus blazei*. *Master's Thesis, National Chung-Hsing University, Taichung, Taiwan*.

Hudzicki, J. (2009). Kirby-Bauer disk diffusion susceptibility test protocol. *American society for microbiology*, *15*(1), 1-23.

Ilyasov, I. R., Beloborodov, V. L., Selivanova, I. A., & Terekhov, R. P. (2020). ABTS/PP decolorization assay of antioxidant capacity reaction pathways. *International journal of molecular sciences*, *21*(3), 1131.

Iqbal, S. M., Rauf, C. A., & Sheikh, M. I. (2005). Yield performance of oyster mushroom on different substrates. *International Journal of Agriculture and Biology*, 7(6), 900-903.

Irshad, A., Tahir, A., Sharif, S., Khalid, A., Ali, S., Naz, A., Sadia H. & Ameen, A. (2023). Determination of Nutritional and Biochemical Composition of Selected *Pleurotus* spps. *BioMed Research International*, *2023*(1), 8150909.

Iwuagwu, M. O., Nwaukwa, D. S., & Nwaru, C. E. (2020). Use of different agro-wastes in the cultivation of *Pleurotus ostreatus* (Jacq.) Kummer. *Journal of Bioresource Management*, *7*(2), 4.

Jantrapanukorn, B., Powthong, P., & Luprasong, C. (2018). In vitro biological properties of crude methanol extract from mushroom; *flammulina velutipes* (golden needle mushroom). *Asian Journal of Pharmaceutical and Clinical Research*, *11*(9).

Jayakumar, T., Thomas, P. A., & Geraldine, P. (2009). In-vitro antioxidant activities of an ethanolic extract of the oyster mushroom, *Pleurotus ostreatus*. *Innovative Food Science & Emerging Technologies*, *10*(2), 228-234.

Jayasuriya, W. B. N., Handunnetti, S. M., Wanigatunge, C. A., Fernando, G. H., Abeytunga, D. T. U., & Suresh, T. S. (2020). Anti-inflammatory activity of *Pleurotus ostreatus*, a culinary medicinal mushroom, in Wistar rats. *Evidence-Based Complementary and Alternative Medicine*, *2020*(1), 6845383.

Jin, Z., Li, Y., Ren, J., & Qin, N. (2018). Yield, nutritional content, and antioxidant activity of *Pleurotus ostreatus* on corncobs supplemented with herb residues. *Mycobiology*, *46*(1), 24-32.

Justyńska, W., Grabarczyk, M., Smolińska, E., Szychowska, A., Glabinski, A., & Szpakowski, P. (2025). Dietary Polyphenols: Luteolin, Quercetin, and Apigenin as Potential Therapeutic Agents in the Treatment of Gliomas. *Nutrients*, *17*(13), 2202.

Kadhila-Muandingi, N. P., Mubiana, F. S., & Halueendo, K. L. (2008). Mushroom Cultivation: a beginners guide. *University of Namibia, Namibia*.

Kandikattu Karthik, K. K., Kumar, P. B. R., Priya, R. V., Kumar, K. S., & Rathore, R. S. B. (2013). Evaluation of anti-inflammatory activity of Canthium parviflorum by in-vitro method. *Indian Journal of Research in Pharmacy and Biotechnology*, 1(5), 729-731.

Kedare, S. B., & Singh, R. P. (2011). Genesis and development of DPPH method of antioxidant assay. *Journal of food science and technology*, *48*(4), 412-422.

Khan, R. A., Khan, M. R., Sahreen, S., & Ahmed, M. (2012). Assessment of flavonoids contents and in vitro antioxidant activity of Launaea procumbens. *Chemistry Central Journal*, *6(1), 43.*

Khanna, P. and H. S. Garcha. (1982). Utilization of paddy straw for cultivation of *Pleurotus* species. *Mushroom Newsl*. Trop. 2(1):5-9.

Kılıç, C., Gürgen, A., Yıldız, S., Can, Z., & Değirmenci, A. (2024). Total phenolics, tannin contents, antioxidant properties, protein and sensory analysis of *Pleurotus ostreatus*, *Pleurotus citrinopileatus* and *Pleurotus djamor* cultivated on different sawdusts. *Maderas. Ciencia y tecnología*, *26*.

Kim, H., Jeon, Y. E., Kim, S. M., Jung, J. I., Ko, D., & Kim, E. J. (2023). *Agaricus bisporus* extract exerts an anti-obesity effect in high-fat diet-induced obese C57BL/6N Mice by inhibiting pancreatic lipase-mediated fat absorption. *Nutrients*, *15*(19), 4225.

Kim, Y. J., Kang, K. S., & Yokozawa, T. (2008). The anti-melanogenic effect of pycnogenol by its anti-oxidative actions. *Food and chemical toxicology*, *46*(7), 2466-2471.

Kissel, D. E., Cabrera, M. L., & Ferguson, R. B. (1988). Reactions of ammonia and urea hydrolysis products with soil. *Soil Science Society of America Journal*, *52*(6), 1793-1796.

Koba, Y., & Ishizaki, A. (1990). Chemical composition of palm fiber and its feasibility as cellulosic raw material for sugar production. *Agricultural and Biological Chemistry*, *54*(5), 1183-1187.

Kocheki, A. (2015). Investigation of physicochemical properties of crust and core dietary fiber from date seed. *Journal of food science and technology (Iran).* 12:153-161.

Kolaylı, S., Baltas, N., Sahin, H., & Karaoglu, S. (2017). Evaluation of anti-*Helicobacter pylori* activity and urease inhibition by some Turkish authentic honeys. *JFSE*, *7*, 67-73.

Kostelnik, A., & Pohanka, M. (2018). Inhibition of acetylcholinesterase and butyrylcholinesterase by a plant secondary metabolite boldine. *BioMed research international*, *2018*(1), 9634349.

Koutrotsios, G., Kalogeropoulos, N., Kaliora, A.C., Zervakis, G.I. (2018). Toward an increased functionality in oyster (*Pleurotus*) mushrooms produced on grape marc or olive mill wastes serving as sources of bioactive compounds. *Journal of agricultural and food chemistry*. 66(24):5971-5983.

Krishna, K. V., Murugan, J. M., Khan, H., Kumar, M., Veeramanikandan, V., Hatamleh, A. A., Al-Dosary, M. A., Venkatachalam K. & Balaji, P. (2023). Exploring the therapeutic potential of edible *Pleurotus* mushroom species for oxidative stress and diabetes management. *Journal of King Saud University-Science*, *35*(9), 102926.

Kumar, S., & Pandey, A. K. (2013). Chemistry and biological activities of flavonoids: an overview. *The scientific world journal*, *2013*(1), 162750.

Lakey-Beitia, J., Burillo, A. M., La Penna, G., Hegde, M. L., & Rao, K. S. (2021). Polyphenols as potential metal chelation compounds against Alzheimer's disease. *Journal of Alzheimer's Disease*, *82*(s1), S335-S357.

Lee, H. J., & Kim, K. W. (2012). Anti-inflammatory effects of arbutin in lipopolysaccharide-stimulated BV2 microglial cells. *Inflammation Research*, *61*(8), 817-825.

Leong, C. C., Ho, W. Y., Yeap, S. K., Krishnen, G., Chong, Z. X., Ho, J. S., Lim, P. T., & Ten, S. T. (2021). Assessment of phylogenetic, growth, and antioxidant capacity of *Pleurotus* spp. in Malaysia. *Journal of Food Processing and Preservation*, *45*(6), e15554.

Li, G., Wang, Y., Yu, D., Zhu, P., Zhao, G., Liu, C., & Zhao, H. (2022). Ligninolytic characteristics of *Pleurotus ostreatus* cultivated in cotton stalk media. *Frontiers in Microbiology*, *13*, 1035040.

Lin-Vien, D., Colthup, N. B., Fateley, W. G., & Grasselli, J. G. (1991). The handbook of infrared and Raman characteristic frequencies of organic molecules. *Elsevier*.

Liu, G., Qin, P., Cheng, X., Wu, L., Zhao, W., & Gao, W. (2024). Evaluation of the mechanistic basis for the antibacterial activity of ursolic acid against *Staphylococcus aureus*. *Frontiers in Microbiology*, *15*, 1389242.

Liu, J., Jia, L., Kan, J., & Jin, C. H. (2013). In vitro and in vivo antioxidant activity of ethanolic extract of white button mushroom (*Agaricus bisporus*). *Food and chemical toxicology*, *51*, 310-316.

López-Alarcón, C., & Denicola, A. (2013). Evaluating the antioxidant capacity of natural products: A review on chemical and cellular-based assays. *Analytica chimica acta*, *763*, 1-10.

Lopez-Llorca, L. V., Carbonell, T., & Salinas, J. (1999). Colonization of plant waste substrates by entomopathogenic and mycoparasitic fungi—a SEM study. *Micron*, *30*(4), 325-333.

Luz, J. M. R. D., Nunes, M. D., Paes, S. A., Torres, D. P., Silva, M. D. C. S. D., & Kasuya, M. C. M. (2012). Lignocellulolytic enzyme production of *Pleurotus ostreatus* growth in agroindustrial wastes. *Brazilian Journal of Microbiology*, *43*, 1508-1515.

Mahari, W.A.W., Nam, W.L., Sonne, C., Peng, W., Phang, X.Y., Liew, R.K., Yek, P.N.Y, Lee, X.Y., Wen, O.W., Show, P.L., Chen, W.H., Chang, J.S., Lam, S.S. (2020). Applying microwave vacuum pyrolysis to design moisture retention and pH neutralizing palm kernel shell biochar for mushroom production. *Bioresource technology*. 312:123572.

Mahdi, Z., El Hanandeh, A., & Yu, J. (2015). Date palm (*Phoenix Dactylifera* L.) seed characterization for biochar preparation. In *EPPM 2015*. Griffith University.

Mahernia, S., Bagherzadeh, K., Mojab, F., & Amanlou, M. (2015). Urease inhibitory activities of some commonly consumed herbal medicines. *Iranian journal of pharmaceutical research: IJPR*, *14*(3), 943.

Manai, S., Boulila, A., Silva, A. S., Barbosa-Pereira, L., Sendón, R., & Khwaldia, K. (2024). Recovering functional and bioactive compounds from date palm by-products and their application as multi-functional ingredients in food. *Sustainable Chemistry and Pharmacy*, *38*, 101475.

Mandeel, Q.A., Al-Laith, A.A. & Mohamed, S.A. (2005). Cultivation of oyster mushrooms (*Pleurotus* spp.) on various lignocellulosic wastes. *World Journal of Microbiology and Biotechnology*, *21*, 601-607. https://doi.org/10.1007/s11274-004-3494-4

Mau, J. L., Chao, G. R., & Wu, K. T. (2001). Antioxidant properties of methanolic extracts from several ear mushrooms. *Journal of Agricultural and Food Chemistry*, *49*(11), 5461-5467.

May, N., de Sousa Alves Neri, J. L., Clunas, H., Shi, J., Parkes, E., Dongol, A., Wang Z., Naranjo C. J., Yu Y., Huang X. F., Charlton K. & Weston-Green, K. (2023). Investigating the therapeutic potential of plants and plant-based medicines: relevance to antioxidant and neuroprotective effects. *Nutrients*, 15(18), 3912.

McDonald, J. H. (2014). *Handbook of biological statistics* (3rd ed.). Baltimore, MD: Sparky House Publishing.

Melanouri, E.M., Dedousi, M., Diamantopoulou, P. (2022). Cultivating *Pleurotus ostreatus* and *Pleurotus eryngii* mushroom strains on agro-industrial residues in solid-state fermentation. Part I: Screening for growth, endoglucanase, laccase and biomass production in the colonization phase. *Carbon Resources Conversion*. 5(1):61-70.

Mihai, R. A., Melo Heras, E. J., Florescu, L. I., & Catana, R. D. (2022). The edible gray oyster fungi *Pleurotus ostreatus* (Jacq. ex Fr.) P. Kumm a potent waste consumer, a biofriendly species with antioxidant activity depending on the growth substrate. *Journal of Fungi*, *8*(3), 274.

Mizutani, T., Inatomi, S., Inazu, A., & Kawahara, E. (2010). Hypolipidemic effect of *Pleurotus eryngii* extract in fat-loaded mice. *Journal of nutritional science and vitaminology*, *56*(1), 48-53.

Mkhize, S. S., Cedric Simelane, M. B., Mongalo, I. N., & Pooe, O. J. (2022). The effect of supplementing mushroom growing substrates on the bioactive compounds, antimicrobial activity, and antioxidant activity of *Pleurotus ostreatus*. *Biochemistry Research International*, *2022*(1), 9436614.

Mkhize, S. S., Cloete, J., Basson, A. K., & Zharare, G. E. (2016). Performance of *Pleurotus ostreatus* mushroom grown on maize stalk residues supplemented with various levels of maize flour and wheat bran. *Food Science and Technology*, *36*, 598-605.

Mohamed, R. M., Fageer, A. S., Eltayeb, M. M., & Mohamed Ahmed, I. A. (2014). Chemical composition, antioxidant capacity, and mineral extractability of S udanese date palm (*Phoenix dactylifera* L.) fruits. *Food Science & Nutrition*, *2*(5), 478-489.

Morales, D., Rutckeviski, R., Villalva, M., Abreu, H., Soler-Rivas, C., Santoyo, S., Iacomini M. & Smiderle, F. R. (2020). Isolation and comparison of α-and β-D-glucans from shiitake mushrooms (*Lentinula edodes*) with different biological activities. *Carbohydrate Polymers*, *229*, 115521.

Moran, J. F., Klucas, R. V., Grayer, R. J., Abian, J., & Becana, M. (1997). Complexes of iron with phenolic compounds from soybean nodules and other legume tissues: prooxidant and antioxidant properties. *Free Radical Biology and Medicine*, *22*(5), 861-870.

Movasaghi, Z., Rehman, S., & ur Rehman, D. I. (2008). Fourier transform infrared (FTIR) spectroscopy of biological tissues. *Applied Spectroscopy Reviews*, *43*(2), 134-179.

Mrabet, A., Jiménez-Araujo, A., Fernández-Prior, Á., Bermúdez-Oria, A., Fernández-Bolaños, J., Sindic, M., & Rodríguez-Gutiérrez, G. (2022). Date Seed: Rich source of antioxidant phenolics obtained by hydrothermal treatments. *Antioxidants, 11(10), 1914.*

Munteanu, I. G., & Apetrei, C. (2021). Analytical methods used in determining antioxidant activity: A review. *International journal of molecular sciences*, *22*(7), 3380.

Murthy, P. S., & Manonmani, H. K. (2008). Bioconversion of Coffee industry wastes with white rot fungus Pleurotus florida.

Muruke, M. H. (2014). Evaluation of antioxidant and iron chelating activities of a wild edible oyster mushroom *Pleurotus cystidiosus* from Tanzania. *Evaluation*, *29*.

Nabili, A., Fattoum, A., Brochier-Salon, M. C., Bras, J., and Elaloui, E. (2017). "Synthesis of cellulose triacetate-I from microfibrillated date seeds cellulose (*Phoenix dactylifera* L.)," Iranian Polymer Journal 26, 137-147.

Naim, L., Alsanad, M. A., El Sebaaly, Z., Shaban, N., Abou Fayssal, S., & Sassine, Y. N. (2020). Variation of *Pleurotus ostreatus* (Jacq. Ex Fr.) P. Kumm.(1871) performance subjected to different doses and timings of nano-urea. *Saudi Journal of Biological Sciences*, *27*(6), 1573-1579.

Naraian, R., Sahu, R. K., Kumar, S., Garg, S. K., Singh, C. S., & Kanaujia, R. S. (2008). Influence of different nitrogen rich supplements during cultivation of *Pleurotus florida* on maize cobs substrate. *The Environmentalist*, 29(1), 1-7. http://dx.doi.org/10.1007/s10669008-9174-4

National Center for Biotechnology Information (2025). PubChem Taxonomy Summary for Taxonomy *Pleurotus ostreatus*. Retrieved August 30, 2025 from https://pubchem.ncbi.nlm.nih.gov/taxonomy/Pleurotus-ostreatus.

Neelam, S., Chennupati, S., Singh, S. (2011). Comparative studies on growth parameters and physio-chemical analysis of *Pleurotus ostreatus* and *Pleurotus florida*. *Asian Journal of Plant Science & Research.*

Nieuwenhuijzen, B.V., Oei, P. (2005). Small-scale mushroom cultivation: oyster, shiitake and wood ear mushrooms, 1st ed. Agrodok.

Niloy, M. A. H. M., Islam, S., Ferdous, T., Rahman, S., Yesmin, S., Bin Rasul, S., & Khandakar, J. (2025). Deciphering the role of substrate carbon to nitrogen ratio in preventing orange mold contamination caused by *Neurospora sitophila* in mushroom cultivation. *Frontiers in Industrial Microbiology, 2, 1508079.*

Noor, S., Mohammad, T., Rub, M. A., Raza, A., Azum, N., Yadav, D. K., Hassan M.d I. & Asiri, A. M. (2022). Biomedical features and therapeutic potential of rosmarinic acid. *Archives of Pharmacal Research*, *45*(4), 205-228.

Nosalova N, Bobek P, Cerna S, GalbavyS and Stvrtina S. (2001). Effects of Pleuran (β-Glucan isolated from *Pleurotus ostreatus*) on experimental colitis in Rats. Journal of Physiological Research, 50(6):575-581,

Nwaokobia, K., Ogboru, R. O., & Idibie, C. A. (2018). Investigating the proximate, ultimate and chemical composition of four cultivars of date seed, *Phoenix dactylifera* L. *World News of Natural Sciences*, *18*(2).

Obodai, M., Vowotor, K.A., Marfo, K. (2002). Performance of various strains of *Pleurotus* species under Ghanaian conditions. *Mushroom Biology and Mushroom Products.* 461-466.

Oei, P. (2003). Mushroom cultivation–appropriate technology for mushroom growers, 3rd ed. Backhuys Publishers, Leiden.

Oei, P., & Nieuwenhuijzen, B. V. (2005). La culture des champignons à petite échelle: pleurotes, shiitakes et auriculaires. *Agromisa*.

Osorio-Tobón, J. F. (2020). Recent advances and comparisons of conventional and alternative extraction techniques of phenolic compounds. *Journal of Food Science and Technology*, *57*(12), 4299-4315.

Östbring, K., Lager, I., Chagas, J. C. C., Ramin, M., Ahlström, C., & Hultberg, M. (2023). Use of oyster mushrooms (*Pleurotus ostreatus*) for increased circularity and valorization of rapeseed residues. *Journal of Environmental Management*, *344*, 118742.

Otieno, O.D., Mulaa, F.J., Obiero, G., Midiwo, J. (2022). Utilization of fruit waste substrates in mushroom production and manipulation of chemical composition. *Biocatalysis and Agricultural Biotechnology*. 39:102250.

Owaid, M. N., Al-Saeedi, S. S. S., & Abed, I. A. (2016). Recycling of date-palm fiber to produce Pleurotus cornucopiae var. citrinopileatus mushroom. *International Journal of Environment*, *5*(4), 56-65.

Oyaizu, M. (1986). Studies on products of browning reactions: antioxidative activities of browning reaction prepared from glucosamine. Japanese Journal of Nutrition, 44, 307–315.

Oyetayo, O. V. (2011). Medicinal uses of mushrooms in Nigeria: towards full and sustainable exploitation. *African Journal of Traditional, Complementary and Alternative Medicines*, *8*(3).

Pandey, K., Ghosh, S. K., Sanyal, T., Bera, T., & Pal, S. (2023). Mycochemistry, antioxidant content, and antioxidant potentiality of the ethanolic extract of *Pleurotus florida* and its

anti-cancerous effect on HeLa cancer cell line, and antitumor effect on HeLa-implanted mice. *International Journal of Health Sciences*, *17*(1), 18.

Parí, S. M., Saldaña, E., Rios-Mera, J. D., Quispe Angulo, M. F., & Huaman-Castilla, N. L. (2025). Emerging Technologies for Extracting Antioxidant Compounds from Edible and Medicinal Mushrooms: An Efficient and Sustainable Approach. *Compounds*, *5*(3), 29.

Paudel, S., Dhakal, D. (2020). Archives of Agriculture and Environmental Science. *Archives of Agriculture and Environmental Science*. 5(2):190-195.

Pellegrino, R. M., Blasi, F., Angelini, P., Ianni, F., Alabed, H. B., Emiliani, C., Venanzoni, R. & Cossignani, L. (2022). LC/MS Q-TOF metabolomic investigation of amino acids and dipeptides in *Pleurotus ostreatus* grown on different substrates. *Journal of Agricultural and Food Chemistry*, *70*(33), 10371-10382.

Pérez, M., Dominguez-López, I., & Lamuela-Raventós, R. M. (2023). The chemistry behind the folin–ciocalteu method for the estimation of (poly) phenol content in food: Total phenolic intake in a mediterranean dietary pattern. *Journal of agricultural and food chemistry*, *71*(46), 17543-17553.

Pillaiyar, T., Manickam, M., & Namasivayam, V. (2017). Skin whitening agents: Medicinal chemistry perspective of tyrosinase inhibitors. *Journal of enzyme inhibition and medicinal chemistry*, *32*(1), 403-425.

Pisoschi, A. M., & Pop, A. (2015). The role of antioxidants in the chemistry of oxidative stress: A review. *European journal of medicinal chemistry*, *97*, 55-74.

Polito, F., De Martino, L., Mirabile, G., Venturella, G., Gargano, M. L., De Feo, V., Elshafie H. S. & Camele, I. (2024). Composition and antimicrobial activity of hydroalcoholic extracts of *Pleurotus eryngii* var. *ferulae* and *P. eryngii* var. *elaeoselini*. *Frontiers in Chemistry*, *12*, 1498787.

Prabu, M., & Kumuthakalavalli, R. (2014). In Vitro And In Vivo Antiinflammatory Activity Of The Methanolic Extract Of White Oyster Mushroom *Pleurotus Florida* (Mont.) Singer. *Int J Pharm Biol Sci*, *5*, 370-5.

Prieto, P., Pineda, M., & Aguilar, M. (1999). Spectrophotometric quantitation of antioxidant capacity through the formation of a phosphomolybdenum complex: specific application to the determination of vitamin E. *Analytical biochemistry*, *269*(2), 337-341.

Pukalski, J., & Latowski, D. (2022). Secrets of flavonoid synthesis in mushroom cells. *Cells*, *11*(19), 3052.

Rahimah, S. B., Djunaedi, D. D., Soeroto, A. Y., & Bisri, T. (2019). The phytochemical screening, total phenolic contents and antioxidant activities in vitro of white oyster mushroom (*Pleurotus ostreatus*) preparations. *Open access Macedonian journal of medical sciences*, *7*(15), 2404.

Raman, J., Jang, K. Y., Oh, Y. L., Oh, M., Im, J. H., Lakshmanan, H., & Sabaratnam, V. (2021). Cultivation and nutritional value of prominent *Pleurotus* spp.: an overview. *Mycobiology*, *49*(1), 1-14.

Randhawa, K., & Shri, R. (2018). Comparison of antioxidant and anticholinesterase activities of selected Pleurotus species (Agaricomycetes) from India. *International Journal of Medicinal Mushrooms*, *20*(8).

Re, R., Pellegrini, N., Proteggente, A., Pannala, A., Yang, M., & Rice-Evans, C. (1999). Antioxidant activity applying an improved ABTS radical cation decolorization assay. *Free radical biology and medicine*, *26*(9-10), 1231-1237.

Reis, F. S., Martins, A., Barros, L., & Ferreira, I. C. (2012). Antioxidant properties and phenolic profile of the most widely appreciated cultivated mushrooms: A comparative study between in vivo and in vitro samples. *Food and chemical toxicology*, *50*(5), 1201-1207.

Rendleman Jr, J. A. (2003). The reaction of starch with iodine vapor. Determination of iodide-ion content of starch–iodine complexes. *Carbohydrate Polymers*, *51*(2), 191-202.

Rivero-Pérez, N., Ayala-Martínez, M., Zepeda-Bastida, A., Meneses-Mayo, M., & Ojeda-Ramírez, D. (2016). Anti-inflammatory effect of aqueous extracts of spent *Pleurotus ostreatus* substrates in mouse ears treated with 12-O-tetradecanoylphorbol-13-acetate. *Indian Journal of pharmacology*, *48*(2), 141-144.

Rizki, M., and Tamai, Y. (2011). Effects of different nitrogen rich substrates and their combination to the yield performance of oyster mushroom (*Pleurotus ostreatus*), *World Journal of Microbiology and Biotechnology* 27, 1695-1702. DOI: 10.1007/s11274-010-0624-z

Sales-Campos, C., Araujo, L.M., Minhoni, M.T.D.A., Andrade, M.C.N.D. (2011). Physiochemical analysis and centesimal composition of *Pleurotus ostreatus* mushroom grown in residues from the Amazon. *Food Science and Technology*. 31:456-461.

Salmones, D., Mata, G., & Waliszewski, K. N. (2005). Comparative culturing of *Pleurotus* spp. on coffee pulp and wheat straw: biomass production and substrate biodegradation. *Bioresource technology*, *96*(5), 537-544.

Samuel, A.A., Eugene, T.L. (2012). Growth performance and yield of oyster mushroom (*Pleurotus ostreatus*) on different substrates composition in Buea South West Cameroon. *Science journal of biochemistry*. 2012.

Sánchez-Moreno, C. (2002). Methods used to evaluate the free radical scavenging activity in foods and biological systems. *Food science and technology international*, *8*(3), 121-137.

Sánchez-Vioque, R., Polissiou, M., Astraka, K., De Los Mozos-Pascual, M., Tarantilis, P., Herraiz-Peñalver, D., & Santana-Méridas, O. (2013). Polyphenol composition and antioxidant and metal chelating activities of the solid residues from the essential oil industry. *Industrial Crops and Products*, *49*, 150-159.

Sanna, D., & Fadda, A. (2022). Role of the hydroxyl radical-generating system in the estimation of the antioxidant activity of plant extracts by electron paramagnetic resonance (EPR). *Molecules*, *27*(14), 4560.

Seethapathy, P., Thangaraj, P., Pandita, A., Sankaralingam, S., & Pandita, D. (2023). Oyster Mushroom (*Pleurotus ostreatus*). In *Mushrooms* (pp. 302-321). CRC Press.

Selvaananthi, A., & Alphonse, A. J. (2022). *Pleurotus* cultivation: a sustainable way to utilize agrowaste. *Acta agriculturae Slovenica*, *118*(1), 1-7.

Selvamani, S., El-Enshasy, H. A., Dailin, D. J., Malek, R. A., Hanapi, S. Z., Ambehabati, K. K., Sukmawati, D. Leng O. M. & Moloi, N. (2018). Antioxidant compounds of the edible mushroom *Pleurotus ostreatus*. *Int J Biotechnol Wellness Ind*, *7*(1), 1-14.

Shamtsyan, M., & Pogačnik, L. (2020). Antiradical and antidiabetic activity of Pleurotus ostreatus extracts. In *E3S web of conferences*. 215, p. 05006). EDP Sciences.

Shokrollahi, S., Denayer, J. F., & Karimi, K. (2023). Efficient bioenergy recovery from different date palm industrial wastes. *Energy*, *272*, 127057.

Siddique, M., Soomro, S. A., & Aziz, S. (2021). Lignin rich energy recovery from lignocellulosic plant biomass into biofuel production. *J Nat Appl Res*, *1*(2), 57-69.

Silva, A. M., Preto, M., Grosso, C., Vieira, M., Delerue-Matos, C., Vasconcelos, V., Reis, M., Barros, L. & Martins, R. (2023). Tracing the path between mushrooms and Alzheimer's disease—A literature review. *Molecules*, *28*(14), 5614.

Singh, A. (2022). Hyperlipidemia in cardiovascular health and digestion. In *Nutrition and Functional Foods in Boosting Digestion, Metabolism and Immune Health* (pp. 141-150). Academic Press.

Skanda, S., & Vijayakumar, B. S. (2021). Antioxidant and anti-inflammatory metabolites of a soil-derived fungus Aspergillus arcoverdensis SSSIHL-01. *Current Microbiology*, *78*(4), 1317-1323.

Skroza, D., Šimat, V., Vrdoljak, L., Jolić, N., Skelin, A., Čagalj, M., Frleta R. & Generalić Mekinić, I. (2022). Investigation of antioxidant synergisms and antagonisms among phenolic acids in the model matrices using FRAP and ORAC methods. *Antioxidants*, *11*(9), 1784.

Smirnoff N, Cumbes QJ. (1989). Hydroxyl radical scavenging activity of compatible solutes. Phytochemistry. 28:1057–1060.

Smith, B. C. (2011). Fundamentals of Fourier transform infrared spectroscopy. CRC press.

Sonnenberg, A. S., Baars, J. J., Straatsma, G., Hendrickx, P. M., Hendrix, E., Blok, C., & van Peer, A. (2022). Feeding growing button mushrooms: The role of substrate mycelium to feed the first two flushes. *Plos one*, *17*(7), e0270633.

Souza, P. M. D. (2010). Application of microbial α-amylase in industry-A review. *Brazilian journal of microbiology*, *41*, 850-861.

Souza, S. P. D., Pereira, L. L., Souza, A. A., & Santos, C. D. D. (2011). Inhibition of pancreatic lipase by extracts of *Baccharis trimera* (Less.) DC., Asteraceae: evaluation of antinutrients and effect on glycosidases. *Revista Brasileira de Farmacognosia*, *21*, 450-455.

Stamets P (2000). Growing Gourmet and Medicinal Mushrooms. 3rd ed. Ten Speed Press, Berkley (CA): pp. 574.

Su, C. H., Lai, M. N., & Ng, L. T. (2013). Inhibitory effects of medicinal mushrooms on α-amylase and α-glucosidase–enzymes related to hyperglycemia. *Food & function*, *4*(4), 644-649.

Subedi, S., Kunwar, N,. Pandey, K.R. ,Joshi, YR. (2023). Performance of oyster mushroom (*Pleurotus ostreatus*) on paddy straw, water hyacinth and their combinations. Heliyon. 9:e19051

Suleiman, R. K., Iali, W., El Ali, B., & Umoren, S. A. (2021). New constituents from the leaves of date palm (*Phoenix dactylifera* L.) of Saudi origin. *Molecules*, *26*(14), 4192.

Suliman, M., & Tahir, M. (2025). Date palm-derived graphene materials: a review on recent advances in synthesis, characterization and environmental applications. *Frontiers in Nanotechnology*, *7*, 1518715.

Sulistiany, H., Sudirman, L. I., & Dharmaputra, O. S. (2016). Production of fruiting body and antioxidant activity of wild Pleurotus. *HAYATI Journal of Biosciences*, *23*(4), 191-195.

Sutthisa, W., & Anujakkawan, S. (2023). Antibacterial Potential of Oyster Mushroom (*Pleurotus ostreatus* (Jacq. Ex Fr.) P. Kumm.) Extract against Pathogenic Bacteria. *Journal of Pure & Applied Microbiology*, *17*(3).

Syedd-León, R., Sandoval-Barrantes, M., Trimiño-Vásquez, H., Villegas-Peñaranda, L. R., & Rodríguez-Rodríguez, G. (2020). Revisiting the fundamentals of p-nitrophenol analysis for its application in the quantification of lipases activity. A graphical update. *Uniciencia*, *34*(2), 31-43.

Tabi, A. N. M., Zakil, F. A., Fauzai, W. N. F. M., Ali, N., & Hassan, O. (2008). The usage of empty fruit bunch (EFB) and palm pressed fibre (PPF) as substrates for the cultivation of Pleurotus ostreatus. *Jurnal Teknologi*, *49*(F), 189-196.

Tahri, I., Devin, I. Z., Ruelle, J., Segovia, C., & Brosse, N. (2016). Extraction and characterization of fibers from palm tree. *BioResources*, *11*(3), 7016-7025.

Talkad, M. S., Das, R. K., Bhattacharjee, P., Ghosh, S., & Shivajirao, U. P. (2015). Establishment of enzyme inhibitory activities of lovastatin, isolated from *Pleurotus ostreatus*. *International Journal of Applied sciences and biotechnology*, *3*(3), 408-416.

Taofiq, O., Heleno, S. A., Calhelha, R. C., Alves, M. J., Barros, L., Barreiro, M. F., González-Paramás M. & Ferreira, I. C. (2016). Development of mushroom-based

cosmeceutical formulations with anti-inflammatory, anti-tyrosinase, antioxidant, and antibacterial properties. *Molecules*, *21*(10), 1372

Tekeste, N., Dessie, K., Taddesse, K., & Ebrahim, A. (2020). Evaluation of different substrates for yield and yield attributes of oyster mushroom (*Pleurotus ostreatus*) in crop-livestock farming system of northern Ethiopia. *The Open Agriculture Journal*, *14*(1).

Tel, G., Ozturk, M., Duru, M. E., & Turkoglu, A. (2015). Antioxidant and anticholinesterase activities of five wild mushroom species with total bioactive contents. *Pharmaceutical biology*, *53*(6), 824-830.

Tomczyk, M., Ceylan, O., Locatelli, M., Tartaglia, A., Ferrone, V., & Sarikurkcu, C. (2019). *Ziziphora taurica* subsp. *taurica*: analytical characterization and biological activities. *Biomolecules, 9(8), 367.*

Torres-Martínez, B. D. M., Vargas-Sánchez, R. D., Torrescano-Urrutia, G. R., Esqueda, M. C., Rodríguez-Carpena, J. G., Fernández-López, J., José Pérez-Álvarez Á. & Sánchez-Escalante, A. (2023). Physicochemical, techno-functional and antioxidant properties of *Pleurotus* spp. powders. *TIP. Revista especializada en ciencias químico-biológicas*, *26*. 1-10.

Trabzuni, D. M., Ahmed, S. E. B., & Abu-Tarboush, H. M. (2014). Chemical composition, minerals and antioxidants of the heart of date palm from three Saudi cultivars. *Food and Nutrition Sciences*, *5*(14), 1379.

Tsai, S. Y., Huang, S. J., Lo, S. H., Wu, T. P., Lian, P. Y., & Mau, J. L. (2009). Flavour components and antioxidant properties of several cultivated mushrooms. *Food Chemistry*, *113*(2), 578-584.

Tupa, M., Sarijan, A., & Ekowati, N. Y. (2022). Oyster mushroom (*Pleurotus ostreatus*) growth and production on straw and brands substrate supplied with nasa liquid organic fertilizer (POC). *Jurnal Agronomi Tanaman Tropika (Juatika)*, *4*(2), 158-168.

Valério, T. P., Szeremeta, L. A., Pacheco, J. T. M. R., Barros, B. C. B., Sydney, E. B., & Danesi, E. D. G. (2024). Production of Oyster Mushroom (*Pleurotus ostreatus*) in Peach Palm By-Products: Effects on Composition and Maximization of Antioxidants Extraction. *Brazilian Archives of Biology and Technology*, *67*, e24230467.

Valverde, M. E., Hernández-Pérez, T., & Paredes-López, O. (2015). Edible mushrooms: improving human health and promoting quality life. *International journal of microbiology*, *2015*(1), 376387.

Vamanu, E. (2012). In vitro antimicrobial and antioxidant activities of ethanolic extract of lyophilized mycelium of *Pleurotus ostreatus* PQMZ91109. *Molecules*, *17*(4), 3653-3671.

Varghese, B. P., & Amritkumar, P. (2020). Comparative Study on Cultivation of Oyster Mushrooms using Nutrition Enhancing Substrates. 7. *Int. J. Sci. Res. in Biological Sciences Vol*, *7*(2).

Venturella, G., Ferraro, V., Cirlincione, F., & Gargano, M. L. (2021). Medicinal mushrooms: bioactive compounds, use, and clinical trials. *International journal of molecular sciences*, *22*(2), 634.

Vetayasuporn, S. (2007). The feasibility of using coconut residue as a substrate for oyster mushroom cultivation.

Vieira Júnior, W. G. (2025). Avaliação da eficiência e viabilidade do substrato exaurido de cogumelo em ciclos subsequentes de *Pleurotus ostreatus* e *Lentinula edodes*.

Vl, S. (1999). Analysis of total phenols and other oxidation substrates and antioxidants by means of Folin-Ciocalteu reagent. *Methods in Enzymology*, *299*, 152-178

Walker, G.M., White, N.A. (2017). Introduction to fungal physiology. *Fungi: biology and applications*, 1-35.

Weatherburn, M. (1967). Phenol-hypochlorite reaction for determination of ammonia. *Analytical chemistry*, *39*(8), 971-974.

Wiafe-Kwagyan, M., Odamtten, G. T., & Kortei, N. K. (2022). Influence of substrate formulation on some morphometric characters and biological efficiency of *Pleurotus ostreatus* EM-1 (Ex. Fr) Kummer grown on rice wastes and “wawa”(*Triplochiton scleroxylon*) sawdust in Ghana. *Food Science & Nutrition*, *10*(6), 1854-1863.

Woldegiorgis, A. Z., Abate, D., Haki, G. D., & Ziegler, G. R. (2014). Antioxidant property of edible mushrooms collected from Ethiopia. *Food chemistry*, *157*, 30-36.

Wu, F., Wang, H., Chen, Q., Pang, X., Jing, H., Yin, L., & Zhang, X. (2023). Lignin promotes mycelial growth and accumulation of polyphenols and ergosterol in *Lentinula edodes*. *Journal of Fungi*, *9*(2), 237.

Yadav, P., & Zelder, F. (2021). Detection of glyphosate with a copper (ii)-pyrocatechol violet based GlyPKit. *Analytical Methods*, *13*(38), 4354-4360.

Yakobi, S. H., Mkhize, S., & Pooe, O. J. (2023). Screening of antimicrobial properties and bioactive compounds of *Pleurotus ostreatus* extracts against *Staphylococcus aureus*, *Escherichia coli*, and *Neisseria gonorrhoeae*. *Biochemistry Research International*, *2023*(1), 1777039.

Yang, W., Guo, F., & Wan, Z. (2013). Yield and size of oyster mushroom grown on rice/wheat straw basal substrate supplemented with cotton seed hull. *Saudi journal of biological sciences*, *20*(4), 333-338.

Yılmaz, A., Yıldız, S., Kılıç, C., & Can, Z. (2017). Protein contents and antioxidant properties of *Pleurotus ostreatus* cultivated on tea and espresso wastes. *International Journal of Secondary Metabolite*, *4*(3, Special Issue 1), 177-186.

Zaidi, K. U., Ali, A. S., & Ali, S. A. (2014). Purification and characterization of melanogenic enzyme tyrosinase from button mushroom. *Enzyme research*, *2014*(1), 120739.

Zakil, F. A., Sueb, M. S. M., & Isha, R. (2019). Growth and yield performance of *Pleurotus ostreatus* on various agro-industrial wastes in Malaysia. In *AIP Conference Proceedings* (Vol. 2155, No. 1, p. 020055). AIP Publishing LLC.

Zhang, L., Larsson, A., Moldin, A., & Edlund, U. (2022). Comparison of lignin distribution, structure, and morphology in wheat straw and wood. *Industrial Crops and Products*, *187*, 115432.

Zinjarde, S. S., Bhargava, S. Y., & Kumar, A. R. (2011). Potent α-amylase inhibitory activity of Indian Ayurvedic medicinal plants. *BMC complementary and alternative medicine*, *11*(1), 1-10.

APPENDECES

APPENDIX

Appendix A: Liquid Chromatography–Mass Spectrometry

Table A1

Characteristic ionization (m/z) values of identified polyphenolic compounds by LC-MS/MS

POLYPHENOL	m/z	POLYPHENOL	m/z
Isorhamnetin- 3-O Rutinoside	623,1	oleochantal SIM	303,2
Quercetin-3-O.hexose deoxyhexose	609,1	Hesperetin	301,3
Kaempferol-3-O-glucose	609,1	quercetin sim	301
Rutin	609	cathechin\epicathechin	289
Kaempferol-3-O-hexose deohyhexose	593,1	Kaempeferol	285
Narigin	579	Luteoilin	284,9
Procianidin	577	Arbutin	271,2
oleuropein SIM	539	Apigenin	269
Amentoflavone	537,1	Sinapic acid	223
quercetin-3-O- glucuronic acid	477	syringic acid SIM	198,9
quercetin-3-O-glucoside	463,1	syringic acid	197
Kaempferol-3-O-glucuronic acid	461,1	trans ferulic acid SIM	193
gallocathechin\epigallocathechin gallate	457	Ferulic acid	193
ursolic acid	455	Caffeic acid	179
luteoilin 7-O-glucoside	447,1	gallic acid SIM	168,9
Isorhamnetin-7-O- Pentose	447,1	Vanillic acid	167
cathechin gallate	441	p coumarci acid SIM	162,9
Kaempferol-3-O-pentose	417,1	Tyrosol	153,4
Rosmarinic acid	359	hydroxytyrosol SIM	153,05
Chlorogenic acid	353	Protocathecoic acid	153
Myricetin	317	Gentisic acid	153
Trimethoxyflavone	312	Trans-cinnamic acid	147
gallocathechin\epigallocathechin	305	p-hydroxybenzoic\salicilic acid	137

Appendix B: extraction yield

Table B1

Pleurotus ostreatus mushroom extraction yield with 80% methanol maceration

Sample	Extraction yield (%)		
	1st flush	**2nd flush**	**3rd flush**
WS	26,12	25,65	23,98
K25	31,76	27,68	22,32
K50	32,76	34,08	30,28
K75	29,44	30,28	32,4
K100	30,04	37,56	38
P25	23,6	26,48	24,04
P50	28,92	24,84	30,28
P75	39,12	29,8	29,76
P100	40,32	29,64	32,12

Appendix C: total phenolic and flavonoids content

Table C1

Pleurotus ostreatus mushroom total phenolic (mg GAE) and flavonoids (mg QE) content per g of extract and g of Dry Mushroom

SAMPLE	TPC		TFC	
	mg GAE/g extract	mg GAE/g DM	mg QE/g extract	mg QE/g DM
W1	9,252 ± 0,556^{bcdefg}	2,416 ± 0,145^{defg}	4,634 ± 0,116^{abc}	1,210 ± 0,030^{abcde}
K25/1	8,73 ± 0,113^{defg}	2,628 ± 0,207^{cdefg}	2,673 ± 0,066^{abcdefgh}	1,825 ± 0,029^{a}
K50/1	9,252 ± 0,065^{cdefg}	3,405 ± 0,128^{abcdef}	2,73 ± 0,009^{abcdefgh}	1,035 ± 0,020^{abcdefg}
K75/1	8,926± 0,704^{defg}	3,966 ± 0,081^{abc}	6,199 ± 0,099^{a}	1,510 ± 0,037^{ab}
K100/1	11,335 ± 0,427^{abcdefg}	3,071 ± 0,180^{abcdefg}	3,446 ± 0,066^{abcdef}	1,092 ± 0,019^{abcde}
P25/1	16,804 ± 0,345^{ab}	3,462 ± 0,086^{abcde}	6,397 ± 0,156a	1,043 ± 0,031^{abcdefg}
P50/1	10,619 ± 0,621^{abcdefg}	3,572 ± 0,243^{abcde}	3,776 ± 0,066^{abcd}	0,645 ± 0,011^{efghi}
P75/1	8,86 ± 0,456^{defg}	2,935 ± 0,146^{abcdefg}	2,447 ± 0,133^{cdefgh}	0,806 ± 0,027^{bcdefghi}
P100/1	10,229 ± 0,8^{abcdefg}	2,546 ± 0,139^{defg}	3,541 ± 0,028^{abcde}	1,043 ± 0,016^{abcdefg}
W2	11,726 ± 0,734^{abcde}	2,776 ± 0,036^{bcdefg}	5,624 ± 0,111^{ab}	0,850 ± 0,021^{abcdefghi}
K25/2	11,074 ± 0,407^{abcdef}	3,466 ± 0,178^{abcde}	2,739 ± 0,009a^{bcdefgh}	0,957 ± 0,052^{abcdefgh}
K50/2	11,726 ± 0,734^{abcde}	4,124 ± 0,323^{ab}	2,57 ± 0,0411^{bcdefgh}	1,428 ± 0,011^{abcd}
K75/2	12,051 ± 0,704^{abcd}	3,007 ± 0,188^{abcdefg}	2,032 ± 0,019^{efgh}	1,442 ± 0,029^{abc}
K100/2	10,814 ± 0,846^{abcde}	3,065 ± 0,113^{abcdefg}	1,929 ± 0,059^{fgh}	0,758 ± 0,003^{cdefghi}
P25/2	17,845 ± 0,396^{a}	1,774 ± 0,140^{g}	3,616 ± 0,111^{abcde}	0,603 ± 0,020^{ghi}
P50/2	15,046 ± 1,437^{abc}	1,638 ± 0,156^{g}	4,201 ± 0,125^{abc}	0,424 ± 0,014^{i}
P75/2	11,986 ± 0,816^{abcd}	2,976 ± 0,238^{abcdefg}	2,164 ± 0,038^{defgh}	0,597 ± 0,011^{ghi}
P100/2	9,903 ± 0,491^{abcdefg}	4,109 ± 0,346^{ab}	2,721 ± 0,091^{abcdefgh}	0,554 ± 0,013^{hi}
W3	10,619 ±0,579^{abcdefg}	3,031 ± 0,021^{abcdefg}	4,351 ± 0,066^{abc}	0,894 ± 0,003^{abcdefghi}
K25/3	7,949 ± 0,628^{efg}	3,996 ± 0,250^{abc}	2,702 ± 0,09^{abcdefgh}	0,876 ± 0,014^{abcdefghi}
K50/3	5,41 ± 0,517^{g}	3,649 ± 0,213^{abcd}	1,401 ± 0,047^{h}	0,615 ± 0,006^{fghi}
K75/3	9,186± 0,733^{defg}	4,062 ± 0,318^{abc}	1,844 ± 0,033^{gh}	0,724 ± 0,022^{efghi}
K100/3	10,814 ± 0,912^{abcdefg}	4,725 ± 0,105^{a}	1,457 ± 0,034^{h}	0,958 ± 0,029^{abcdefgh}
P25/3	9,447 ± 0,396^{bcdefg}	2,271 ± 0,095^{efg}	2,155 ± 0,043^{defgh}	0,518 ± 0,010^{hi}
P50/3	9,382 ± 0,68^{bcdefg}	2,841 ± 0,206^{bcdefg}	2,475 ± 0,148^{bcdefgh}	0,750 ± 0,045^{defghi}
P75/3	6,7124 ± 0,792^{fg}	1,998 ± 0,236^{fg}	2,551 ± 0,212^{bcdefgh}	0,759 ± 0,063^{cdefghi}
P100/3	8,73 ± 0,851^{defg}	2,804 ± 0,273^{bcdefg}	3,333 ± 0,093^{abcdefg}	1,071 ± 0,030^{abcdef}

Values with different superscript letters differ significantly (Kruskal–Wallis + Dunn's test, Benjamini–Hochberg correction, $p < 0.05$). Letters follow activity ranking, with "a" indicating the highest activity

Figure C1

Gallic acid standard calibration curve for total phenolic content (TPC) determination

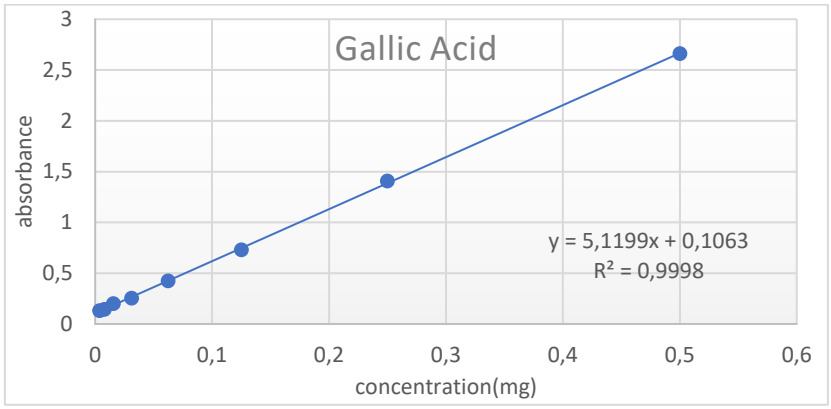

Figure C2

Quercetin standard calibration curve for total flavonoid content (TFC) determination

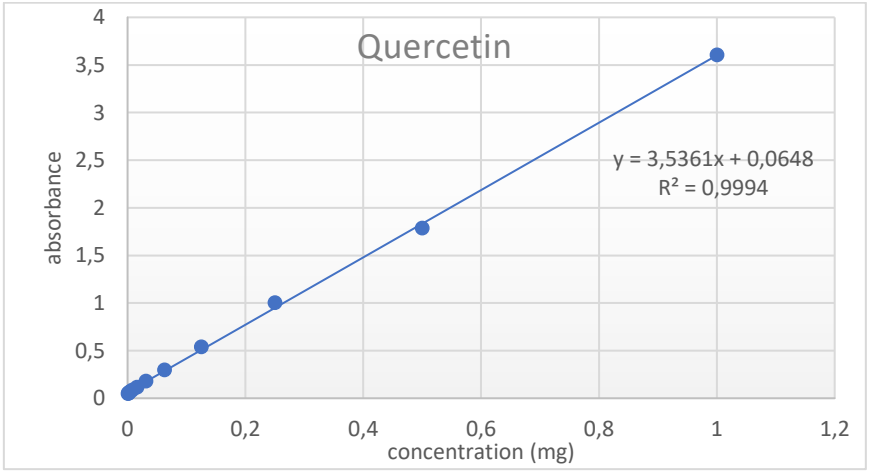

Appendix D: FTIR analysis

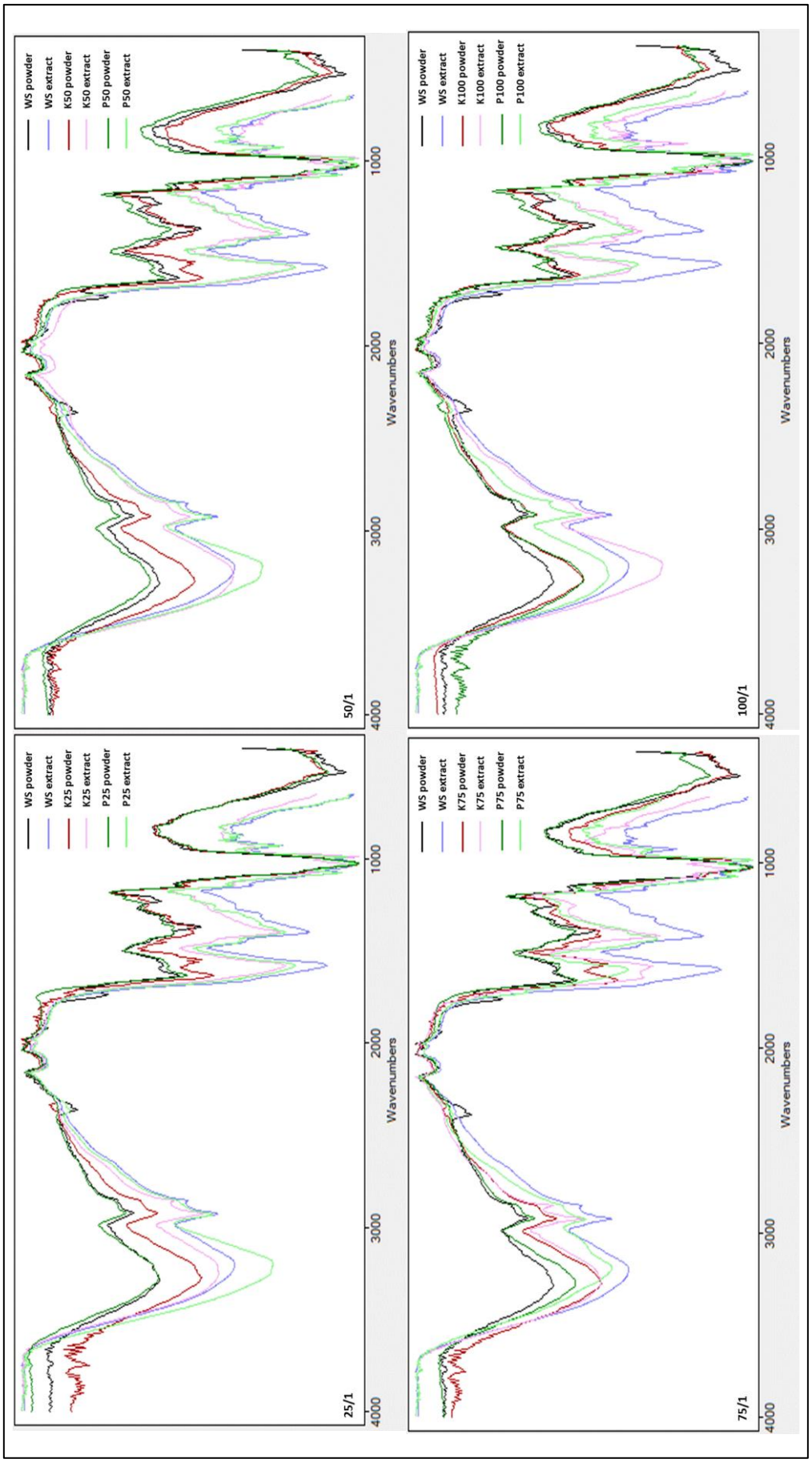

Figure D1

FTIR of 1st flush

Figure D2

FTIR of 2nd flush

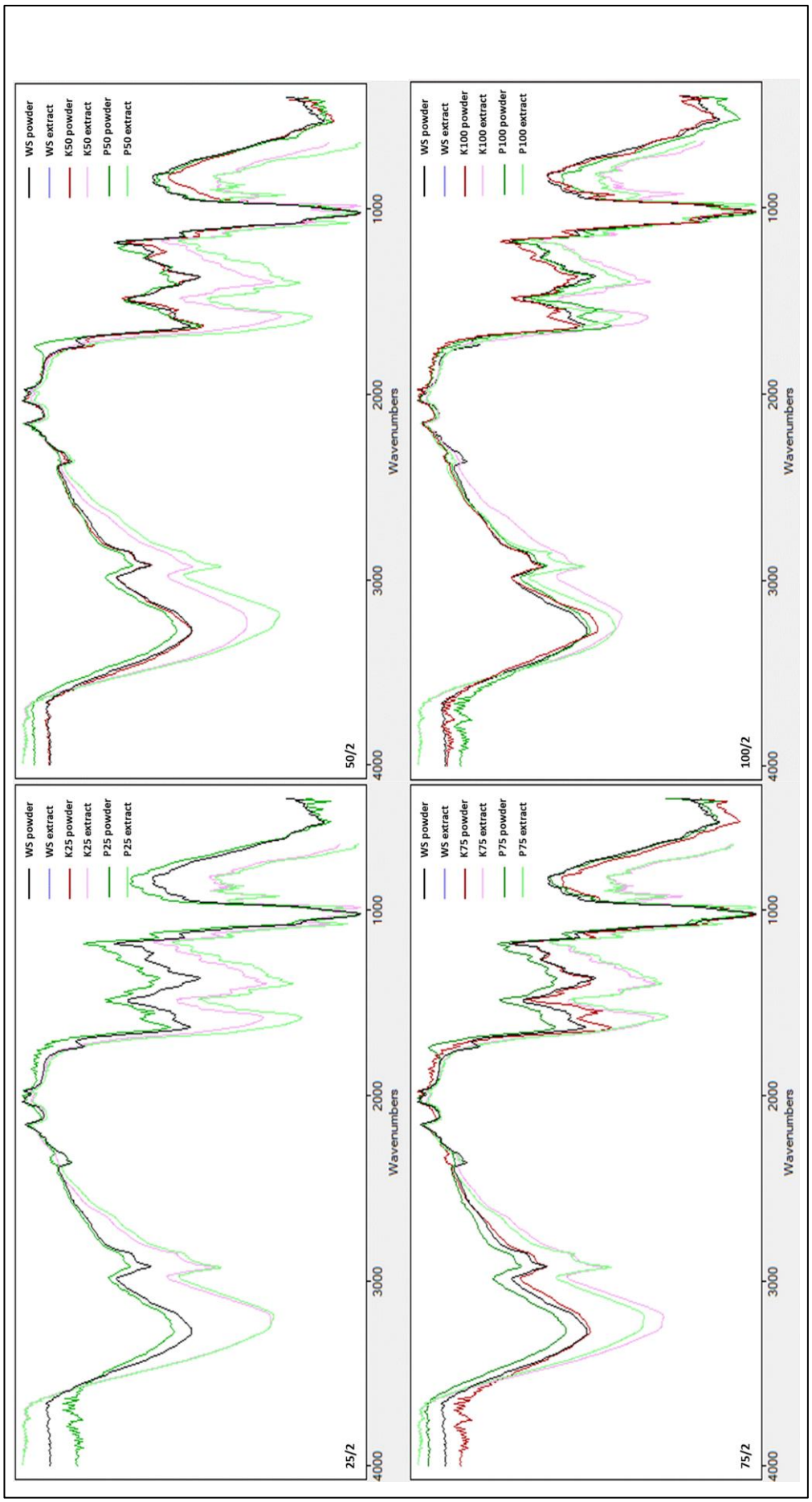

Figure D3

FTIR of 3rd flush

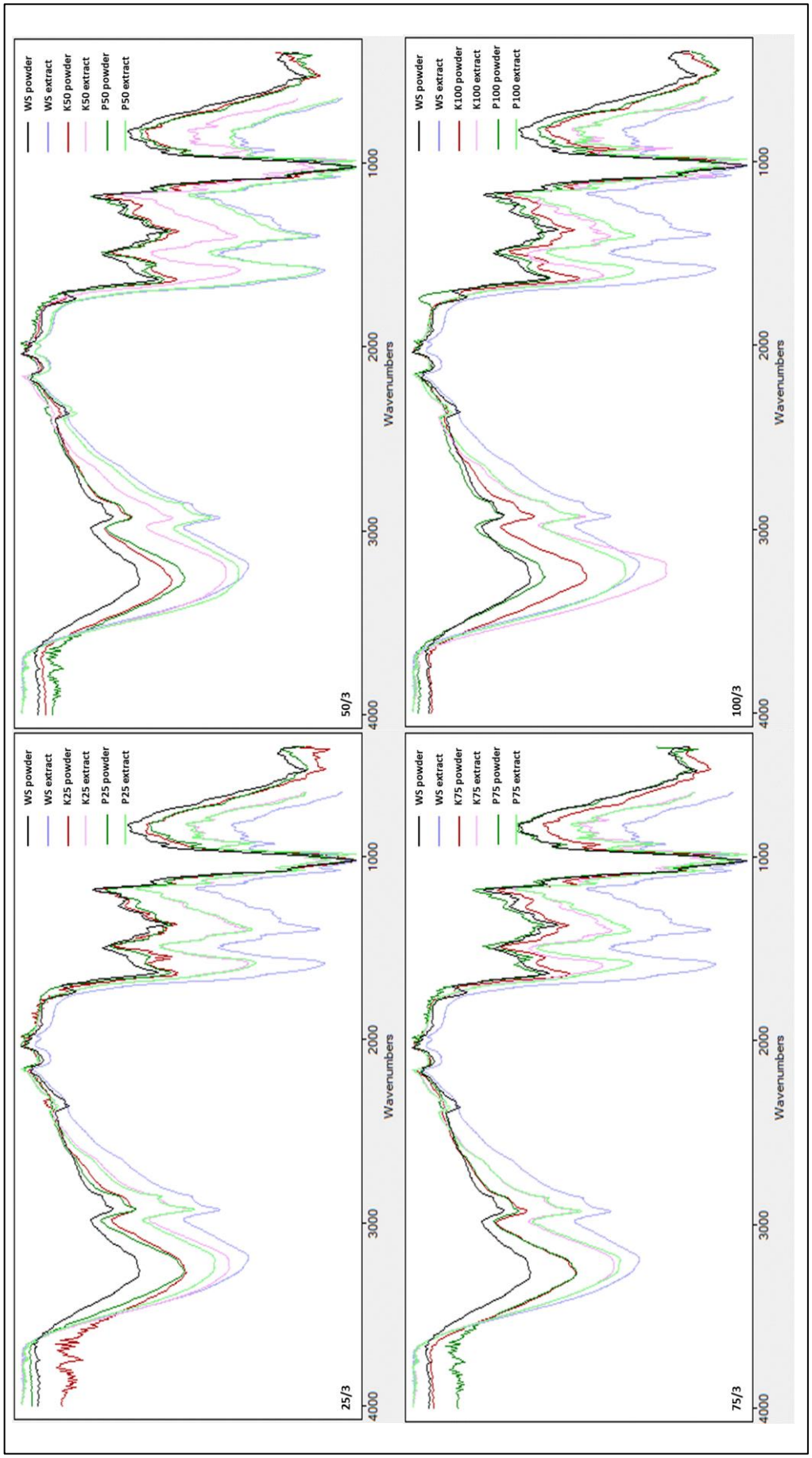

Figure D4

FTIR of powdered samples

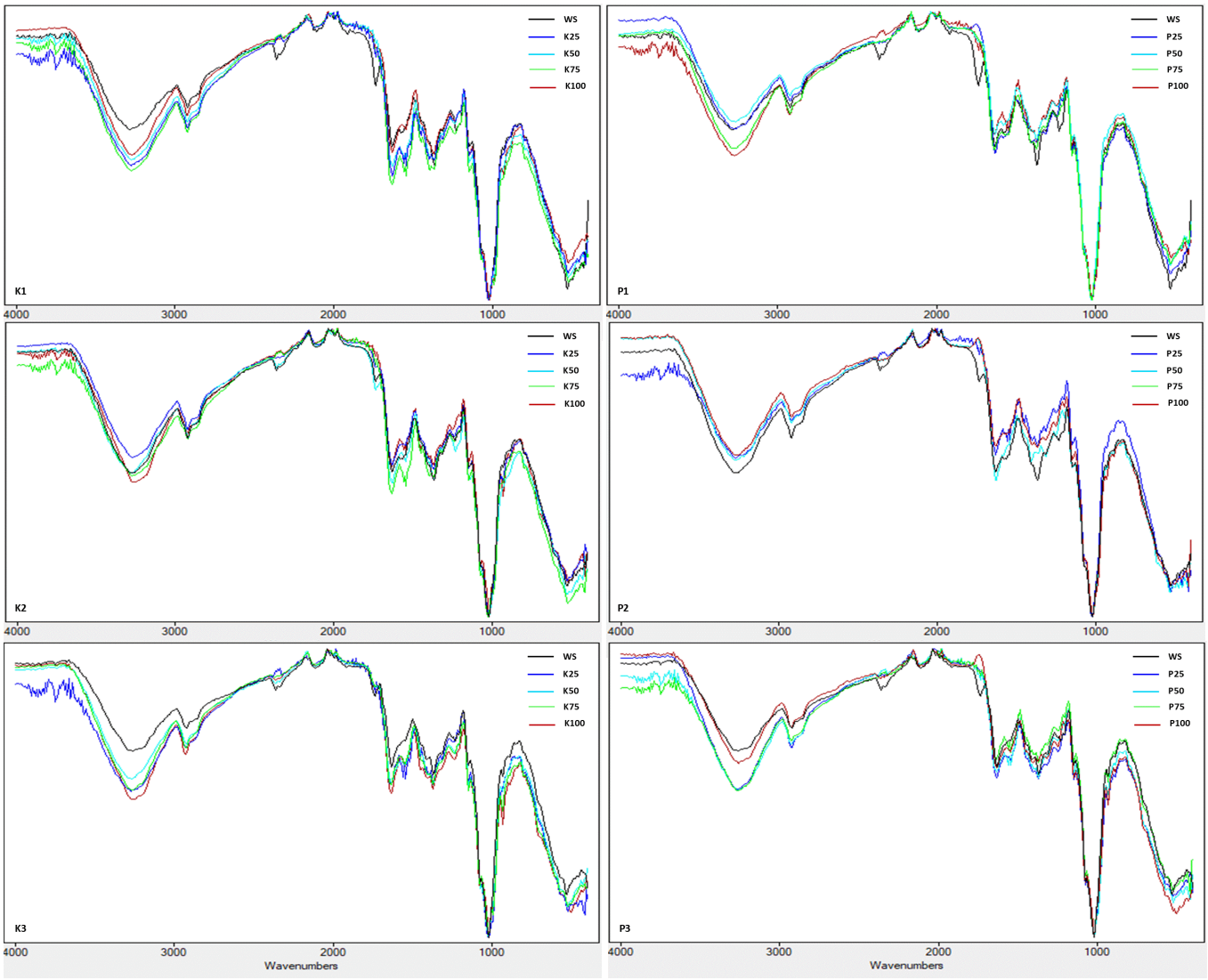

Figure D5

FTIR of extract samples

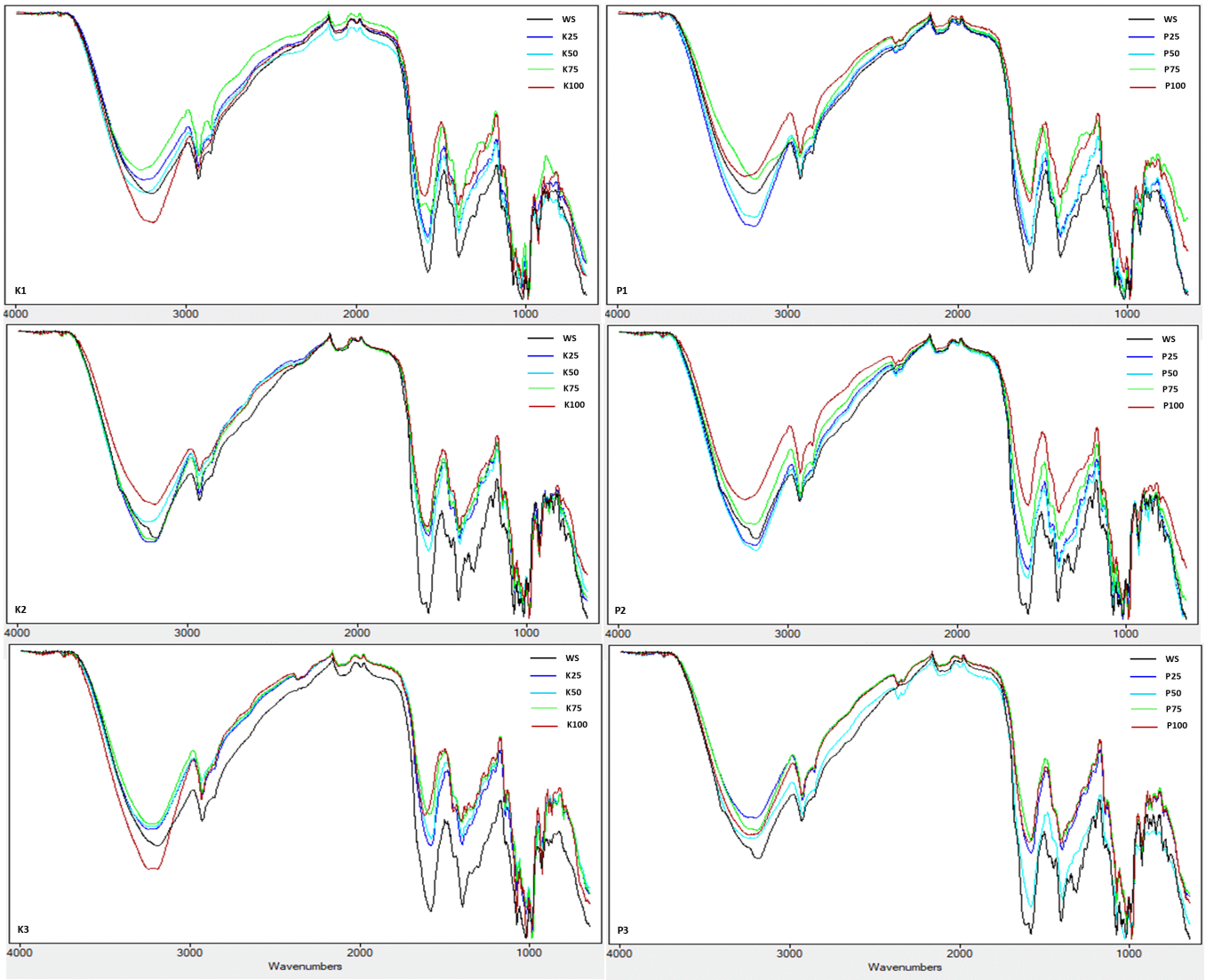

Appendix E: Scavenging Antioxidant Activity

Table E1

Table: IC_{50} Values (µg/ml) of DPPH, ABTS, and Hydroxyl Radical scavenging assays of ***three flushes Pleurotus ostreatus extracts cultivated in different substrate formulas***

Sample		IC_{50} (µg/ml)		
Substrate	**Flush**	**DPPH**	**ABTS**	**HR**
WS	**1st**	604,23 ± 5,71^{abc}	142,75 ± 1,39^{ab}	1105,33± 16,22^{abcd}
	2nd	537,54± 8,72^{ab}	195,20± 8,82^{abcde}	1240,12± 4,26^{abcdefg}
	3rd	529,85± 20,77^{ab}	172,36± 3,13^{abcd}	1186,96± 10,99^{abcdef}
K25	**1st**	716,45± 12,43^{abcdef}	249,18± 8,98^{abcdef}	1019,80± 38,47^{abc}
	2nd	767,22± 10,04^{bcde}	214,00± 3,52a^{abcde}	1568,59± 6,87^{g}
	3rd	855,80± 10,56^{cdef}	260,02± 4,87^{abcdef}	2232,22± 32,79^{efg}
K50	**1st**	713,03± 19,23^{abcdef}	231,03± 0,22^{abcdef}	1041,89± 14,67^{abc}
	2nd	628,51± 15,94^{abcd}	189,56± 5,06^{abcde}	1178,72± 8,95^{abcdef}
	3rd	836,80± 20,01^{cdef}	279,72± 4,76 ^{cdef}	1626,55± 36,42^{bcdefg}
K75	**1st**	657,12± 5,62^{abcdef}	152,35± 4,02^{abc}	915,54± 22,60^{ab}
	2nd	649,32± 9,54^{abcde}	153,04± 2,66^{abc}	3610,37± 73,71^{abcdefg}
	3rd	793,74± 2,29^{bcdef}	430,32± 11,53^{f}	2071,07± 33,40^{bcdefg}
K100	**1st**	709,86± 4,59^{abcdef}	221,47± 1,96^{abcdef}	1585,88± 9,11^{abcdefg}
	2nd	546,88± 9,14^{ab}	190,29± 1,89^{abcde}	873,71± 19,62^{a}
	3rd	559,72± 4,23d^{ab}	234,69± 1,64bcd^{ab}	3336,30± 44,45^{fg}
P25	**1st**	786,39± 5,70^{abcdef}	122,39± 5,64a	1197,46±39,83^{abcdefg}
	2nd	936,46± 26,73^{ef}	237,14±3,50^{abcdef}	1924,03± 28,16^{abcdefg}
	3rd	502,93± 11,01^{a}	210,62± 0,59^{abcdef}	2283,91± 90,55^{efg}
P50	**1st**	915,38± 20,84^{def}	227,59± 2,56^{abcdef}	1159,08± 20,53^{abcde}
	2nd	916,92± 10,25^{def}	186,42± 3,98^{abcde}	868,38± 9,92^{a}
	3rd	658,73±16,25^{abcdef}	331,82± 0,68^{ef}	1587,29± 84,05^{abcdefg}
P75	**1st**	962,02± 9,63^{f}	442,15± 0,65f	1234,24± 2,73^{abcdefg}
	2nd	926,01± 15,23^{ef}	301,62± 4,75^{def}	1214,49± 24,06^{abcdefg}
	3rd	782,16± 11,76^{abcdef}	367,15± 10,35^{ef}	1876,68± 123,73^{abcdefg}
P100	**1st**	752,47± 13,22^{abcdef}	264,14± 7,47^{bcdef}	2071,35± 98,40^{cdefg}
	2nd	779,25± 6,48^{abcdef}	1157,65± 23,31^{f}	2198,84± 58,98^{defg}
	3rd	690,36± 15,65^{abcdef}	333,13± 13,29^{ef}	2018,71± 37,99^{bcdefg}

Values with different superscript letters differ significantly (Kruskal–Wallis + Dunn's test, Benjamini–Hochberg correction, $p < 0.05$). Letters follow activity ranking, with "a" indicating the highest activity

Table E2

Table: Antioxidant Capacities (µM TE/g DW) determined by DPPH, ABTS, and Hydroxyl Radical scavenging assays in three flushes of Pleurotus Ostreatus grown on various substrate formulations

Sample		TEAC (µM TE/g DW)		
Substrate	**Flushes**	**DPPH**	**ABTS**	**HR**
W	**1st**	6,85 ± 0,06 abcdefgh	25,10 ± 0,24 abc	48,62 ± 0,72 abcdef
	2nd	7,57 ± 0,12 abc	18,10 ± 0,86 abcdefgh	42,53 ± 0,15 abcdefg
	3rd	7,19 ± 0,28 abcde	19,10 ± 0,34 abcdef	41,55 ± 0,38 abcdefgh
K25	**1st**	7,03 ± 0,12 abcdefg	17,53 ± 0,61 abcdefgh	64,22 ± 2,34 abc
	2nd	5,72 ± 0,08 cdefgh	17,75 ± 0,30 abcdefgh	36,29 ± 0,16 cdefgh
	3rd	4,13 ± 0,05 h	11,78 ± 0,22 efgh	20,57 ± 0,31 gh
K50	**1st**	7,29 ± 0,20 abcd	19,45 ± 0,02 abcde	64,69 ± 0,90 abc
	2nd	8,60 ± 0,22 ab	24,70 ± 0,68 abc	59,46 ± 0,46 abcd
	3rd	5,74 ± 0,14 cdefgh	14,86 ± 0,25 cdefgh	38,32 ± 0,86 bcdefgh
K75	**1st**	7,10 ± 0,06 abcdef	26,54 ± 0,68 ab	66,21 ± 1,61 ab
	2nd	7,39 ± 0,11 abcd	27,16 ± 0,48 ab	17,26 ± 0,35 h
	3rd	6,47 ± 0,02 bcdefgh	10,34 ± 0,27 gh	32,19 ± 0,53 defgh
K100	**1st**	6,71 ± 0,04abcdefgh	18,61 ± 0,16 abcdefg	38,96 ± 0,22 abcdefgh
	2nd	10,89 ± 0,18 a	27,08 ± 0,26 a	88,49 ± 1,96 a
	3rd	10,76 ± 0,08 a	22,21 ± 0,16 abcd	23,43 ± 0,31 fgh
P25	**1st**	4,76 ± 0,03 fgh	26,56 ± 1,22 ab	40,62 ± 1,39 abcdefgh
	2nd	4,49 ± 0,12 fgh	15,32 ± 0,22 cdefgh	28,31 ± 0,41 efgh
	3rd	7,58 ± 0,17 abc	15,66 ± 0,04 bcdefgh	21,72 ± 0,88 gh
P50	**1st**	5,01 ± 0,12 efgh	17,44 ± 0,19 abcdefgh	51,34 ± 0,93 abcde
	2nd	4,29 ± 0,05 gh	18,29 ± 0,39 abcdefgh	58,84 ± 0,67 abcd
	3rd	7,29 ± 0,18 abcde	12,52 ± 0,03 defgh	39,44 ± 2,02 abcdefgh
P75	**1st**	6,45 ± 0,06 bcdefgh	12,14 ± 0,02 efgh	65,18 ± 0,14 abc
	2nd	5,10 ± 0,08 defgh	13,56 ± 0,21 defgh	50,50 ± 1,00 abcde
	3rd	6,03 ± 0,09 cdefgh	11,14 ± 0,31 fgh	32,91 ± 2,29 defgh
P100	**1st**	8,50 ± 0,15 ab	20,97 ± 0,59 abcd	40,22 ± 1,99 abcdefgh
	2nd	6,03 ± 0,05 cdefgh	3,51 ± 0,07 h	27,76 ± 0,75 efgh
	3rd	7,3 8± 0,16 abcd	13,27 ± 0,53 defgh	32,74 ± 0,62 defgh

Values with different superscript letters differ significantly (Kruskal–Wallis + Dunn's test, Benjamini–Hochberg correction, $p < 0.05$). Letters follow activity ranking, with "a" indicating the highest activity

Appendix F: Reducing Antioxidant Activity

Table F1

Table: IC_{50} values (µg/ml) of FRAP, CUPRAC, and TAC assays of three flushes of Pleurotus ostreatus extracts cultivated in different substrate formulas

sample		A_{50} (µg/ml)		
Substrate	**Flush**	**FRAP**	**CUPRAC**	**TAC**
WS	**1st**	43,07± 1,23^{abcdef}	482,28± 18,21^{e}	96,60± 0,93^{ab}
	2nd	20,50± 0,94^{ab}	388,15± 8,79^{de}	85,91± 3,16^{a}
	3rd	33,42± 4,44^{abcdef}	393,99± 2,72^{de}	76,38± 3,02^{a}
K25	**1st**	27,37± 2,08^{abcde}	225,71± 13,03^{abcde}	154,73± 4,68^{abcde}
	2nd	27,00± 0,94^{abcde}	221,92± 1,14^{abcde}	145,49± 1,32^{abcde}
	3rd	75,51± 0,08^{f}	229,78± 2,64^{abcde}	137,89± 2,14^{abcde}
K50	**1st**	55,32± 2,07^{abcde}	203,63± 0,67^{abcde}	146,96± 7,57^{abcde}
	2nd	64,79± 3,92^{cdef}	263,62± 9,79^{bcde}	88,85± 6,23^{ab}
	3rd	12,43± 1,67^{a}	377,58± 6,91^{cde}	145,68± 0,69^{abcde}
K75	**1st**	29,72± 0,62^{abcdef}	205,56± 5,17^{abc}	139,18± 13,07^{abcde}
	2nd	74,27± 0,78^{f}	223,23± 9,78^{abcde}	98,33± 1,17^{ab}
	3rd	37,84± 0,63^{abcdef}	282,74± 2,02^{bcde}	127,78± 2,34^{abcde}
K100	**1st**	46,74± 1,86^{abcdef}	144,57± 5,43^{abcde}	188,54± 5,52^{cde}
	2nd	78,08± 2,68^{f}	115,99± 3,14^{a}	115,63± 2,01^{abcde}
	3rd	26,81± 1,45^{abcde}	114,29± 1,09^{a}	167,36± 5,03^{bcde}
P25	**1st**	25,69± 1,15^{abcd}	130,55± 3,08^{ab}	80,66± 0,60^{a}
	2nd	29,06± 0,61^{abcdef}	98,51± 0,84^{a}	99,25± 1,36^{abc}
	3rd	33,35± 2,36^{abcdef}	139,57± 6,13^{abc}	191,53± 4,08^{cde}
P50	**1st**	53,31± 2,96^{abcdef}	230,54± 5,75^{abcde}	105,49± 1,90^{abcd}
	2nd	26,17± 2,79^{abcde}	259,76± 0,53^{bcde}	94,40± 1,43^{ab}
	3rd	60,73± 2,93^{cdef}	131,37± 2,11^{ab}	145,16± 1,78^{abcde}
P75	**1st**	59,15± 3,26^{cdef}	391,40± 6,23^{de}	152,44± 15,99^{abcde}
	2nd	28,47± 0,70^{abcdef}	182,95± 4,74^{abcd}	128,04± 1,44^{abcde}
	3rd	69,76± 0,75^{ef}	213,44± 10,51^{abcde}	225,51± 4,64^{e}
P100	**1st**	24,66± 1,99^{abc}	221,60± 1,23^{abcde}	167,04± 3,57^{bcde}
	2nd	43,68± 2,96^{abcdef}	217,36± 3,62^{abcde}	171,21± 8,71^{bcde}
	3rd	70,74± 10,72^{def}	228,73± 4,81^{abcde}	197,28± 4,61^{de}

Values with different superscript letters differ significantly (Kruskal–Wallis + Dunn's test, Benjamini–Hochberg correction, $p < 0.05$). Letters follow activity ranking, with "a" indicating the highest activity

Table F2

Table: Antioxidant Capacities (µM TE/g DW) determined by FRAP, CUPRAC, and TAC assays in three flushes of Pleurotus Ostreatus grown on various substrate formulations

Sample		TEAC (µM TE/g DW)		
Substrte	**Flush**	**FRAP**	**CUPRAC**	**TAC**
WS	**1st**	32,36 ± 0,95 ^{cdefghijk}	40,02 ± 1,49 ^{g}	63,77 ± 0,61 ^{abcde}
	2nd	66,93 ± 3,00 ^{abcd}	48,74 ± 1,13 ^{g}	70,59 ± 2,67 ^{abcd}
	3rd	39,82 ± 6,07 ^{abcdefghijk}	44,85 ± 0,31 ^{g}	74,25 ± 2,84 ^{abc}
K25	**1st**	62,54 ± 4,73 ^{abcd}	104,41 ± 6,35 ^{abcdefg}	48,47 ± 1,48 ^{defghi}
	2nd	54,74 ± 1,91 ^{abcdef}	91,90 ± 0,47 ^{bcdefg}	44,85 ± 0,40 ^{efghi}
	3rd	15,75 ± 0,01 ^{k}	71,59 ± 0,83 ^{efg}	38,17 ± 0,60 ^{fghi}
K50	**1st**	31,63 ± 1,19 ^{defghijk}	118,52 ± 0,39 ^{abcdef}	52,80 ± 2,60 ^{bcdefghi}
	2nd	28,25 ± 1,78 ^{efghijk}	95,50 ± 3,47 ^{bcdefg}	91,27 ± 6,18 ^{a}
	3rd	134,39 ± 16,07 ^{a}	59,13 ± 1,10 ^{fg}	48,99 ± 0,24 ^{cdefghi}
K75	**1st**	52,79 ± 1,13 ^{abcdefg}	105,65 ± 2,69 ^{abcdefg}	50,70 ± 4,42 ^{bcdefghi}
	2nd	21,72 ± 0,23 ^{jk}	100,32 ± 4,33 ^{abcdefg}	72,61 ± 0,86 ^{abcd}
	3rd	45,61 ± 0,77 ^{abcdefghij}	84,45 ± 0,60 ^{defg}	59,82 ± 1,11 ^{abcdefgh}
K100	**1st**	34,32 ± 1,32 ^{bcdefghijk}	153,55 ± 6,00 ^{abc}	37,63 ± 1,13 ^{ghi}
	2nd	25,69 ± 0,86 ^{hijk}	238,92 ± 6,56 ^{a}	76,62 ± 1,35 ^{ab}
	3rd	75,99 ± 4,24 ^{abc}	245,00 ± 2,34 ^{a}	53,62 ± 1,58 ^{abcdefghi}
P25	**1st**	49,11 ± 2,11 ^{abcdefghi}	133,36 ± 3,13 ^{abcd}	68,97 ± 0,50 ^{abcd}
	2nd	48,57 ± 1,01 ^{abcdefghij}	198,04 ± 1,68 ^{ab}	62,90 ± 0,85 ^{abcdef}
	3rd	38,83 ± 2,87 ^{abcdefghijk}	127,40 ± 5,61 ^{abcde}	29,61 ± 0,63 ^{i}
P50	**1st**	29,08 ± 1,71 ^{efghijk}	92,53 ± 2,36 ^{cdefg}	64,68 ± 1,17 ^{abcde}
	2nd	51,72 ± 5,44 ^{abcdefgh}	70,46 ± 0,15 ^{efg}	62,06 ± 0,94 ^{abcdefg}
	3rd	26,70 ± 1,26 ^{fghijk}	169,88 ± 2,78 ^{abc}	49,18 ± 0,61 ^{cdefghi}
P75	**1st**	35,47 ± 2,08 ^{abcdefghijk}	73,68 ± 1,16 ^{defg}	61,99 ± 7,15 ^{abcdefg}
	2nd	55,84 ± 1,40 ^{abcde}	120,16 ± 3,07 ^{ancdef}	54,88 ± 0,61 ^{abcdefghi}
	3rd	22,73 ± 0,25 ^{ijk}	103,25 ± 5,07 ^{abcdefg}	31,13 ± 0,64 ^{hi}
P100	**1st**	88,23 ± 7,26 ^{ab}	134,07 ± 0,73 ^{abcd}	56,95 ± 1,23 ^{abcdefghi}
	2nd	36,46 ± 2,40 ^{abcdefghijk}	100,54 ± 1,66 ^{abcdefg}	41,03 ± 2,10 ^{efghi}
	3rd	25,20 ± 3,35 ^{ghijk}	103,56 ± 2,17 ^{abcdefg}	38,42 ± 0,89 ^{fghi}

Values with different superscript letters differ significantly (Kruskal–Wallis + Dunn's test, Benjamini–Hochberg correction, $p < 0.05$). Letters follow activity ranking, with "a" indicating the highest activity

Appendix G: Chelating Antioxidant Activity

Table G1

Table: A_{50} Values (µg/ml) of FIC and CCA assays of three flushes of Pleurotus ostreatus extracts cultivated in different substrate formulas

Sample		A_{50} (µg/ml)	
Substrate	**Flush**	**FIC**	**CCA**
WS	**1st**	150,25 ± 2,96^{abcdef}	413,89± 8,84^{a}
	2nd	236,97± 35,28^{cdef}	715,25± 8,01^{abcde}
	3rd	210,13± 5,28^{bcdef}	823,49± 18,71^{abcdef}
K25	**1st**	352,65± 16,44^{f}	1095,70± 48,70^{ef}
	2nd	87,20± 0,24^{ab}	1163,32± 89,21^{abcdef}
	3rd	132,52± 0,24^{abcdef}	1994,74± 111,71^{abcdef}
K50	**1st**	93,15± 1,56^{abc}	1027,79± 29,24^{abcdef}
	2nd	86,77± 1,48^{a}	2133,30± 90,06^{f}
	3rd	217,99± 11,11^{cdef}	1067,57± 147,05^{abcdef}
K75	**1st**	209,46± 1,55^{cdef}	1783,56± 22,73^{cdef}
	2nd	82,67± 4,82^{a}	1740,18± 68,96^{cdef}
	3rd	194,55± 1,02^{abcdef}	1851,72± 58,85^{def}
K100	**1st**	122,29± 6,51^{abcdef}	3013,65± 86,17^{f}
	2nd	84,54± 0,56^{a}	2135,75± 108,02^{f}
	3rd	198,74± 2,21^{abcdef}	1921,07± 66,14^{ef}
P25	**1st**	99,30± 7,75^{abc}	609,48± 5,06^{abc}
	2nd	155,19± 1,53^{abcdef}	618,71± 85,95^{abcd}
	3rd	187,09± 3,13^{abcdef}	1069,77± 102,21^{abcdef}
P50	**1st**	111,79± 1,12^{abcde}	511,88± 28,78^{ab}
	2nd	172,06± 2,66^{abcdef}	631,87± 17,08d^{ab}
	3rd	171,07± 2,22^{abcdef}	658,49± 46,78^{abcd}
P75	**1st**	95,80± 7,00d^{ab}	710,18± 18,80^{abcde}
	2nd	106,36± 5,34^{abcd}	835,04± 46,18^{abcdef}
	3rd	305,21± 5,74^{ef}	935,67± 56,05^{abcdef}
P100	**1st**	155,13 ± 1,69^{abcdef}	1120,52± 67,64^{abcdef}
	2nd	299,17 ± 7,29^{def}	1385,28± 93,32^{bcdef}
	3rd	253,64 ± 3,43^{def}	1073,48± 106,26^{abcdef}

Values with different superscript letters differ significantly (Kruskal–Wallis + Dunn's test, Benjamini–Hochberg correction, $p < 0.05$). Letters follow activity ranking, with "a" indicating the highest activity

Table G2

Table: Antioxidant Capacities (µM EDTAE/g DW) determined by FIC, and CCA, assays in three flushes of Pleurotus Ostreatus grown on various substrate formulations

Sample		TEAC (µM EDTAE/g DW)	
Substrate	**Flush**	**FIC**	**CCA**
W1	**1st**	134,15 ± 23,44 abcde	332,62 ± 7,22 a
	2nd	76,13 ± 11,68 bcdefg	188,90 ± 2,12 abcdef
	3rd	87,79 ± 2,18 abcdefg	153,51 ± 3,56 abcdefg
K25/1	**1st**	39,63 ± 1,91 g	153,21 ± 6,53 abcdefg
	2nd	182,98 ± 0,50 a	126,74 ± 9,39 bcdefg
	3rd	149,40 ± 0,28 ab	59,30 ± 3,37 g
K50/1	**1st**	144,89 ± 2,36 abcd	168,11 ± 4,69 abcdefg
	2nd	149,50 ± 2,56 abc	84,42 ± 3,45 fg
	3rd	67,27 ± 3,32 defg	155,12 ± 21,11 abcdefg
K75/1	**1st**	71,64 ± 0,53 bcdefg	86,95 ± 1,09 fg
	2nd	177,65 ± 9,78 a	91,92 ± 3,69 fg
	3rd	70,10 ± 0,36 defg	92,32 ± 2,84 fg
K100/1	**1st**	120,91 ± 6,11 abcdef	52,58 ± 1,52 g
	2nd	139,11 ± 0,93 abcd	93,06 ± 4,51 fg
	3rd	58,52 ± 0,64 efg	104,41 ± 3,65 efg
P25/1	**1st**	191,05 ± 16,12 a	203,94 ± 1,71 abcde
	2nd	107,53 ± 1,06 abcdefg	235,72 ± 37,36 abcde
	3rd	98,29 ± 1,68 abcdefg	120,34 ± 10,50 cdefg
P50/1	**1st**	136,68 ± 1,39 abcde	299,48 ± 17,65 ab
	2nd	103,42 ± 1,61 abcdefg	207,31 ± 5,50 abcde
	3rd	85,34 ± 1,13 bcdefg	244,68 ± 17,89 abcd
P75/1	**1st**	119,15 ± 8,63 abcdef	290,48 ± 7,89 abc
	2nd	140,14 ± 7,42 abcd	189,09 ± 10,59 abcdef
	3rd	48,67 ± 0,93 fg	168,63 ± 9,56 abcdefg
P100/1	**1st**	70,67 ± 0,76 cdefg	190,92 ± 11,87 abcdef
	2nd	49,88 ± 1,19 fg	113,68 ± 7,52 defg
	3rd	54,25 ± 0,74 fg	160,63 ± 15,60 abcdefg

Values with different superscript letters differ significantly (Kruskal–Wallis + Dunn's test, Benjamini–Hochberg correction, $p < 0.05$). Letters follow activity ranking, with "a" indicating the highest activity

Appendix H: Antioxidant activity of standards

Table H1

Table: IC_{50} Values (µg/ml) of different antioxidant assays for different standards

Standard	IC50 (µg/ml)							
	DPPH	ABTS	FRAP	FIC	CCA	CUPRAC	TAC	HR
Gallic/A	1,21± 0,02	0,36± 0,04	0,91± 0,14	-	73,09± 0,89	-	2,34± 0,02	-
Ascorbic/A	4,00± 0,08	4,19± 0,07	7,70± 0,07	-	258,05± 1,88	-	4,59± 0,04	77,01± 0,72
BHA	5,72± 0,31	1,74± 0,02	0,53± 0,02	-	-	8,47± 2,48	2,64± 0,14	611,67± 38,61
BHT	48,25± 0,70	1,04± 0,04	0,59± 0,06	-	-	8,47± 0,54	6,56± 0,77	-
Catechin	-	0,98± 0,02	0,93± 0,03	-	-	10,71± 1,45	1,37± 0,03	-
Quercetin	2,15± 0,01	0,32± 0,04	0,50± 0,01	-	-	-	1,93± 0,09	-
Trolox	3,97± 0,13	3,40± 0,03	1,37± 0,04	-	-	21,48± 2,93	5,88± 0,78	51,47 ± 2,7
EDTA				35.94 ± 0,17	131,79 ± 1,57			-

The numbers in the table representing the means ± standard error ($P < 0.05$)

Appendix I: Anti-inflammatory activity

Table I1

IC_{50} values (µg/mL) of anti-inflammatory activity of Pleurotus ostreatus extracts from three successive flushes cultivated on different substrate formulas

Sample	Anti-inflammatory IC_{50} (µg/ml)		
	1st flush	2nd flush	3rd flush
WS	124,61 ± 7,35^{ab}	109,83 ± 0,09^{a}	106,73 ± 1,99^{a}
K25	149,53 ± 2,96^{abcd}	226,03 ± 2,41^{bcde}	200,83 ± 5,27^{abcde}
K50	148,82 ± 1,97^{abcd}	211,36 ± 1,52^{abcde}	195,90 ± 1,97^{abcde}
K75	145,69 ± 0,21^{abcde}	160,07 ± 3,45^{abcde}	194,79 ± 1,78^{abcde}
K100	245,82 ± 10,03^{cde}	229,07 ± 4,59^{bcde}	204,88 ± 9,14^{abcde}
P25	126,54 ± 6,54^{ab}	177,62 ± 4,71^{abcde}	263,27 ± 7,46^{de}
P50	132,9 ± 2,91^{ab}	150,19 ± 0,77^{abcd}	230,98 ± 4,94^{bcde}
P75	208,97 ± 14,48^{abc}	224,45 ± 1,44^{bcde}	368,24 ± 9,33^{e}
P100	155,25 ± 5,09^{abcde}	261,43 ± 7,51^{de}	269,82 ± 9,81^{de}
Diclofenac		25,09 ± 0,47	

Values with different superscript letters differ significantly (Kruskal–Wallis + Dunn's test, Benjamini–Hochberg correction, $p < 0.05$). Letters follow activity ranking, with "a" indicating the highest activity

Appendix J: Enzyme Inhibition Activity

Table J1

IC_{50} values (µg/mL) of Tyrosinase inhibition activity of Pleurotus ostreatus extracts from three successive flushes cultivated on different substrate formulas.

Sample	IC_{50} Tyrosinase inhibition (µg/ml)		
	1st flush	2nd flush	3rd flush
WS	664,80 ± 2,62^{abcdef}	740,19 ± 26,46^{abcdef}	804,24 ± 14,34^{ef}
K25	627,39 ± 3,70^{abcdef}	723,22 ± 26,04^{abcdef}	652,32 ± 9,25^{abcdef}
K50	768,54 ± 37,88^{cdef}	544,59 ± 17,74^{abcde}	676,12 ± 13,15^{abcdef}
K75	744,44 ± 7,02^{abcdef}	775,16 ± 8,49^{cdef}	509,37 ± 9,21^{abcd}
K100	638,81 ± 11,92^{abcdef}	758,24 ± 11,48^{abcdef}	609,16 ± 10,86^{abcdef}
P25	575,98 ± 8,12^{abcde}	325,18 ± 7,64^{ab}	1420,73 ± 55,95^{f}
P50	827,31 ± 5,39^{ef}	551,50 ± 16,10^{abcde}	1143,69 ± 27,26^{f}
P75	895,77 ± 82,32^{ef}	797,86 ± 18,30^{def}	491,69 ± 26,55^{abc}
P100	616,33 ± 8,67^{abcdef}	266,68 ± 6,33^{a}	508,47 ± 15,59^{abcd}
Kojic acid	3,82 ± 0,57		

Values with different superscript letters differ significantly (Kruskal–Wallis + Dunn's test, Benjamini–Hochberg correction, $p < 0.05$). Letters follow activity ranking, with "a" indicating the highest activity

Table J2

IC_{50} values (µg/mL) of Tyrosinase inhibition activity of Pleurotus ostreatus extracts from three successive flushes cultivated on different substrate formulas.

Sample	IC_{50}Urease inhibition (µg/ml)		
	1st flush	2nd flush	3rd flush
WS	871,11 ± 10,25^{cdefg}	485,20 ± 22,65^{abc}	662,22 ± 10,42^{abcdefg}
K25	519,05 ± 1,78^{abcd}	555,06 ± 12,05^{abcde}	821,60 ± 12,89^{bcdefg}
K50	489,14 ± 18,26^{abc}	570,32 ± 7,04^{abcdef}	625,82 ± 4,56^{abcdefg}
K75	380,02 ± 16,39^{ab}	513,23 ± 15,02^{abcd}	825,13 ± 26,67^{bcdefg}
K100	320,77 ± 8,77^{a}	495,77 ± 1,09^{abc}	643,52 ± 8,00^{abcdefg}
P25	751,31 ± 15,29^{abcdefg}	725,12 ± 9,57^{abcdefg}	576,28 ± 11,22^{abcdefg}
P50	738,0 ± 11,22^{abcdefg}	686,48 ± 13,92^{abcdefg}	1113,17 ± 41,32^{efg}
P75	825,71 ± 6,60^{bcdefg}	860,78 ± 9,75^{cdefg}	1416,10 ± 55,26g
P100	952,92 ± 5,78^{defg}	1081,64 ± 17,71^{efg}	1313,46 ± 31,01^{fg}
Thiourea	9,743 ± 0,002		

Values with different superscript letters differ significantly (Kruskal–Wallis + Dunn's test, Benjamini–Hochberg correction, $p < 0.05$). Letters follow activity ranking, with "a" indicating the highest activity

Table J3

enzyme inhibition values (%) (α-amylase, AChE, BChE and lipase) of 1mg/ml of P.ostreatus extracts of three successive flushes cultivated on different substrate formulas.

Sample	Inhibition (%) of 1 µg/ml			
	α-amylase	**AChE**	**BChE**	**Lipase**
WS1	24,729 ± 0,314^{gh}	29,726 ± 0,508^{abcdefghij}	35,750 ± 0,433^{g}	6,860 ± 0,006^{bcdefgh}
K25/1	20,302 ± 0,575^{cdefgh}	42,915 ± 0,586^{ghij}	24,960 ± 0,419^{abcdefg}	4,951 ± 0,079^{abc}
K50/1	18,793 ± 0,272^{abcdefgh}	14,404 ± 0,177f^{abcd}	20,456 ± 0,552^{ab}	4,423 ± 0,259^{bc}
K75/1	17,582 ± 0,129^{abcdefgh}	24,259 ± 0,383^{abcdefghij}	35,101 ± 0,545^{fg}	9,986 ± 0,559^{cdefgh}
K100/1	30,015 ± 0,685^{h}	36,822 ± 0,337^{fghij}	22,156 ± 0,173^{abcde}	9,169 ± 0,098^{abcdefg}
P25/1	15,696 ± 0,288^{abcdef}	44,817 ± 0,509^{hij}	31,043 ± 0,627^{defg}	9,704 ± 0,134^{cdefgh}
P50/1	14,325 ± 0,270^{defgh}	30,705 ± 0,506^{bcdefghij}	25,476 ± 0,994^{abcdefg}	11,269 ± 0,510^{fgh}
P75/1	13,168 ± 0,181^{ab}	13,566 ± 0,781^{abcd}	30,811 ± 1,092^{defg}	7,040 ± 0,189^{abcdefg}
P100/1	10,613 ± 0,233^{a}	27,274 ± 0,947^{abcdefghij}	21,714 ± 0,657^{abcd}	9,201 ± 0,332^{bcdefgh}
WS2	18,029 ± 0,273^{abcdefgh}	15,996 ± 0,227^{abcdef}	20,802 ± 0,245^{abc}	14,210 ± 0,089^{h}
K25/2	21,495 ± 0,208^{efgh}	32,966 ± 0,919^{cdefghij}	20,536 ± 0,341^{bc}	12,916 ± 0,121^{gh}
K50/2	15,717 ± 1,836^{abcdef}	34,755 ± 0,361^{defghij}	27,396 ± 0,809^{bcdefg}	11,914 ± 0,356^{gh}
K75/2	20,886 ± 0,504^{efgh}	35,325 ± 0,298^{efghij}	31,332 ± 0,253^{efg}	7,887 ± 0,165^{abcdefgh}
K100/2	17,062 ± 0,467^{abcdefg}	20,870 ± 0,175^{abcdefgh}	30,873 ± 0,858^{defg}	5,509 ± 0,077^{abcde}
P25/2	21,922 ± 0,207^{fgh}	23,647 ± 0,263^{abcdefghij}	26,257 ± 0,404^{abcdefg}	5,047 ± 0,137^{abcde}
P50/2	20,538 ± 0,236^{cdefgh}	20,841 ± 0,633^{abcdefghi}	30,551 ± 0,439^{cdefg}	13,429 ± 0,258^{fgh}
P75/2	20,705 ± 0,290^{defgh}	14,140 ± 0,774^{abcd}	18,692 ± 0,647^{ab}	10,849 ± 0,071^{efgh}
P100/2	17,659 ± 0,561^{abcdefgh}	11,880 ± 0,419^{hij}	24,299 ± 0,540^{abcdef}	8,909 ± 0,092^{abcdefgh}
WS3	11,435 ± 0,236^{ab}	7,606 ± 0,557^{ab}	24,295 ± 0,877^{abcdefg}	9,727 ± 0,227^{defgh}
K25/3	14,148 ± 0,212f^{ab}	5,354 ± 0,565^{a}	31,319 ± 1,163^{defg}	6,229 ± 0,083^{abcdef}
K50/3	27,111 ± 0,462^{h}	13,887 ± 0,926^{abcd}	22,397 ± 1,093^{abcde}	5,781 ± 0,282^{abcdef}
K75/3	19,471 ± 0,079^{bcdefgh}	17,758 ± 0,270^{abcdefg}	15,798 ± 0,274^{a}	3,984 ± 0,054^{ab}
K100/3	6,201 ± 0,157^{a}	33,298 ± 0,297^{cdefghij}	16,165 ± 0,640^{a}	5,013 ± 0,173^{abcd}
P25/3	19,205 ± 0,266^{bcdefgh}	46,004 ± 0,768^{ij}	25,710 ± 0,234^{abcdefg}	2,957 ± 0,119^{a}
P50/3	16,618 ± 0,339^{abcdef}	44,716 ± 1,522^{hij}	25,402 ± 0,371^{abcdefg}	10,824 ± 0,427^{fgh}
P75/3	17,597 ± 0,207^{abcdefgh}	33,512 ± 1,289^{defghij}	25,397 ± 0,367^{abcdefg}	6,145 ± 0,256^{abcdef}
P100/3	16,713 ± 0,062^{abcdef}	52,860 ± 0,970^{j}	34,304 ± 0,623^{fg}	7,831 ± 0,270^{abcdefgh}

Values with different superscript letters differ significantly (Kruskal–Wallis + Dunn's test, Benjamini–Hochberg correction, $p < 0.05$). Letters follow activity ranking, with "a" indicating the highest activity

Appendix K: Enzyme Inhibition Activity

Table K1

inhibition zone (mm) including disk diameter (6mm) of three first flushes of Pleurotus ostreatus mushroom Extracts cultivated of different substrate formulas against different bacetria gram-positive and gram-negative

	Gram-positive				Gram-negative			
Sample	**E.Coli**	**K. Pneumonia**	**P. Aerogenosa**	**Selmonella**	**B.subtilis**	**B.cereus**	**S.aureus**	**E.faecalis**
W1	6,29 ± 0,29	6,50 ± 0,15	6	6	8,43 ± 0,90	9,03 ± 0,10	7,37 ± 0,22	6
K25/1	6,46 ± 0,02	6,29 ± 0,06	6	6	8,46 ± 0,40	8,93 ± 0,02	7,59 ± 0,29	6
K50/1	6,75 ± 0,39	6,25 ± 0,22	6	6	8,11 ± 0,03	6,43 ± 0,12	7,06 ± 0,07	6
K75/1	6	6	6	6	7,16 ± 0,33	7,73 ± 0,50	7,13 ± 0,47	6
K100/1	6,57 ± 0,00	6,39 ± 0,00	6	6	7,12 ± 0,38	6,62 ± 0,12	6,56 ± 0,28	6
P25/1	6,25 ± 0,25	6	6	6	6,48 ± 0,13	7,56 ± 0,26	6	6
P50/1	6	6	6	6	7,89 ± 0,36	6,82 ± 0,18	6,65 ± 0,18	6
P75/1	6	6,37 ± 0,00	6	6	8,21 ± 0,11	6	6,82 ± 0,24	6
P100/1	6,69 ± 0,03	6	6	6	8,04 ± 0,40	6,84 ± 0,04	6,59 ± 0,00	6
W2	6	6	6	6	7,82 ± 0,15	7,00 ± 0,16	12,90 ± 0,09	6
K25/2	6	6,32 ± 0,12	6	6	8,86 ± 0,20	7,18 ± 0,00	6,58 ± 0,17	6
K50/2	6,23 ± 0,23	6	6	6	6,93 ± 0,30	7,64 ± 0,26	6,36 ± 0,08	6
K75/2	6	6	6	6	7,34 ± 0,34	8,42 ± 0,30	14,67 ± 0,19	6
K100/2	6,70 ± 0,70	6,39 ± 0,12	6	6	7,62 ± 0,37	6,20 ± 0,02	6,54 ± 0,04	6
P25/2	6,51 ± 0,08	6,25 ± 0,01	6	6	6,23 ± 0,09	6,31 ± 0,06	6,63 ± 0,29	6
P50/2	6	6	6	6	7,67 ± 0,15	8,20 ± 0,33	8,07 ± 0,68	6
P75/2	6,60 ± 0,33	6	6	6	8,05 ± 0,28	6,95 ± 0,35	6,63 ± 0,09	6
P100/2	6,59 ± 0,15	6	6	6	7,00 ± 0,13	7,43 ± 0,02	6,81 ± 0,06	6
W3	6,63 ± 0,00	6	6	6	7,82 ± 0,21	8,74 ± 0,14	7,39 ± 0,00	6
K25/3	6,62 ± 0,32	6	6	6	8,62 ± 0,20	6,70 ± 0,02	6,88 ± 0,04	6
K50/3	6	6	6	6	7,21 ± 0,41	7,53 ± 0,43	7,13 ± 0,11	6
K75/3	6,84 ± 0,22	6	6	6	7,21 ± 0,65	6	6,55 ± 0,16	6
K100/3	6,18 ± 0,18	6	6	6	7,30 ± 0,03	6,64 ± 0,27	6,49 ± 0,19	6
P25/3	6,19 ± 0,19	6	6	6	6,60 ± 0,10	7,72 ± 0,46	6,83 ± 0,21	6
P50/3	6	6	6	6	6,89 ± 0,31	6	6,38 ± 0,14	6
P75/3	6	6	6	6	6	6,45 ± 0,07	6,12 ± 0,12	6
P100/3	6,43 ± 0,16	6	6	6	6	6,90 ± 0,35	6,47 ± 0,09	6
AMPiciline	20,83 ± 0,00	6	6	/	6,28 ± 0,00	6	41,99 ± 0,91	/
AMoxiciline	28,48 ± 1,04	23,39 ± 0,55	8,69 ± 0,26	30,27 ± 0,17	14,52± 0,31	11,09 ± 0,16	49,86 ± 3,49	6